A COMPARATIVE STUDY ON BIOLOGICAL DEGRADATION OF PLASTIC FROM ISOLATED MICROBES USING VARIOUS METHOD

Malini, R[1]., Vanitha, M[2] and K. Arunthathi K[1]*

[1]Dept. of Microbiology, Thassim Beevi Abdul Kader College for Women, Kilakarai-623517
[2]Dept. of Biotechnology, Madha Engineering College, Kundrathur, Chennai-600069
**Corresponding author: arunthathi.kr@gmail.com*

ABSTRACT

Plastic eradication is one of the most important need in our life and it becomes necessary factor to lead our healthy generation. Plastic is widely used as various products like plastic bags, plastic bottles and pipes among people. Meanwhile, enormous usage of plastic leads to environmental threats. The existing method of Plastic degradation achieved by physical chemical and biological method. In recent year plastic degradation by microbes were the important research area where the application of various microbes and various methods were analysing. Bacteria and fungi play vital role in the degradation process. The present study aims polyethylene, polypropylene and polyvinyl chloride biodegradation using four different method such as artificial media method, modified ASTM G21 70 method, dip hanging method and Compost burial method. The five bacterial and three fungal strains were isolated from compost which is prepared from mixture of cow dung, vegetables waste, Paddy's straw, and saw dust. After that isolates were allowed to characterization test such as staining, biochemical test and antibiotic sensitivity test, isolates allowed for degradation property. Out of eight isolates, white and green fungi highly degrade the polyethylene with 78.8% of weight loss, polypropylene highly degraded by creamy bacteria with 20.4% weight loss, then, polyvinyl chloride highly degraded by black fungi with 4.6% of weight loss. Besides weight loss method, morphological changes was identified by FTIR and SEM analysis.

Keywords: Biodegradation, compost, modified ASTM G21 70 method, dip hanging method, polyethylene, polypropylene, polyvinyl chloride.

INTRODUCTION

Plastics are high-molecular-weight organic polymers. Plastics are typically produced by human industrial processes. These polymers are produced from a variety of hydrocarbons and petroleum derivatives (Abraham et al., 2016) and various renewable materials, like cotton or corn derivatives, are utilized in current industrial processes. According to Kale et al., in 2015 plastics are polymers that can be moulded into moulds by heating them up except for biodegradable bioplastics (Akmal et al., 2015). Plastics versatility makes them an

essential material in different applications; they are used in packaging (39.9%), construction (19.8%), the automotive industry (9.8%), electronics and communication (6.2%), agriculture (3.4%), household leisure and sport (4.1%), and other fields (16.7%). Among the different plastics, the most commonly used in packaging are polypropylene 4 (PP), low-density polyethylene (LDPE), high-density polyethylene (HDPE), vinyl chloride (PVC), polyurethane (PU), polyethylene terephthalate (PETE), and polystyrene (PS).

According to Plastic Pollution (2014), PE is linked to hormonal disturbances, developmental issues, cancer, decreased sperm count, infertility, and diminished immunity. PVC, a type of plastic used in cosmetics, containers, packaging, and utility items, has been linked to cancer, birth defects, and other genetic conditions. Additionally, it may cause problems with 6 digestion and the liver, bronchitis, skin disease, deafness, and vision. Mercury, dioxins, and phthalates, among other dangerous poisonous chemicals released during the PVC life cycle, may pose health risks that cannot be reversed over time. Dioxins, one of the most potent synthetic chemicals ever tested, are released when PVC plastic is made or burned. These dioxins can cause cancer and harm the immune and reproductive systems. According to Zeenat et al (2021), the compound bisphenol A, which is found in some plastic water bottles, is thought to cause cancer, weaken the immune system, cause early puberty, and lead to the development of obesity and diabetes.

In past years polyethylene degrading bacteria has been reported such as, Acinetobacter baumannii, Arthrobacter spp, Viscosus spp, Pseudomonas spp, Arthrobacter viscosus, Bacillus amyloliquefaciens, thuringiensis, mycoides, cereus, pumilus, Staphylococcuscohnii, Xylosus spp, Pseudomonas fluorescens, Rahnella aquatills, Micrococcus luteus, lylae, Paenibacillus macerans, Flavobacterium spp, Delftia acidovorans, Ralstonia spp Rhodococcus erythropolis, Pseudomonas aeruginosa [Koutny et al., 2009] and Bacillus brevies [Watanabe et al., 2009]. The purpose of this study was to isolate microorganisms from compost and screen for the potential plastic degrading microorganisms and identifying the high potential microorganisms that degrade plastic.

MATERIALS AND METHODS

The cow dung, saw dust, paddy’s straw, egg shells and vegetable waste are collected from mahar nonpu pottal, kenkarai, Ramanathapuram district.The collected waste materials were allowed to be dried and chopped into small materials. Next, a plastic container was prepared with a hole for aeration. The collected waste materials were added one by one and mixed with the materials. The prepared plastic container was placed in the shaded area and leaves to composing process bacteria isolated and characterized by biochemical test.

Muller hinton agar was prepared. A petri dish and five bacterial and three fungal broth cultures were obtained. Swab was taken and dipped into broth cultures. Using a dipped swab, streak on the plates in even to obtain a uniform growth. Plates were rotated and reswabed. Using sterile forceps, the antibiotic disc (amoxycillin, ampicillin, pencilin G, gentamycin, vancomycin, streptomycin, kanamycin, nystatin) were taken aseptically and then placed on plates. Plates were incubated at 37℃ for 24 hours. Results were observed that zone of inhibition was noted (Albertsson,, 1980).

Three types of plastic samples were selected, such as polyethylene, polypropylene, polyvinyl chloride. These three samples were more harmful to the environment as well as human health.Biodegradation carriedout by artifical method (Montazer et al., 2020), Dip Hanging method (Alshehrei, 2017) and ASTM G21-70 method (Alshehrei, 2017).Plastic samples were obtained after 15 days of incubation. Samples were washed using 2% sodium lauryl sulphate to remove bacterial and fungal biomass, dried overnight and then 28 weighed. The weight loss of the sample was measured by weighing samples before inoculation as initial sample Weight (Wo) and after 15 days of inoculation process (Wf). Per cent weight loss was calculated.

RESULT AND DISCUSSION

A plastic container was filled full of waste material on the 1 st day. But on the 28th day the mixed materials were converted into a small powder format, a large space appeared on top of the container and an earthy smell developed. Biochemical tes results of isolated microbes were noted in table 1.

Antibiotic sensitivity was used to decide how powerful an antibiotic was against the test life form. The eight separate one were screened for susceptibility towards eight anti- toxins (pencillin, gentamycin, vancomycin, nystatin, streptomycin, amoxycilin, kanamycin) and the outcome was noted. Half white (smooth), white, slight yellow, black and white and green fungi have no antimicrobial movement (Table 2).

All plastic samples were pre-treated with 70% ethanol.

In the artificial media method, polyethylene, polypropylene and polyvinyl chloride pieces were added at an initial weight of 0.0142 g, 0.2328 g and 1.5700 g along with 1ml of inoculum. There are five selected bacteria and three selected fungi separately into dubos mineral salt medium for bacteria and czapek dox medium for fungi. After 15 days of incubation, each plastic sample was reduced in it’s weight and some color changes were observed. Compared to another study, the ability of selected isolates to degrade LDPE was very similar to that of previous research. After 60 days of incubation in MSMB under shaking

conditions (at 130 rpm) (Munir E et al., 2018), Das and Kumar discovered that Apergillus reduced the weight of LDPE film by 5-8% and Fusarium by 9%. The total weight loss of LDPE has also been found to be significantly higher. According to Singh and COMPOST BURIAL METHOD FIGURE 13: SODIUM LAURYL SULFATE TREATED PLASTIC SAMPLES 74 Gupta, Mucor sp., Aspergillus japonicus, Aspergillus flavus, and Aspergillus niger all reduced weight by 30%, 20%, and 36%, respectively. In this present study, colour changes observed on the polyethylene and polyvinyl chloride samples. The colour of polyethylene sample into the faded and blue colour of the polyvinyl chloride sample changed into grey and white and polyethylene samples degraded into 65.2%, polypropylene samples into 6% and polyvinyl chloride into 25%.

Dip hanging method, the specific media are not used. So, the carbon source for bacterial and fungal growth only comes from plastic samples. After incubation of 15 days of incubation, bacterial and fungal colonies stick on the plastic samples. Compared to another study,the decomposition time for PCL from England and PLA from Japan is 60 days, according to the ASTM standard. In linear polymers, chemical degradation reactions result in a decrease in molecular weight or a shorter chain length. Acetal bonds in starch are very simple to degrade. Because the bioplastic's composition was a natural material that microbes could easily digest, this mass reduction was significant. A natural polymer with a hydroxyl group (-OH) was the primary characteristic of a polymer that could be degraded naturally; consequently, this group was easily degraded by microorganisms (Zeenat et al., 2021), A. niger lost 11.5% of its weight. The dip-hanging method resulted in poor growth (R.C Nissa et al 2019). But in this study, On the 15 th day, polyethylene samples faded and polyvinyl chloride samples were changed to grey and black with some dots appearing and weight also reduced. The weight of polyethylene, polypropylene and polyvinyl chloride is 61.6%, 8.1% and 15 % reduced.

By the ASTM method, organisms take nutrients from glucose salt agar. The inoculum was spread on the surface of the agar plates and plastic samples were placed on it. So, organisms grow around and on the plastic samples. Compared with Alshehrei,2017, in the modified ASTM G21-70 method, A. niger flourished on the bioplastic sample’s surface, indicating that the bioplastic could be degraded by the fungus. In this study after incubation, the weight of the polyethylene samples degraded into 61.3%, polypropylene samples in 19.6% and polyvinyl chloride degraded into 15.8%. But colour change was not observed.

CONCLUSION

The five bacterial and three fungal strains were tested for their ability to degrade polyethylene, polypropylene and polyvinyl chloride. Biodegradation occur four different methods. From this study, out of eight isolates, three strains were well performed after 15 days of incubation. The well performed isolates consist of two fungal and one bacterial strain. Those three are white and green fungi, slight yellow bacteria and black fungi. White and green fungi promising strain to degrade polyethylene, slight yellow to degrade polypropylene and black fungi to polyvinyl chloride degradation. The three well performed strains highly degrade the respective plastic samples at the presence of nutrients such as artificial media method. So, artificial media method was suitable method for plastic degradation.

TABLE 1: BIOCHEMICAL CHARACTERS OF ISOLATES

S.NO	TEST	Bacterial Colonies				
		Pink	Half white, smooth	Half white, rough	White	Yellow
1	Indole	+	+	-	-	+
2	Methyl red	+	+	-	+	+
3	Voges proskauer	+	+	+	+	+
4	Catalase	+	+	+	+	+
5	Citrate	+	+	-	+	+
6	Urease	-	-	+	+	-
7	Starch hydrolysis/ amylase enzyme	-	-	+	+	-
8	Casein hydrolysis/ protease enzyme	+	-	+	+	-
9	Gelatin hydrolysis	+	-	+	+	+
10	Nitrate reduction	+	+	-	+	+
11	Oxidase	+	-	+	+	+
12	Cellulose enzyme	+	-	-	+	+
13	Glucose fermentation	-	+	+	+	+
14	Gas production	+	+	+	+	+

TABLE 2:ANTIBIOTIC ASSAY OF ISOLATED STRAINS

S.NO	ISOLATES	ANTIBIOTIC DISC assay (mm)			
		AMOXYCILIN (30mg)	PENCILIN G (10mg)	KANAMYCIN (30mg)	STREPTOMYCIN (10mg)
1	Half white, rough	14	-	-	18
2	Pink	14	-	-	-
3	Half white, smooth	-	-	-	-
4	Yellow	-	-	-	-
5	White	-	-	-	-

REFERNCE

Abraham, J., Ghosh, E., Mukherjee, P., & Gajendiran, A. (2016). Microbial degradation of low density polyethylene. Environmental Progress & Sustainable Energy, 36(1), 147–154.

Akmel, D. C., Kakou, K. E., Kone, K. Y., Assidjo, N. E., & Kouame, P. (2015). Desorption isotherms and isosteric heats of fermented cocoa beans (Theobroma cocoa). Journal of Food Research, 4(3), 138.

Albertsson, A. C., 1980. The shape of the biodegradation curve for low and high density polyethylenes in prolonged series of experiments. Eur. Polym. J. 16, 623-630.

Alshehrei, F. (2017). Biodegradation of low density polyethylene by fungi isolated from Red Sea Water. International Journal of Current Microbiology and Applied Sciences, 6(8), 1703– 1709.

Koutny, M., Amato, P., Muchova, M., Ruzicka, J., & Delort, A.-M. (2009). Soil bacterial strains able to grow on the surface of oxidized polyethylene film containing prooxidant additives. International Biodeterioration & Biodegradation, 63(3), 354–357

Montazer, Z.; Habibi Najafi, M.B.; Levin, D.B. Challenges with Verifying Microbial Degradation of Polyethylene. Polymers 2020, 12, 123.

Watanabe, T., Ohtake, Y., Asabe, H., Murakami, N., & Furukawa, M. (2009). Biodegradability and degrading microbes of low-density polyethylene. Journal of Applied Polymer Science, 111(1), 551–559.

Zeenat, Elahi, A., Bukhari, D. A., Shamim, S., & Rehman, A. (2021). Plastics degradation by microbes: A sustainable approach. Journal of King Saud University – Science, 33(6), 101538.

EVALUATING AND IDENTIFYING THE PHARMOCOLOGICAL ACTIVIES OF *Cissus quadrangularis* USING MOLECULAR DOCKING AND ANIMAL MODEL

Afra M.J., Thenmozhi, M[2], Arunthathi K*

Department of Microbiology, Thassim Beevi Abdul Kader College for Women, Kilakarai-623517
[2]Dept. of Biotechnology, Madha Engineering College, Kundrathur, Chennai- 69
**Corresponding author: arunthathi.kr@gmail.com*

ABSTRACT:

Cissus quadrangularis is a succulent plant belongs to the family of *Vitaceae*. It is a fleshy, cactus in nature. It is additionally acknowledged as *Vitis quadrangularis*. It is commonly observed in tropical and sub-tropical xeric wood. It is an historical remedy plant native to hotter components of Ceylon and India. This plant has been said to include flavonoids, triterpenoids, phytosterols, glycosides and wealthy supply of calcium. This learns about targets to deliver a systematic evaluate of *Cissus quadrangularis* in a variety of pharmacological mechanisms. Evidences from the preceding research recommended the efficacy of *Cissus quadrangularis* with anti-microbial, anti-diabetic, anti-inflammatory, anti-obesity, bone turnover, cell reinforcement, ache relief, gastro-intestinal treatments, cardiovascular and hepatoprotective activities. In conclusion, the plant seems helpful of pharmacological investigations for new drug formula for inflammation.

Keywords: *Cissus quadrangularis*, bone turnover, calcium, pharmacological, anti-inflammatory, flavonoids, *Vitis quadrangularis*

INTRODUCTION:

Cissus quadrangularis is a perennial plant of the grape family. It is usually recognized as Veldt Grape or Devil's Backbone (Ganesan & Choi 2016). The plant generally acknowledged as a "bone setter"- it is referred to as Asthisandhani in Sanskrit and Hodjod in Hindi due to the fact of its potential to join bones. *Cissus quadrangularis* is used as a medicinal plant (Abu Bakar et al., 2020). In siddha medication, it is regarded as tonic and analgesic. It is additionally used to heal damaged bones, injured ligaments and tendons (Liebsch et al., 2011). Therefore, it is identified as Asthisamharaka (that which prevents the destruction of bones). The clean stem and leaves of *Cissus quadrangularis* are used for the therapy of hemorrhoids, menstrual disorders, scurvy and flatulence. It requires a heat tropical climate. It is propagated the usage of the stem slicing techniques in the months of June to July (Kubo et al., 2006). The plant is successfully reproduced using its mature stem cuttings. Sickness free, healthful and mature plant of Cissus quadrangularis was once used as

a supply of stem cuttings for further development (Evans, W. C. 2009). It can immediately grownup in the organized beds with average supply of water and appropriate substratum to climb). A developed plant of *Cissus quadrangularis* is beneficial to switch the plant life is easily from one region to any other as per need. The above activities no longer solely support the plants for fast multiplication (Balouiri et al., 2016). However, additionally for their dissemination. The *Cissus quadrangularis*, invites the interest of the global researchers for its pharmacologic things to do such as anti- analgesic, anti-inflammatory, anti-oxidant, and free radical anti-scavenging activities, anti-osteoporosis endeavor and bone restoration activity. It is a tendril-climbing shrub barring stout, fleshy quadrangular stems. The important that are components discovered in the plant are ascorbic acid, carotene, ketosteroid, calcium, triterpenoids (Wagner & Ulrich-Merzenich 2009). It was mentioned to include three unsymmetric tetracyclic triterpenoids alongside with the β-sitosterol, β-amyrin, and β-amyrone. In addition, It carries the flavonoids, phytosterols, δ-amyrin, δ-amyron, resveratrol, piceatannol, pallidol, parthenocissine, quadragularins and water-soluble glycosides (Raj, et.al., 2011).

MATERIALS AND METHODS:

The fresh stem parts of the plant Cissus quadrangularis was collected from the Kilakarai, Ramanathapuram, Tamilnadu. Collected stems were rinsed with distilled water and allowed to dry in shadow for 20-30 days. The completely dried stem was powdered for further studies (John et al., 2011). The studies such as extraction, phytochemical analysis, thin-layer chromatography, gas chromatography – mass spectrometry was accomplished (Kagan et al., 2014).

The identified phytocompounds from the gas chromatography – mass spectrometry was undergone with the molecular docking with the aid of PyRx Python Virtual Screening Tool (version 0.8) against Human C-Reactive Protein, an inflammatory agent in human (Morris, G. M., Lim-Wilby, M. 2008). The method hemolysis was implemented using an animal model (Albino Rat) with different concentrations of the extract (Du Clos, T. W. 2000). The antibacterial activity was conducted using both Gram-positive and Gram-negative strains of bacteria, including Bacillus subtilis, Staphylococcus aureus, Klebsiella sp., and *Escherichia coli (*Mohanty et al., 2011*).* By observing the results of all the above studies, the anti-inflammatory gel-based product was developed with the help of activators, buffers and preservative (Grada et al., 2018).

RESULTS AND DISSCUSSION:

Phytochemical Analysis:

Preliminary phytochemical analysis of the aqueous, ethanol and methanol extracts of *Cissus quadrangularis* indicated the presence of certain metabolites in a different manner.

Table 1: Phytochemical Analysis of Aqueous, Methanol and Ethanol Extracts

S.NO	TEST		REAGENT	AQUEOUS	METHANOL	ETHANOL
1	Alkaloids	Mayer's Test	Mayer's Reagent	+	+	-
		Wagner's Test	Wagner's Reagent	+	+	-
2	Coumarins	Sodium Hydroxide Test	NaOH	+	+	+
3	Terpenoids	Salkowski's Test	$CHCl_3$ H_2SO_4	+	+	+
4	Phenols	Ferric Chloride Test	$FeCl_3$	+	+	-
5	Quinones	Alkali Test	10% NaOH	+	-	-
6	Anthraquinones	Hydrochloric Acid Test	HCl	+	-	-
7	Tannins	Gelatin Test	NaCl	+	+	+
8	Phlobatannins	Ammonia Test	NH_4OH	-	+	+
9	Carbohydrates	Molish's Test	Alphanapthol	+	+	-
		Benedict's Test	Benedict's Reagent	+	+	-
		Fehling's Test	Fehling's Reagent	+	+	-
10	Glycosides	Legal's Test	$CHCL_3$ NH_4OH	-	-	+
11	Cardiac Glycosides	Keller-killani Test	CH_3COOH $FeCl_3$ H_2SO_4	-	-	+
12	Proteins	Million's Test	Million's Reagent	+	+	-
		Biuret's Test	Biuret's Reagent	+	+	-
13	Amino Acids	Ninhydrin Test	Ninhydrin Reagent	+	+	+
14	Steroids	Ferric Chloride – Acetic acid test	$CHCL_3$ $FeCl_3$ CH_3COOH H_2SO_4	-	+	+
15	Phytosteroids	Chloroform – Sulphuric Acid Test	$CHCL_3$ H_2SO_4	-	+	-

16	Acids	Sodium Bicarbonate Test	$NaHCO_3$	+	+	-
17	Saponins	Foam Test	H_2O	+	+	-
18	Carboxylic Acids	Phenolphthalein Test	$C_{20}H_{14}O_4$ NaOH	-	+	+
19	Fixed Oils	Oil Detection Test	Whattman Filter Paper	-	-	-
20	Fats	Saponification Test	KOH $C_{20}H_{14}O_4$	-	-	-
21	Gums And Mucilages	Distilled water and Alcohol Test	C_2H_5OH	+	+	+
22	Flavanoids	Aqueous Test	NaOH	+	+	+
		Sulphuric Acid Test	H_2SO_4	+	+	+

TABLE 2: Phenol and Flavonoid compounds quantified in the extract

S. No	Phytochemicals	Amount (µg/mg)
1.	Phenols	744.2 ±1.05
2.	Flavonoids	152.5 ±0.22

The total phenol content was 744.2 ±1.05 µg/mg of GAE and the total flavonoid content was 152.5 ± 0.22 µg/mg in the extract.

Gas chromatography mass spectrometry:

The total phytocompounds identified in the GC-MS analysis was about Aqueous = 13 phytocompounds and Methanol = 16 phytocompounds.

Figure 1: Chromatogram of the result observed from GC-MS Analysis of Aqueous Extract and Methanol Extract of *Cissus quadrangularis*

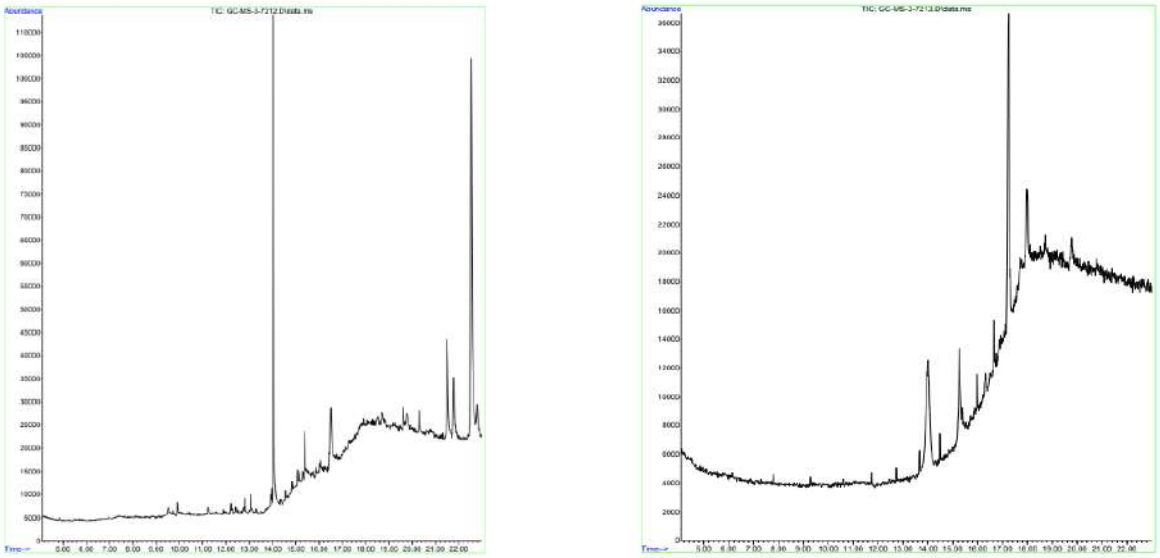

Molecular docking studies:

The molecular docking was done between the phytocompounds observed in the Gas Chromatography – Mass Spectrometry with the Human C-Reactive Protein.

TABLE 3: Results of the molecular docking (Methanol Extract)

Compound	Binding Affinity (Kcal/Mol)	Mode	Rmsd Lower Bounding	Rmsd Upper Bounding
5-Methyl-2-Phenylindolizine	-6.8	0	0.0	0.0
	-6.8	1	0.801	2.402
	-6.4	2	1.183	1.647
	-6.3	3	1.204	2.944
	-5.6	4	19.015	19.975
	-5.6	5	18.391	19.579
	-4.4	6	19.344	20.154
	-3.9	7	20.172	21.263
Acetic acid	-3.2	0	0.0	0.0
	-3.1	1	20.398	20.946
	-3.1	2	15.483	15.534
	-3.0	3	20.408	20.881
	-2.9	4	23.811	24.267
	-2.7	5	16.383	16.597
	-2.7	6	22.404	22.911
	-2.6	7	17.26	17.631
Dimethylaminoethyl	-4.9	0	0.0	0.0
	-2.8	1	1.123	2.331
	-2.0	2	8.535	11.037
Benzoxazepine	-6.7	0	0.0	0.0
	-5.8	1	2.188	3.17
	-5.2	2	2.533	5.116
	-5.0	3	2.18	40705
	-4.0	4	3.046	5.77
	-3.8	5	17.797	18.501
Cyclotrisiloxane	-4.7	0	0.0	0.0
	-4.1	1	26.415	27.355
	-3.8	2	12.973	16.116
	-3.6	3	1.034	21.91
	-3.6	4	9.935	13.071
	-3.2	5	9.76	13.557
	-3.0	6	1.526	5.660
	-2.7	7	12.912	16.139
	-2.4	8	22.655	27.677
Benzo [H] quinoline	-5.2	0	0.0	0.0
	-5.1	1	2.334	5.29
	-5.1	2	18.856	19.669
	-5.1	3	1.422	2.436

	-4.6	4	3.136	5.677
	-4.3	5	3.432	5.655
	-4.3	6	1.042	2.011
	-4.3	7	10.993	12.233
	-4.2	8	20.371	21.146
	-6.0	0	0.0	0.0
1,2-Benzisothiazol	-3.0	1	1.885	2.425
	-3.9	0	0.0	0.0
	-3.9	1	0.27	0.277
	-3.9	2	0.259	2.528
	-3.4	3	2.466	3.395
Benzene	-3.4	4	2.391	3.927
	-3.3	5	20.106	20.769
	-3.3	6	20.117	20.724
	-3.3	7	20.048	20.701
	-3.3	8	20.194	20.885
Cycloheptatrien	-.3.8	0	0.0	0.0
	-3.8	1	0.264	1.447
	-3.8	2	0.248	2.3
	-3.8	3	19.652	20.794
	-3.7	4	19.567	20.467
	-3.7	5	0.243	2.293
Heptamethyltrisiloxane	0	0	0	0
	-4.7	0	0.0	0.0
	-4.1.	1	26.415	27.355
	-3.8	2	12.973	16.116
	-3.6	3	1.034	4.91
Cyclotrisiloxane	-3.6	4	9.935	13.071
	-3.2	5	9.76	13.557
	-3.0	6	1.526	5.666
	-2.7	7	12.912	16.139
	2.4	8	26.655	27.677

TABLE 4: Results of the molecular docking (Aqueous Extract)

Compound	Binding Affinity (Kcal/Mol)	Mode	RMSD Lower Bounding	RMSD Upper Bounding
Phytol	-4.3	0	0.0	0.0
	-4.1	1	3.612	10.606
	-3.1	2	9.552	14.333
	-2.4	3	5.424	10.287
	-2.0	4	3.797	6.336
	-1.7	5	3.88	6.134

Isophytol	-4.1	0	0.0	0.0
	-3.8	1	1.454	2.116
	-3.1	2	4.764	12.006
	-2.9	3	1.475	2.239
	-1.7	4	3.132	5.64
	-1.4	5	3.941	11.203
1-Hexadecen-3-ol	5.0	0	0.0	0.0
	5.4	1	1.366	2.044
	55	2	2.943	9.801
	6.1	3	1.275	2.153
	6.7	4	3.503	10.146
	7.7	5	3.383	10.095
	7.8	6	1.568	2.569
Sulfurous Acid	-2.6	0	0.0	0.0
	-1.6	1	5.085	6.488
	-0.6	2	5.798	6.919
2,4-Dimethylcyclopentanol	-4.4	0	0.0	0.0
	-4.3	1	2.412	3.214
	-4.0	2	20.166	20.693
	-4.0	3	2.312	3.464
	-3.9	4	2.02	3.719
	-3.8	5	19.983	20.882
Butylcyclopentane	-4.6	0	0.0	0.0
	-4.3	1	19.003	19.817
	-4.2	2	18.661	19.336
	-4.0	3	19.698	20.288
	-3.8	4	19.342	19.907
	-3.7	5	3.014	5.96
1-Nonadecanol	-3.9	0	0.0	0.0
	-3.8	1	1.06	2.295
	-3.4	2	1.56	3.429
	-33	3	1.652	2.894
	-3.1	4	1.534	3.177
Isocholesteryl Methylether	0.5	0	0.0	0.0
	0.6	1	2.18	3.14
	1.2	2	8.116	6.784
Carbonic Acid	-5.6	0	0.0	0.0
	-5.4	1	1.352	2.202
	-5.3	2	20.765	21.535
	-5.3	3	20.393	21.196
	-5.1	4	19.304	20.16
	-5.1	5	19.741	20.643

	-5.1	6	19.277	20.174
2-Benzothiazolythio	-7.6	0	0.0	0.0
	-7.4	1	1.326	2.985
	-6.6	2	6.94	5.095
	-6.5	3	1.931	4.723
	-5.9	4	1.51	4.939
	-5.5	5	2.162	4.78
1,4-Oxazepine	-6.8	0	0.0	0.0
	-5.9	1	2.21	3.195
1-Methyl-2-Phenyl-1H Indole	-7.2	0	0.0	0.0
	-6.5	1	1.69	5.889
	-6.1	2	17.994	19.074
	-5.4	3	18.78	19.454
	-5.4	4	17.635	18.542

Animal Studies:

The outcome showed that extract has significant anti-inflammatory properties at different concentrations. The IC50 was 85.52 g/ml concentration, and the maximum hemolysis inhibition was 46.770.66 at 80 g/ml concentration. Asprin was used as the reference standard (IC50 = 137.14 g/ml concentration).

TABLE 5: The inhibition results of the extract

CONCENTRATION(µg/ml)	OD at 517nm	% OF INHIBITION
Control	0.17	-
20	0.179	4.92±0.58
40	0.184	7.28±1.03
60	0.195	11.09±2.41
80	0.322	46.77±0.66
100	0.411	58.33±0.46
120	0.698	75.04±0.53

Figure 2: Anti-inflammatory activity of the extract

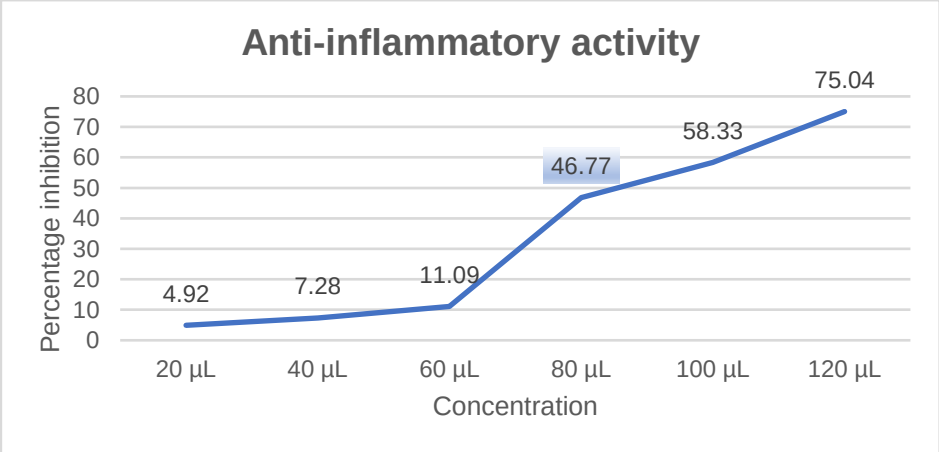

Anti-Bacterial Activity:

The extract was investigated for in vitro antibacterial activity against microorganism including Gram-positive bacteria (Bacillus subtilis, Staphylococcus aureus) and Gram-negative bacteria (*Klebsiella Sp. and Escherichia coli*). The maximum zone of inhibition of combination extract against Bacillus subtilis was 12mm in 500µg/ml and Escherichia coli was 13mm in 500µg/ml.

TABLE 6: Zone of inhibition in Anti-bacterial activity

S.NO	ORGANISM	ZONE OF INHIBITION			
		750 µg	250µg	375µg	500µg
1.	*Klebsiella Sp.*	16mm	10mm	12mm	13mm
2.	*Bacillus subtilis*	14mm	10mm	11mm	12mm
3.	*Escherichia coli*	15mm	10mm	11mm	13mm
4.	*Staphylococcus aureus*	21mm	11mm	13mm	15mm

Product Development:

The extract was treated with activators, buffers and preservatives results in the production of gel -based external use medication.

FIG 3: Gel-based external use product using plant extract

Patch test on skin:

A patch test is a skin test used to find the cause of a possible allergic reaction on the skin. The product applied in the inflamed skin for about one hour results in no allergic reactions.

CONCLUSION:

The active components that give medicinal plants their pharmacological potential are their phytochemicals. The extracts of *Cissus quadrangularis* in water, ethanol, and methanol showed varied patterns of the presence of certain metabolites according to preliminary phytochemical examination. Significant chemical components such flavonoids, alkaloids, coumarins, quinones, glycosides, and phytosteroids, among others, have been identified according to reports. The antioxidant activity appeared to be caused by the phenol and flavonoid components that were measured in the composition of the herbal extract. The extract's total phenol content was 744.2 1.05 g/mg and its total flavonoid content was 152.5 0.22 g/mg. The results of the molecular docking against the CRP shows the binding affinity which results in the potential to eradicate the inflammation. The results of the animal model demonstrated that extract, at various doses, has considerable anti-inflammatory activities. The maximal

hemolysis inhibition was 46.770.66 at an 80 g/ml concentration, while the IC50 was 85.52 g/ml. The reference standard was asprin (IC50 = 137.14 g/ml concentration).

The plant *Cissus quadrangularis* show the potential against inflammation. Thus, the plant can be modified and used as a natural source of medications which can heal the inflammation.

REFERENCES:

Abu Bakar, F. I., Abu Bakar, M. F., Abdullah, N., Endrini, S., & Fatmawati, S. (2020). Optimization of extraction conditions of phytochemical compounds and anti-gout activity of Euphorbia hirta L.(Ara Tanah) using response surface methodology and liquid chromatography-mass spectrometry (LC-MS) Analysis.

Balouiri, M., Sadiki, M., & Ibnsouda, S. K. (2016). Methods for in vitro evaluating antimicrobial activity: A review. *Journal of pharmaceutical analysis*, *6*(2), 71-79.

Du Clos, T. W. (2000). Function of C-reactive protein. *Annals of medicine*, *32*(4), 274-278.

Evans, W. C. (2009). *Trease and Evans' pharmacognosy*. Elsevier Health Sciences

Ganesan, P., & Choi, D. K. (2016). Current application of phytocompound-based nanocosmeceuticals for beauty and skin therapy. *International journal of nanomedicine*, *11*, 1987.

Grada, A., Mervis, J., & Falanga, V. (2018). Research techniques made simple: animal models of wound healing. *Journal of Investigative Dermatology*, *138*(10), 2095-2105.

John De Britto, A., Sebastian, S. R., & Mary Sujin, R. (2011). Phytochemical analysis of eight medicinal plants of Lamiaceae. *Journal of Research in Plant Sciences*, *1*, 001-006.

Kagan, I. A., & Flythe, M. D. (2014). Thin-layer chromatographic (TLC) separations and bioassays of plant extracts to identify antimicrobial compounds. *JoVE (Journal of Visualized Experiments)*, (85), e51411.

Kubo, I., Xiao, P., & Fujita, K. I. (2002). Anti-MRSA activity of alkyl gallates. *Bioorganic & Medicinal Chemistry Letters*, *12*(2), 113-116.

Kumar, T. S., & Jegadeesan, M. (2006). Physico-chemical profile of *Cissus quadrangularis* L. Var-i in different soils. *Ancient science of life*, *26*(1-2), 50.

Liebsch, M., Grune, B., Seiler, A., Butzke, D., Oelgeschläger, M., Pirow, R., ... & Luch, A. (2011). Alternatives to animal testing: current status and future perspectives. *Archives of toxicology*, *85*, 841-858.

Mohanty, C., Das, M., & Sahoo, S. K. (2012). Sustained wound healing activity of curcumin loaded oleic acid based polymeric bandage in a rat model. *Molecular pharmaceutics*, *9*(10), 2801-2811.

Morris, G. M., & Lim-Wilby, M. (2008). Molecular docking. *Molecular modeling of proteins*, 365-382.

Wagner, H., & Ulrich-Merzenich, G. (2009). Synergy research: approaching a new generation of phytopharmaceuticals. *Phytomedicine*, *16*(2-3), 97-110.

PHARMACOGNOSTIC ASSESSMENT OF SILVER NANOPARTICLES FROM ENDOPHYTIC BACTERIA

Hemachandran, M., Malini, R* ., Geethika, M and A. Aruna

Department of Biotechnology, Madha Engineering College, Chennai- 69
**Dept. of Microbiology, Thassim Beevi Abdul Kader College for Women, Kilakarai-623517*

ABSTRACT

The field of nanotechnology is the most promising area of the research, Plant leaves are potential hosts to a plethora of beneficial microorganism like endophytic bacteria. Endophytic bacteria live symbiotically with the plant and in turn helping the plants in number of ways. The present assessment were undertaken to isolate and identify bacterial endophytes in leaf tissues of *Moringa oleifera* plants growing at India also in Asia, Africa ,south America .A total of two endophytic bacteria were isolate from the parts of the plant. On the basis of the morphological and biochemical characterization of the endophytes they are identified as staphylococcus species. Endophytic based silver nanoparticles were found to possess significant antioxidant (DPPH and Phosphomolybdenum) and antidiabetic activity (alpha amylase assay).

Keywords: Moringa oleifera, Endophytic bacteria, nano particles, Phosphomolybdenum, DPPH, alpha amylase activity.

INTRODUCTION

Moringaoleifera, the most widely found species of the Moringaceae family thrives in tropical. Insular climate and is found in abundance nears rivers. The tree ranges from 5- 10 m in height. (Anwar et al., 2007). It can withstand humid and dry lands, deprived soils and tolerate a wide. Range of rainfall (Morton, 1991). Many parts of the Moringa tree are edible and numerous nutritional and medicinal properties have been attributed to its roots, bark, leaves, flowers, fruits, and seeds (Mbikay, 2012). Phytochemical analyses have revealed that Moringa leaves are a rich source of potassium, calcium, phosphorous, iron, vitamins A and D and essential amino acid (Gowrishankar et al., 2010). Antioxidants and flavonoids have also been reported from other parts of the plant such as seeds and fruits (Anjorin et al., 2010).Traditionally Moringa isalso known as Drumstick in countries like India and Nigeria where it is cultivated as a crop. Its pods are cooked and eaten whereas the leaves can be cooked or stored as dried powder both of which are a rich source of proteins (Mbikay, 2012). The leaf extracts of Moringa contain antioxidant properties and inhibit the peroxidation of linoleic acid. Extracts of leaves were also shown to prevent the bleaching of carotene and scavenge radicals in the DPPH radical scavenging assay (Sindhuraju & Becker, 2003). *Moringaoleifera* is a plant that is often called the drumstick tree, themiracle tree, the

ben oil tree, or the horseradish tree. Moringa has been used for centuries due to its medicinal properties and health benefits. It also has antifungal, antiviral, antidepressant, and anti-inflammatory properties. Itcontains a variety of proteins vitamins and minerals. Moringa contains many healthful compounds such as Vitamin A, VitaminB1, VitaminB2, VitaminB3,VitaminB6and ascorbic acid, calcium, potassium, and magnesium Phosphorus zinc. Moringa is also extremely low in fat and contains no harmful cholesterol. The tree is native to India but also grows in Asia, Africa and South American. Protecting on nourishing skin and hair treating edema, protecting the liver, preventing and treating cancer, treating stomach complaint, fighting against bacterial disease, making bones healthy, treating mood disorders, protecting the cardiovascular system, helping wounds to heal, treating diabetes, treating asthma, protecting against Kidney disorder, Reducing high blood pressure, Treatinganemia and sickle cell disease. Moringa (*Moringaoleifera* Lam.) is a multipurpose tropical tree. It is mainly used for food and has numerous industrial, medicinal and agricultural uses, including animal feeding. Nutritious, fast-growing and drought-tolerant, this traditional plant was rediscovered in the 1990s and its cultivation has since become increasingly popular in Asia and Africa, where it is among the most economically valuable crops. It has been dubbed the "miracle tree" or "tree of life" by the media (FAO, 2014; Radovich, 2009; Orwa et al., 2009; Bosch, 2004). Plant inner tissues are colonized by bacterial organisms known as endophytes. The relatively recent application of culture independent and molecular high throughput techniques allowed the description of a large diversity of endophyticbacterial taxa. These microorganisms can be found in any plant organ, including fruits and legume nodules. Nanotechnology as the manipulation of matter with at least one dimension sized from 1 to 100 nanometers. Two main approaches are used in nanotechnology. Inthe "bottom-up" approach, materials and devices are built from molecular components which assemble themselves chemically by principles of molecular recognition. In the "top-down" approach, nano-objects are constructed from larger entities without atomic-level control**.** Nanoparticles (also known as ultrafine particles 225) are defined as having one structural dimension of less than 100nm making them comparable in size to subcellular structures, including cell organelles or biological macromolecules, thereby enabling their ready incorporation into biological systems.

MATERIALS AND METHODS:

Glass were soaked in cleaning solution and washed thoroughly withrunning tap water. They were then cleaned with detergent solution and rinsed several times with tap water and finally in distilled water and air dried. The glassware and media were sterilized in autoclave at 15psi for 20 minutes, at120˚c. *Moringo oleifera* leaf samples were collected from healthy trees. Collectedleaves were covered with paper and were placed in dry and clean plastic bags. Debris were removed from the leaf samples by rinsing with tap water, afterwards, all explants were surface sterilized by washing with combination of distilled water and 70%ethanol.The surface sterilized explants were then transferred to plates contain nutrient agar (NA).Four explants were transferred to each plate with a total of two plates per sampled tree. All plates were incubated at 30 c for up to 1week, and were observed for bacterial growth every two days. Emerging mycelia from the end of explants were subculture in freshly prepared agar

(NA) plates to obtain pure cultures. Stock cultures were maintained in nutrient broth (NB) and stored at 30 degree Celsius A 10ml of culture filtrates were mixed with 45ml of 5mM aqueous silver nitrate (AgNo3) in 250ml flask and incubate at 30 c for 2 weeks. Positive synthesis of silver nanoparticles were determined based on the color change to dark brown. The expansion of nanotechnology in various research areas has led to the need to use analytical techniques for the analysis and characterization of nanoparticles. Several characterization techniques are available, including microscopic, separation and spectroscopic techniques. Nanoparticles are usually characterized in the literature by their size distribution, morphology, surface properties, stability and interactions. The main characterization techniques of nanoparticles in general and AgNP in particular Gram staining was carried out by following standard staining procedures and techniques the microscope examination was performed with the oil immersion objective of the bright field microscope Catalase is the enzyme that breaks hydrogen peroxide (H_2O_2) into H_2O and O_2. Hydrogen Peroxide is often used as a topical disinfectant in wounds, and the bubbling that is seen is due to the evolution of O_2 gas. H_2O_2 is a potent oxidizing agent that can wreak havoc in a cell; because Of this, any cell thatuses O_2 or can live in the presence of O_2 must have a way to get rid of the Peroxide. Catalase activity of the isolates was estimates by using H_2O_2 solution onto the microscopic slides containing the culture of the isolates separately observations were taken for immediate bubble formation CO_2 water bubbles Release of O_2 Bubbles indicate positive catalase activity. Basically, this is a test to see if an organism is an aerobe. It is a check for the presence of the electron transport chain that is the final phase of aerobic respiration. Normally, oxygen is the final electron acceptor for this system. In the oxidase test, an artificial final electron acceptor (N,N,N‟,N‟-tetramethylphenylenediaminedihydrochloride) is used in the place of oxygen. This acceptor is a chemical that changes color to a dark blue/purple when ittakes the electron from the last element (cytochrome oxidase) in the electron transport chain. The oxidase tests used to identify bacteria that produce cytochrome oxidase an enzyme of the bacterial electron transport chain when present the cytochrome oxidase oxidizes the reagent tetramethyl-p phenylenediamine to (indophenols) purple colour in product when the enzyme is not present in the reagent reminds reduced and is colourless.

Phytochemical analysis: Test for Carbohydrates, Tannins, Saponins, Flavonoids, Alkaloids, Quinones, Glycosides, Cardiac glycosides, Terpenoids, Phenols, Coumarins, Steroids, hloba tannins, Anthraquinone were analyzed. A total antioxidant activity of methanol and aqueous extract were determined according to the method. The sample was readed with the stable DPPH radical in a methanol solution, the reaction mixture consisted of different concentration of each sample and add 2ml of DPPH solution (0.4 mM) when DPPH reacts with an antioxidant compound which can donate hydrogen, it is reduced, the reaction mixture was incubated at 20 minutes in dark condition the changes in colour (from deep violet to light yellow), were read absorbance at 517 nm using UV- VIS spectrophotometer. The methanol serves as blank. The scavenging activity percentage (AA %) was determined according to the formula. % inhibition = [Control- Sample] ×100 Control The total antioxidant capacity of the methanol, aqueous extracts was according to the Phosphomolybdenum method different concentration of each sample and add 1ml of phosphor molybdenum (0.049g ammonium

molybdenum, sodium phosphate(0.036g), and Sulphuric acid(588ul) reaction mixture was incubated in water bath at 90˚C for 90 minutes. After the samples were cooled to room temperature, the absorbance of methanol and aqueous solution of each sample was measured at 695 nm using UV spectrophotometer. The methanol serves as blank. The higher absorbance value indicated higher antioxidant activity. % inhibition = [sample – control] × 100.

The alpha-Amylase inhibitory activities of the given plant samples were carried out according to the method reported by Nickavar*et al*. (2009). The starch solution (0.5% w/v) used as the substrate was prepared by boiling potato starch in distilled water for 15 min. The enzyme solution was prepared by dissolving 1 mg of porcine pancreatic α - amylasein 20 mM phosphate buffer (100 mL, pH 6.9).The sample solutions were prepared in DMSO (dimethyl sulfoxide) in different concentrations (10 to 100 mg/mL).The DNS solution (20 mL 96 mM 3,5-dinitrosalicylicacid, 12 g sodium potassium tartrate in 8 mL of 2 M NaOH and 12 mL deionized water) was used as the coloring reagent of reaction. Three sets of experiments were conducted: test, blank and control. A mixture of 1mL of each of the test and enzyme solutions, in a test tube, was incubated at 25°C for 30 min. Then, after taking out 1 mL from this mixture, 1 mL of the above mentioned starch solution was added and the mixture was incubated at 25°C for 3 min. Finally, 1 mL of the DNS solution was added. The tube was then covered and heated in water bath at 85ºC for 15 min. After coolingthe tube, the reaction mixture was diluted with distilled water (9 mL). It was mixed well and the absorbance was recorded at 540nm. In case of blank, the DNS solution was added prior tothe addition of the starch solution, while rest of the method was same as for the test. For control, all procedure was again the same except that plant extract was replaced by 1 mL of DMSO. Acarbose, a well-known anti-diabetic medicine, was used as a positive control. The percentage inhibition was calculated by the formula: %Inhibition = [(Ac – As) /Ac] × 100

RESULTS AND DISCUSSION

The presence of phytochemicals in *Moringo oleifera* was checked and theresults were provided in the **table 5.1.1.** The preliminary phytochemical test werehelpful in finding out the biochemical constituents present in the plant material. The extracts of *Moringooleifera* when test with different solvents showed positive results for important phytochemicals such as carbohydrates, alkaloids, glycosides, cardiacglycosides, terpenoids, steroids.

Phytochemical analysis:

S. No	Phytochemical constituents	Results
1.	Carbohydrates	Positive
2.	Tannins	Negative
3.	Saponins	Negative
4.	Flavonoids	Negative
5.	Alkaloids	Positive
6.	Quinones	Negative
7.	Glycosides	Positive
8.	Cardiac glycosides	Positive
9.	Terpenoids	Positive
10.	Triterpenoids	Negative
11.	Phenols	Negative
12.	Coumarins	Negative
13.	Steroids	Positive
14.	Phlobatannins	Negative

Isolation of bacterial endophytes: The isolated endophytic bacteria were identified as *Staphylococcus aureus* based on microbial observation colony growth, morphological characteristics was identified shown in the figure. Staphylococcus species were used in the synthesis of silver nanoparticles.

Mixed culture of endophytes

Pure isolation of bacterial endophytes

Identification of bacterial endophytes

The clear zone of haemolysis –beta haemolytic shows that staphylococcus aureus because hemolysin is one of the important virulence factors for staphylococcus aureus and causes the typical beta haemolytic phenotype which is called complete haemolytic phenotype as well.

Table Identification of bacteria

S. No.	Test	Results
1.	Gram Staining	Gram positive – cocci
2.	Blood agar	Clear zone of haemolysis-beta haemolytic
3.	Catalase	Positive
4.	Oxidase	Negative
5.	Nutrient agar	Golden yellow colonies

Green synthesis of endophytic bacteria:

Silver ions were reduced to silver nanoparticles when added endophytic extractsand it as observed that the color of the mixed solution turned from white solution to dark brown which indicated the formation of silver nanoparticles dueto surface plasmon resonance after 24 h of incubation (fig 5.4). The formation and stability of silver nanoparticles in the solution are confirmed by UV-Visspectrophotometer studies.

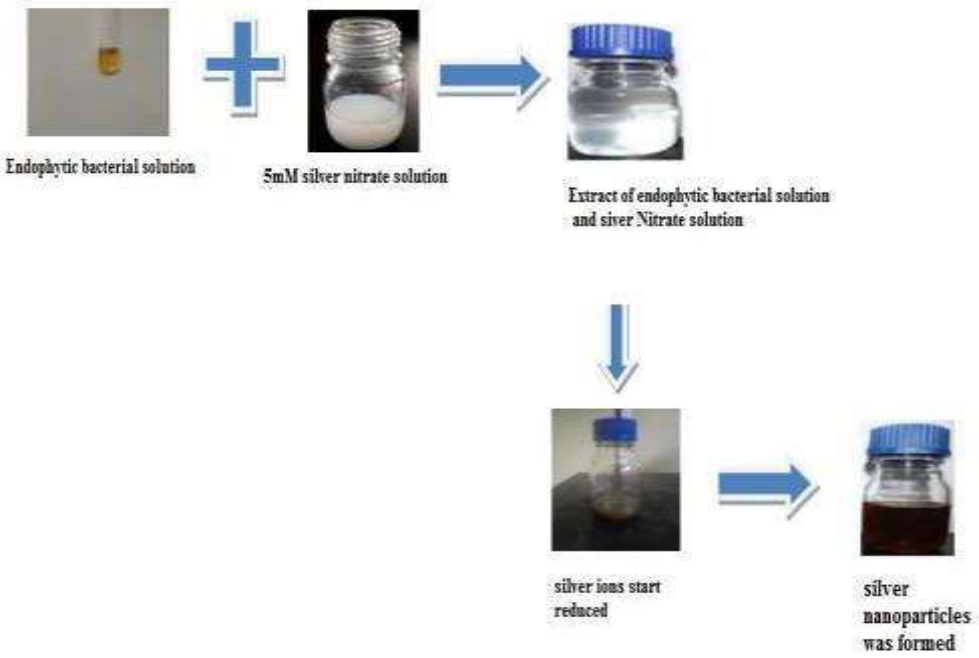

Fig 5.4 shows the schematic representation of the silver Nano particles

UV-Vis Spectrophotometer: The formation and stability of silver nanoparticles in the solution are confirmedby uv-vis spectrophotometer studies shown in fig (5.5).

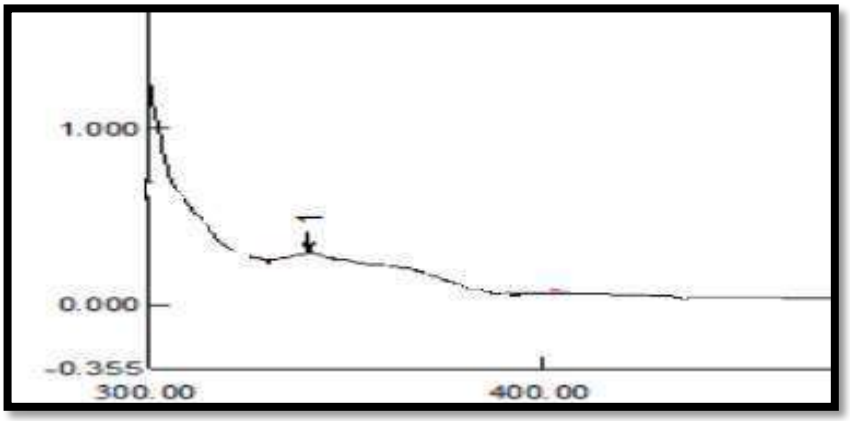

Figure 5.5 UV –visible spectrum of a silver nanoparticles solution is shown.

The absorbance of the visible or ultraviolet light is presented in a calibrationgraph,this is measured by many standard solutions . This absorbance of lightmeasurement of an unknown solutions indicates us to determine its concentration by reading off the graph.

Antioxidant activity

DPPH assay

The antioxidant of the methanol and aqueous endophytic bacterial extractwas measured on the basis of the scavenging activity of the stable DPPH free radical. It shows active site of antioxidant in methanol extract by increasing of inhibition by increasing of concentration and the result was shown in the figure 5.6 (a), (b), (c).

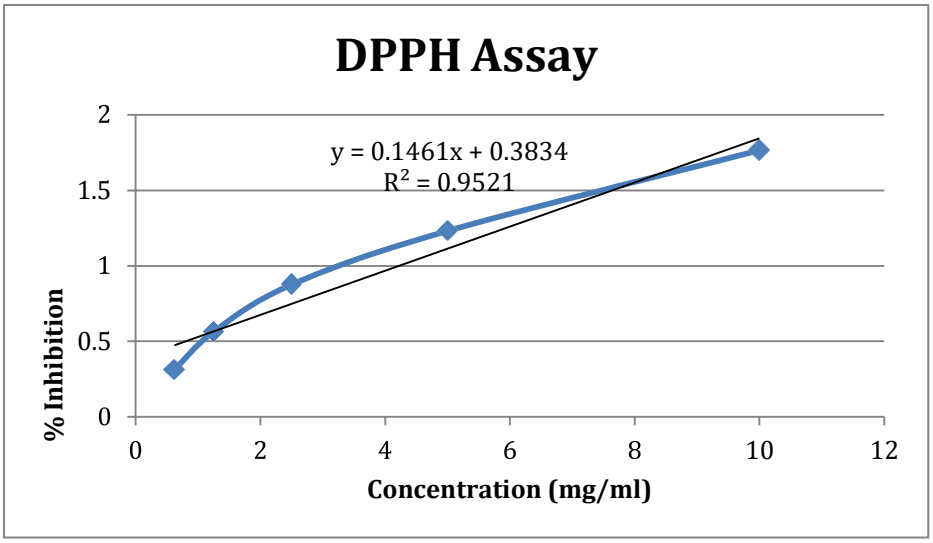

Figure 1.6.1 antioxidant activity by DPPH

Table 1.2.1(a)

Concentration (mg/ml)	Mean OD
10	1.765
5	1.231
2.5	0.876
1.25	0.564
0.62	0.312

Table 1.2.2 (b)

Concentration (mg/ml)	Mean OD	% Inhibition
5	0.039	86.46
2.5	0.100	65.28
1.25	0.106	63.19
0.62	0.193	32.99
0.31	0.203	29.51
Control	0.288	0.00

The active site of antioxidant in methanol extract by increasing of inhibition by increasing of concentration was determined by silver nanoparticle wasdetermined

Antioxidant activity by phosphomolybdenum Assay:

Preliminary test of antioxidant using phosphomolybdenum assay shows presence of scavenging activities in sample shown in the fig 5.5**,**Alpha amylase inhibitory assay.

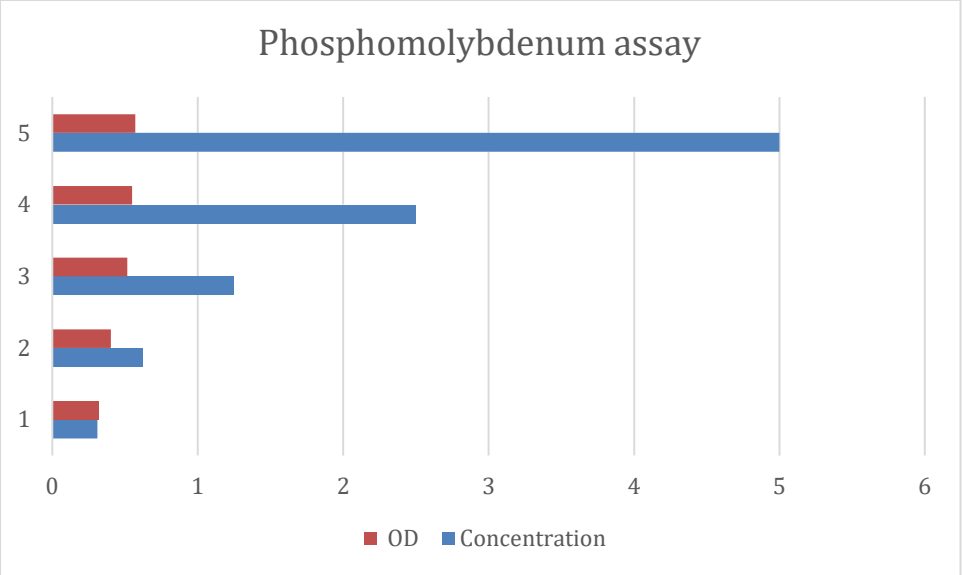

Anti diabetic activity: Alpha amylase inhibitory assay: Result:

Table 1.3

CONCENTRATION (mg/ml)	(OD)	% Inhibition
5	0.318	62.188
2.5	0.403	52.081
1.25	0.515	38.763
0.62	0.547	34.958
0.31	0.57	32.224
Control	0.841	

Table 1.4

Metformin Standard Concentration (µg/ml)	(OD)	% Inhibition
10	0.978	12.13
20	0.864	22.37
40	0.558	49.87
80	0.441	60.38
100	0.253	77.27
Control	1.113	

Figure 1.7.1 showing alpha amylase inhibitory activity by metformin stdconc.

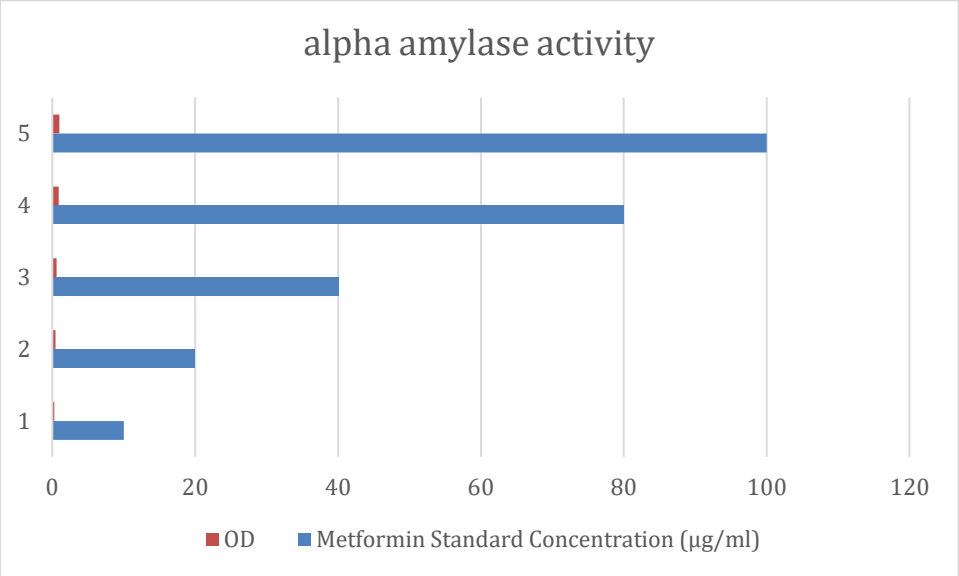

TABLE 1.4 (b)

Nanoparticle Concentration (µg/ml)	(OD)	% Inhibition
10	0.995	10.60
20	0.812	27.04
40	0.703	36.84
80	0.523	53.01
100	0.425	61.81
Control	1.113	

Figure 1.7.2 showing alpha amylase inhibitory activity by nanoparticleconcentration.

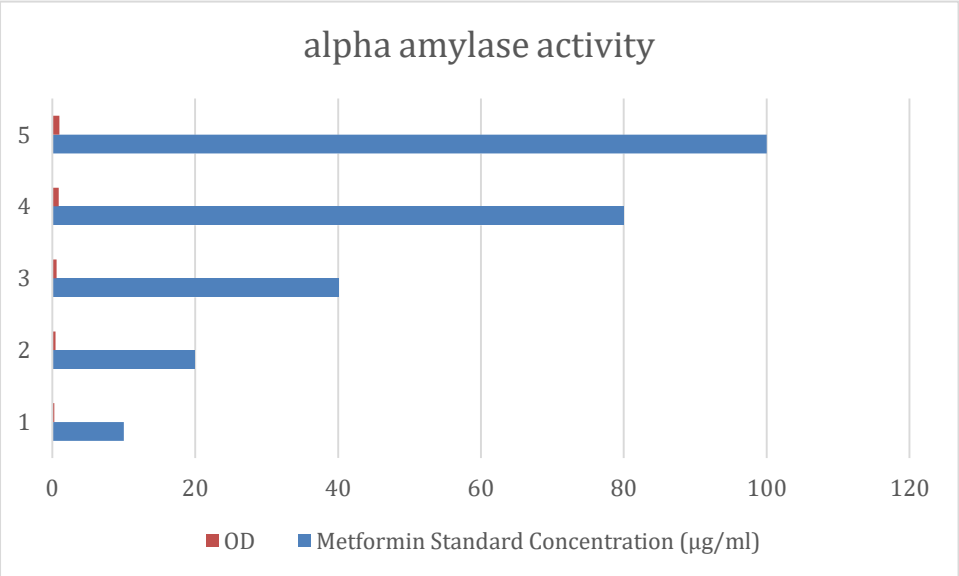

DISCUSSION

Silver ions were reduced to silver nanoparticles when added endophytic extracts and its antioxidant properties was checked and it showing the best response when compare to the other method. The silver Nanomaterial‟s prepared by the green synthesis a good physical and chemical property. The biological method of silver nanomaterial's will paved a new pathway for the preparation of nanomaterial and its importance in material science was understood from the study.

CONCLUSION

A critical need in the field of nanotechnology is the development of reliable and eco-friendly processes for synthesis of silver nanoparticles .Here, we have reported a simple biological and low – cost approach for preparation of stable silver nanoparticles using *Moringooleifera***.**

REFERENCES

Anna Zielinska, EwaSkwarek, Adriana Zaleska, Maria Gazda, Jan Hupka, (2009) Preparation of silver nanoparticles with controlled particle size‟,ProcediaChemistry 1: 1560–1566.

Ajitha.B, Y.A.K. Reddy, P.S. Reddy, Green synthesis and characterization of silver nanoparticles using Lantana camara leaf extract, Mater. Sci. Eng. C 49 (2015) 373–381.

Banerjee M, Mallick S, Paul A, Chattopadhyay A, Ghosh SS.(2010) „Heightened Reactive Oxygen Species Generation in the Antimicrobial Activity of aThree Component Iodinated Chitosan-Silver Nanoparticle Composite, Langmuir 26: 5901–5908.

Bard AJ, Holt KB. Interaction of Silver (I) (2005) Ions with the Respiratory Chain of *Escherichia coli*: An Electrochemical and Scanning Electrochemical Microscopy Study of the Antimicrobial Mechanism of Micromolar Ag+ Biochemistry; 44:13214-13223.

Chaloupka K, Y. Malam, A.M. Seifalian, Nanosilver as a new generation of nanoproduct in biomedical applications, Trends Biotechnol. 28 (11) (2010) 580–588.

Chou, K. and Ren, C. (2000) „Synthesis of nanosized silver particles by chemical reduction method‟, Mater. Chem. Phys. 64, 241.

Deng, Z., Chen, M., Wu, L., 2007. J. Phys. Chem. C 111,Dibrov P, Dzioba J, Gosink KK, Hase CC. (2002) Chemiosmotic mechanism of antimicrobial activity of Ag+ in Vibrio cholerae, Antimicrob. Agents Chemother; 46: 2668-2670.

Duran, N., Marcarto, P., De Souza, G., Alves, O., Esposito, E., 2007. J Biomed Nanotechnol 3, 203.

El-Sayed, M., 2001. Acc. Chem. Res. 34, 257

Feng QL, Wu J, Chen GQ, Cui FZ, Kim TN, Kim JO(2000) „A mechanistic study of the antibacterial effect of silver ions on *Escherichia coli* and *Staphylococcus aureus*‟ J Biomed Mater Res.;52:662-668.

Guo, J., Cui, H., Zhou, W., Wang, W., 2008. J. Photochem. Photobiol. A: Chem. 193,89.

Hahm, J., Lieber, C., 2004. Nano Lett. 4, 51.

Hoonacker, A.V., Englebienne, P., (2006) „Revisiting silver nanoparticle chemicalsynthesis and stability by optical spectroscopy‟, Current Nanoscience 2, 359.

Hu, A. W., & Fu, Z. H. (2003). Nano technology and its application in packaging and packaging

machinery. Packaging Engineering, 24, 22–24.

Jia, X., Ma, X., Wei, D., Dong, J., Qian, W., 2008. Colloids Surf. A: Physicochem. Eng. Aspects 330, 234.

Jung WK, Koo HC, Kim KW, Shin S, Kim SH, Park YH. (2008) „Antibacterial activity and mechanism of action of the silver ion *in Staphylococcus aureus* and *Escherichia coli*", Appl. Environ. Microbiol; 74:2171-2178.

Kheybari S., Samadi N., Hosseini S.V., Fazeli A., Fazeli M.R. (2010) „Synthesis and antimicrobial effects of silver nanoparticles produced by chemical reduction method",DARU Vol. 18, No. 3 pp168-172.

Kim JS, Kuk E, Yu KN, Kim JH, Park SJ, Lee HJ, Kim SH, Park YK, Park YH, Hwang CY, Kim YK, Lee YS, Jeong DH, Cho MH. (2007) „Antimicrobial effects of silver nanoparticles", Nanomedicine.;3:95–101.

Ko¨hler, J., Abahmane, L., Albert, J., Mayer, G., 2008. Chem. Eng. Sci. 63, 5048.

Kurihara, L.K., Chow, G.M. and Schoen, P.E., (1995) „Nanocrystalline metallicpowders and films produced by the polyol method". Nanostructure Materials. 5, 607.

Lakshmi S. Nair and Cato T. Laurencin (2007) Silver Nanoparticles: Synthesis and Therapeutic Applications", Journal of Biomedical Nanotechnology Vol.3, 301–316.

Nanda A, Saravanan M. (2009) „Biosynthesis of silver nanoparticles from *Staphylococcus aureus* and its antimicrobial activity against MRSA and MRSE", Nanomedicine.5:452-456.

Pastoriza-Santos, I. and Liz-Marzan, L.M., (2000) „Reduction of silver nanoparticles in DMF.Formationof monolayers and stable colloids", Pure Appl. Chem. 72-83

Pileni, M.P., Maillard, M. and Giorgio, S. (2003) „Tuning the Size of Silver Nanodisks with Similar Aspect Ratios: Synthesis and Optical Properties" *J. Phys. Chem. B* , 107, 11, 2466–2470

Prasad KS, D. Pathak, A. Patel, P. Dalwadi, R. Prasad, P. Patel, K. Selvaraj, Biogenic synthesis of silver nanoparticles using Nicotianatobaccum leaf extract and study of their antibacterial effect, Afr. J. Biotechnol. 10 (41) (2011) 8122.

Rai M, Yadav A, Gade A. (2009) Silver nanoparticles as a new generation of antimicrobials, Biotechnol Adv; 27:76–83.

Rao, P., Chandraprasad, M.S., Lakshmi, Y.N., Rao, J., Aishwarya, P. and Shetty, S. (2014) Biosynthesis of Silver Nanoparticles Using Lemon Extract and Its Antibacterial Activity, International Journal of Multidisciplinary and Current Research,2, 165-169.

Raveendran, P., Fu, J., and Wallen, S.L. (2003) Completely "Green" synthesis and stabilization of metal nanoparticles", J. Am. Chem. Soc. 125, 1940.

Shrivastava S, Bera T, Roy A, Singh G, Ramachandrarao P, Dash D.(2007) Characterization of enhanced antibacterial effects of novel silver nanoparticles", Nanotechnology. 18:1–9.

Sun Y. and Xia, Y., (2002) „Shape-controlled synthesis of gold and silver nanoparticles", Science 298, 2176.

Thakkar K.N., S.S. Mhatre, R.Y. Parikh, Biological synthesis of metallic nanoparticles, Nanomedicine 6 (2) (2010).

Velikov K. P, Zegers G. E. and van Blaaderen, A. (2003) Synthesis and characterization of large colloidal silver particles, Langmuir 19, 1384.

Wang, J., Wen, L., Wang, Z., Chen, J., 2006. Mater. Chem. Phys. 96, 90.

Yeo, S., Lee, H., Jeong, S., 2003. J. Mater. Sci. 38, 2143.
Zhong, L., Hu, J., Cui, Z., Wan, L., Song, W., 2007. Chem. Mater. 19.

FORMULATION AND CHARACTERIZATION OF BIO FERTILIZER PREPARED FROM FISH WASTE

Lighty George[1]., Arunthathi, K[2] and P. Dhasarathan[3]*

Department of Zoology, Sarah Tucker College (Autonomous), Tirunelveli - 627 007.
[2]Dept. of Microbiology, Thassim Beevi Abdul Kader College for Women, Kilakarai-623517
[3]Dept. of Biotechnology, Madha Engineering College, Kundrathur, Chennai- 69*

ABSTRACT

The bio-stimulant root system has enabled the crop to have a rapid and balanced nutritional intake, since the presence of polysaccharides, phosphorus and other essential trace elements in combination with amino acids allowed to have a well-developed root system, increase the size and length of the primary and secondary roots, stimulate the physiological functions of plants during periods of high activity. In addition, the effect of application of the bio-stimulant on the root part made it possible to detect a development and a growth of the root biomass in comparison with the control maize which was not treated with this bio-stimulant.

The effective utilization of biofertilizer from the fish processing waste would not only provide economic benefits to the farmers but also improve and maintain soil fertility and sustainability in natural ecosystem. The biofertilizer which we prepared by using fish waste was tested in our gardens by spraying it to the plants. The results we got were excellent. The biofertilizer acts as a good manure, it is purely organic .The yield is doubled after using this bio fertilizer. The biofertilizer not only acts as an excellent manure for plants, but also it is a good biopesticide. It is noted that, the land containing the plants is spoiled with some pests but after spraying the biofertilizer for the second time to the plants there were no pests at all. From the biofertilizer various physico chemical parameters and biochemical analysis were tested. From the results obtained, we conclude that the biofertilizer prepared by using fish waste is a pure organic manure. At the same time it is harmless to all the organisms, pollution free and safe to use in our environment.

Keywords: Biofertilizer, Fish waste, Biochemical analysis, plant growth, germination

INTRODUCTION

Fish waste biomasses are locally available resources which contain nutrients. Fermentation of the biomass produces slurries used for plankton production. Bio-refinery of fish waste material can be converted into value added biological products such as biofuels, industrial chemicals, animal and fish feed, human food, neutraceuticals and organic fertilizer, etc. Fish hydrolysate generally shows a beneficial effect on growth performances an feed utilization at low inclusion levels. The performance is postulated to be due to the balance of free amino acids, peptides and proteins in digestion, absorption and utilization. Fish processing industry and fish markets produce more than 60% by-products as waste, which includes skin,

heart, viscera, trimmings, liver, frames, bones and roes. These by-products contain good amount of protein rich nutrient material.

The fish waste contain nutrients and all the essential cofactor for the growth of plants and comparing with the chemical fertilizer and organic fertilizer. Biofertilizer are very popular amoung the farmer to produce quality product. These are eco-friendly and the cheapest source of nutrients. Recently, some studies have examined the reutilization of biodegrade fisheries waste product as liquid fertilizer (Kim and Lee, 2009: Kim *et al*.,2010:Dao and Kim, 2011)

Biofertilizers or biostimulants for the plant are substances and materials which when applied to plants, seeds or growth substrates in a specific formulation have the ability to alter the physiological processes of plants in order to provide potential growth benefits, development and / or stress response. Fish processing generates considerable quantities of solid waste in the form of head and body carapace. These body parts comprise 48-56% depending on the species (Sachindra *et.al*., 2005). Jaggery or molasses are cheap source of sucrose and sucrose is reported to be an ideal carbohydrate source for lactic acid bacterial fermentation (Cira *et al*., 2002). This technique and material should be used to economically present shrimp waste and made into fertilizer and feed for aquaculture and agriculture uses. Sugarcane molasses/Jaggery was provided by local grocery market. Tilapia wastes were chopped with a mineer and sugarcane molasses were added to have a mixture ratio of fish waste: molasses of 50:50(w/w). Although, the analyses of these fish by-products showed a high load of pathogenic microorganisms, they also showed a wealth of organic material including proteins and minerals. These components and others are capitalizing to be used for agricultural or agro-food, hence the need for the establishment of an industrial process of their treatments and their valuations. That's why our laboratory, has made a biotechnological method based on the use of a fermentation leaven and carbon-rich source of carbohydrates, A hydrolyzate rich in amino acids and trace elements was obtained with excellent hygienic quality. It will be used as a fertilizer and soil improver. Its use will be as factors for fertilizer and soil amendment. We produced two biostimulants necessary for plant growth: Rooting- development, elongation-production.

A hydrolyzate rich in amino acids and trace elements was obtained with excellent hygienic quality. Numerous long-term experiments carried out in the last decade of the twentieth century showed that national management of mineral fertilizers and organic amendments made it possible to increase crop yields and to sustain soil fertility sustainably. (Bado *et al.*, 1997; Bationo and Makwuney, 1999; Berger *et al.*, 1987;Pichotétal.1981; Piéri, 1989; Sédogo, 1981, 1993). Bio-refinery of fish waste material can be converted into value added biological products such as biofuels, industrial chemicals, animal and fish feed, human food, neutraceuticals and organic fertilizer, etc. Fish processing waste could be regarded as a promising renewable biomass resource for biorefineries.

MATERIALS AND METHODS

Collection of fish waste: 4kg of fish wastes were collected from various fish markets at Tirunelveli.They were split into half kg and filled in 8 plastic bottles.

Collection of sugar: Two types of sugars were collected. Jaggerry (2kg) and Udankudi Jaggerry (2kg).2kg of Jaggerry were split into half kg and filled in 4 plastic bottles.2 kg of Udankudi Jaggerry were split into half kg and filled in another 4 plastic bottles.

Mixing and incubation: Both the fish waste and jaggery were mixed in equal proportions and filled in 4 plastic bottles.Similarly the fish waste and udankudi jaggery were also mixed in equal proportions and filled in 4 plastic bottles.The 8 bottles were kept undisturbed for about 50 days.

Analysis time periods: In 30 days 2 bottles were opened one from jaggery and one from udankudi jaggery. The colour and odour were noted. In 40 days another 2 bottles were opened and the colour and odour were noted. In 50 days another 2 bottles were opened and the colour and odour were noted. As the days goes on colour of mixture becomes darker. Similarly the odour of the mixture becomes lesser.

Biochemical analysis: For biochemical analysis the fish waste sample were collected from local markets. Catalase test, Indole test, Oxidase test, Urea test, Gelatin test, **Nitrate reduction test**, **Starch test**, **Yoges proskauer** were performed.

Growth in nutrient agar: Nutrient agar is used as a general purpose medium for the growth of a wide variety of non- fastidious microorganisms.

NPK analysis: The nutrients that are required by crops in the largest amounts are N,P and K. For that reason they are often considered as the most important nutrients. The important nutrient available in the organic fertilizer are nitrogen (N), phosphorous (P) and potassium (K),micro and macro elements which are important for plant and animal growth.

Nitrogen analysis: Nitrogen is a necessary component which is used for the growth of the plant. Plants need a limited amount of nitrogen for their growth. Some crops need more nitrogen for their growth. In recent years biofertilizer have emerged as a promising component of integrating nutrient supply system in agriculture.(Mishra and Dadhich, 2010). For soils that are nitrogen deficient, treat, manure,wheats, grass clippings, and other garden waste with CBPA and add the resulting compost to the soil. This will result in a simultaneous improvement in humus and nitrogen content. During processing, the total Kjeldahl nitrogen content marks stabilization for M1 composition. Unlike other tests, such rates increased during the 15 days of biotransformation.

Phosphorus analysis: A natural phosphate rock product can be the best sourse of phosphorus. Phosphate rock is most effective when applied in combination with manure. Treat the manure with CBPA and work into the soil. A richer formula in fish waste and molasses allows phosphorus rates to be improved.

Potassium analysis: Among the three, potassium is the third important macronutrient element of plant nutrient that plays a significant role in the activation of several metabolic processes, including photosynthesis, protein synthesis and ezymes as well as in resistance to diseases, insects, etc (Rehm and Schmitt 2002) potassium though is present as an abundant element in the soil are is applied to filled as natural are synthetic fertilizers, only 1-2% of this available to plants, the rest being bound to other minerals and therefore unavailable to plants. Soil

microorganisms influence the availability of soil minerals, playing a central role in ion cycling and soil fertility (Lian *et al.* 2008)

Chromatography analysis: High performance liquid chromatography is a specific form of column chromatography generaly used in biochemistry and analysis to separated, identify, quantity the active compounds.

Total ion chromatogram (tic): A TIC (Total Ion Chromatogram) is a chromatogram created by summing up intensities of all mass spectral peaks belonging to the same scan. The TIC is compared to a GC chromatogram. Note that the TIC includes background noise as well as sample components.

Isolation of 27kDa protein from fertilizer: The nitrogen in CAN is made by the slow ammonium nitrogen and the fast nitrate nitrogen at equal ratio, therefore it can be applied for both top dressing and basic fertilization for any kind of soil types and vegetation.

The dolomite content with the nitrogen reduces the source of soil. So it is specifically recommended for treating sour soils, calcium (magnesium)improves the soil structure, as its clay/humin complexes make it crumbly (water, heat, and air retaining capacity of the soil will be better due to porosity), and increases its fertility. It increases the absorption and utilization of other nutrient through improving the ion balance.

Treatment: concentration exposure germination and growth: To evaluate the phytotoxicity of the mixture culture (which is based on fish waste) a seed germination test was carried out according to Kyun Kim (2010) . For tests of seed germination and root length, 10 ml of filtrate was pipetted into a sterile Petri dish lined with Whatman filter paper. Seed germination and root length in each plate were measured. It is very important to improve the utilization of fertilizer nutrients, since the growth of plants and their quality are mainly a function of the quantity of fertilizer.

Germination: To evaluate the phytotoxicity of the mixture culture, a seed germination test was carried out according to Kyun Kim (2010).For tests of seed germination, 5 ml of filtrate was pipetted into a sterile petri dish lined with Whatman filter paper.

Plant growth: Plant growth promoting bacteria reduce susceptibility to diseases caused by plant pathogens, and improve tolerance of stress conditions such as drought, salinity and nutrient deficiency.

RESULT AND DISCUSSION:

The sugars were made into small pieces and mixed with fish waste.The fish waste along with the sugars were mixed in equal proportions and kept in anaerobic condition for about 50-60 days.Then the fish waste with two types of sugars were converted into biofertilizer.

Odour At Different Time Intervals: As the time goes on, the odour of biofertilizer gets lessened. First interval: At 30 days the odour of bio fertilizer is heavier. Second interval: At 40 days the odour of biofertilizer becomes lesser. Third interval: At 50 days there is no odour. AND Physico Chemical analysis of Jaggery were interpreted in Table.1. Figure .1 represents the diagrammatic representation of Table.1.

Physical Nature of Compost At Different Time Intervals: As the time passes on, the physical structure changes. First interval: At 30 days the appearanc of biofertilizer is light in

colour. Second interval: At 40 days the appearance of biofertilizer becomes thick in colour. Third interval: At 50 days the appearance of biofertilizer thick brown in colour.

Fish waste is a potentially valuable resource from which high value protein can be obtained. Anaerobic digestion of the original fish waste and the fish sludge remaining after enzymatic pre treatment to extract fish oil and fish protein hydrolysate was evaluated regarding the potential for methane production. Physico Chemical analysis of Udankudi Jaggery were interpreted in Table.2. Figure.2 represents the Diagrammatic representation of Table.2.

Table-1 Physico Chemical Parameters of Jaggery

EXPRIMENTAL VALUE	Initial	30 days	40 days	50 days
pH	8.77	3.41	3.82	3.92
Acidity	0	0.57	0.32	0.21
Colour at 430nm in EBC	4.25	2.4	4.1	3.02
Bitterness at 275 in IBU	18.7	12.5	11.5	12.8
Growth rate at 600 nm	0.03	0.07	0.35	0.26
Antioxidant activity	10%	28%	32%	41%

Figure 1: Diagrammatic representation of Table.1

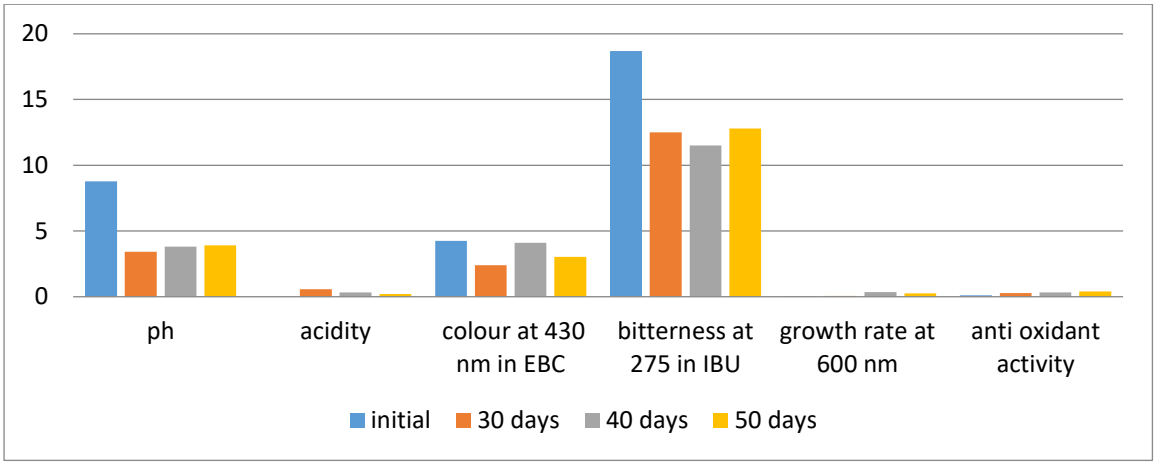

Table 2. Physico- Chemical parameters of Udankudi Jaggery

EXPRIMENTAL VALUE	Initial	20days	30 days	40 days
pH	8.77	4.41	4.77	4.84
Acidity	0	0.87	0.39	0.30
Colour at 430nm in EBC	4.25	3.5	4.5	3.25
Bitterness at 275 in IBU	18.7	18.65	17.5	16.8
Growth rate at 600 nm	0.03	0.165	0.675	0.766
Antioxidant activity	10%	35%	40%	54%

Figure :2 Diagrammatic representation of Table.2

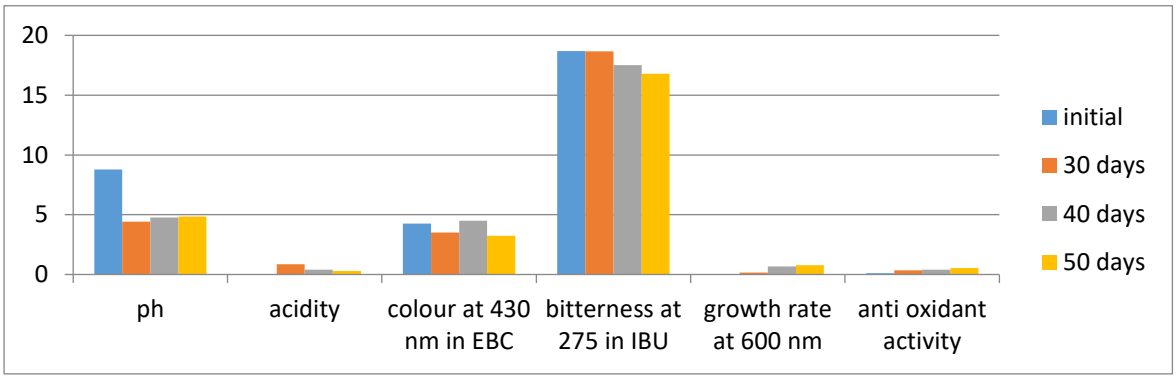

Biochemical Analysis: The result of analysis reveal that the quality of fish feed formulation. The availability of good quality raw material at an affordable price must ensured for achieving high yields and optimum growth of fish stalk in public and private sectors fish farms. For biochemical analysis the fish waste sample were collected from local markets. The result obtained indicated that the nutritional values of the commercial available fish waste ingredients was comparable with the standard values. Bio chemical analysis of fish waste were interpreted in Table 3.

Table 3: **Bio-chemical analysis of fish waste**

S.NO	TEST	RESULT
1	Catalase	Positive
2	Indole	Negative
3	Oxidase	Positive
4	Urea	Negative
5	Gelatin	Positive
6	Growth in Nutrient Agar	Positive
7	Nitrate reduction	Positive
8	Starch	Positive
9	Voges Proskauer	Positive

Final product **Manure**

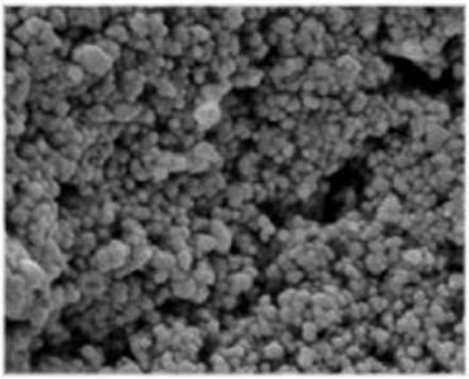

Characterization of the biofertilizer from fish waste using chromatogram / plant germination and growth. Figure 4 represents the Isolation of Protein from bio fertilizer. Table.4 represents the peak report of TIC.

Figure 4 27 kDa protein isolated from fertilizer

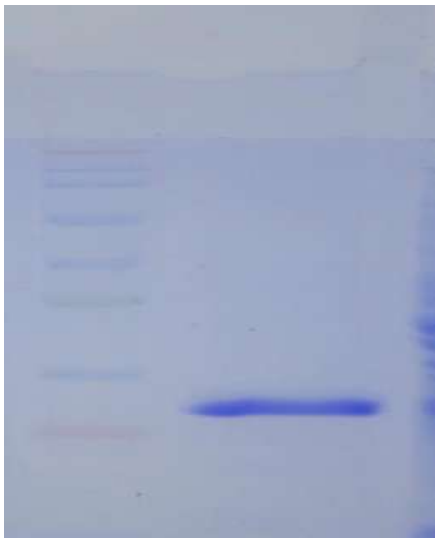

Table : 4 Peak Report Of TIC

Peak Report TIC

Peak#	R.Time	Name	Area	Area%	Height	Height%
1	5.425	4-Ethoxystyrene	4635275	3.45	596655	2.75
2	6.551	Ninhydrin	339723	0.25	184052	0.85
3	6.991	1,3-Benzodioxole	4170441	3.11	673602	3.11
4	7.632	4-Hydroxy-3-nitrobenzaldehyde	3185698	2.37	490485	2.26
5	8.609	Ethyl hydrogen suberate	199285	0.15	62612	0.29
6	8.650	Solasonine	66151	0.05	43908	0.20
7	9.385	2-Aminobenzophenone	613876	0.46	140898	0.65
8	9.506	Phenol, 4-nitro-	3225458	2.40	626097	2.89
9	11.198	Chloromethyl phenyl sulfide	690989	0.51	169825	0.78
10	11.600	Tributyl phosphate	22273629	16.59	6736563	31.09
11	11.916	l-Tyrosyl-l-alanyl-l-phenylalanine	165347	0.12	52187	0.24
12	12.192	Salicylidene aniline	391138	0.29	105208	0.49
13	12.356	Corymbolone	384195	0.29	79211	0.37
14	14.316	Thiophanate	2394958	1.78	646208	2.98
15	15.098	Heptafluorobutyric acid, n-octadecyl ester	833249	0.62	129922	0.60
16	15.531	Isopropyl Myristate	169241	0.13	64704	0.30
17	16.065	Carbonodithioic acid, S,S-diphenyl ester	2310937	1.72	503207	2.32
18	22.545	Isopropyl Palmitate	513403	0.38	105998	0.49

Figure: 5 Chromatogram Analysis

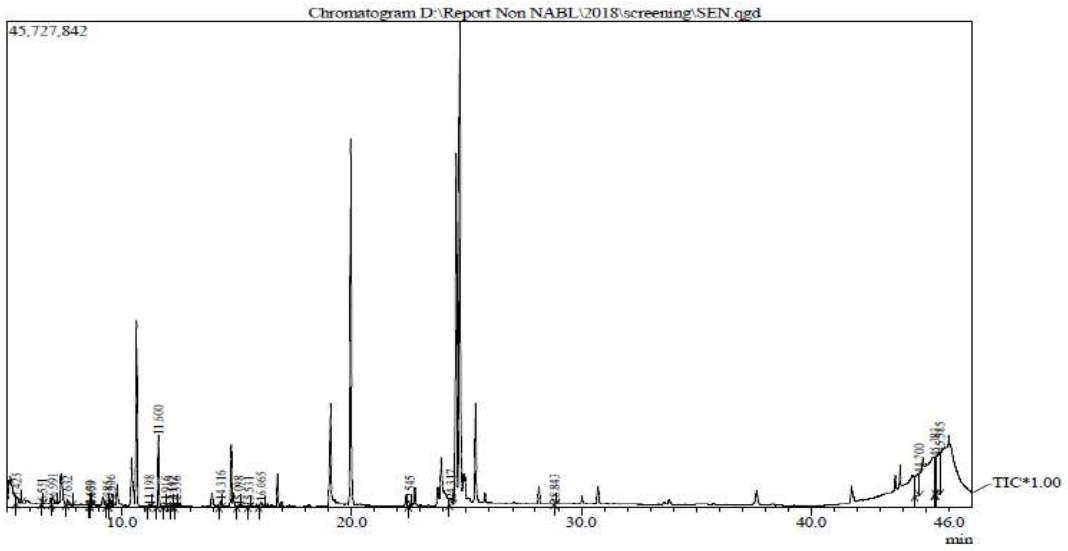

Germination of plants

4 th day **7 th day**


Comparison of the control and treated plants.

Growth of Ladies Finger on first week

Growth of Indian Broad Beans on third week

The final product, compost, can be used as a soil amendment that improves soil texture and fertility and thus reduces the use of synthetic fertilizers applied to the soil. In this case, the conversion should be performed by implementation of novel technologies for the recycling of waste in the form of compost for their use in agriculture. In addition to the usage of compost as a fertilizer, applying compost to the soil may increase the carbon storage capacity within the soil, which reduces greenhouse gas (GHG) emissions into the atmosphere . Biofertilizer are very popular among the farmer to produce quality product. These are eco-friendly and the cheapest source of nutrients. Recently, some studies have examined the reutilization of biodegrade fisheries waste product as liquid fertilizer (Kim and Lee, 2009: Kim *et al.*,2010:Dao and Kim, 2011). The above-mentioned material is of great potential use in agriculture. Numerous long-term experiments carried out in the last decade of the twentieth century showed that national management of mineral fertilizers and organic amendments made it possible to

increase crop yields and to sustain soil fertility sustainably. (Bado *et al.,* 1997; Bationo and Makwuney, 1999; Berger *et al.,* 1987; Pichotétal.1981;

The difference in physico chemical parameters of both Jaggery and Udankudi Jaggery are clearly noted. As the days goes on ,The pH level of both becomes reduced. The acid content is low at the initial period ,at 30 th day it gets increases ,but at the 40 th and 50 th day there is a reduction in acid content.

The bitterness level gets reduced . The growth rate of the plants gets increases. The percentage of anti oxidant activity becomes increases. The biochemical analysis of certain amino acids shows both Positive and Negative values. The amino acids like Catalase, Oxidase, Gelatin, Growth in Nutrient Agar, Nitrate reduction, Starch, Voges Proskauer shows positive effects. The amino acids Indole and Urea shows negative effects

CONCLUSION: Thus we can conclude that bio fertilizer have positive effects on plant growth in all organs. It also increases the photosynthesis, lengthens the vegetative cycle, promotes pollination, improves the size and early maturity of the fruit and improves the over all condition of the plant. Bio fertilizer are very popular among the farmers to produce quality products.

REFERENCES

Arbia .W., Arbia. L., Adour, L., Amrane,A.(2013) Chitin extraction from crustaceans shells using biological methods.

Bado B.V Sedogo, M .P.Sescas M.P. Lompo F and Pationo A.1997.Effect de long term des fumures sur le sol et les rendements du Mais Au Burkina Faso.

Chatterjee R and Bandyopadhyay S .(2014) Studies on effect of organic, inorganic and biofertilizer on plant nutrient status and availability of major nutrients in tomato .

Cira, L A., Hoerta, S, Hall, G.M and Shirai, K.(2002).Pilots scale lactic acid fermentation of shrimp waste for chitin recovery.

Clausen,E., Gildberg,A .,Rao J. (1985). Preparation and testing of autolysate of fush viscera as growth substrate for bacteria.

Cornevale E (2000) Attualicriteri per la valutazion edella qualitative nutrizion In conferenz an azion ealesulle ducazione alimentare, Rome 2000.

Dao VT and Kim JK 2011. Scaled-up bioconversion of fish waste to liquid fertilizer using a 5 L ribbon-type reactor.

Faid, A., Zouiten, A., Elongrakchi, A. and Achkari-Bagdouri, A. (1997). Bio transformation of fish waste into a stable feed ingredient. Food Chem. Col: 13-18.

Gao, M., Hirata, M., Toarisaka, E and Hano, T.(2006). Acid hydrolysis of fish waste for lactic acid fermentation. Bio Resourse Technology 97:2414-2420.

Ghisselini, P., Ciallani, C., and Ulgiati,S.(2015). A review on circular economy: the expected transition to a balance inter interplag of environmental and economic system.

Gustavsson J, Cederberg, C., Sonesson, U.(2011). Extent of food losses and waste in Global food losses and food waste, Gothernderg: Swedish. Institute for food and Biotechnology (Silk) pp.4-9.

Hasson and Heath (1986) Biological fermentation of fish waste for potential used in animal and poultry feeds. Agri Wastes 15, 1-15.

Keller S.1990.Making profits out of sea food wastes. In Specifications for marine By-products for agriculture. HardyRW and masumoto T, eds. Alaska sea Grant college program, Anchorage, AK, US, pp.109-120.

Keller and Hall. 1986. Fish processing technology. In Fishery By Products. Okerman HW,ed.VCH Publisher, New York, NY, US, pp.155-192.

Kristinson, HG., Rasco, B.A.(2000). Fish protein hydrolysate production, Biochemical and functional properties. Crit. Rev. Food Sci. Nutr., Kyun kim,J., Vanthingocdao, N., Kong, I.S., Lee, H.H:Identification And characterization of microorganisms from earthworm viscera. Bioresource Technology,

Lio PH Jones L, Lau AK Walkemeyers, Egan B And Holbek N, 1997 Composting of fish wastes in a full-scale in-vessel system. Bioresource Technology.

Sachindra,N.M.,Bhaskar,N., Mahendra,Kar ,N.S.(2005). Carotenoids in different body componends of Indian shrimps.J. Sci Food Agri.

Vazquez JA, Docasal SF, Prieto MA, Gonzalez MP and Murada MA. (2008) Growth and metabolic features of lactic acid bacteria in media with hydrolyzed fish viscera: an approach to bio-silage of fishing by products. Bioresour Technol 99, 6246-6257.

Yamamoto M,Saleh F, Ohtsuka A and Hayashi K.(2005) New fermentation Technique to process fish waste. Anim Sci J 76,245-248.

Chalamaiah, M., Dinesh Kumar, B.,n Hemalatha, R., Jyothirmayi, T. (2012). Fish protein hydrolysate proximate composition, amino acid composition, anti-oxidant activities and applications.

Hammoutou, S., Aziane,A., Chaouch, A., and Elyachiouy, M., (2017) Characterization , treatment and recovery of fish by products as a stable bio Fertilizer.

Bationo A.et Makewuney A.U 1999. Role of manures and cop residue in alleviating sol fertility constraints to crop production with special reference to the sahelian and soudanian zone West Africa.

Laabioui H., Elmoualdi L., Oouhsine M,et EL Yachioui M., 2006. Essai de valorization des dechets des abattoirs comme UN stable bio-engrais Journal Afericain des sciences de l'Environnement.

Russell L, Stokes AR, Macdonald H, Muscolo A, Nardi S 2006. Stomata Response to humic substances and auxin are sensitive to Inhibition phospholipase A2. Plant and soil.

Vedie, H: Fertilie chimique du sol: savoir interpreter les analysers pourgerer les apports d' elements majeurs en maraichage biologique.

Sachindra N.M. and bhaskar N, (2008). Invitro antioxidant activity of liquor from fermented shrimp bio-waste. Bio resources Technology.

Branger, M, Richer, M, Roustel, S: Microbiochimie et alimentation Educagri Edition

Schumacher, B.A: Method for the determination of total organic carbon (TOC) in soils and sedmints. United States Lsa vegas. Sciences division National Exposure Research Laboratory.

Zabar, M., Benkerroum, N, Guerourali, A, Baou,S., Alahiane,L. Biological ensiling of sardine wastes in sugarcane molesse for their valorization in animals feeding . Microbiollohical study. Proceedings of international symposium on Environment pollution control and waste management.

frontiers | Frontiers in Microbiology

TYPE Review
PUBLISHED 17 April 2023
DOI 10.3389/fmicb.2023.1149418

OPEN ACCESS

EDITED BY
Rami M. Elshazli,
Horus University, Egypt

REVIEWED BY
Padmani Sandhu,
Institute of Microbial Technology (CSIR), India
Martijn Zwama,
Osaka University, Japan

*CORRESPONDENCE
Shiela Chetri
✉ sony240689@gmail.com

SPECIALTY SECTION
This article was submitted to Antimicrobials, Resistance and Chemotherapy, a section of the journal Frontiers in Microbiology

RECEIVED 21 January 2023
ACCEPTED 13 March 2023
PUBLISHED 17 April 2023

CITATION
Chetri S (2023) The culmination of multidrug-resistant efflux pumps vs. meager antibiotic arsenal era: Urgent need for an improved new generation of EPIs. *Front. Microbiol.* 14:1149418. doi: 10.3389/fmicb.2023.1149418

The culmination of multidrug-resistant efflux pumps vs. meager antibiotic arsenal era: Urgent need for an improved new generation of EPIs

Shiela Chetri*

Department of Microbiology, Thassim Beevi Abdul Kader College for Women, Kilakarai, Tamil Nadu, India

Efflux pumps function as an advanced defense system against antimicrobials by reducing the concentration of drugs inside the bacteria and extruding the substances outside. Various extraneous substances, including antimicrobials, toxic heavy metals, dyes, and detergents, have been removed by this protective barrier composed of diverse transporter proteins found in between the cell membrane and the periplasm within the bacterial cell. In this review, multiple efflux pump families have been analytically and widely outlined, and their potential applications have been discussed in detail. Additionally, this review also discusses a variety of biological functions of efflux pumps, including their role in the formation of biofilms, quorum sensing, their survivability, and the virulence in bacteria, and the genes/proteins associated with efflux pumps have also been explored for their potential relevance to antimicrobial resistance and antibiotic residue detection. A final discussion centers around efflux pump inhibitors, particularly those derived from plants.

KEYWORDS

efflux pump, MDR, antibiotic resistance, resistance nodulation division superfamily, efflux pump inhibitors (EPIs), *Escherichia coli*

Introduction

Bacteria are already well known for their ability to persist in extreme environments *via* their evolving numerous defense mechanisms against various substances that are lethal for their survival. Currently, antimicrobial resistance, the most complicated health concern across the world, which is primarily associated with an extended hospital stay, expensive treatment, and high mortality and morbidity rates, needs undeniable attention and multiple operative approaches involving the "One Health" concept. As the concept specifies, the interrelatedness among food, animals, and human health with the environment and the intentional collaboration between different sectors' efforts to confront the standing challenge (Taneja and Sharma, 2019), but regrettably, of antimicrobial resistance (AMR) development due to environmental influences have received less care as compared to human and animal health in spite of the significant deviations in the geographical dissemination of AMR associated with environment (O'Neill, 2015). The ultimate result of the increasing incidences of AMR is the development of multidrug-resistant phenotypes, and the multidrug-resistant (MDR) bacteria is a serious problem worldwide (Cooper and Shlaes, 2011; Blair et al., 2014; O'Neill, 2015; Venter, 2019). Moreover, unexpectedly, this problem occurs at the same time when several pharmaceutical companies stopped investing in research to find

new drugs to treat MDR due to a lack of high financial returns. In the bacterial cell membrane, the presence of transporters helps in the extrusion of noxious compounds, ultimately decreasing the concentration of external and unwanted or irrelevant substances and enhancing growth. However, the role of some transporters in the biodegradation of various deadly substances present in our environment is also well known (Ganas et al., 2007). As per the previous reports available, there are various resistance mechanisms contributing toward the development of resistant phenotypes—both extrinsic and intrinsic (Ganas et al., 2007). However, the role of intrinsic mechanisms such as the overexpression of multidrug-resistant efflux pump systems in evolving MDR phenotypes has gained partial attention (Nikaido and Pagès, 2012). The role of these efflux pumps is not only limited to functions as an efficient transporter but also limited to combat the stress from external environmental for bacterial survivability. However, it should be noted that some efflux pumps are substrate specific while others have a broad range of substrate specificity, which means that they can pump out multiple substrates including different classes of antibiotics, thus prompting multidrug resistance in bacteria (Nikaido and Pagès, 2012). Therefore, the efflux pump systems which form an important antibiotic resistance mechanism are widely considered due to their unique ability to extrude a variety of noxious compounds including dyes, detergents, different classes of antibiotics, and disinfectants (Nikaido and Pagès, 2012; Venter et al., 2015) outside the cell and thus are intensely associated with MDR expansion. Moreover, these specific features of the efflux pump systems have made them more prominent as multidrug efflux pumps (Webber and Piddock, 2003; Piddock, 2006a).

For the survivability of bacteria, these transporters located in the bacterial cell membrane play a crucial role in facilitating the reduction of external and irrelevant substance concentrations and promoting bacterial growth. However, evidence indicating the role of these transporters in the biodegradation of deadly compounds that are present in the environment has previously been reported (Ganas et al., 2007), suggesting the role of these efflux pump systems not only as a transporter but also in defending bacterial growth and survivability under various environmental stresses. Substrate specificity of these efflux pumps against various substrates, such as different antimicrobial classes, induces the pathogens to become multidrug resistant (Hernando-Amado et al., 2016). However, in some cases it has also been observed that the ejection of the substrates or organic solvents results into overexpression of transporters, which further, triggers the co-selection of the altered features of antimicrobial resistance in bacteria (Blair and Piddock, 2016). As a consequence of overexpression of the efflux pump systems, biofilm formation and quorum sensing (QS) will also be impacted by bacterial pathogenicity (Alcalde-Rico et al., 2016; Kong et al., 2017). In addition to antimicrobials, efflux pumps also have the potential to export virulence determinants, such as adhesins, toxins, and other crucial proteins, which are very critical for colonization within host cells (Piddock, 2006b). Several studies have already been reported on unfolding the development of antibiotic resistance associated with efflux pump systems along with numerous novel efflux pump transporters and simultaneous proteins. Additionally, in recent years, several other functions of an efflux pump system besides antibiotic resistance, such as virulence and bacterial self-protection against various environmental pollutants, were investigated. However, the particular mechanisms of regulation of these efflux pump systems and the active domains of the transporters are still not clearly understood. There are several inducing factors located on the inner and outer membranes of bacteria that stimulate the activity of efflux pump systems and promote their structural alterations within the fluid membrane environment. A brief overview of the role of efflux pumps in Gram-positive and Gram-negative bacteria is presented in this review article. Furthermore, the applications of efflux pump regulators to identify antimicrobial resistance and antibiotic residues, as well as the discovery of new efflux pump inhibitors derived from plants, have been discussed in this study.

Efflux pump families

Efflux pump systems are predominantly classified into six major superfamilies based on their energy source utilized to export the substrates: ATP-binding cassette (ABC) superfamily, multidrug and toxic compound extrusion (MATE) superfamily, major facilitator superfamily (MFS), resistance nodulation and cell division (RND) superfamily, small multidrug resistance (SMR) superfamily, and proteobacterial antimicrobial compound efflux (PACE) (Hassan et al., 2018) (Figure 1). One of the chief differentiating features of these efflux pumps is the source of energy they utilize; for example, the ABC superfamily draws energy *via* ATP hydrolysis (Verchère et al., 2012); however, other EP families such as RND, MFS, SMR, and MATE utilize either proton motive force (PMF) derived from H+ or electrochemical gradient of Na+ for exporting their substrates and for extruding several compounds (Kim and Hummer, 2012). Additionally, there are some other features as well for differentiating these efflux pumps based upon their composition or structure of the efflux pump transporters; for example, in an RND efflux pump system, three components, namely, an outer membrane protein (OMP) channel, an inner membrane transporter protein, and two modules that were connected *via* a membrane fusion protein (MFP) combine to form a composite known as a tripartite complex, which ultimately works together for the extrusion of noxious agents (Daury et al., 2016; Neuberger et al., 2018). However, research on novel multidrug-resistant (MDR) efflux pump systems in bacteria is still underway.

ATP-binding cassette superfamily

The MacAB-TolC efflux pump system is a tripartite complex belonging to the ABC and is the most comprehensively studied EP system among gram negative bacteria which is actively associated with the extrusion of macrolides and polypeptides virulence factors driven *via* ATPase MacB and further participates in enterotoxin heat stable enterotoxins (TII) secretion in *Escherichia coli* (Lu and Zgurskaya, 2013; Fitzpatrick et al., 2017; Jo et al., 2017). Additionally, lipopolysaccharides (LPS) and analogous glycolipids can be considered as organic substrates of the MacAB-TolC pump

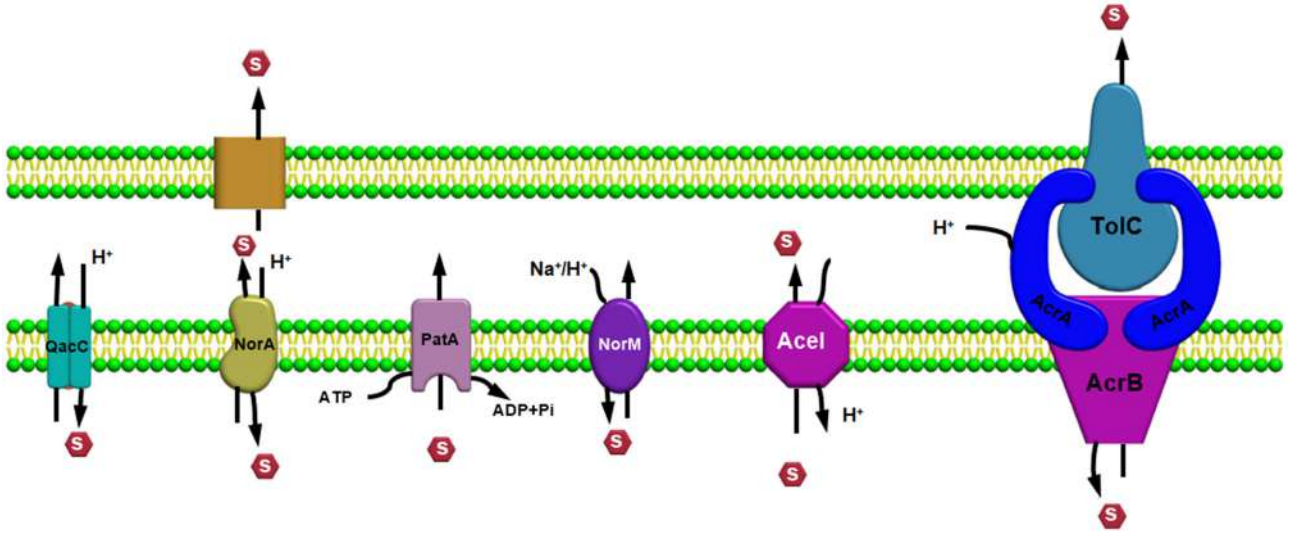

FIGURE 1
Efflux pump major super-families based on their energy source utilized to export the substrates.

systems (Lu and Zgurskaya, 2013). As the MacAB-TolC (pump system) is a tripartite complex with three components, including MacB, which is an inner membrane protein that functions as a homodimer complex and consists of two domains, namely, the (i) N-terminal, a nucleotide-binding domain that enables power generation *via* ATP hydrolysis and the (ii) C-terminal cytoplasmic tail (Lu and Zgurskaya, 2013). Other important components of the EP system are MacA, a periplasmic adaptor protein (PAP) that gets stimulated when ATPase binds specifically with the lipopolysaccharide core, and an outer membrane channel protein TolC that functions as an exit duct for substrate transport (Lu and Zgurskaya, 2013; Fitzpatrick et al., 2017). We observed from previous literature that, in *Serratia marcescens*, the absence of the MacAB (efflux pump system) resulted in increased susceptibility to polymixins and aminoglycosides, with a significant decrease in swimming motility and biofilm formation ability, and even caused impairment in defense capability to combat superoxide stress (Shirshikova et al., 2021). In addition, in their research study, Shi et al. (2019) observed that, in *Agrobacterium tumefaciens* 5A {a strain that is arsenite [As (III)] resistant}, MacAB efflux pump confers resistance against a variety of macrolide and penicillin-like antibiotics along with arsenite [As (III)].

However, Gram-positive bacteria harboring the ABC efflux pump systems, containing single component or transmembrane protein, have also been observed: for example, EfrAB transporter in *Enterococcus faecalis*, Msr protein in *Streptococcus*, LmrA in *Lactococcus lactis* (Hellmich et al., 2015), and PatA/B in *Streptococcus pneumoniae* (Garvey et al., 2011a; Iannelli et al., 2014). EfrAB, an MDR efflux pump system, is a heterodimeric protein conferring resistance toward different antibiotics such as gentamicin, chloramphenicol, and streptomycin (Lerma et al., 2014). In addition, the expression of the EfrAB pump was found to be highly induced when exposed to these antibiotics in sub-inhibitory concentration, and a decline in the expression was observed in the presence of a sub-inhibitory concentration of EDTA (3 mM) (Lerma et al., 2014). The LmrA transporter protein in *L. lactis* is a homodimer protein having one nucleotide-binding domain and six α-helix domains, which initially identifies and then proceeds toward the extrusion of macrolides and lincosamides (Hellmich et al., 2012). In *Streptococcus*, the Msr protein, comprising only two nucleotide-binding domains [without any transmembrane domain (TMD)], was found to be responsible for conferring resistance against macrolides and to collaborate with the Mef transport family (Zhang et al., 2016; Tatsuno et al., 2018). Further, in the case of the PatA/B efflux pump system, nearly the entire hydrophilic fluoroquinolone family members, such as ciprofloxacin, function as a substrate for this pump (Baylay and Piddock, 2015).

Multidrug and toxic compound extrusion superfamily

Members of the multidrug and toxic compound extrusion (MATE) family are broadly disseminated among the three domains, namely, archaea, bacteria, and eukarya (Kuroda and Tsuchiya, 2009). This class of transporters belongs to the multidrug/oligosaccharide-lipid/polysaccharide (MOP) family, which is further categorized into two subfamilies, namely, (i) NorM and DinF found in prokaryotes and (ii) the eMATE subfamily in eukaryotes based on their sequence similarity (Brown et al., 1999; Omote et al., 2006). MATE transporter proteins in bacteria are mainly involved in the extrusion process of amphiphilic cationic drugs, such as norfloxacin, outside the cell. However, in plants, these transporters are involved in physiological roles like developing resistance toward herbicides, leaf senescence, auxin synthesis, tolerance against aluminum, homeostasis, and sequestration of organic compounds (which are plant-based) inside the vacuoles (Remy and Duque, 2014). Further, the MATE transporters were found to be located in both the proximal

(convoluted and straight) tubules in the kidney in the case of mammals and in the canalicular domain inside hepatocytes, where the organic compounds are transported across this membrane domain during the final round of drug elimination process (Omote et al., 2006; Terada and Inui, 2008).

All life forms on earth need a balanced extrusion of exogenous noxious substances outside to sustain homeostasis. Therefore, the extrusion of lethal compounds such as xenobiotics requires the efficient involvement of the transporters. First, MATE family transporters were known for their ability to develop antibiotic resistance in *Vibrio parahaemolyticus* (Morita et al., 1998) but they later became well-known in other domains as well. Moreover, MATE is abundant throughout the human body, but its expression is highly concentrated in the bile canaliculi of the liver and within the brush border membrane of the kidney (Otsuka et al., 2005). Metformin, cimetidine, procainamide, and acyclovir (Masuda et al., 2006; Tanihara et al., 2007) are the cationic drugs that are recognized by the MATE transporter, and therefore, they act as influential factors in controlling plasma concentrations. However, previous literature suggests the significant role of MATE in inducing drug-associated nephrotoxicity during the last phase of pharmacodynamics of cationic drugs. An example is cisplatin, a clinically vital anticancer agent which has not been recognized by the MATE efflux transporter and has ultimately resulted in nephrotoxicity due to renal accumulation (Yokoo et al., 2007). Moreover, cimetidine, which is a histamine (H2) receptor antagonist that is a well-known MATE inhibitor functioning as a gastric acid inhibitor (Ito et al., 2012; Wagner et al., 2016), must be carefully handled and administered. Therefore, a deep understanding of the MATE transporter's working mechanisms is necessary for refining the efficiencies of cationic drugs. The MATE transporters are energetically involved in several physiological functions, which makes them attractive pharmaceutical targets. The MATE transporter protein structure is composed of 12-transmembrane helices arranged in two six-transmembrane (TM) domains, namely, the N- and C-lobes.

However, the positioning of these helices is arranged in an altered manner so as to make it different from the transporters belonging to the major facilitator superfamily (MFS) (He et al., 2010; Van Veen, 2010), supporting the previous assumptions that these two transporters should be considered as distinct superfamilies (Brown et al., 1999). Previous studies on the effective changes in the mechanisms, which are required either for the survivability of a particular microbe or for the development of a multidrug-resistant variant, have been observed in the case of a variety of transporter proteins. As a result of consecutive conformational variations, the transporter protein substitutes within two main conformations, one of which functions *via* exposing the substrate binding pocket (located centrally) to the inside and the other disclosures the pocket toward the outside of the cell. However, the structure and catalytic reactions mediated desired conformational changes are still not properly understood and one of the main reason behind this is the evidence indicating two crystal structures of the MATE transporter protein having an outward fronting conformation. Additionally, transporter proteins belonging to the MATE family were primarily well-known for mediating drugs or ions antiport *via* utilizing Na+ or H+ energy sources. The difference in the utilization of different energy sources such as H+ or Na+ gradient in different family members within the MATE superfamily has been suggested according to previous x-ray crystallographic studies concerning the NorM subfamily depending upon Na+ coupling in the C-lobe (He et al., 2010; Lu et al., 2013a), and a quite similar pattern was noticed in case of the eMATE subfamily (Miyauchi et al., 2017; Tanaka et al., 2017) but the DinF subfamily members was found to utilize H+ in the N-lobe (Lu et al., 2013b; Tanaka et al., 2013; Radchenko et al., 2015; Mousa et al., 2017; Kusakizako et al., 2019).

Major facilitated superfamily

Several secondary carrier families having similar topological features were identified before 1993, but no information was available to prove or to relate these families by a common origin. Among these families, a sugar porter's family including glucose facilitators found in mammals, two families of specific and multidrug efflux pump transporters, a metabolic uptake transporter family, and an oligosaccharide transporting family, including lactose permease present in *E. coli*, have been well studied. In addition, the knowledge and effort of bioinformatics helped us to understand the mechanisms and provided evidence to relate these families, and further, the name "major facilitator superfamily" (MFS) was coined (Marger and Saier, 1993). The major facilitator superfamily (MFS) transporters can be categorized into three main groups based on the mode of transportation of their substrates: (i) uniporters, which are responsible for the transference of a single substrate, (ii) symporters, which transport a substrate along with the simultaneous transportation of a coupling ion (e.g., H+), and (iii) antiporters, which are responsible for the simultaneous transportation of two substrates in opposite directions in such a way that the transportation of one substrate is dependent on prior discharge of the co-substrate (Forrest et al., 2011) (Figures 2A–C). In addition, it has been observed that the uniporters are able to transport their substrates without utilizing any energy source below their concentration gradient, while in the case of antiporters and symporters, the stored energy of the coupling ion concentration gradient is utilized for substrate transportation against their concentration gradient. However, irrespective of the differences in the mode of transportation of the substrates, all the members belonging to the major facilitator superfamily have the identical core structure comprising 12 TM helices, which are organized on two domains, namely, the N-domain and the C-domain (having similar structure) (Hirai et al., 2002; Yan, 2013), and are further partitioned into two inverted repeats of three helices.

One of the most well-studied MFS transporters in bacteria is the lactose permease (LacY) present in *E. coli,* which has worked as an appropriate protein model, for understanding the diverse features of the mechanisms involved in transportation associated with MFS transporters (Guan and Kaback, 2006; Smirnova et al., 2011; Kaback, 2015). However, in humans, the most studied MFS efflux pump (EP) system is the glucose transporter which plays a very crucial role in maintaining glucose homeostasis

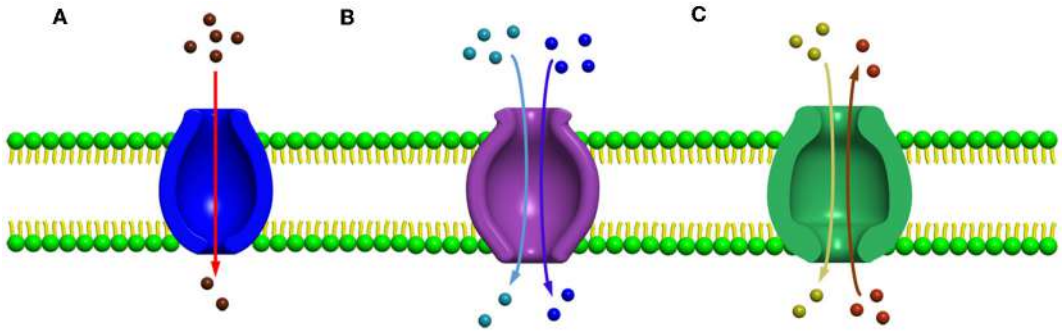

FIGURE 2
Major facilitator super family (MFS) transporters can be categorized into three main groups based upon their mode of transportation of their substrates **(A)** uniport, **(B)** symport, and **(C)** antiport.

in the human body, which is also referred to as the SLC2 protein. Moreover, the deterioration or faulty regulation of these proteins may lead to important diseases such as diabetes (Type II) (Augustin, 2010; Cura and Carruthers, 2012). Further, the roles of the Msr transporter belonging to the ABC superfamily and the Mef system of the MFS family were found to increase the macrolides extrusion co-actively, which further enhanced the resistance toward 14–15-member ring macrolides (Nunez-Samudio and Chesneau, 2013). Besides their active participation in the extrusion process, these MFS transporters are also linked with other biological pathways, such as the role of MdrT and MdrM in promoting the immune response in hosts by activating the production of interferon-β (IFN-B, which is a type I interferon response) and in maintaining the stability of the cell wall (Pasqua et al., 2021). In the case of *Staphylococcus aureus*, the presence of a constitutively expressing MFS efflux pump system Tet38 has been reported to influence the progression of host cell invasion comprising internalization, adhesion, and relocation within epithelial cells and the consequent step involved in epithelial cell infection due to *Staphylococcus aureus*, which includes the viability of bacteria and trafficking within phagolysosomes (Pasqua et al., 2021).

However, in *Acinetobacter baumannii*, loss of the MFS transporter protein AbaQ resulted in a significant decrease in bacterial virulence and motility capability (Pasqua et al., 2021), and furthermore, a substantial reduction in bacterial motility and virulence was detected when the efflux pumps encoding genes (such as RND, MATE, SMR, and ABC) are inactivated (Pérez-Varela et al., 2019). The working mechanisms of MFS transporters still require more explanation. However, an updated form of the classical rocker–switch model for understanding the changes emerging in the conformation of the MFS transporter associated with a form of substrate transportation known as the "clamp-and-switch" model has been previously proposed (Quistgaard et al., 2016), which also discussed the function of gating residues, binding of substrates, and the conformational change observed in the updated model (Quistgaard et al., 2016). In the past decades, many molecular biology, biochemical, and biophysical experiments have been conducted to understand the function of MFS transporters due to their physiological and pharmacological significance.

Resistance nodulation division superfamily

Resistance nodulation division (RND) superfamily members are the most well-known efflux pump systems because of their astonishing capability of extruding a wide range of substrates, which includes various classes of antibiotics, such as tetracyclines, chloramphenicol, different β-lactam antibiotics, and besides antibiotics, several other compounds such as dyes, detergents, metals, bacterial metabolites are also utilized as a substrate by this pump (Munita and Arias, 2016). The only feature which is common among these compounds is the amphiphilic nature of the substrates utilized by this pump (Yamaguchi et al., 2015). RND family members are part of multiprotein complexes which are arranged within the bacteria in a way that connects the outer membrane, periplasmic space, and the inner membrane to form a tripartite complex; thus, the RND transporters can facilitate the transport of compounds into these compartments by allowing them to work in conjunction with other transmembrane transporters. RND transporters are capable of capturing substrates not only from the cytoplasm but also from the inner membrane's outer leaflets or from the periplasm (Du et al., 2015). Consequently, it has been observed that these protein complexes are larger than several other transmembrane proteins of bacteria, which usually range over only a single membrane. Resistance nodulation division (RND) family members is comprised of three components, including (i) a periplasmic adaptor protein (PAP) (ii) an outer membrane protein (OMP) channel, and (iii) an MFP, which connects IMP and OMP, and are referred as a tripartite system for having three components together to form a complex (Figure 3). The main function of this tripartite complex is to identify and bind the substrates found in the periplasmic space, outer leaflet of the inner membrane, or the cytoplasm and lastly extrude or expel outside the cell through the outer membrane channel. However, other transporter protein functions as a single unit within the inner membrane for transporting substrates *via* the membrane bilayer (Nikaido, 2011; Du et al., 2018). Besides the participation of efflux pumps in the development of antibiotic resistance, other mechanisms such as alteration in drug target or inactivation or modification of antibiotics also have a vital role in AMR (Walsh, 2003; Blair et al., 2015; Colque et al., 2020). However,

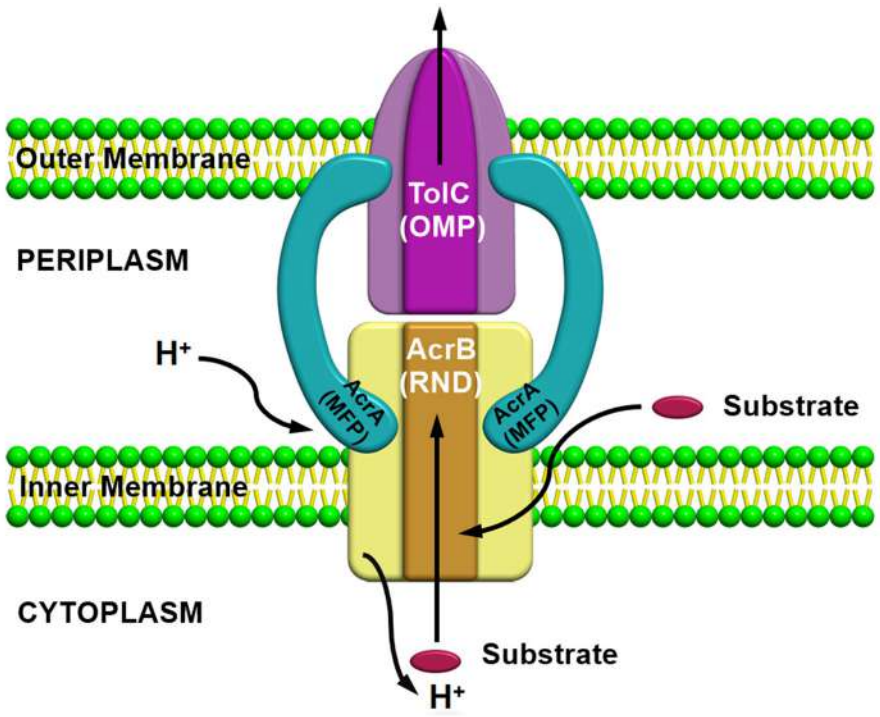

FIGURE 3
AcrAB-TolC a tripartite efflux pump system containing three components together to form a complex.

it has been noticed that comparative to the single factor that contributes to the resistance development against a particular class or group of antibiotics, multidrug resistance (MDR) can progress due to a reduction in bacterial membrane permeability (Nikaido, 2009) and *via* overexpression of the MDR efflux pump system in both Gram-positive and Gram-negative bacteria (Nikaido, 2009; Allen et al., 2010; Li et al., 2015). Besides being intrinsically expressed or present, bacteria also acquire resistance by RND efflux pumps *via* plasmids, etc. (Levy and Marshall, 2004; Allen et al., 2010), and mutation is intensely associated with the significant rise in the expression level of both intrinsic and extrinsic efflux pump systems in the clinical strains (Blair et al., 2015). This resulted in an increase in the expression level, which is one of the chief reasons for MDR development (Blair et al., 2014). In the current scenario, resistance nodulation division (RND) superfamily members are considered among the core contributors to MDR progress in clinical isolates (Nikaido, 1996; Blair et al., 2014).

Besides, the ability of these RND transporters to work as a tripartite pump in the extrusion of a wide variety of substrates such as different classes of antibiotics, detergents (Zwama and Yamaguchi, 2018), dyes, and various other noxious compounds outside the cell (Du et al., 2014), the overexpression of the efflux pump genes as a result of an increase in the transcriptional level of the operonic genes due to mutations in their regulatory proteins and genes (Nishino et al., 2008, 2009) has already been well studied and established in pathogenic bacteria within clinical settings (Oethinger et al., 1998; Nishino et al., 2008, 2009; Blair et al., 2015; Yu et al., 2020; Salehi et al., 2021). Examples of some of the well-studied RND efflux pump systems observed in Gram-negative bacteria are AcrAB-TolC in *E. coli* and *Salmonella enterica*, MexAB-OprM in *Psedomonas aeruginosa*, and the AdeABC system in *A. baumannii* (Bhakdi et al., 1988; Nikaido, 1996; Xu et al., 2020; Lv et al., 2021) are intensely associated with the extrusion process of a wide range of lethal compounds. Other examples such as the CmeABC system in *Campylobacter jejuni*, SmeABC in *S. enterica*, and the MtrCDE efflux pump system in *Neisseria gonorrhoeae*, have also been reported previously (Gilson et al., 1990; Singh et al., 2006; Wehmeier et al., 2009; Guérin et al., 2014; Wright and Tate, 2015; Lv et al., 2021). An important role of the RND transporter proteins, such as MtrD, MexB, AcrB, and AdeB, within the system, is in the substrate binding step (where the substrate may be specific) and in the drug transportation process, which is crucial for resistance development clinically (Delmar et al., 2014). An example is the mutation in AcrB gene which resulted in ciprofloxacin treatment failure (B). According to the previous literature, the transcriptional level of the regulatory proteins belonging to the TetR family such as AcrR (Blanco et al., 2016; Chetri et al., 2019a), MtrR (Lin et al., 2017), CmeR (Zwama and Nishino, 2021), TtgR (Bay and Turner, 2009), MexR (Srinivasan and Rajamohan, 2013), NalC/NalD (Bay et al., 2008), SmeT (Lytvynenko et al., 2016), and RarA belonging to the AraC family (Chetri et al., 2018b) influences the expression of these efflux pumps. The amino acid (AA) residues within the efflux pump systems are very crucial and actively participate in the substrate binding course and the substitution, or any changes in the AA residues probably can modify the substrate affinity (Banigan et al., 2015). Further, alteration in prominent AA residues was demonstrated to associate with efflux pump-facilitated

resistance toward various drugs (Padariya et al., 2018). AcrAB-TolC, MexAB-OprM, and CmeABC are among the most well-characterized multidrug resistant efflux pump systems belonging to the RND superfamily and are responsible for survivability and pathogenicity in bacteria. There are reports indicating the co-existence of different defense mechanisms including porin deficiencies and β-lactamase production with the overexpression of efflux pumps in *E. coli* (Chetri et al., 2019a,c), but rare evidence of insertions into penicillin-binding protein 3 (PBP3) of *E. coli* affecting their activity against monobactams and cephalosporins has already been reported (Alm et al., 2015). In carbapenem-resistant *E. coli* isolates, the overexpression of the AcrAB-TolC efflux pump simultaneously with the downregulation of OmpF due to regulation *via* the MarA gene was observed (Chetri et al., 2020). Further, for a comparative analysis study in carbapenem-resistant *E. coli* isolates, the β-lactamase gene (*bla*NDM-1, *bla*CTX-M-14, and *bla*CTX-M-3) were targeted and amplified (Shimizu et al., 2017; Chetri et al., 2019b). However, a study showing the capability of the AcrAB-TolC efflux pump system in influencing bacterial attachment, then penetration within the host, and further proliferation and persistence within animals has been reported (Piddock, 2006b) previously. Besides, the role of the AcrAB-TolC efflux pump in *E. coli*, AcrEF-TolC has also been reported to have a significant role in developing resistance toward different antibiotics (Chetri et al., 2018a).

Extensive usage of heavy metals (HME) in antimicrobials is not an infrequent event, for example, in disinfectants, and as a result, the RND efflux pump superfamily has developed the ability to resist these compounds for their survivability. Further, these RND superfamily is divided into two main categories: (i) hydrophobic and amphiphilic (HAE)-RND family, for example, AcrB, AcrD, AcrF, MdtC, MdtD, and YhiV, (ii) HME-RND family, for example, CusA which utilizes Cu(I) and Ag(I) as the most important substrate (Delmar et al., 2014), where CusA functions as a membrane fusion protein, CusC as an outer membrane channel protein to form a tripartite complex, the CusCBA efflux pump system (Long et al., 2012). However, the mechanical pathways required for the exportation of metal ions have previously been predicted (Long et al., 2012). Further, for survival, bacteria adapts in different ways such as efflux pump-associated biodegradation to get rid of the harmful effects of the lethal chemical compounds resulting from organic pollutants, for example, in *Pseudomonas Putida*, the occurrence of the TtgABC efflux pump system is responsible for conferring tolerance toward toluene (Blanco et al., 2016). Consequently, due to pressure exerted *via* overuse of antimicrobials, mutations in functional genes occurs, which may influence various changes in the AA residues located in the binding sites, which affect the substrate specificity of an efflux pump, and as a result, bacteria become less receptive toward antimicrobials, i.e., antimicrobial-resistant phenotype significantly altering the scenario in the environmental, clinical, and laboratory settings (Zwama and Nishino, 2021). The genetic changes occurring in an efflux pump denote an evolutionary adaptation within a microorganism against antimicrobials, and it is undoubtedly complexing the entire therapeutic option management system of pathogenic bacteria (Zwama and Nishino, 2021).

Small multidrug resistance family

Small multidrug resistance (SMR) family members utilize proton gradient to export a wide range of antibiotics, hence contributing toward MDR development. On the basis of the sequence, the SMR family can be divided into two main physiological subtypes (Kermani et al., 2020): (i) guanidinium exporter (representative of "Gdx") which is responsible for the allocation of bacterial metabolites such as guanidinium ion in exchange of two protons (Nelson et al., 2017; Kermani et al., 2018) and (ii) quaternary ammonium compound (Qac) representative subtype, which is responsible for the export of certain hydrophobic, cationic, and quaternary ammonium compounds (Nelson et al., 2017; Kermani et al., 2018). After the discovery of the first antiseptics containing quaternary ammonium around 100 years ago, Qac cluster proteins were found to be nearly associated with the propagation of multidrug resistance elements (Russell, 2002; Pal et al., 2015; Gillings, 2017; Zhu et al., 2017). Several bacteria harboring both subtypes of SMR transporter proteins were detected. Additionally, it was observed that the two subtypes do not interfere with each other's physiological role, for example, Qac protein will not participate in the transportation of guanidinium ion (Gdm+) and likewise, the guanidinium exporter will not involve in the export of any cationic or quaternary ammonium compounds but will require a substrate that is having guanidine moiety (Kermani et al., 2020). In *E. coli*, an example of the most well-studied Qac transporter protein is EmrE, and also an EmrE mutant, i.e., S64V that is having diminished conformational exchange dynamics based on extensive NMR measurements has been recently reported (Shcherbakov et al., 2021). SMR family members comprise short polypeptide chains of 100–150 amino acids and can stretch the cytoplasmic membrane as 4 TM α-helices (Bay et al., 2008). Proteins with short hydrophilic loops allow solubilization of a broad range of drugs, noxious lipophilic compounds that comprise DNA intercalating agents, lethal metabolites such as nicotine, and polyamine compounds such as spermidine (Bay et al., 2008; Bay and Turner, 2009). There are several reports indicating the active role of these family members in developing resistance toward different substrates—like in *A. baumannii*—AbeS transporter is found to be responsible for the transportation of ethidium, benzalkonium, and acriflavine, which simultaneously increases resistance toward amikacin (Lytvynenko et al., 2016; Lin et al., 2017). Similarly, in *Klebsiella pneumoniae* activation of the efflux pump system, KpnEF confers resistance against chlorhexidine, other antiseptics, benzalkonium chloride, etc. (Srinivasan and Rajamohan, 2013). In both *P. aeruginosa* and *E. coli*, the role of EmrE transporter protein in recognizing the substrates and mediating the elimination of polyaromatic compounds has already been reported (Banigan et al., 2015; Chetri et al., 2018b), but the Qac proteins are particularly associated in resistance development against different antibiotics and antiseptics (Jaglic and Cervinkova, 2012). Frequent incidences of QacA or QacB genes in *E. faecalis* and *S. aureus* have been observed, whereas in the case of *Enterobacteriaceae* and *Pseudomonas* spp., the dissemination of qacE gene was more prevalent (Jaglic and Cervinkova, 2012). SMR family members are plasmid-encoded and can often occur on integrons (the

mobile genetic elements [MGEs]), which influences the menace of horizontal spread of resistance (Bay and Turner, 2009). Incidences of QAC exposure influencing the overexpression of the efflux pump supports the horizontal transfer of integrons or MGEs harboring fluoroquinolone resistance determinants within Class I intergron (QacED1) (Anandapadamanaban et al., 2016; Buffet-Bataillon et al., 2016). The transfer of both the antibiotic-resistant and disinfectant-resistant genes between diverse species regulates the bactericidal effect of these lethal compounds.

Proteobacterial antimicrobial compound efflux family

The abundance of these efflux pump systems in proteobacteria has provided a purpose for the naming of the family as the proteobacterial antimicrobial compound efflux (PACE) family (Hassan et al., 2015a). One of the well-studied transporter proteins of the PACE family, *Acinetobacter* chlorhexidine efflux (AceI) found to be responsible for developing resistance toward different compounds and additionally, numerous homologs of AceI conferring resistance against various biocides and mediating transportation of fluorescent dyes, such as proflavine and acriflavine, has been observed which differentiates this family from other families of efflux pump (Hassan et al., 2015a). Presently, PACE family members responsible for the extrusion of around 10 substrates have been reported and the transporter proteins belonging to this family are included in the Database of Transporter Classification (Saier et al., 2016), which comes under proteobacterial chlorhexidine efflux (CHX) family (Elbourne et al., 2017). Transporter protein of the PACE superfamily has been reported for the export of biocides such as acriflavine and chlorhexidine; however, transporter AbgT having a role in the extrusion of sulphonamides was observed. Regulators play an important role in modulation the efflux pump systems for drug extrusion, and the factors influencing drug resistance such as under tetracycline exposure, TetR regulates TetB expressional level and in case of cationic antimicrobials pressure, QacR controls qacA expression (Grkovic et al., 2002). In bacterial membranes, the regulators control the systems in such a way that, when there is a requirement of efflux, and only the expression of the efflux pump will proceed; thus, avoiding lethal effect of overexpressed efflux pumps that are constitutively expressing within the bacteria and saving the cellular resources (Andersson and Levin, 1999). From a research viewpoint, the identification of the efflux pump (EP) system recognizing the substrates or novel factors associated with resistance or tolerance against drugs can be analyzed through observation of the changes occurring in their transcriptional level, and it is possible because of the constricted regulatory control of EP genes. The analysis of the transcriptional response of *A. baumannii* toward chlorhexidine (a membrane-active biocide) revealed the role of *Acinetobacter* chlorhexidine efflux protein (AceI) system in *A. baumannii* (Hassan et al., 2013, 2015b). Antibiotic-resistant strains of *A. baumannii* are becoming increasingly prevalent in hospitals because they have emerged as a major cause of Gram-negative infections.

Function and regulation mechanism of efflux pump

Efflux pump genes are present in all species of bacteria, and the efflux pump encoding genes are located either on a chromosome or a plasmid, especially in clinical cases (Piddock, 2006b; Poole, 2007). The understanding of the regulation of these efflux pumps, finding their function, their participation in developing resistance toward specific or multiple substrates, and their response under different environmental conditions, all of which were very crucial for the implementation of an accurate action plan. For a variety of membrane transporters, alternating access mechanisms have shown evolutionary persistence over the past few decades (Jardetzky, 1966). During sequential conformational modifications, a substrate-binding pocket in the middle of the transporter is exposed to the inner cellular space, while the other exposes the pocket to the outer cellular space through multiple conformational changes (Raturi et al., 2021). However, the structure and catalysis of MATE transporters underlying conformational changes are still not clearly understood. Partly, this is due to the fact that, particularly, two previously reported crystal structures of MATE transporters were with an outward-facing orientation (Raturi et al., 2021). Therefore, the MATE transporters facilitating drug/ion coupled transportation *via* Na+ or H+ coupling (Lu et al., 2013a) have already been described. The functionally diverse ABC family members utilize ATP to export their substrates and some act as ion channel modulators (Li et al., 2017). The structure of the ABC family transporter consists of two domains—one with substrate binding pocket (TMDs) and another with nucleotide-binding domain (NBDs)—which binds and initiates hydrolysis of ATP to stimulate the transport cycle (Dawson and Locher, 2006; Jin et al., 2012; Choudhury et al., 2014; Kodan et al., 2014; Johnson and Chen, 2017; Verhalen et al., 2017). An "alternating access" mechanism involved in the transportation of the substrate has been observed based on the functional and structural data available, in which the transportation triggers the switch in the conformation between inward-open, occluded, and outward-open states required for substrate transportation, and additionally, these conformational alterations are associated with the dimerization and dissociation of the nucleotide-binding domain-mediated *via* binding and hydrolysis of ATP (Khare et al., 2009; Korkhov et al., 2012; Woo et al., 2012). Consequently, in *E. coli*, the presence of ABC transporter protein MsbA utilizing the ATPase activity to transfer lipopolysaccharide precursor lipid A from the inner-cytoplasmic membrane to the outer-periplasmic membrane has been observed (Woebking et al., 2005), and as a result of its catalytic action, this enzyme is referred to as a flippase. Further, the cryogenic electron microscopy (cryo-EM) studies of the structural aspects of MsbA protein helped to understand the functional states and the visualization of the transportation route (Mi et al., 2017). However, some ABC transporters have shown that the MacB exhibits only outward-directed transport mechanism for the substrate entering through the periplasmic side, and as a result, the state of the substrate binding pocket remains in the outward direction. The transporters have the ability to interfere with their substrates from the outside facing binding pocket followed by a conformational alteration coupled with ATP hydrolysis, which

enables the reduction in the affinity toward the ligand inducing its shifting into the exterior part (Perez et al., 2015; Locher, 2016). Similar to the ABC transporter family, the mechanism of alternating access was also reported in MFS transporters as well where in the course of a transport cycle the conformational switch of the two domains within inward to outward open states has been reported (Jardetzky, 1966). According to the data obtained from lactose permease symporter (LacY), the conformational switch of the alternating access mechanism is activated *via* induced fit from the ligand binding and further, and the transport rate is governed by the electrochemical proton gradients (Kaback, 2015). The fundamental component of the model is the formation of a ternary complex when the proton and substrate bind in an ordered manner. However, various MFS transporters bind in different sequences as well, such as initiated with binding with proton, then substrate, or with a substrate first and then proton. Additionally, it has been observed that the transportation cycle of MFS protein generally involves the binding (as an initial step) followed by the release of substrate and proton, however, variations in the stoichiometric drug–proton interconversion within family members have been reported (Schaedler and Van Veen, 2010; Fluman et al., 2014). Small multidrug resistance (SMR) efflux pump system utilizes proton motive force as an energy source was previously reported *via* an experiment with *S. aureus* Smr (Sau-Smr) conducted first by Grinius and Goldberg in 1994 (Littlejohn et al., 1992; Grinius and Goldberg, 1994). Moreover, this experiment revealed that an electrochemical proton gradient was utilized as the energy source for tetraphenylphosphonium (TPP) efflux due to the reconstitution of Sau-Smr efflux within proteoliposomes. Further, under similar experimental conditions, similar results were obtained for Eco-EmrE, the SMR homolog (Yerushalmi et al., 1995, 1996). Therefore, SMR proteins are considered a proton-dependent MDR efflux pump system (Paulsen et al., 1996). Despite QACs, SMR proteins are able to transport neutral and negatively charged compounds (Jack et al., 2000; Nishino and Yamaguchi, 2001). However, previous studies revealed that the nature of the compound has a significant effect on the energy required for substrate transportation observed in Eco-EmrE studies, for example, the transportation of TPP requires movement of the charge for an active efflux besides the transportation of methyl viologen (MV) (a lipophilic divalent cation) (Yerushalmi et al., 1995; Rotem and Schuldiner, 2004). Further, as a result of several structural studies of the AcrB protein of *E. coli* by utilizing X-ray crystallography (Murakami et al., 2002; Nakashima et al., 2011; Eicher et al., 2012) and cryo-EM techniques (Du et al., 2014), the transporter protein was well-studied and became the most expansively characterized member of RND family (Zgurskaya, 2009; Zwama et al., 2019). Additionally, the interaction of AcrB with a wide range of substrates, which are chemically distinct, was analyzed to understand the poly-specificity feature of the transporter protein (Murakami et al., 2006; Nakashima et al., 2011; Eicher et al., 2012, 2014; Hung et al., 2013; Mousa et al., 2016; Sjuts et al., 2016; Zwama et al., 2018). Further, the movement of the substrates *via* the transporter is driven by the conformational changes taking place within the system, which is also revealed by the previous studies (Du et al., 2014; Blair et al., 2015). Moreover, the understanding of the function of these EP systems and the inhibition mediated *via* small molecules was simplified with the help of molecular simulation studies (Vargiu and Nikaido, 2012; Vargiu et al., 2018). The entire protein domains present were defined by the initial crystal structure developed for AcrB, which revealed that the region of transmembrane consists of 12 α-helices that anchor the inner membrane protein and supports proton movement and is accompanied by the transportation of the substrates and energy supply to drive translocation (Murakami et al., 2006; Seeger et al., 2006). Further, the entry of the substrates into the multiprotein complex is facilitated by the groove located between 8 and 9 transmembrane helices, which provide one out of two distinct access sites for the substrates, and the remaining protein residue projects into periplasm which is required for binding of the substrates and to link up with AcrA (periplasmic protein) as well as with the outer membrane channel protein TolC that is rooted in the outer membrane. The carrier domain of AcrB having the ability to span periplasm consist of four sub-domains, namely, PN1, PN2, PC1, and PC2, each of which comprises a common motif pattern, namely, two β-strand–α-helix–β-strand motif. The carrier sub-domains of all three protomers are arranged in such a way that a central pore along with a long channel extending through the membrane has been formed for the translocation of the substrate (Zwama and Yamaguchi, 2018).

Further, it has been reported that a second access site for substrate was found to be located in a cleft that formed in between PC1 and PC2 domains. The binding of AcrA and TolC is facilitated by the docking domains (DN and DC), which are located on the top of the porter domain. Additionally, tight binding of the top of AcrB with the TolC base is very essential for preventing the substrate leakage into periplasm aided by β-strands, which are placed antiparallel to generate a funnel-like construction. The crystal structure initially reported by Murakami et al. (2002) revealed the crystallized symmetrical homotrimeric structure without any bound ligand and explained the entire structural design of AcrB. According to three consequent studies published in 2006, it has been first reported that the establishment of an AcrB complex with various ligands that demonstrated the adoption of diverse conformations by each of the three protomers resulted in an asymmetrical homotrimeric structure assembly (Murakami et al., 2006; Seeger et al., 2006; Su et al., 2006), which has been indicated to be an active state. Therefore, under these circumstances, three different conformations have been well-defined as follows: (i) loose (L) that is mainly associated with the access for the substrates, (ii) tight (T) that is linked with the binding course, and (iii) open (O) state coupled with the extrusion conformation (Seeger et al., 2009; Nikaido, 2011; Eicher et al., 2012). As the substrates move over the protein, the monomer rotates between L, T, and O and returns back to L, and this "L conformer" which is accessible for substrate binding is also recognized as the resting state (Murakami et al., 2006; Seeger et al., 2006; Nakashima et al., 2011). First, the substrate enters into AcrB during the unliganded L state either from the periplasm or inner membrane envelope *via* one of the two defined entry sites, which are then released into a proximal binding pocket (PBP). Additionally, as a result of the movement of substrates *via* AcrB in the direction of the distal binding pocket (DBP), which is situated deep in the carrier domain, a conformational alteration toward the T state assisting the transfer of the substrate from the central pore of AcrB toward TolC entrance has been observed.

Subsequently, the ejection of the substrate from AcrB into TolC occurs *via* the rotating functional mechanism, which involves the protein transitional step, i.e., from state T to state O (Murakami et al., 2006; Seeger et al., 2006). Under that situation, state O which indicates an open state, a channel which is generated for substrate extrusion from AcrB to TolC and during the transportation of substrate, and several compressions and hindrances occurred inside the porter domain which facilitated the transportation of substrate in a unidirectional way toward central funnel referred as "peristaltic pump mechanism" (Seeger et al., 2006, 2008; Pos, 2009). In AcrB, the substrate entry *via* the two primary sites, primarily, *via* the proximal binding pocket (PBP) and then toward the distal binding pocket (DBP), plays an important role in defining the poly-specificity feature of the transporter.

However, in the case of hydrophobic substrates which are separated in the inner membrane's outer leaflet can enter through the TMD, containing hydrophobic grooves and are well defined as TM8 and TM9 (Murakami et al., 2006; Pos, 2009). Thereafter, tunnel 1 is formed which then elongates from the periplasmic membrane plane at the end of the TM8/TM9 groove till it links the proximal binding pocket (PBP) 2. However, comparatively, the entry of compounds confined to periplasm occurs *via* another site placed within the porter domains PC1 and PC2, ∼15 Å on top of the membrane plane, leads toward tunnel 2, which further elongates in the direction of the protein center (Eicher et al., 2012). Finally, after linking tunnels 1 and 2, it leads toward a distal binding pocket located deep within AcrB protein, where the presence of a glycine-rich switch loop that is proposed to contribute to the unidirectional movement of the substrates further facilitates the separation of distal and proximal binding pockets (Eicher et al., 2012; Zwama et al., 2018; Tam et al., 2020). As per the previous AcrB structural studies, the high molecular mass drugs, such as erythromycin and rifampicin, co-crystallize within the proximal binding pocket; however, the distal binding pockets are found to be responsible for holding both the low and high molecular mass drugs such as minocycline, doxorubicin, and neopentyl glycol derivative C7NG (Nakashima et al., 2011; Ababou and Koronakis, 2016; Sakurai et al., 2019). AcrB in *E. coli* and MexB homolog in *P. aeruginosa* and have similar structures and substrate-binding sites; therefore, both have similarities in a broad substrate specificity as well. Distal binding pocket (DBP) is a huge chamber surrounded by hydrophobic phenylalanine (Phe) residues and polar residues (Vargiu et al., 2018); further, the side chains present on these hydrophobic residues interact with the substrates through Pi–Pi stacking and van der Waals interaction, and on the contrary, polar residues interact *via* H-bonding. There are several pieces of evidence supporting the manifestation of broad substrate specificity of the pump as demonstrated by the different binding positions adopted by minocycline and doxorubicin. Moreover, according to previous structural studies, the role of a switch loop containing Gln 616–Gly 619 in regulating substrate's entrance into the distal binding pocket (Vargiu et al., 2018) and also in functioning as a barrier to separate the distal binding pocket from proximal pocket has been observed. Additionally, it has been suggested that physical contact between the substrate with the switch loop is essential for the translocation of the substrate before leaving the proximal binding pocket, and the movement instigated *via* the flexible loop facilitated the transportation of the substrates deep inside the distal binding site; however, without passing through the loop, the extrusion of the substrates *via* TolC is not possible (Nakashima et al., 2011; Eicher et al., 2012; Vargiu and Nikaido, 2012; Jamshidi et al., 2018). Immediately, after the binding of the substrate into the distal binding pocket occurs, it leads to a conformational change in the protein from state T to O and subsequently, the disintegration of tunnels 1 and 2 because of a transition of the coil to helix at N-terminal end of TM8 and extensive reorientation of carrier domains has been noticed (Zwama et al., 2017). Furthermore, for substrate transportation, a third tunnel that directs the substrates from AcrB on the way to TolC for extrusion is created in the state O (Eicher et al., 2012). Besides AcrB, the role of AcrA is also very crucial as repacking of AcrA helps to inhibit the leaking of the substrate into the periplasm *via* closing the cavities that exist inside the pump, and further, the changes arising in AcrA which result into the opening of the closed base of TolC are obviously initiated *via* the ligand binding phase due to the conformational changes occurring in AcrB. In addition, if the assemblage is exposed to the periplasm, it will restrict the opening of the TolC channel and the absence of any substrate inside a pump or extrusion of a substrate facilitates the conformational changes in AcrB from the drug transportation state to the resting state L (Wang Y. et al., 2017; Wang Z. et al., 2017). According to the aforementioned discussion regarding the homotrimeric symmetrical structure of AcrB which crystallizes immediately and forms substrate or inhibitor bound protein co-complexes because of their flexibility and multiple binding site mechanisms of AcrB, the movement for transportation of the substrates driven *via* multiple structural changes has been observed (Sakurai et al., 2019). A well-organized protein crystal required for the investigation of x-ray diffraction patterns can be difficult to grow when either of these processes is involved. However, currently, a number of compound-bounded AcrB structural studies have been carried out, which facilitated our understanding of the molecular foundation of inhibition (Murakami et al., 2006; Sennhauser et al., 2009; Nakashima et al., 2011, 2013; Eicher et al., 2012; Sjuts et al., 2016; Wang Y. et al., 2017; Wang Z. et al., 2017). Distal binding pockets (DBP) contain two characteristics crucial to inhibitor binding: (i) channels that translocate hydrophilic substrates and bind multiple drugs and (ii) a hydrophobic catcher that is located proximate to the distal binding pocket that divides this channel, which gives more attention to AcrB targeted small molecule inhibitors designing.

Efflux pumps influencing biofilm foundation and quorum sensing

Besides the contribution of efflux pumps in the development of antibiotic resistance, some other mechanisms such as biofilm formation, which is clearly a community of microbes affixed to a surface, also contribute to the progress of bacterial resistance and tolerance; additionally, it has been suggested that the efflux pump system has the capability to influence the function of biofilm either directly or indirectly (Hall and Mah, 2017; Alav et al., 2018). In *A. baumannii*, biofilm formation is inhibited due to tigecycline exposure in sub-inhibitory concentration *via* the downregulation of the adeG gene encoding for efflux pumps (Chen et al., 2017). Quorum sensing (QS) is a network that is generated

within cells to encourage mutual communication at the cellular level, and the utilization of signal transduction for participation in activities occurring inside bacteria has already been observed. The association between biofilm and QS improves bacterial viability in response to different variations in environmental signals. As an example, the ejection of acylated homoserine lactone (AHL) *via* the efflux pump system MexAB-OprM in *P. aeruginosa* is maintained by the QS contribution and overexpression of the efflux pump, which ultimately resulted in the release of QS signals (Piddock, 2006b). According to the available literature, it has been assumed that the bacterial QS mechanism is restricted if inhibitors hinder the efflux pump activity (Gupta et al., 2017). Similarly, in *S. aureus*, the inhibition of the NorA efflux pump activity due to the presence of an appropriate concentration of efflux pump inhibitor has also been described in a previous study (Sabatini et al., 2017). Additionally, the role of efflux pump systems in facilitating the pathogens in adapting to the harsh environment present within a mature biofilm, which involves response against envelope stress in maintaining the membrane rigidity and in conferring resistance toward high osmotic stress (Robin et al., 2022), such as the essential role played by the MacAB-TolC efflux pump in biofilm formation (Robin et al., 2022), has been reported. Pmt and AbaF are the two well-known MFS transporter proteins found in *A. baumannii*, which play an important role in the formation of biofilms such as Pmt in extracellular DNA extrusion and active participation of AbaF in emancipating biofilm materials (Pasqua et al., 2021). There is evidence indicating variations in bacterial membrane influencing the functioning of biofilm formation mediated *via* different MDR efflux pump systems belonging to the RND family (Yoon et al., 2016), as shown in *A. baumannii*, where the inhibition of adeAB gene expression or deletion resulting in reduced expression or hindrance of biofilm and QS systems have been described earlier (Richmond et al., 2016; Dou et al., 2017). A previous study proposed the incidence of a positive association between mRNA levels of efflux pump genes and biofilm formation, which can be influenced by the MIC levels of antibiotics such as polymyxin B or colistin (Sato et al., 2018). For example, MexGHI, an efflux pump system recognized in *P. aerugiosa* responsible for phenazine transportation, plays a crucial role in biofilm morphogenesis (Sakhtah et al., 2016). Similarly, the QS system also has a similar correlation with the efflux pump system (Liang et al., 2016). Additionally, a study evidenced the mutation in mexI, an efflux pump gene of *P. aeruginosa,* mediating the loss and reduced expression of quorum sensing molecules or virulence factors (Wolloscheck et al., 2018). The role of ATP-binding cassette (ABC) type efflux pump systems in conferring resistance toward antifungal agents that are used against fungi, mostly *Candida* species, is well known and their involvement in QS molecules secretion and influential capability toward biofilm formation is found to be similar to that of RND family members (Cannon and Holmes, 2015).

Role of efflux pump inhibitors toward antimicrobial resistance

Efflux pumps largely contribute toward multidrug resistance, both intrinsic and extrinsic in bacteria; therefore, the active participation of efflux pump inhibitors (EPIs) have a potential impact in preventing antimicrobial resistance globally. A significant challenge in the discovery of EPI has been its highly hydrophobic nature and the substrate-binding poly-specific site for the target. However, the primary studies on the x-ray crystal structures of different compounds such as pyranopyridine (Sjuts et al., 2016) and pyridopyrimidine (Nakashima et al., 2013) (Table 1) revealed that the EPIs bound to different efflux pumps of RND family of *P. aeruginosa* and *E. coli* have helped to facilitate the rapid advancement in our understanding of different mechanisms involved and the binding interactions of these EPIs. Moreover, a strong binding interface between the Phe-abundant hydrophobic trap and the inhibitor D13-9001 participates in inhibiting the conformational change from state L to T and further hinders the functional rotation mechanism. Further, it has been suggested that the entry of the substrates into the binding cleft situated between the domains PC1 and PC2 is blocked by the hydrophilic moiety existing on the inhibitor D13-9001. Phe 178 is an imperative amino acid that exists in the hydrophobic trap, which plays a vital role in the binding of inhibitors with the aromatic substrates *via* utilizing π-π stacking (Nakashima et al., 2013; Sjuts et al., 2016), and it has been reported that, by applying a structure-guided design for an effective inhibitors development, the hydrophobic trap discovery has a major role (Aron and Opperman, 2018). As these efflux pumps are considered excellent targets for antimicrobial combination treatment, facilitating the usage of synthetic (Table 1) or plant-based (Table 2) efflux pump inhibitors (EPIs) to support antimicrobial therapeutic options toward bacterial infections (Opperman and Nguyen, 2015; Alibert et al., 2017). There are several effective approaches to restrict or avoid the activity of an active efflux pump system found in bacteria such as decreasing the antibiotic binding affinity toward transporters *via* chemical structural modification of the drug, escalating the OM permeability to increase the drug concentration within cell, knocking out or impeding the efflux pump associated genes, and disrupting the supply of ATP or *via* designing compounds which have the capability to compete with the antimicrobial agents for active sites for their action to obstruct the efflux pump activity (Jamshidi et al., 2016). Additionally, approaches such as computational analysis or artificial abstraction from plants were utilized for the detection of numerous inhibitors active against both Gram-positive and Gram-negative bacteria. Researchers working on screening different natural EP inhibitor compounds *via* utilizing high-throughput methods have observed a natural compound referred to as *Terminalia chebula*, which is isolated from an Indian medicinal plant, having the ability to abolish the binding of ligands with Na+, which resulted in a change in the conformation of the transporter protein NorM found in *N. gonorrhea* to closed state (Kesherwani et al., 2017). In *E. coli*, *P. aeruginosa*, and *A. baumannii*, one of the most widely studied efflux pump inhibitors of AcrB, phenylalanyl-arginine-β-naphthylamide (PAβN), is recognized for its ability to bind with the hydrophobic pocket located within AcrB, further inhibiting the drug extrusion activity (Lomovskaya et al., 2001; Ribera et al., 2002; Kinana et al., 2016). However, few other EPIs (MBX inhibitors) having the ability to bind strongly to AcrB have also been reported (Sjuts et al., 2016). Additionally, this inhibitor can be combined with a secondary metabolite, i.e., carolacton produced by mycobacteria, which can be utilized as a

TABLE 1 Examples of synthetic efflux pump inhibitors (EPIs) having inhibitory action against Gram-negative bacteria.

S. No	Efflux pump inhibitor (EPI) types	Efflux pump substrate (s)	Effective against bacteria	References
1	Peptidomimetics	Chloramphenicol, fluoroquinolones, macrolides, carbapenem, tetracyclines	*E. coli, P. aeruginosa, K. pneumoniae, S. enterica, Campylobacter* spp., *E. aerogenes, A. baumanii*	Renau et al., 1999; Malléa et al., 2002; Mamelli et al., 2003; Lomovskaya and Bostian, 2006; Cortez-Cordova and Kumar, 2011; Vera-Leiva et al., 2018
2	Quinoline derivatives	Chloramphenicol, tetracycline, norfloxacin	*E. aerogenes, K. pneumoniae*	Chevalier et al., 2001; Gallo et al., 2003; Malléa et al., 2003; Ghisalberti et al., 2006; Mahamoud et al., 2006
3	Trimethoprim	Chloramphenicol, tetracycline, ciprofloxacin, erythromycin	*Enterobacteriaceae, P. aeruginosa*	Piddock et al., 2010
4	Aminoglycoside analogs	Tetracycline, gentamicin	*H. influenza*	Van Bambeke and Lee, 2006
5	Microbial EPIs	Levofloxacin	*P. aeruginosa*	Lee et al., 2001
6	Arylpiperazines	Chloramphenicol, tetracyclines, fluoroquinolones, macrolides, linezolid	*A. baumanii, P. aeruginosa, C. jejuni Enterobacteriaceae*	Bohnert and Kern, 2005; Kern et al., 2006; Pannek et al., 2006; Schumacher et al., 2006; Kurinčič et al., 2012; Sonnet et al., 2012
7	Indole derivatives	Chloramphenicol, erythromycin, ciprofloxacin, tetracycline	*E. coli*	Zeng et al., 2010
8	sRNA and antisense oligonucleotides	Ciprofloxacin, erythromycin	*E. coli, C. jejuni*	Van Bambeke and Lee, 2006; Mu et al., 2013
9	Arylpiperidines	Linezolid	*E. coli*	Thorarensen et al., 2001
10	Substituted polyamines	Unknown	*H. influenza*	Mahmood et al., 2016
11	Hydantoins	Chloramphenicol, nalidixic acid, sparfloxacin, doxycycline, erythromycin	*E. coli, E. aerogenes*	Handzlik et al., 2011; Otreebska-Machaj et al., 2016
12	Epinephrine	Chloramphenicol, tetracycline, ciprofloxacin, erythromycin	Enterobacteriaceae, *P. aeruginosa*	Piddock et al., 2010
13	Antibiotic analogs, tetracycline analogs	Tetracyclines	*E. coli*	Nelson et al., 1993, 1994
14	Quinazoline derivatives	Chloramphenicol, nalidixic acid, sparfloxacin	*E. aerogenes, P. aeruginosa*	Chevalier et al., 2010
15	Pyranopyridines	Fluoroquinolones, piperacillin	Enterobacteriaceae	Opperman et al., 2014; Vargiu et al., 2014; Aron and Opperman, 2016; Sjuts et al., 2016
16	Phenothiazines	Chloramphenicol, tetracyclines, nalidixic acid, levofloxacin, triclosan, erythromycin, aminoglycosides	*E. coli, S. enterica, B. pseudomallei*	Chan et al., 2007; Bailey et al., 2008; Martins et al., 2008
17	Serum compounds	Minocycline, ciprofloxacin	*A. baumanii, P. aeruginosa*	Blanchard et al., 2014
18	Antibiotics globomycin	Chloramphenicol, norfloxacin	*E. aerogenes*	Malléa et al., 2002
19	Fluoroquinolone analogs	Fluoroquinolones, macrolides	*E. coli, P. aeruginosa*	Van Bambeke and Lee, 2006
20	Pyridopyrimidines	Fluoroquinolones, B-lactams	*P. aeruginosa*	Yoshida et al., 2006, 2007
21	Naphthamides	Chloramphenicol, tetraphenylphosphonium, erythromycin	*E. coli*	Wang Y. et al., 2017; Wang Z. et al., 2017; Wang et al., 2018

potential therapeutic option against pathogens over-expressing the AcrAB-TolC efflux pump system (Donner et al., 2017). Another example of EPIs is tannic acid, which inhibits the multidrug efflux pump systems, such as Tet and Msr (Tintino et al., 2017), and is well studied in *S. aureus*. Tannic acid has also been reported to reduce the MIC levels of different antibiotics such as erythromycin and tetracycline significantly (Tintino et al., 2017). However, in clinical settings, the usage of an antibiotic along with an efflux pump inhibitor (EPI) as combination therapy is a potential challenge that depends upon the internal permeability characteristics of the bacterial outer membrane. Further, in a study done by Yang et al. (2017) the use of combination therapy against multidrug-resistant *P. aeruginosa* comprising tobramycin and EPI (NMP, paroxetine, or DBP) encourages the binding of EPI with tetracycline; additionally, the response of the combination of tobramycin plus EPI along with rifampicin, fluoroquinolone, and fosfomycin was also analyzed, which revealed that they exert a robust effect cooperatively upon the bacteria, which resulted into reduction in the MIC80 level against these antibiotics (Yang et al., 2018). Another example of combination therapy containing levofloxacin and EPI (trimethoprim and sertraline) used against *P. aeruginosa* harboring the MexAB-OprM efflux

TABLE 2 List of plant-derived efflux pump inhibitors (EPIs) having inhibitory action toward Gram-negative bacteria.

Plant	Compound extracted	Effective against	References
Ipomoea muricata	Lysergol	*E. coli*	Maurya et al., 2013
Glycine max	Daidzein	*E. coli*	Dwivedi et al., 2015
Baccharoides adoensis, Callistemon citrinus	Ethanolic extract	*Pseudomonas aeruginosa*	Chitemerere and Mukanganyama, 2014
Larrea tridentata	Nordihydroguaretic acid	*E. coli*	Ohene-Agyei et al., 2014
Lithospermum erythrorhizon	Shikonin		
Plumbagin	*Plumbago indica*		
Digitalis lanata	Lanatoside C	*E. coli, Pseudomonas aeruginosa*	Aparna et al., 2014
Acer saccharum	Phenolic-rich maple syrup extracts (PRMSE)	*E. coli, Proteus mirabilis, Pseudomonas aeruginosa*	Maisuria et al., 2015
Ammannia spp.	4-Hydroxy-alpha-tetralone + semisynthetic derivatives	*E. coli*	Dwivedi et al., 2014
Eucalyptus tereticornis	Ursolic acid	*E. coli*	Dwivedi et al., 2015
Berveris bulgaris	Berberine, palmatine	*Pseudomonas aeruginosa*	Aghayan et al., 2017
Holarrhena antidysenterica	Conessine		Siriyong et al., 2017

pump system showed a progressive advantage over monotherapy (using levofloxacin alone) (Adamson et al., 2015). Similar research conducted by Prasch and Bucar (2015) has also validated that a reduction in the antibiotic dose was observed when the combination therapy comprising EPI inhibitor and antibiotics was co-administered. Besides the aforementioned EPIs, several plant-based EPIs, have also been investigated, and above 20 different EPIs derived from plants have been reported based on their extraction mechanisms (Garvey et al., 2011b; Shiu et al., 2013). Additionally, vegetable-derived compounds, such as artesunate, berberine (Table 2), and curcumin, have also been reported to have the ability to inhibit EP activity in *E. coli* and *P. aeruginosa*, besides their anti-inflammatory and antibacterial activities (Li et al., 2011; Negi et al., 2014; Laudadio et al., 2019). Different food items such as vegetables, including *Momoedica balsamina*, spices, such as cumin and pepper, and oils extracted from aromatic plants are known for being an exceptional source of EPIs (Karumathil et al., 2018; Li et al., 2019; Tariq et al., 2019; Solnier et al., 2020; Muniz et al., 2021); further, the application of flavonoids such as flavonolignans in combating MDR *via* inhibiting efflux pump systems have been described previously (Chambers et al., 2019).

However, incidences of another resistance mechanism associated with membrane-embedded MDR efflux pumps which can extrude a wide range of noxious compounds such as antibiotics, dyes, and biocides have been reported (Mitchell et al., 2019; Jesin et al., 2020), which can be a promising novel approach for tackling the increasing risk of antibiotic-resistant bacteria. Based on previous studies, all the bacterial species possess MDR efflux pumps, conferring intrinsic resistance against antibiotics (Bay and Turner, 2009), and six different superfamilies of efflux pumps have already been reported, but mostly, the small multidrug resistance efflux pump family was studied extensively (Sun et al., 2014). In hospitals, the commonly used disinfectants, the quaternary ammonium compounds (QACs), toxic compounds such as ethidium bromide, and many other compounds such as biocides, cetyltrimethylammonium bromide (CTAB), and benzalkonium chloride (BZK) are utilized as a substrate for acquiring energy by the SMRs family members (Bay et al., 2008). A study by Kadry et al. (2017) revealed the existence of a strong correlation between the gene encoding SMR protein with the enhanced level of resistance toward compounds such as benzalkonium chloride in clinical isolates of *P. aeruginosa*.

Conclusions

In this review study, we have discussed the important role played by efflux pump family members in developing resistance against single or multiple antibiotics as well as against various compounds other than the antimicrobial agents including heavy metals, preservatives, and toxins. Apart from different classes of antibiotics, efflux pumps also provide resistance against disinfectants and virulence factors and even develop cross-resistance against other different noxious compounds, which further leads to the development of a multidrug-resistant phenotype. The working mechanism along with the regulation of an efflux pump system is an intricate process that actively participates in different biological processes in bacteria such as biofilm formation, quorum sensing, and adhesion of bacteria to host, and their progressive multiplication have been highlighted in this review. This review further highlights the importance of the discovery of novel EPIs, which should be plant-based, safe, and non-toxic, and many efflux pump inhibitors that are under clinical trial as well. Efflux pump inhibitors derived from plants are of great importance and are studied widely presently. However, the variations in function and regulatory mechanisms of the efflux pump systems along with the progress

and utilization of a variety of efflux pump inhibitors still need further exploration. According to the progressive research work, it has been suggested that TetR family members can be studied further for the discovery of antibiotic residues associated with multidrug resistance. In addition to the role of the aforementioned active regulatory proteins, some other proteins with an ability to identify single or multiple substrates and specific substrate-binding domains that can be utilized to identify antibiotic residues involved in substrate binding have been reported earlier. Therefore, other than the TetR regulatory protein, the detection of residues of antibiotics and transcriptional regulatory protein requires the utilization of efflux pump concomitant genes. Additionally, the proteins with a high substrate binding specificity toward diverse antimicrobials with more appropriate features are very demanding. Moreover, this review discussed the association of the expressional levels of efflux pump systems with various other defense mechanisms such as biofilm formation and quorum sensing, which provides novel insights for expanding the extent of fundamental research. In this article, we provided an overview of efflux genes and significant transporters indicating an area which requires persistent exploration to provide supervision for clinical practices.

Author contributions

SC was involved in the literature review, writing of the original draft, figure illustrations, conceptualization, preparing the draft of the manuscript, reviewing, editing, revising the manuscript, has contributed to the article, and approved the submitted version.

Acknowledgments

SC would like to acknowledge the support of management, Dr. S. Sumaya (Principal, Thassim Beevi College, Kilakarai, Tamil Nadu, India) and Dr. M. S. Irfan Ahmed (Director—Research and Industry–Institute Relations) for providing a stimulating environment.

Conflict of interest

The author declares that the research was conducted in the absence of any commercial or financial relationships that could be construed as a potential conflict of interest.

Publisher's note

All claims expressed in this article are solely those of the authors and do not necessarily represent those of their affiliated organizations, or those of the publisher, the editors and the reviewers. Any product that may be evaluated in this article, or claim that may be made by its manufacturer, is not guaranteed or endorsed by the publisher.

References

Ababou, A., and Koronakis, V. (2016). Structures of gate loop variants of the AcrB drug efflux pump bound by erythromycin substrate. *PLoS ONE* 11, e159154. doi: 10.1371/journal.pone.0159154

Adamson, D. H., Krikstopaityte, V., and Coote, P. J. (2015). Enhanced efficacy of putative efflux pump inhibitor/antibiotic combination treatments versus MDR strains of *Pseudomonas aeruginosa* in a Galleria mellonella *in vivo* infection model. *J. Antimicrob. Chemother.* 70, 2271–2278. doi: 10.1093/jac/dkv111

Aghayan, S. S., Mogadam, H. K., Fazli, M., Darban-Sarokhalil, D., Khoramrooz, S. S., Jabalameli, F., et al. (2017). The effects of berberine and palmatine on efflux pumps inhibition with different gene patterns in *Pseudomonas aeruginosa* isolated from burn infections. *Avicenna J. Med. Biotechnol.* 9, 2.

Alav, I., Sutton, J. M., and Rahman, K. M. (2018). Role of bacterial efflux pumps in biofilm formation. *J. Antimicrob. Chemother.* 73, 2003–2020. doi: 10.1093/jac/dky042

Alcalde-Rico, M., Hernando-Amado, S., Blanco, P., and Martínez, J. L. (2016). Multidrug efflux pumps at the crossroad between antibiotic resistance and bacterial virulence. *Front. Microbiol.* 7, 1483. doi: 10.3389/fmicb.2016.01483

Alibert, S., N'gompaza Diarra, J., Hernandez, J., Stutzmann, A., Fouad, M., Boyer, G., et al. (2017). Multidrug efflux pumps and their role in antibiotic and antiseptic resistance: a pharmacodynamic perspective. *Expert Opin. Drug Metab. Toxicol.* 13, 301–309 doi: 10.1080/17425255.2017.1251581

Allen, H. K., Donato, J., Wang, H. H., Cloud-Hansen, K. A., Davies, J., and Handelsman, J. (2010). Call of the wild: antibiotic resistance genes in natural environments. *Nat. Rev. Microbiol.* 8, 251–259. doi: 10.1038/nrmicro2312

Alm, R. A., Johnstone, M. R., and Lahiri, S. D. (2015). Characterization of *Escherichia coli* NDM isolates with decreased susceptibility to aztreonam/avibactam: role of a novel insertion in PBP3. *J. Antimicrob. Chemother.* 70, 1420–1428. doi: 10.1093/jac/dku568

Anandapadamanaban, M., Pilstål, R., Andresen, C., Trewhella, J., Moche, M., Wallner, B., et al. (2016). Mutation-induced population shift in the MexR conformational ensemble disengages DNA binding: a novel mechanism for MarR family derepression. *Structure* 24, 1311–1321. doi: 10.1016/j.str.2016.06.008

Andersson, D. I., and Levin, B. R. (1999). The biological cost of antibiotic resistance. *Curr. Opin. Microbiol.* 2, 489–493. doi: 10.1016/s1369-5274(99)00005-3

Aparna, V., Dineshkumar, K., Mohanalakshmi, N., Velmurugan, D., and Hopper, W. (2014). Identification of natural compound inhibitors for multidrug efflux pumps of *Escherichia coli* and *Pseudomonas aeruginosa* using *in silico* high-throughput virtual screening and *in vitro* validation. *PLoS ONE* 9, e101840. doi: 10.1371/journal.pone.0101840

Aron, Z., and Opperman, T. J. (2016). Optimization of a novel series of pyranopyridine RND efflux pump inhibitors. *Curr. Opin. Microbiol.* 33, 1–6. doi: 10.1016/j.mib.2016.05.007

Aron, Z., and Opperman, T. J. (2018). The hydrophobic trap—the Achilles heel of RND efflux pumps. *Res. Microbiol.* 169, 393–400. doi: 10.1016/j.resmic.2017.11.001

Augustin, R. (2010). The protein family of glucose transport facilitators: it's not only about glucose after all. *IUBMB Life* 62, 315–333. doi: 10.1002/iub.315

Bailey, A. M., Paulsen, I. T., and Piddock, L. J. (2008). RamA confers multidrug resistance in *Salmonella enterica via* increased expression of acrB, which is inhibited by chlorpromazine. *Antimicrob. Agents Chemother.* 52, 3604–3611. doi: 10.1128/AAC.00661-08

Banigan, J. R., Gayen, A., Cho, M. K., and Traaseth, N. J. (2015). A structured loop modulates coupling between the substrate-binding and dimerization domains in the multidrug resistance transporter EmrE. *J. Biol. Chem.* 290, 805–814. doi: 10.1074/jbc.M114.601963

Bay, D. C., Rommens, K. L., and Turner, R. J. (2008). Small multidrug resistance proteins: a multidrug transporter family that continues to grow. *Biochim. Biophys. Acta. Biomembr.* 1778, 1814–1838. doi: 10.1016/j.bbamem.2007.08.015

Bay, D. C., and Turner, R. J. (2009). Diversity and evolution of the small multidrug resistance protein family. *BMC Evol. Biol.* 9, 1–27. doi: 10.1186/1471-2148-9-140

Baylay, A. J., and Piddock, L. J. (2015). Clinically relevant fluoroquinolone resistance due to constitutive overexpression of the PatAB ABC transporter in *Streptococcus pneumoniae* is conferred by disruption of a transcriptional attenuator. *J. Antimicrob. Chemother.* 70, 670–679. doi: 10.1093/jac/dku449

Bhakdi, S., Mackman, N., Menestrina, G., Gray, L., Hugo, F., Seeger, W., et al. (1988). The hemolysin of *Escherichia coli*. *Eur. J. Epidemiol.* 4, 135–143. doi: 10.1007/BF00144740

Blair, J., Webber, M. A., Baylay, A. J., Ogbolu, D. O., and Piddock, L. J. (2015). Molecular mechanisms of antibiotic resistance. *Nat. Rev. Microbiol.* 13, 42–51. doi: 10.1038/nrmicro3380

Blair, J. M., and Piddock, L. J. (2016). How to measure export *via* bacterial multidrug resistance efflux pumps. *MBio* 7, e00840-16. doi: 10.1128/mBio.00840-16

Blair, J. M., Richmond, G. E., and Piddock, L. J. (2014). Multidrug efflux pumps in Gram-negative bacteria and their role in antibiotic resistance. *Future Microbiol.* 9, 1165–1177. doi: 10.2217/fmb.14.66

Blanchard, C., Barnett, P., Perlmutter, J., and Dunman, P. M. (2014). Identification of *Acinetobacter baumannii* serum-associated antibiotic efflux pump inhibitors. *Antimicrob. Agents Chemother.* 58, 6360–6370. doi: 10.1128/AAC.03535-14

Blanco, P., Hernando-Amado, S., Reales-Calderon, J. A., Corona, F., Lira, F., Alcalde-Rico, M., et al. (2016). Bacterial multidrug efflux pumps: much more than antibiotic resistance determinants. *Microorganisms* 4, 14. doi: 10.3390/microorganisms4010014

Bohnert, J. A., and Kern, W. V. (2005). Selected arylpiperazines are capable of reversing multidrug resistance in *Escherichia coli* overexpressing RND efflux pumps. *Antimicrob. Agents Chemother.* 49, 849–852. doi: 10.1128/AAC.49.2.849-852.2005

Brown, M. H., Paulsen, I. T., and Skurray, R. A. (1999). The multidrug efflux protein NorM is a prototype of a new family of transporters. *Mol. Microbiol.* 31, 394–395. doi: 10.1046/j.1365-2958.1999.01162.x

Buffet-Bataillon, S., Tattevin, P., Maillard, J. Y., Bonnaure-Mallet, M., and Jolivet-Gougeon, A. (2016). Efflux pump induction by quaternary ammonium compounds and fluoroquinolone resistance in bacteria. *Future Microbiol.* 11, 81–92. doi: 10.2217/fmb.15.131

Cannon, R. D., and Holmes, A. R. (2015). Learning the ABC of oral fungal drug resistance. *Mol. Oral Microbiol.* 30, 425–437. doi: 10.1111/omi.12109

Chambers, C. S., Viktorová, J., Rehorová, K., Biedermann, D., Turková, L., Macek, T., et al. (2019). Defying multidrug resistance! Modulation of related transporters by flavonoids and flavonolignans. *J. Agric. Food Chem.* 68, 1763–1779. doi: 10.1021/acs.jafc.9b00694

Chan, Y. Y., Ong, Y. M., and Chua, K. L. (2007). Synergistic interaction between phenothiazines and antimicrobial agents against *Burkholderia pseudomallei*. *Antimicrob. Agents Chemother.* 51, 623–630. doi: 10.1128/AAC.01033-06

Chen, H., Cao, J., Zhou, C., Liu, H., Zhang, X., and Zhou, T. (2017). Biofilm formation restrained by subinhibitory concentrations of tigecyclin in *Acinetobacter baumannii* is associated with downregulation of efflux pumps. *Chemotherapy* 62, 128–133. doi: 10.1159/000450537

Chetri, S., Bhowmik, D., Dhar, D., Chakravarty, A., and Bhattacharjee, A. (2019b). Effect of concentration gradient carbapenem exposure on expression of blaNDM-1 and acrA in carbapenem resistant *Escherichia coli*. *Infect. Genet. Evol.* 73, 332–336. doi: 10.1016/j.meegid.2019.05.024

Chetri, S., Bhowmik, D., Paul, D., Pandey, P., Chanda, D. D., Chakravarty, A., et al. (2019a). AcrAB-TolC efflux pump system plays a role in carbapenem non-susceptibility in *Escherichia coli*. *BMC. microbial.* 19, 1–7. doi: 10.1186/s12866-019-1589-1

Chetri, S., Das, B. J., Bhowmik, D., Chanda, D. D., Chakravarty, A., and Bhattacharjee, A. (2020). Transcriptional response of mar, sox and rob regulon against concentration gradient carbapenem stress within *Escherichia coli* isolated from hospital acquired infection. *BMC Res. Notes.* 13, 1–7. doi: 10.1186/s13104-020-04999-2

Chetri, S., Dolley, A., Bhowmik, D., Chanda, D. D., Chakravarty, A., and Bhattacharjee, A. (2018a). Transcriptional response of AcrEF-TolC against fluoroquinolone and carbapenem in *Escherichia coli* of clinical origin. *Indian J. Med. Microbiol.* 36, 537–540. doi: 10.4103/ijmm.IJMM_18_308

Chetri, S., Singha, K., Bhowmik, D., Chanda, D. D., Chakravarty, A., and Bhattacharjee, A. (2018b). Sub-inhibitory concentration of ertapenem induces overexpression of regulator of antibiotic resistance A in *Escherichia coli*. *Indian J. Med. Microbiol.* 36, 569–572. doi: 10.4103/ijmm.IJMM_18_436

Chetri, S., Singha, M., Bhowmik, D., Nath, K., Chanda, D. D., Chakravarty, A., et al. (2019c). Transcriptional response of OmpC and OmpF in *Escherichia coli* against differential gradient of carbapenem stress. *BMC Res. Notes.* 12, 1–6. doi: 10.1186/s13104-019-4177-4

Chevalier, J., Atifi, S., Eyraud, A., Mahamoud, A., Barbe, J., and Pagès, J. M. (2001). New pyridoquinoline derivatives as potential inhibitors of the fluoroquinolone efflux pump in resistant enterobacter a erogenes strains. *J. Med. Chem.* 44, 4023–4026. doi: 10.1021/jm010911z

Chevalier, J., Mahamoud, A., Baitiche, M., Adam, E., Viveiros, M., Smarandache, A., et al. (2010). Quinazoline derivatives are efficient chemosensitizers of antibiotic activity in Enterobacter aerogenes, Klebsiella pneumoniae and Pseudomonas aeruginosa resistant strains. *Int. J. Antimicrob. Agents.* 36, 164–168. doi: 10.1016/j.ijantimicag.2010.03.027

Chitemerere, T. A., and Mukanganyama, S. (2014). Evaluation of cell membrane integrity as a potential antimicrobial target for plant products. *BMC Complement. Altern. Med.* 14, 1–8. doi: 10.1186/1472-6882-14-278

Choudhury, H. G., Tong, Z., Mathavan, I., Li, Y., Iwata, S., Zirah, S., et al. (2014). Structure of an antibacterial peptide ATP-binding cassette transporter in a novel outward occluded state. *Proc. Natl. Acad. Sci. USA* 111, 9145–9150. doi: 10.1073/pnas.1320506111

Colque, C. A., Albarracín Orio, A. G., Feliziani, S., Marvig, R. L., Tobares, A. R., Johansen, H. K., et al. (2020). Hypermutator *Pseudomonas aeruginosa* exploits multiple genetic pathways to develop multidrug resistance during long-term infections in the airways of cystic fibrosis patients. *Antimicrob. Agents Chemother.* 64, e02142-19. doi: 10.1128/AAC.02142-19

Cooper, M. A., and Shlaes, D. (2011). Fix the antibiotics pipeline. *Nature* 472, 32–32. doi: 10.1038/472032a

Cortez-Cordova, J., and Kumar, A. (2011). Activity of the efflux pump inhibitor phenylalanine-arginine β-naphthylamide against the AdeFGH pump of *Acinetobacter baumannii*. *Int. J. Antimicrob. Agents.* 37, 420–424. doi: 10.1016/j.ijantimicag.2011.01.006

Cura, A. J., and Carruthers, A. (2012). The role of monosaccharide transport proteins in carbohydrate assimilation, distribution, metabolism and homeostasis. *Compr. Physiol.* 2, 863. doi: 10.1002/cphy.c110024

Daury, L., Orange, F., Taveau, J. C., Verchere, A., Monlezun, L., Gounou, C., et al. (2016). Tripartite assembly of RND multidrug efflux pumps. *Nat. Commun.* 7, 1–8. doi: 10.1038/ncomms10731

Dawson, R. J., and Locher, K. P. (2006). Structure of a bacterial multidrug ABC transporter. *Nature*. 443, 180–185. doi: 10.1038/nature05155

Delmar, J. A., Su, C. C., and Yu, E. W. (2014). Bacterial multidrug efflux transporters. *Annu. Rev. Biophys.* 43, 93–117. doi: 10.1146/annurev-biophys-051013-022855

Donner, J., Reck, M., Bunk, B., Jarek, M., App, C. B., Meier-Kolthoff, J. P., et al. (2017). The biofilm inhibitor carolacton enters gram-negative cells: studies using a TolC-deficient strain of *Escherichia coli*. *Msphere* 2, e00375-17. doi: 10.1128/mSphereDirect.00375-17

Dou, Y., Song, F., Guo, F., Zhou, Z., Zhu, C., Xiang, J., et al. (2017). *Acinetobacter baumannii* quorum-sensing signalling molecule induces the expression of drug-resistance genes. *Mol. Med. Rep.* 15, 4061–4068. doi: 10.3892/mmr.2017.6528

Du, D., van Veen, H. W., and Luisi, B. F. (2015). Assembly and operation of bacterial tripartite multidrug efflux pumps. *Trends Microbiol.* 23, 311–319. doi: 10.1016/j.tim.2015.01.010

Du, D., Wang, Z., James, N. R., Voss, J. E., Klimont, E., Ohene-Agyei, T., et al. (2014). Structure of the AcrAB–TolC multidrug efflux pump. *Nature* 509, 512–515. doi: 10.1038/nature13205

Du, D., Wang-Kan, X., Neuberger, A., Van Veen, H. W., Pos, K. M., Piddock, L. J., et al. (2018). Multidrug efflux pumps: structure, function and regulation. *Nat. Rev. Microbiol.* 16, 523–539. doi: 10.1038/s41579-018-0048-6

Dwivedi, G. R., Maurya, A., Yadav, D. K., Khan, F., Darokar, M. P., and Srivastava, S. K. (2015). Drug resistance reversal potential of ursolic acid derivatives against nalidixic acid-and multidrug-resistant *Escherichia coli*. *Chem. Biol. Drug Des.* 86, 272–283. doi: 10.1111/cbdd.12491

Dwivedi, G. R., Upadhyay, H. C., Yadav, D. K., Singh, V., Srivastava, S. K., Khan, F., et al. (2014). 4-Hydroxy-α-tetralone and its derivative as drug resistance reversal agents in multi drug resistant *Escherichia coli*. *Chem. Biol. Drug Des.* 83, 482–492. doi: 10.1111/cbdd.12263

Eicher, T., Cha, H. J., Seeger, M. A., Brandstätter, L., El-Delik, J., Bohnert, J. A., et al. (2012). Transport of drugs by the multidrug transporter AcrB involves an access and a deep binding pocket that are separated by a switch-loop. *Proc. Natl. Acad. Sci. USA* 109, 5687–5692. doi: 10.1073/pnas.1114944109

Eicher, T., Seeger, M. A., Anselmi, C., Zhou, W., Brandstätter, L., Verrey, F., et al. (2014). Coupling of remote alternating-access transport mechanisms for protons and substrates in the multidrug efflux pump AcrB. *Elife* 3, e03145. doi: 10.7554/eLife.03145

Elbourne, L. D., Tetu, S. G., Hassan, K. A., and Paulsen, I. T. (2017). TransportDB 2.0: a database for exploring membrane transporters in sequenced genomes from all domains of life. *Nucleic. Acids. Res.* 45, D320–D324. doi: 10.1093/nar/gkw1068

Fitzpatrick, A. W., Llabrés, S., Neuberger, A., Blaza, J. N., Bai, X. C., Okada, U., et al. (2017). Structure of the MacAB–TolC ABC-type tripartite multidrug efflux pump. *Nat. Microbiol.* 2, 1–8. doi: 10.1038/nmicrobiol.2017.70

Fluman, N., Adler, J., Rotenberg, S. A., Brown, M. H., and Bibi, E. (2014). Export of a single drug molecule in two transport cycles by a multidrug efflux pump. *Nat. Commun.* 5, 4615. doi: 10.1038/ncomms5615

Forrest, L. R., Krämer, R., and Ziegler, C. (2011). The structural basis of secondary active transport mechanisms. *Biochim. Biophys. Acta. Bioenerg.* 1807, 167–188. doi: 10.1016/j.bbabio.2010.10.014

Gallo, S., Chevalier, J., Mahamoud, A., Eyraud, A., Pagès, J. M., and Barbe, J. (2003). 4-alkoxy and 4-thioalkoxyquinoline derivatives as chemosensitizers for the

chloramphenicol-resistant clinical Enterobacter aerogenes 27 strain. *Int. J. Antimicrob. Agents.* 22, 270–273. doi: 10.1016/S0924-8579(03)00215-2

Ganas, P., Mihasan, M., Igloi, G. L., and Brandsch, R. (2007). A two-component small multidrug resistance pump functions as a metabolic valve during nicotine catabolism by Arthrobacter nicotinovorans. *Microbiology* 153, 1546–1555. doi: 10.1099/mic.0.2006/004234-0

Garvey, M. I., Baylay, A. J., Wong, R. L., and Piddock, L. J. (2011a). Overexpression of patA and patB, which encode ABC transporters, is associated with fluoroquinolone resistance in clinical isolates of *Streptococcus pneumoniae*. *Antimicrob. Agents Chemother.* 55, 190–196. doi: 10.1128/AAC.00672-10

Garvey, M. I., Rahman, M. M., Gibbons, S., and Piddock, L. J. (2011b). Medicinal plant extracts with efflux inhibitory activity against Gram-negative bacteria. *Int. J. Antimicrob. Agents.* 37, 145–151.doi: 10.1016/j.ijantimicag.2010.10.027

Ghisalberti, D., Mahamoud, A., Chevalier, J., Baitiche, M., Martino, M., Pagès, J. M., et al. (2006). Chloroquinolines block antibiotic efflux pumps in antibiotic-resistant *Enterobacter aerogenes* isolates. *Int. J. Antimicrob. Agents.* 27, 565–569. doi: 10.1016/j.ijantimicag.2006.03.010

Gillings, M. R. (2017). Class 1 integrons as invasive species. *Curr. Opin. Microbiol.* 38, 10–15. doi: 10.1016/j.mib.2017.03.002

Gilson, L., Mahanty, H. K., and Kolter, R. (1990). Genetic analysis of an MDR-like export system: the secretion of colicin V. *EMBO J.* 9, 3875–3884. doi: 10.1002/j.1460-2075.1990.tb07606.x

Grinius, L. L., and Goldberg, E. B. (1994). Bacterial multidrug resistance is due to a single membrane protein which functions as a drug pump. *J. Biol. Chem.* 269, 29998–30004. doi: 10.1016/S0021-9258(18)43980-4

Grkovic, S., Brown, M. H., and Skurray, R. A. (2002). Regulation of bacterial drug export systems. *Microbiol. Mol. Biol. Rev.* 66, 671–701. doi: 10.1128/MMBR.66.4.671-701.2002

Guan, L., and Kaback, H. R. (2006). Lessons from lactose permease. *Annu. Rev. Biophys. Biomol. Struct.* 35, 67. doi: 10.1146/annurev.biophys.35.040405.102005

Guérin, F., Galimand, M., Tuambilangana, F., Courvalin, P., and Cattoir, V. (2014). Overexpression of the novel MATE fluoroquinolone efflux pump FepA in Listeria monocytogenes is driven by inactivation of its local repressor FepR. *PLoS ONE* 9, e106340. doi: 10.1371/journal.pone.0106340

Gupta, D., Singh, A., and Khan, A. U. (2017). Nanoparticles as efflux pump and biofilm inhibitor to rejuvenate bactericidal effect of conventional antibiotics. *Nanoscale Res. Lett.* 12, 1–6. doi: 10.1186/s11671-017-2222-6

Hall, C. W., and Mah, T. F. (2017). Molecular mechanisms of biofilm-based antibiotic resistance and tolerance in pathogenic bacteria. *FEMS Microbiol. Rev.* 41, 276–301. doi: 10.1093/femsre/fux010

Handzlik, J., Szymańska, E., Chevalier, J., Otrebska, E., Kieć-Kononowicz, K., Pagès, J. M., et al. (2011). Amine–alkyl derivatives of hydantoin: new tool to combat resistant bacteria. *Eur. J. Med. Chem.* 46, 5807–5816. doi: 10.1016/j.ejmech.2011.09.032

Hassan, K. A., Elbourne, L. D., Li, L., Gamage, H. K., Liu, Q., Jackson, S. M., et al. (2015b). An ace up their sleeve: a transcriptomic approach exposes the AceI efflux protein of *Acinetobacter baumannii* and reveals the drug efflux potential hidden in many microbial pathogens. *Front. Microbiol.* 6, 333. doi: 10.3389/fmicb.2015.00333

Hassan, K. A., Jackson, S. M., Penesyan, A., Patching, S. G., Tetu, S. G., Eijkelkamp, B. A., et al. (2013). Transcriptomic and biochemical analyses identify a family of chlorhexidine efflux proteins. *Proc. Natl. Acad. Sci. USA* 110, 20254–20259. doi: 10.1073/pnas.1317052110

Hassan, K. A., Liu, Q., Elbourne, L. D., Ahmad, I., Sharples, D., Naidu, V., et al. (2018). Pacing across the membrane: the novel PACE family of efflux pumps is widespread in Gram-negative pathogens. *Res. Microbiol.* 169, 450–454. doi: 10.1016/j.resmic.2018.01.001

Hassan, K. A., Liu, Q., Henderson, P. J., and Paulsen, I. T. (2015a). Homologs of the *Acinetobacter baumannii* AceI transporter represent a new family of bacterial multidrug efflux systems. *MBio* 6, e01982–14. doi: 10.1128/mBio.01982-14

He, X., Szewczyk, P., Karyakin, A., Evin, M., Hong, W. X., Zhang, Q., et al. (2010). Structure of a cation-bound multidrug and toxic compound extrusion transporter. *Nature* 467, 991–994. doi: 10.1038/nature09408

Hellmich, U. A., Lyubenova, S., Kaltenborn, E., Doshi, R., van Veen, H. W., Prisner, T. F., et al. (2012). Probing the ATP hydrolysis cycle of the ABC multidrug transporter LmrA by pulsed EPR spectroscopy. *J. Am. Chem. Soc.* 134, 5857–5862. doi: 10.1021/ja211007t

Hellmich, U. A., Mönkemeyer, L., Velamakanni, S., van Veen, H. W., and Glaubitz, C. (2015). Effects of nucleotide binding to LmrA: a combined MAS-NMR and solution NMR study. *Biochim. Biophys. Acta- Biomembr.* 1848, 3158–3165. doi: 10.1016/j.bbamem.2015.10.003

Hernando-Amado, S., Blanco, P., Alcalde-Rico, M., Corona, F., Reales-Calderón, J. A., Sánchez, M. B., et al. (2016). Multidrug efflux pumps as main players in intrinsic and acquired resistance to antimicrobials. *Drug Resist. Updat.* 28, 13–27. doi: 10.1016/j.drup.2016.06.007

Hirai, T., Heymann, J. A., Shi, D., Sarker, R., Maloney, P. C., and Subramaniam, S. (2002). Three-dimensional structure of a bacterial oxalate transporter. *Nat. Struct. Biol.* 9, 597–600. doi: 10.1038/nsb821

Hung, L. W., Kim, H. B., Murakami, S., Gupta, G., Kim, C. Y., and Terwilliger, T. C. (2013). Crystal structure of AcrB complexed with linezolid at 3.5 Å resolution. *J. Struct. Funct. Genomics.* 14, 71–75. doi: 10.1007/s10969-013-9154-x

Iannelli, F., Santagati, M., Santoro, F., Oggioni, M. R., Stefani, S., and Pozzi, G. (2014). Nucleotide sequence of conjugative prophage *Φ*1207. 3 (formerly Tn 1207.3) carrying the mef (A)/msr (D) genes for efflux resistance to macrolides in Streptococcus pyogenes. *Front. Microbiol.* 5, 687. doi: 10.3389/fmicb.2014.00687

Ito, S., Kusuhara, H., Yokochi, M., Toyoshima, J., Inoue, K., Yuasa, H., et al. (2012). Competitive inhibition of the luminal efflux by multidrug and toxin extrusions, but not basolateral uptake by organic cation transporter 2, is the likely mechanism underlying the pharmacokinetic drug-drug interactions caused by cimetidine in the kidney. *J. Pharmacol. Exp. Ther.* 340, 393–403. doi: 10.1124/jpet.111.184986

Jack, D. L., Storms, M. L., Tchieu, J. H., Paulsen, I. T., and Saier Jr, M. H. (2000). A broad-specificity multidrug efflux pump requiring a pair of homologous SMR-type proteins. *J. Bacteriol.* 182, 2311–2313. doi: 10.1128/JB.182.8.2311-2313.2000

Jaglic, Z., and Cervinkova, D. (2012). Genetic basis of resistance to quaternary ammonium compounds–the qac genes and their role: a review. *Vet. Med.* 57, 275–281. doi: 10.17221/6013-VETMED

Jamshidi, S., Sutton, J. M., and Rahman, K. M. (2016). An overview of bacterial efflux pumps and computational approaches to study efflux pump inhibitors. *Future Med. Chem.* 8, 195–210. doi: 10.4155/fmc.15.173

Jamshidi, S., Sutton, J. M., and Rahman, K. M. (2018). Mapping the dynamic functions and structural features of acrb efflux pump transporter using accelerated molecular dynamics simulations. *Sci. Rep.* 8, 1–13. doi: 10.1038/s41598-018-28531-6

Jardetzky, O. (1966). Simple allosteric model for membrane pumps. *Nature* 211, 969–970. doi: 10.1038/211969a0

Jesin, J. A., Stone, T. A., Mitchell, C. J., Reading, E., and Deber, C. M. (2020). Peptide-based approach to inhibition of the multidrug resistance efflux pump AcrB. *Biochemistry* 59, 3973–3981. doi: 10.1021/acs.biochem.0c00417

Jin, M. S., Oldham, M. L., Zhang, Q., and Chen, J. (2012). Crystal structure of the multidrug transporter P-glycoprotein from *Caenorhabditis elegans*. *Nature* 490, 566–569. doi: 10.1038/nature11448

Jo, I., Hong, S., Lee, M., Song, S., Kim, J. S., Mitra, A. K., et al. (2017). Stoichiometry and mechanistic implications of the MacAB-TolC tripartite efflux pump. *Biochem. Biophys. Res. Commun.* 494, 668–673. doi: 10.1016/j.bbrc.2017.10.102

Johnson, Z. L., and Chen, J. (2017). Structural basis of substrate recognition by the multidrug resistance protein MRP1. *Cell.* 168, 1075–1085. doi: 10.1016/j.cell.2017.01.041

Kaback, H. R. (2015). A chemiosmotic mechanism of symport. *Proc. Natl. Acad. Sci. USA* 112, 1259–1264. doi: 10.1073/pnas.1419325112

Kadry, A. A., Serry, F. M., El-Ganiny, A. M., and El-Baz, A. M. (2017). Integron occurrence is linked to reduced biocide susceptibility in multidrug resistant *Pseudomonas aeruginosa*. *Br. J. Biomed. Sci.* 74, 78–84. doi: 10.1080/09674845.2017.1278884

Karumathil, D. P., Nair, M. S., Gaffney, J., Kollanoor-Johny, A., and Venkitanarayanan, K. (2018). Trans-cinnamaldehyde and eugenol increase *Acinetobacter baumannii* sensitivity to beta-lactam antibiotics. *Front. Microbiol.* 9, 1011. doi: 10.3389/fmicb.2018.01011

Kermani, A. A., Macdonald, C. B., Burata, O. E., Ben Koff, B., Koide, A., Denbaum, E., et al. (2020). The structural basis of promiscuity in small multidrug resistance transporters. *Nat. Commun.* 11, 1–9. doi: 10.1038/s41467-020-19820-8

Kermani, A. A., Macdonald, C. B., Gundepudi, R., and Stockbridge, R. B. (2018). Guanidinium export is the primal function of SMR family transporters. *Proc. Natl. Acad. Sci. USA* 115, 3060–3065. doi: 10.1073/pnas.1719187115

Kern, W. V., Steinke, P., Schumacher, A., Schuster, S., Baum, H. V., and Bohnert, J. A. (2006). Effect of 1-(1-naphthylmethyl)-piperazine, a novel putative efflux pump inhibitor, on antimicrobial drug susceptibility in clinical isolates of *Escherichia coli*. *J. Antimicrob. Chemother.* 57, 339–343. doi: 10.1093/jac/dki445

Kesherwani, M., Michael Gromiha, M., Fukui, K., and Velmurugan, D. (2017). Identification of novel natural inhibitor for NorM—a multidrug and toxic compound extrusion transporter—an insilico molecular modeling and simulation studies. *J. Biomol. Struct. Dyn.* 35, 58–77. doi: 10.1080/07391102.2015.1132391

Khare, D., Oldham, M. L., Orelle, C., Davidson, A. L., and Chen, J. (2009). Alternating access in maltose transporter mediated by rigid-body rotations. *Mol. Cell.* 33, 528–536. doi: 10.1016/j.molcel.2009.01.035

Kim, Y. C., and Hummer, G. (2012). Proton-pumping mechanism of cytochrome c oxidase: a kinetic master-equation approach. *Biochim. Biophys. Acta. Bioenerg.* 1817, 526–536. doi: 10.1016/j.bbabio.2011.09.004

Kinana, A. D., Vargiu, A. V., May, T., and Nikaido, H. (2016). Aminoacyl β-naphthylamides as substrates and modulators of AcrB multidrug efflux pump. *Proc. Natl. Acad. Sci. USA* 113, 1405–1410. doi: 10.1073/pnas.1525143113

Kodan, A., Yamaguchi, T., Nakatsu, T., Sakiyama, K., Hipolito, C. J., Fujioka, A., et al. (2014). Structural basis for gating mechanisms of a eukaryotic P-glycoprotein homolog. *Proc. Natl. Acad. Sci. USA* 111, 4049–4054. doi: 10.1073/pnas.1321562111

Kong, E. F., Tsui, C., Kucharíková, S., Van Dijck, P., and Jabra-Rizk, M. A. (2017). Modulation of *Staphylococcus aureus* response to antimicrobials by the *Candida albicans* quorum sensing molecule farnesol. *Antimicrob. Agents. Chemother.* 61, e01573-17. doi: 10.1128/AAC.01573-17

Korkhov, V. M., Mireku, S. A., and Locher, K. P. (2012). Structure of AMP-PNP-bound vitamin B12 transporter BtuCD–F. *Nature*. 490, 367–372. doi: 10.1038/nature11442

Kurinčič, M., Klančnik, A., and Smole Možina, S. (2012). Effects of efflux pump inhibitors on erythromycin, ciprofloxacin, and tetracycline resistance in *Campylobacter* spp. isolates. *Microb. Drug Resist.* 18, 492–501. doi: 10.1089/mdr.2012.0017

Kuroda, T., and Tsuchiya, T. (2009). Multidrug efflux transporters in the MATE family. *Biochim. Biophys. Acta. Proteins Proteom*. 1794, 763–768. doi: 10.1016/j.bbapap.2008.11.012

Kusakizako, T., Claxton, D. P., Tanaka, Y., Maturana, A. D., Kuroda, T., Ishitani, R., et al. (2019). Structural basis of H+-dependent conformational change in a bacterial MATE transporter. *Structure* 27, 293–301. doi: 10.1016/j.str.2018.10.004

Laudadio, E., Cedraro, N., Mangiaterra, G., Citterio, B., Mobbili, G., Minnelli, C., et al. (2019). Natural alkaloid berberine activity against *Pseudomonas aeruginosa* MexXY-mediated aminoglycoside resistance: *in silico* and *in vitro* studies. *J. Nat. Prod.* 82, 1935–1944. doi: 10.1021/acs.jnatprod.9b00317

Lee, M. D., Galazzo, J. L., Staley, A. L., Lee, J. C., Warren, M. S., Fuernkranz, H., et al. (2001). Microbial fermentation-derived inhibitors of efflux-pump-mediated drug resistance. *IL Farmaco* 56, 81–85. doi: 10.1016/S0014-827X(01)01002-3

Lerma, L. L., Benomar, N., Valenzuela, A. S., Muñoz, M. D. C. C., Gálvez, A., and Abriouel, H. (2014). Role of EfrAB efflux pump in biocide tolerance and antibiotic resistance of *Enterococcus faecalis* and Enterococcus faecium isolated from traditional fermented foods and the effect of EDTA as EfrAB inhibitor. *Food Microbiol.* 44, 249–257. doi: 10.1016/j.fm.2014.06.009

Levy, S. B., and Marshall, B. (2004). Antibacterial resistance worldwide: causes, challenges and responses. *Nat. Med.* 10, S122–S129. doi: 10.1038/nm1145

Li, B., Yao, Q., Pan, X. C., Wang, N., Zhang, R., Li, J., et al. (2011). Artesunate enhances the antibacterial effect of β-lactam antibiotics against *Escherichia coli* by increasing antibiotic accumulation *via* inhibition of the multidrug efflux pump system AcrAB-TolC. *J. Antimicrob. Chemother.* 66, 769–777. doi: 10.1093/jac/dkr017

Li, J., Liu, D., Tian, X., Koseki, S., Chen, S., Ye, X., et al. (2019). Novel antibacterial modalities against methicillin resistant *Staphylococcus aureus* derived from plants. *Crit. Rev. Food Sci. Nutr.* 59, S153–S161. doi: 10.1080/10408398.2018.1541865

Li, N., Wu, J. X., Ding, D., Cheng, J., Gao, N., and Chen, L. (2017). Structure of a pancreatic ATP-sensitive potassium channel. *Cell*. 168, 101–110. doi: 10.1016/j.cell.2016.12.028

Li, X. Z., Plésiat, P., and Nikaido, H. (2015). The challenge of efflux-mediated antibiotic resistance in Gram-negative bacteria. *Clin. Microbiol. Rev.* 28, 337–418. doi: 10.1128/CMR.00117-14

Liang, Z. B., Chen, Y. M., Chen, Y. F., Cheng, Y. Y., and Zhang, L. H. (2016). RND efflux pump and its interrelationship with quorum sensing system. *FEMS Microbiol. Lett.* 38, 894–901. doi: 10.16288/j.yczz.16-139

Lin, M. F., Lin, Y. Y., Tu, C. C., and Lan, C. Y. (2017). Distribution of different efflux pump genes in clinical isolates of multidrug-resistant *Acinetobacter baumannii* and their correlation with antimicrobial resistance. *J. Microbiol. Immunol. Infect.* 50, 224–231. doi: 10.1016/j.jmii.2015.04.004

Littlejohn, T. G., Paulsen, I. T., Gillespie, M. T., Tennent, J. M., Midgley, M., Jones, I. G., et al. (1992). Substrate specificity and energetics of antiseptic and disinfectant resistance in *Staphylococcus aureus*. *FEMS Microbiol. Lett*. 95, 259–265. doi: 10.1111/j.1574-6968.1992.tb05376.x

Locher, K. P. (2016). Mechanistic diversity in ATP-binding cassette (ABC) transporters. *Nat. Struct. Mol. Biol*. 23, 487–493. doi: 10.1038/nsmb.3216

Lomovskaya, O., and Bostian, K. A. (2006). Practical applications and feasibility of efflux pump inhibitors in the clinic—a vision for applied use. *Biochem. Pharmacol.* 71, 910–918. doi: 10.1016/j.bcp.2005.12.008

Lomovskaya, O., Warren, M. S., Lee, A., Galazzo, J., Fronko, R., Lee, M. A. Y., et al. (2001). Identification and characterization of inhibitors of multidrug resistance efflux pumps in *Pseudomonas aeruginosa*: novel agents for combination therapy. *Antimicrob. Agents Chemother*. 45, 105–116. doi: 10.1128/AAC.45.1.105-116.2001

Long, F., Su, C. C., Lei, H. T., Bolla, J. R., Do, S. V., and Yu, E. W. (2012). Structure and mechanism of the tripartite CusCBA heavy-metal efflux complex. *Philos. Trans. R. Soc. B Biol. Sci.* 367, 1047–1058. doi: 10.1098/rstb.2011.0203

Lu, M., Radchenko, M., Symersky, J., Nie, R., and Guo, Y. (2013b). Structural insights into H+-coupled multidrug extrusion by a MATE transporter. *Nat. Struct. Mol. Biol.* 20, 1310–1317. doi: 10.1038/nsmb.2687

Lu, M., Symersky, J., Radchenko, M., Koide, A., Guo, Y., Nie, R., et al. (2013a). Structures of a Na+-coupled, substrate-bound MATE multidrug transporter. *Proc. Natl. Acad. Sci. USA* 110, 2099–2104. doi: 10.1073/pnas.1219901110

Lu, S., and Zgurskaya, H. I. (2013). MacA, a periplasmic membrane fusion protein of the macrolide transporter MacAB-TolC, binds lipopolysaccharide core specifically and with high affinity. *J. Bacteriol*. 195, 4865–4872. doi: 10.1128/JB.00756-13

Lv, Z., Zhao, M., Wang, W., Wang, Q., Huang, M., Li, C., et al. (2021). Changing Gly311 to acidic amino acid in the MATE family protein DTX6 leads to enhanced resistance of *Arabidopsis* to the dihydropyridine herbicides. *Mol. Plant.* 14, 2115–2125. doi: 10.1016/j.molp.2021.09.002

Lytvynenko, I., Brill, S., Oswald, C., and Pos, K. M. (2016). Molecular basis of polyspecificity of the small multidrug resistance efflux pump AbeS from *Acinetobacter baumannii*. *J. Mol. Biol.* 428, 644–657. doi: 10.1016/j.jmb.2015.12.006

Mahamoud, A., Chevalier, J., Davin-Regli, A., and Barbe, J. (2006). Quinoline derivatives as promising inhibitors of antibiotic efflux pump in multidrug resistant Enterobacter aerogenes isolates. *Curr. Drug Targets*. 7, 843–847. doi: 10.2174/138945006777709557

Mahmood, Y. H., Jamshidi, S., Mark Sutton, J. M., and Rahman, K. (2016). Current advances in developing inhibitors of bacterial multidrug efflux pumps. *Curr. Med. Chem.* 23, 1062–1081. doi: 10.2174/0929867323666160304150522

Maisuria, V. B., Hosseinidoust, Z., and Tufenkji, N. (2015). Polyphenolic extract from maple syrup potentiates antibiotic susceptibility and reduces biofilm formation of pathogenic bacteria. *Appl. Environ. Microbiol.* 81, 3782–3792. doi: 10.1128/AEM.00239-15

Malléa, M., Chevalier, J., Eyraud, A., and Pagès, J. M. (2002). Inhibitors of antibiotic efflux pump in resistant Enterobacter aerogenes strains. *Biochem. Biophys. Res. Commun.* 293, 1370–1373. doi: 10.1016/S0006-291X(02)00404-7

Malléa, M., Mahamoud, A., Chevalier, J., Alibert-Franco, S., Brouant, P., Barbe, J. et al. (2003). Alkylaminoquinolines inhibit the bacterial antibiotic efflux pump in multidrug-resistant clinical isolates. *Biochem. J.* 376, 801–805. doi: 10.1042/BJ20030963

Mamelli, L., Amoros, J. P., Pagès, J. M., and Bolla, J. M. (2003). A phenylalanine–arginine β-naphthylamide sensitive multidrug efflux pump involved in intrinsic and acquired resistance of Campylobacter to macrolides. *Int. J. Antimicrob. Agents.* 22, 237–241. doi: 10.1016/S0924-8579(03)00199-7

Marger, M. D., and Saier Jr, M. H. (1993). A major superfamily of transmembrane facilitators that catalyse uniport, symport and antiport. *Trends Biochem. Sci.* 18, 13–20. doi: 10.1016/0968-0004(93)90081-w

Martins, M., Dastidar, S. G., Fanning, S., Kristiansen, J. E., Molnar, J., Pages, J. M., et al. (2008). Potential role of non-antibiotics (helper compounds) in the treatment of multidrug-resistant Gram-negative infections: mechanisms for their direct and indirect activities. *Int. J. Antimicrob. Agents.* 31, 198–208. doi: 10.1016/j.ijantimicag.2007.10.025

Masuda, S., Terada, T., Yonezawa, A., Tanihara, Y., Kishimoto, K., Katsura, T., et al. (2006). Identification and functional characterization of a new human kidney–specific H+/organic cation antiporter, kidney-specific multidrug and toxin extrusion 2. *J. Am. Soc. Nephrol.* 17, 2127–2135. doi: 10.1681/ASN.2006030205

Maurya, A., Dwivedi, G. R., Darokar, M. P., and Srivastava, S. K. (2013). Antibacterial and synergy of clavine alkaloid lysergol and its derivatives against nalidixic acid-resistant *Escherichia coli*. *Chem. Biol. Drug Des.* 81, 484–490. doi: 10.1111/cbdd.12103

Mi, W., Li, Y., Yoon, S. H., Ernst, R. K., Walz, T., and Liao, M. (2017). Structural basis of MsbA-mediated lipopolysaccharide transport. *Nature*. 549, 233–237. doi. 10.1038/nature23649

Mitchell, C. J., Stone, T. A., and Deber, C. M. (2019). Peptide-based efflux pump inhibitors of the small multidrug resistance protein from Pseudomonas aeruginosa. *Antimicrob. Agents Chemother.* 63, e00730–e00719. doi: 10.1128/AAC.00730-19

Miyauchi, H., Moriyama, S., Kusakizako, T., Kumazaki, K., Nakane, T., Yamashita, K., et al. (2017). Structural basis for xenobiotic extrusion by eukaryotic MATE transporter. *Nat. Commun.* 8, 1–11. doi: 10.1038/s41467-017-01541-0

Morita, Y., Kodama, K., Shiota, S., Mine, T., Kataoka, A., and Mizushima, T. (1998). NorM, a putative multidrug efflux protein, of *Vibrio parahaemolyticus* and its homolog in *Escherichia coli*. *Antimicrob. Agents Chemother.* 42, 1778–1782. doi: 10.1128/aac.42.7.1778

Mousa, J. J., Newsome, R. C., Yang, Y., Jobin, C., and Bruner, S. D. (2017). ClbM is a versatile, cation-promiscuous MATE transporter found in the colibactin biosynthetic gene cluster. *Biochem. Biophys. Res. Commun*. 482, 1233–1239. doi: 10.1016/j.bbrc.2016.12.018

Mousa, J. J., Yang, Y., Tomkovich, S., Shima, A., Newsome, R. C., Tripathi, P., et al. (2016). MATE transport of the *E. coli*-derived genotoxin colibactin. *Nat. Microbiol.* 1, 1–7. doi: 10.1038/nmicrobiol.2015.9

Mu, Y., Shen, Z., Jeon, B., Dai, L., and Zhang, Q. (2013). Synergistic effects of anti-CmeA and anti-CmeB peptide nucleic acids on sensitizing *Campylobacter jejuni* to antibiotics. *Antimicrob. Agents Chemother.* 57, 4575–4577. doi: 10.1128/AAC.00605-13

Munita, J. M., and Arias, C. A. (2016). Mechanisms of antibiotic resistance. *Microbiol. Spectr.* 4, 4–2. doi: 10.1128/microbiolspec.VMBF-0016-2015

Muniz, D. F., dos Santos Barbosa, C. R., de Menezes, I. R. A., de Sousa, E. O., Pereira, R. L. S., Júnior, J. T. C., et al. (2021). *In vitro* and *in silico* inhibitory effects of synthetic and natural eugenol derivatives against the NorA efflux pump in *Staphylococcus aureus*. *Food. Chem.* 337, 127776. doi: 10.1016/j.foodchem.2020.127776

Murakami, S., Nakashima, R., Yamashita, E., Matsumoto, T., and Yamaguchi, A. (2006). Crystal structures of a multidrug transporter reveal a functionally rotating mechanism. *Nature* 443, 173–179. doi: 10.1038/nature05076

Murakami, S., Nakashima, R., Yamashita, E., and Yamaguchi, A. (2002). Crystal structure of bacterial multidrug efflux transporter AcrB. *Nature* 419, 587–593. doi: 10.1038/nature01050

Nakashima, R., Sakurai, K., Yamasaki, S., Hayashi, K., Nagata, C., Hoshino, K., et al. (2013). Structural basis for the inhibition of bacterial multidrug exporters. *Nature* 500, 102–106. doi: 10.1038/nature12300

Nakashima, R., Sakurai, K., Yamasaki, S., Nishino, K., and Yamaguchi, A. (2011). Structures of the multidrug exporter AcrB reveal a proximal multisite drug-binding pocket. *Nature* 480, 565–569. doi: 10.1038/nature10641

Negi, N., Prakash, P., Gupta, M. L., and Mohapatra, T. M. (2014). Possible role of curcumin as an efflux pump inhibitor in multi drug resistant clinical isolates of *Pseudomonas aeruginosa*. *J. Clin. Diagnostic. Res.* 8, DC04. doi: 10.7860/JCDR/2014/8329.4965

Nelson, J. W., Atilho, R. M., Sherlock, M. E., Stockbridge, R. B., and Breaker, R. R. (2017). Metabolism of free guanidine in bacteria is regulated by a widespread riboswitch class. *Mol. Cell* 65, 220–230. doi: 10.1016/j.molcel.2016.11.019

Nelson, M. L., Park, B. H., Andrews, J. S., Georgian, V. A., Thomas, R. C., and Levy, S. B. (1993). Inhibition of the tetracycline efflux antiport protein by 13-thio-substituted 5-hydroxy-6-deoxytetracyclines. *J. Med. Chem.* 36, 370–377. doi: 10.1021/jm00055a008

Nelson, M. L., Park, B. H., and Levy, S. B. (1994). Molecular requirements for the inhibition of the tetracycline antiport protein and the effect of potent inhibitors on the growth of tetracycline-resistant bacteria. *J. Med. Chem.* 37, 1355–1361. doi: 10.1021/jm00035a016

Neuberger, A., Du, D., and Luisi, B. F. (2018). Structure and mechanism of bacterial tripartite efflux pumps. *Res. Microbiol.* 169, 401–413. doi: 10.1016/j.resmic.2018.05.003

Nikaido, H. (1996). Multidrug efflux pumps of gram-negative bacteria. *J. Bacteriol.* 178, 5853–5859. doi: 10.1128/jb.178.20.5853-5859.1996

Nikaido, H. (2009). Multidrug resistance in bacteria *Annu. Rev. Biochem.* 78, 119–146. doi: 10.1146/annurev.biochem.78.082907.145923

Nikaido, H. (2011). Structure and mechanism of RND-type multidrug efflux pumps. *Adv. Enzymol. Relat. Areas Mol. Biol.* 77, 1. doi: 10.1002/9780470920541.ch1

Nikaido, H., and Pagès, J. M. (2012). Broad-specificity efflux pumps and their role in multidrug resistance of Gram-negative bacteria. *FEMS Microbiol. Rev.* 36, 340–363. doi: 10.1111/j.1574-6976.2011.00290.x

Nishino, K., Nikaido, E., and Yamaguchi, A. (2009). Regulation and physiological function of multidrug efflux pumps in *Escherichia coli* and Salmonella. *Biochim. Biophys. Acta Proteins. Proteom.* 1794, 834–843. doi: 10.1016/j.bbapap.2009.02.002

Nishino, K., Senda, Y., and Yamaguchi, A. (2008). The AraC-family regulator GadX enhances multidrug resistance in *Escherichia coli* by activating expression of mdtEF multidrug efflux genes. *J. Infect. Chemother.* 14, 23–29. doi: 10.1007/s10156-007-0575-y

Nishino, K., and Yamaguchi, A. (2001). Analysis of a complete library of putative drug transporter genes in *Escherichia coli*. *J. Bacteriol.* 183, 5803–5812. doi: 10.1128/JB.183.20.5803-5812.2001

Nunez-Samudio, V., and Chesneau, O. (2013). Functional interplay between the ATP binding cassette Msr (D) protein and the membrane facilitator superfamily Mef (E) transporter for macrolide resistance in *Escherichia coli*. *Res. Microbiol.* 164, 226–235. doi: 10.1016/j.resmic.2012.12.003

Oethinger, M., Podglajen, I., Kern, W. V., and Levy, S. B. (1998). Overexpression of the marA or soxS regulatory gene in clinical topoisomerase mutants of *Escherichia coli*. *Antimicrob. Agents. Chemother.* 42, 2089–2094. doi: 10.1128/aac.42.8.2089

Ohene-Agyei, T., Mowla, R., Rahman, T., and Venter, H. (2014). Phytochemicals increase the antibacterial activity of antibiotics by acting on a drug efflux pump. *Microbiologyopen* 3, 885–896. doi: 10.1002/mbo3.212

Omote, H., Hiasa, M., Matsumoto, T., Otsuka, M., and Moriyama, Y. (2006). The MATE proteins as fundamental transporters of metabolic and xenobiotic organic cations. *Trends Pharmacol. Sci.* 27, 587–593. doi: 10.1016/j.tips.2006.09.001

O'Neill, J. (2015). *Antimicrobials in Agriculture and the Environment: Reducing Unnecessary Use and Waste. The Review on Antimicrobial Resistance*. 1–41.

Opperman, T. J., Kwasny, S. M., Kim, H. S., Nguyen, S. T., Houseweart, C., D'Souza, S., et al. (2014). Characterization of a novel pyranopyridine inhibitor of the AcrAB efflux pump of *Escherichia coli*. *Antimicrob. Agents Chemother.* 58, 722–733. doi: 10.1128/AAC.01866-13

Opperman, T. J., and Nguyen, S. T. (2015). Recent advances toward a molecular mechanism of efflux pump inhibition. *Front. Microbiol.* 6, 421. doi: 10.3389/fmicb.2015.00421

Otreebska-Machaj, E., Chevalier, J., Handzlik, J., Szymańska, E., Schabikowski, J., Boyer, G., et al. (2016). Efflux pump blockers in Gram-negative bacteria: the new generation of hydantoin based-modulators to improve antibiotic activity. *Front. Microbiol.* 7, 622. doi: 10.3389/fmicb.2016.00622

Otsuka, M., Matsumoto, T., Morimoto, R., Arioka, S., Omote, H., and Moriyama, Y. (2005). A human transporter protein that mediates the final excretion step for toxic organic cations. *Proc. Natl. Acad. Sci. USA* 102, 17923–17928. doi: 10.1073/pnas.0506483102

Padariya, M., Kalathiya, U., and Baginski, M. (2018). Structural and dynamic insights on the EmrE protein with TPP+ and related substrates through molecular dynamics simulations. *Chem. Phys. Lipids.* 212, 1–11. doi: 10.1016/j.chemphyslip.2017.12.004

Pal, C., Bengtsson-Palme, J., Kristiansson, E., and Larsson, D. G. (2015). Co-occurrence of resistance genes to antibiotics, biocides and metals reveals novel insights into their co-selection potential. *BMC Genom.* 16, 1–14. doi: 10.1186/s12864-015-2153-5

Pannek, S., Higgins, P. G., Steinke, P., Jonas, D., Akova, M., Bohnert, J. A., et al. (2006). Multidrug efflux inhibition in *Acinetobacter baumannii*: comparison between 1-(1-naphthylmethyl)-piperazine and phenyl-arginine-β-naphthylamide. *J. Antimicrob. Chemother.* 57, 970–974. doi: 10.1093/jac/dkl081

Pasqua, M., Bonaccorsi di Patti, M. C., Fanelli, G., Utsumi, R., Eguchi, Y., Trirocco, R., et al. (2021). Host-Bacterial pathogen communication: the Wily role of the multidrug efflux pumps of the MFS family. *Front. Mol. Biosci.* 8, 723274. doi: 10.3389/fmolb.2021.723274

Paulsen, I. T., Brown, M. H., and Skurray, R. A. (1996). Proton-dependent multidrug efflux systems. *Microbiol. Rev.* 60, 575–608. doi: 10.1128/mr.60.4.575-608.1996

Perez, C., Gerber, S., Boilevin, J., Bucher, M., Darbre, T., Aebi, M., et al. (2015). Structure and mechanism of an active lipid-linked oligosaccharide flippase. *Nature.* 524, 433–438. doi: 10.1038/nature14953

Pérez-Varela, M., Corral, J., Aranda, J., and Barbé, J. (2019). Roles of efflux pumps from different superfamilies in the surface-associated motility and virulence of *Acinetobacter baumannii* ATCC 17978. *Antimicrob. Agents Chemother.* 63, e02190–e02118. doi: 10.1128/AAC.02190-18

Piddock, L. J. (2006a). Clinically relevant chromosomally encoded multidrug resistance efflux pumps in bacteria. *Clin. Microbiol. Rev.* 19, 382–402. doi: 10.1128/CMR.19.2.382-402.2006

Piddock, L. J. (2006b). Multidrug-resistance efflux pumps? Not just for resistance. *Nat. Rev. Microbiol.* 4, 629–636. doi: 10.1038/nrmicro1464

Piddock, L. J., Garvey, M. I., Rahman, M. M., and Gibbons, S. (2010). Natural and synthetic compounds such as trimethoprim behave as inhibitors of efflux in Gram-negative bacteria. *J. Antimicrob. Chemother.* 65, 1215–1223. doi: 10.1093/jac/dkq079

Poole, K. (2007). Efflux pumps as antimicrobial resistance mechanisms. *Ann. Med.* 39, 162–176. doi: 10.1080/07853890701195262

Pos, K. M. (2009). Drug transport mechanism of the AcrB efflux pump. *Biochim. Biophys. Acta Proteins. Proteom.* 1794, 782–793. doi: 10.1016/j.bbapap.2008.12.015

Prasch, S., and Bucar, F. (2015). Plant derived inhibitors of bacterial efflux pumps: an update. *Phytochem. Rev.* 14, 961–974. doi: 10.1007/s11101-015-9436-y

Quistgaard, E. M., Löw, C., Guettou, F., and Nordlund, P. (2016). Understanding transport by the major facilitator superfamily (MFS): structures pave the way. *Nat. Rev. Mol. Cell. Biol.* 17, 123–132. doi: 10.1038/nrm.2015.25

Radchenko, M., Symersky, J., Nie, R., and Lu, M. (2015). Structural basis for the blockade of MATE multidrug efflux pumps. *Nat. Commun.* 6, 1–11. doi: 10.1038/ncomms8995

Raturi, S., Nair, A. V., Shinoda, K., Singh, H., Bai, B., Murakami, S., et al. (2021). Engineered MATE multidrug transporters reveal two functionally distinct ion-coupling pathways in NorM from Vibrio cholerae. *Commun. Biol.* 4, 558. doi: 10.1038/s42003-021-02081-6

Remy, E., and Duque, P. (2014). Beyond cellular detoxification: a plethora of physiological roles for MDR transporter homologs in plants. *Front. Physiol.* 5, 201. doi: 10.3389/fphys.2014.00201

Renau, T. E., Léger, R., Flamme, E. M., Sangalang, J., She, M. W., Yen, R., et al. (1999). Inhibitors of efflux pumps in *Pseudomonas aeruginosa* potentiate the activity of the fluoroquinolone antibacterial levofloxacin. *J. Med. Chem.* 42, 4928–4931. doi: 10.1021/jm9904598

Ribera, A., Ruiz, J., Jiminez de Anta, M. T., and Vila, J. (2002). Effect of an efflux pump inhibitor on the MIC of nalidixic acid for *Acinetobacter baumannii* and *Stenotrophomonas maltophilia* clinical isolates. *J. Antimicrob. Chemother.* 49, 697–698. doi: 10.1093/jac/49.4.697

Richmond, G. E., Evans, L. P., Anderson, M. J., Wand, M. E., Bonney, L. C., Ivens, A., et al. (2016). The Acinetobacter baumannii two-component system AdeRS

regulates genes required for multidrug efflux, biofilm formation, and virulence in a strain-specific manner. *MBio* 7, e00430–e00416. doi: 10.1128/mBio.00430-16

Robin, B., Nicol, M., Le, H., Tahrioui, A., Schaumann, A., Vuillemenot, J. B., et al. (2022). MacAB-TolC contributes to the development of *Acinetobacter baumannii* biofilm at the solid–liquid interface. *Front. Microbiol.* 12, 3878. doi: 10.3389/fmicb.2021.785161

Rotem, D., and Schuldiner, S. (2004). EmrE, a multidrug transporter from *Escherichia coli,* transports monovalent and divalent substrates with the same stoichiometry. *J. Biol. Chem.* 279, 48787–48793. doi: 10.1074/jbc.M408187200

Russell, A. D. (2002). Introduction of biocides into clinical practice and the impact on antibiotic-resistant bacteria. *J. Appl. Microbiol.* 92, 121S—135S. doi: 10.1046/j.1365-2672.92.5s1.12.x

Sabatini, S., Piccioni, M., Felicetti, T., De Marco, S., Manfroni, G., Pagiotti, R., et al. (2017). Investigation on the effect of known potent *S. aureus* NorA efflux pump inhibitors on the staphylococcal biofilm formation. *RSC. Adv.* 7, 37007–37014. doi: 10.1039/C7RA03859C

Saier Jr, M. H., Reddy, V. S., Tsu, B. V., Ahmed, M. S., Li, C., and Moreno-Hagelsieb, G. (2016). The transporter classification database (TCDB): recent advances. *Nucleic Acids Res.* 44, D372–D379. doi: 10.1093/nar/gkv1103

Sakhtah, H., Koyama, L., Zhang, Y., Morales, D. K., Fields, B. L., Price-Whelan, A., et al. (2016). The *Pseudomonas aeruginosa* efflux pump MexGHI-OpmD transports a natural phenazine that controls gene expression and biofilm development. *Proc. Natl. Acad. Sci. USA* 113, E3538–E3547. doi: 10.1073/pnas.1600424113

Sakurai, K., Yamasaki, S., Nakao, K., Nishino, K., Yamaguchi, A., and Nakashima, R. (2019). Crystal structures of multidrug efflux pump MexB bound with high-molecular-mass compounds. *Sci. Rep.* 9, 1–9. doi: 10.1038/s41598-019-40232-2

Salehi, B., Ghalavand, Z., Yadegar, A., and Eslami, G. (2021). Characteristics and diversity of mutations in regulatory genes of resistance-nodulation-cell division efflux pumps in association with drug-resistant clinical isolates of *Acinetobacter baumannii*. *Antimicrob. Resist. Infect. Control.* 10, 1–12. doi: 10.1186/s13756-021-00924-9

Sato, Y., Unno, Y., Ubagai, T., and Ono, Y. (2018). Sub-minimum inhibitory concentrations of colistin and polymyxin B promote *Acinetobacter baumannii* biofilm formation. *PLoS ONE* 13, e0194556. doi: 10.1371/journal.pone.0194556

Schaedler, T. A., and Van Veen, H. W. (2010). A flexible cation binding site in the multidrug major facilitator superfamily transporter LmrP is associated with variable proton coupling. *FASEB J.* 24, 3653–3661. doi: 10.1096/fj.10-156927

Schumacher, A., Steinke, P., Bohnert, J. A., Akova, M., Jonas, D., and Kern, W. V. (2006). Effect of 1-(1-naphthylmethyl)-piperazine, a novel putative efflux pump inhibitor, on antimicrobial drug susceptibility in clinical isolates of Enterobacteriaceae other than *Escherichia coli*. *J. Antimicrob. Chemother.* 57, 344–348. doi: 10.1093/jac/dki446

Seeger, M. A., Diederichs, K., Eicher, T., Brandstatter, L., Schiefner, A., Verrey, F., et al. (2008). The AcrB efflux pump: conformational cycling and peristalsis lead to multidrug resistance. *Curr. Drug. Targets* 9, 729–749. doi: 10.2174/138945008785747789

Seeger, M. A., Schiefner, A., Eicher, T., Verrey, F., Diederichs, K., and Pos, K. M. (2006). Structural asymmetry of AcrB trimer suggests a peristaltic pump mechanism. *Science* 313, 1295–1298. doi: 10.1126/science.1131542

Seeger, M. A., von Ballmoos, C., Verrey, F., and Pos, K. M. (2009). Crucial role of Asp408 in the proton translocation pathway of multidrug transporter AcrB: evidence from site-directed mutagenesis and carbodiimide labeling. *Biochemistry* 48, 5801–5812. doi: 10.1021/bi900446j

Sennhauser, G., Bukowska, M. A., Briand, C., and Grütter, M. G. (2009). Crystal structure of the multidrug exporter MexB from *Pseudomonas aeruginosa*. *J. Mol. Biol.* 389, 134–145. doi: 10.1016/j.jmb.2009.04.001

Shcherbakov, A. A., Hisao, G., Mandala, V. S., Thomas, N. E., Soltani, M., Salter, E. A., et al. (2021). Structure and dynamics of the drug-bound bacterial transporter EmrE in lipid bilayers. *Nat. Commun.* 12, 1–13. doi: 10.1038/s41467-020-20468-7

Shi, K., Cao, M., Li, C., Huang, J., Zheng, S., and Wang, G. (2019). Efflux proteins MacAB confer resistance to arsenite and penicillin/macrolide-type antibiotics in *Agrobacterium tumefaciens* 5A. *World J. Microbiol. Biotechnol.* 35, 1–10. doi: 10.1007/s11274-019-2689-7

Shimizu, T., Harada, K., Tsuyuki, Y., Kimura, Y., Miyamoto, T., Hatoya, S., et al. (2017). *In vitro* efficacy of 16 antimicrobial drugs against a large collection of β-lactamase-producing isolates of extraintestinal pathogenic *Escherichia coli* from dogs and cats *J. Med. Microbiol.* 66, 1085–1091. doi: 10.1099/jmm.0.000535

Shirshikova, T. V., Sierra-Bakhshi, C. G., Kamaletdinova, L. K., Matrosova, L. E., Khabipova, N. N., Evtugyn, V. G., et al. (2021). The ABC-type efflux pump MacAB is involved in protection of *Serratia marcescens* against aminoglycoside antibiotics, polymyxins, and oxidative stress. *Msphere* 6, e00033–e00021. doi: 10.1128/mSphere.00033-21

Shiu, W. K., Malkinson, J. P., Rahman, M. M., Curry, J., Stapleton, P., Gunaratnam, M., et al. (2013). A new plant-derived antibacterial is an inhibitor of efflux pumps in *Staphylococcus aureus*. *Int. J. Antimicrob. Agents.* 42, 513–518. doi: 10.1016/j.ijantimicag.2013.08.007

Singh, A. K., Haldar, R., Mandal, D., and Kundu, M. (2006). Analysis of the topology of Vibrio cholerae NorM and identification of amino acid residues involved in norfloxacin resistance. *Antimicrob. Agents. Chemother.* 50, 3717–3723. doi: 10.1128/AAC.00460-06

Siriyong, T., Srimanote, P., Chusri, S., Yingyongnarongkul, B. E., Suaisom, C., Tipmanee, V., et al. (2017). Conessine as a novel inhibitor of multidrug efflux pump systems in *Pseudomonas aeruginosa*. *BMC Complement Altern. Med.* 17, 1–7. doi: 10.1186/s12906-017-1913-y

Sjuts, H., Vargiu, A. V., Kwasny, S. M., Nguyen, S. T., Kim, H. S., Ding, X., et al. (2016). Molecular basis for inhibition of AcrB multidrug efflux pump by novel and powerful pyranopyridine derivatives. *Proc. Natl. Acad. Sci. USA*. 113, 3509–3514. doi: 10.1073/pnas.1602472113

Smirnova, I., Kasho, V., and Kaback, H. R. (2011). Lactose permease and the alternating access mechanism. *Biochemistry* 50, 9684–9693. doi: 10.1021/bi2014294

Solnier, J., Martin, L., Bhakta, S., and Bucar, F. (2020). Flavonoids as novel efflux pump inhibitors and antimicrobials against both environmental and pathogenic intracellular mycobacterial species. *Molecules* 25, 734. doi: 10.3390/molecules25030734

Sonnet, P., Izard, D., and Mullié, C. (2012). Prevalence of efflux-mediated ciprofloxacin and levofloxacin resistance in recent clinical isolates of *Pseudomonas aeruginosa* and its reversal by the efflux pump inhibitors 1-(1-naphthylmethyl)-piperazine and phenylalanine-arginine-β-naphthylamide. *Int. J. Antimicrob. Agents.* 39, 77–80. doi: 10.1016/j.ijantimicag.2011.08.005

Srinivasan, V. B., and Rajamohan, G. (2013). KpnEF, a new member of the *Klebsiella pneumoniae* cell envelope stress response regulon, is an SMR-type efflux pump involved in broad-spectrum antimicrobial resistance. *Antimicrob. Agents. Chemother.* 57, 4449–4462. doi: 10.1128/AAC.02284-12

Su, C. C., Li, M., Gu, R., Takatsuka, Y., McDermott, G., Nikaido, H., et al. (2006). Conformation of the AcrB multidrug efflux pump in mutants of the putative proton relay pathway. *J. Bacteriol.* 188, 7290–7296. doi: 10.1128/JB.00684-06

Sun, J., Deng, Z., and Yan, A. (2014). Bacterial multidrug efflux pumps: mechanisms, physiology and pharmacological exploitations. *Biochem. Biophys. Res. Commun.* 453, 254–267. doi: 10.1016/j.bbrc.2014.05.090

Tam, H. K., Malviya, V. N., Foong, W. E., Herrmann, A., Malloci, G., Ruggerone, P., et al. (2020). Binding and transport of carboxylated drugs by the multidrug transporter AcrB. *J. Mol. Biol.* 432, 861–877. doi: 10.1016/j.jmb.2019.12.025

Tanaka, Y., Hipolito, C. J., Maturana, A. D., Ito, K., Kuroda, T., Higuchi, T., et al. (2013). Structural basis for the drug extrusion mechanism by a MATE multidrug transporter. *Nature* 496, 247–251. doi: 10.1038/nature12014

Tanaka, Y., Iwaki, S., and Tsukazaki, T. (2017). Crystal structure of a plant multidrug and toxic compound extrusion family protein. *Structure* 25, 1455–1460. doi: 10.1016/j.str.2017.07.009

Taneja, N., and Sharma, M. (2019). Antimicrobial resistance in the environment: the Indian scenario. *Indian. J. Med. Res.* 149, 119–128. doi: 10.4103/ijmr.IJMR_331_18

Tanihara, Y., Masuda, S., Sato, T., Katsura, T., Ogawa, O., and Inui, K. I. (2007). Substrate specificity of MATE1 and MATE2-K, human multidrug and toxin extrusions/H+-organic cation antiporters. *Biochem. Pharmacol.* 74, 359–371. doi: 10.1016/j.bcp.2007.04.010

Tariq, A., Sana, M., Shaheen, A., Ismat, F., Mahboob, S., Rauf, W., et al. (2019). Restraining the multidrug efflux transporter STY4874 of Salmonella Typhi by reserpine and plant extracts. *Lett. Appl. Microbiol.* 69, 161–167. doi: 10.1111/lam.13196

Tatsuno, I., Isaka, M., Masuno, K., Hata, N., Matsumoto, M., and Hasegawa, T. (2018). Functional predominance of msr (D), which is more effective as mef (A)-associated than mef (E)-associated, over mef (A)/mef (E) in macrolide resistance in Streptococcus pyogenes. *Microb. Drug. Resist.* 24, 1089–1097. doi: 10.1089/mdr.2017.0277

Terada, T., and Inui, K. I. (2008). Physiological and pharmacokinetic roles of H+/organic cation antiporters (MATE/SLC47A). *Biochem. Pharmacol.* 75, 1689–1696. doi: 10.1016/j.bcp.2007.12.008

Thorarensen, A., Presley-Bodnar, A. L., Marotti, K. R., Boyle, T. P., Heckaman, C. L., Bohanon, M. J., et al. (2001). 3-Arylpiperidines as potentiators of existing antibacterial agents. *Bioorganic Med. Chem. Lett.* 11, 1903–1906. doi: 10.1016/S0960-894X(01)00330-4

Tintino, S. R., Morais-Tintino, C. D., Campina, F. F., Costa, M. D. S., Menezes, I. R., de Matos, Y. M. L., et al. (2017). Tannic acid affects the phenotype of *Staphylococcus aureus* resistant to tetracycline and erythromycin by inhibition of efflux pumps. *Bioorg. Chem.* 74, 197–200. doi: 10.1016/j.bioorg.2017.08.004

Van Bambeke, F., and Lee, V. J. (2006). Inhibitors of bacterial efflux pumps as adjuvants in antibiotic treatments and diagnostic tools for detection of resistance by efflux. *Recent Pat. Antiinfect. Drug Discov.* 1, 157–175. doi: 10.2174/157489106777452692

Van Veen, H. W. (2010). Last of the multidrug transporters. *Nature* 467, 926–927. doi: 10.1038/467926a

Vargiu, A. V., and Nikaido, H. (2012). Multidrug binding properties of the AcrB efflux pump characterized by molecular dynamics simulations. *Proc. Natl. Acad. Sci. USA* 109, 20637–20642. doi: 10.1073/pnas.1218348109

Vargiu, A. V., Ramaswamy, V. K., Malloci, G., Malvacio, I., Atzori, A., and Ruggerone, P. (2018). Computer simulations of the activity of RND efflux pumps. *Res. Microbiol.* 169, 384–392. doi: 10.1016/j.resmic.2017.12.001

Vargiu, A. V., Ruggerone, P., Opperman, T. J., Nguyen, S. T., and Nikaido, H. (2014). Molecular mechanism of MBX2319 inhibition of *Escherichia coli* AcrB multidrug efflux pump and comparison with other inhibitors. *Antimicrob. Agents Chemother.* 58, 6224–6234. doi: 10.1128/AAC.03283-14

Venter, H. (2019). Reversing resistance to counter antimicrobial resistance in the World Health Organisation's critical priority of most dangerous pathogens. *Biosci. Rep.* 39:BSR20180474. doi: 10.1042/BSR20180474

Venter, H., Mowla, R., Ohene-Agyei, T., and Ma, S. (2015). RND-type drug efflux pumps from Gram-negative bacteria: molecular mechanism and inhibition. *Front. Microbiol.* 6, 377. doi: 10.3389/fmicb.2015.00377

Vera-Leiva, A., Carrasco-Anabalón, S., Lima, C. A., Villagra, N., Domínguez, M., Bello-Toledo, H., et al. (2018). The efflux pump inhibitor phenylalanine-arginine β-naphthylamide (PAβN) increases resistance to carbapenems in Chilean clinical isolates of KPC-producing *Klebsiella pneumoniae*. *J. Glob. Antimicrob. Resist.* 12, 73–76. doi: 10.1016/j.jgar.2017.12.003

Verchère, A., Broutin, I., and Picard, M. (2012). Photo-induced proton gradients for the *in vitro* investigation of bacterial efflux pumps. *Sci. Rep.* 2, 1–4. doi: 10.1038/srep00306

Verhalen, B., Dastvan, R., Thangapandian, S., Peskova, Y., Koteiche, H. A., Nakamoto, R. K., et al. (2017). Energy transduction and alternating access of the mammalian ABC transporter P-glycoprotein. *Nature.* 543, 738–741. doi: 10.1038/nature21414

Wagner, D. J., Hu, T., and Wang, J. (2016). Polyspecific organic cation transporters and their impact on drug intracellular levels and pharmacodynamics. *Pharmacol. Res.* 111, 237–246. doi: 10.1016/j.phrs.2016.06.002

Walsh, C. (2003). Where will new antibiotics come from? *Nat. Rev. Microbiol.* 1, 65–70. doi: 10.1038/nrmicro727

Wang, Y., Mowla, R., Guo, L., Ogunniyi, A. D., Rahman, T., Lopes, M. A. D. B., et al. (2017). Evaluation of a series of 2-napthamide derivatives as inhibitors of the drug efflux pump AcrB for the reversal of antimicrobial resistance. *Bioorg. Med. Chem. Lett.* 27, 733–739. doi: 10.1016/j.bmcl.2017.01.042

Wang, Y., Mowla, R., Ji, S., Guo, L., Lopes, M. A. D. B., Jin, C., et al. (2018). Design, synthesis and biological activity evaluation of novel 4-subtituted 2-naphthamide derivatives as AcrB inhibitors. *Eur. J. Med. Chem.* 143, 699–709. doi: 10.1016/j.ejmech.2017.11.102

Wang, Z., Fan, G., Hryc, C. F., Blaza, J. N., Serysheva, I. I., Schmid, M. F., et al. (2017). An allosteric transport mechanism for the AcrAB-TolC multidrug efflux pump. *Elife* 6, e24905. doi: 10.7554/eLife.24905

Webber, M. A., and Piddock, L. J. V. (2003). The importance of efflux pumps in bacterial antibiotic resistance. *J. Antimicrob. Chemother.* 51, 9–11. doi: 10.1093/jac/dkg050

Wehmeier, C., Schuster, S., Fähnrich, E., Kern, W. V., and Bohnert, J. A. (2009). Site-directed mutagenesis reveals amino acid residues in the *Escherichia coli* RND efflux pump AcrB that confer macrolide resistance. *Antimicrob. Agents. Chemother.* 53, 329–330. doi: 10.1128/AAC.00921-08

Woebking, B., Reuter, G., Shilling, R. A., Velamakanni, S., Shahi, S., Venter, H., et al. (2005). Drug-lipid A interactions on the *Escherichia coli* ABC transporter MsbA. *J. Bacteriol.* 187, 6363–6369. doi: 10.1128/JB.187.18.6363-6369.2005

Wolloscheck, D., Krishnamoorthy, G., Nguyen, J., and Zgurskaya, H. I. (2018). Kinetic control of quorum sensing in *Pseudomonas aeruginosa* by multidrug efflux pumps. *ACS Infect. Dis.* 4, 185–195. doi: 10.1021/acsinfecdis.7b00160

Woo, J. S., Zeltina, A., Goetz, B. A., and Locher, K. P. (2012). X-ray structure of the Yersinia pestis heme transporter HmuUV. *Nat. Struct. Mol. Biol.* 19, 1310–1315. doi: 10.1038/nsmb.2417

Wright, D. J., and Tate, C. G. (2015). Isolation and characterisation of transport-defective substrate-binding mutants of the tetracycline antiporter TetA (B). *Biochim. Biophys. Acta. Biomembr.* 1848, 2261–2270. doi: 10.1016/j.bbamem.2015.06.026

Xu, S., Chen, G., Liu, Z., Xu, D., Wu, Z., Li, Z., et al. (2020). Site-directed mutagenesis reveals crucial residues in *Escherichia coli* resistance-nodulation-division efflux pump OqxB. *Microb. Drug. Resist.* 26, 550–560. doi: 10.1089/mdr.2019.0165

Yamaguchi, A., Nakashima, R., and Sakurai, K. (2015). Structural basis of RND-type multidrug exporters. *Front. Microbiol.* 6, 327. doi: 10.3389/fmicb.2015.0032

Yan, N. (2013). Structural advances for the major facilitator superfamily (MFS) transporters. *Trends. Biochem. Sci.* 38, 151–159. doi: 10.1016/j.tibs.2013.01.003

Yang, X., Domalaon, R., Lyu, Y., Zhanel, G. G., and Schweizer, F. (2018). Tobramycin-linked efflux pump inhibitor conjugates synergize fluoroquinolones, rifampicin and fosfomycin against multidrug-resistant *Pseudomonas aeruginosa*. *J. Clin. Med.* 7, 158. doi: 10.3390/jcm7070158

Yang, X., Goswami, S., Gorityala, B. K., Domalaon, R., Lyu, Y., Kumar, A., et al. (2017). A tobramycin vector enhances synergy and efficacy of efflux pump inhibitors against multidrug-resistant Gram-negative bacteria. *J. Med. Chem.* 60, 3913–3932. doi: 10.1021/acs.jmedchem.7b00156

Yerushalmi, H., Lebendiker, M., and Schuldiner, S. (1995). EmrE, an *Escherichia coli* 12-kDa multidrug transporter, exchanges toxic cations and H+ and is soluble in organic solvents. *J. Biol. Chem.* 270, 6856–6863. doi: 10.1074/jbc.270.12.6856

Yerushalmi, H., Lebendiker, M., and Schuldiner, S. (1996). Negative dominance studies demonstrate the oligomeric structure of EmrE, a multidrug antiporter from *Escherichia coli*. *J. Biol. Chem.* 271, 31044–31048. doi: 10.1074/jbc.271.49.31044

Yokoo, S., Yonezawa, A., Masuda, S., Fukatsu, A., Katsura, T., and Inui, K. I. (2007). Differential contribution of organic cation transporters, OCT2 and MATE1, in platinum agent-induced nephrotoxicity. *Biochem. Pharmacol.* 74, 477–487. doi: 10.1016/j.bcp.2007.03.004

Yoon, E. J., Balloy, V., Fiette, L., Chignard, M., Courvalin, P., and Grillot-Courvalin, C. (2016). Contribution of the Ade resistance-nodulation-cell division-type efflux pumps to fitness and pathogenesis of *Acinetobacter baumannii*. *MBio* 7, e00697–e00616. doi: 10.1128/mBio.00697-16

Yoshida, K. I., Nakayama, K., Kuru, N., Kobayashi, S., Ohtsuka, M., Takemura, M., et al. (2006). MexAB-OprM specific efflux pump inhibitors in *Pseudomonas aeruginosa*. Part 5: Carbon-substituted analogues at the C-2 position. *Bioorg. Med. Chem. Lett.* 14, 1993–2004. doi: 10.1016/j.bmc.2005.10.043

Yoshida, K. I., Nakayama, K., Ohtsuka, M., Kuru, N., Yokomizo, Y., Sakamoto, A., et al. (2007). MexAB-OprM specific efflux pump inhibitors in *Pseudomonas aeruginosa*. Part 7: highly soluble and in vivo active quaternary ammonium analogue D13-9001, a potential preclinical candidate. *Bioorg. Med. Chem. Lett.* 15, 7087–7097. doi: 10.1016/j.bmc.2007.07.039

Yu, K., Zhang, Y., Xu, W., Zhang, X., Xu, Y., Sun, Y., et al. (2020). Hyper-expression of the efflux pump gene adeB was found in *Acinetobacter baumannii* with decreased triclosan susceptibility. *J. Glob. Antimicrob. Resist.* 22, 367–373. doi: 10.1016/j.jgar.2020.02.027

Zeng, B., Wang, H., Zou, L., Zhang, A., Yang, X., and Guan, Z. (2010). Evaluation and target validation of indole derivatives as inhibitors of the AcrAB-TolC efflux pump. *Biosci. Biotechnol. Biochem.* 74, 2237–2241. doi: 10.1271/bbb.100433

Zgurskaya, H. I. (2009). Covalently linked AcrB giant offers a new powerful tool for mechanistic analysis of multidrug efflux in bacteria. *J. Bacteriol.* 191, 1727–1728. doi: 10.1128/JB.01718-08

Zhang, Y., Tatsuno, I., Okada, R., Hata, N., Matsumoto, M., Isaka, M., et al. (2016). Predominant role of msr (D) over mef (A) in macrolide resistance in *Streptococcus pyogenes*. *Microbiology* 162, 46–52. doi: 10.1099/mic.0.000206

Zhu, Y. G., Zhao, Y. I., Li, B., Huang, C. L., Zhang, S. Y., Yu, S., et al. (2017). Continental-scale pollution of estuaries with antibiotic resistance genes. *Nat. Microbiol.* 2, 1–7. doi: 10.1038/nmicrobiol.2016.270

Zwama, M., Hayashi, K., Sakurai, K., Nakashima, R., Kitagawa, K., Nishino, K., et al. (2017). Hoisting-loop in bacterial multidrug exporter AcrB is a highly flexible hinge that enables the large motion of the subdomains. *Front. Microbiol.* 8, 2095. doi: 10.3389/fmicb.2017.02095

Zwama, M., and Nishino, K. (2021). Ever-adapting RND efflux pumps in gram-negative multidrug-resistant pathogens: a race against time. *Antibiotics* 10, 774. doi: 10.3390/antibiotics10070774

Zwama, M., and Yamaguchi, A. (2018). Molecular mechanisms of AcrB-mediated multidrug export. *Res. Microbiol.* 169, 372–383. doi: 10.1016/j.resmic.2018.05.005

Zwama, M., Yamaguchi, A., and Nishino, K. (2019). Phylogenetic and functional characterisation of the *Haemophilus influenzae* multidrug efflux pump AcrB. *Commun. Biol.* 2, 1–11. doi: 10.1038/s42003-019-0564-6

Zwama, M., Yamasaki, S., Nakashima, R., Sakurai, K., Nishino, K., and Yamaguchi, A. (2018). Multiple entry pathways within the efflux transporter AcrB contribute to multidrug recognition. *Nat. Commun.* 9, 124. doi: 10.1038/s41467-017-02493-1

Integrating Seaweed Culture into Shrimp and Fish Farming Systems with Autonomous Underwater Vehicles (AUV)

Ms.M.Nagavalli*& Dr.A.Krishnaveni#
Assistant Professors*#
Department of Computer Science and Research Centre
Thassim Beevi Abdul Kader College For women, Kilakarai.

Abstract

Aquaculture is the fastest-growing food production sector in the world and has come under increasing focus and censure because of coastal pollution. Aquaculture involves major environmental impacts: waste discharge, nutrient pollution, and disease outbreaks. Seaweed aquaculture fulfils a vital role in protecting the marine ecosystem as well as preventing climate change. The Marine Algal Research Station at Mandapam was founded specifically to advance seaweed farming. The centre is well situated on the coastline of the Gulf of Mannar, where seaweed is widespread. Integrating seaweed culture into shrimp and fish farming systems is considered an achievable aquaculture practise. This system integrates the trophic level-specific productivity of a variety of aquatic species. This system's goal is to create a closed loop to minimise waste and decrease harmful impacts on the environment by using one species' waste as nutrients for another. The trophic levels in this system are based on the feeding habits of the aquatic organisms. In order to secure the sustainable production and growth of the coastal environment, it is highly important to protect it. Remote offshore subsea monitoring systems have the potential to become more safe, sustainable, and cost-effective with the help of Autonomous Underwater Vehicle (AUV) technology.

Keywords: Aquaculture, shrimp, coastal, Autonomous Underwater Vehicle, Marine Algal

Introduction

Mariculture is a specialized form of aquaculture that involves growing marine organisms for food and other goods in the open ocean or in seawater-filled tanks, ponds, or raceways. As an illustration, consider the farming of marine fish in salt water resources, including finfish and shellfish like cobia, pompano, sea bass, lobster, oysters, and seaweed. Mariculture also produces cosmetics, nutritional agar, jewelry (like cultivated pearls), and

fish meal, which are non-food items. When compared to fish raised in ponds or tanks, mariculture fish are said to be of greater quality and come in a wider variety of varieties.

Seaweed farming can gain from combined seaweed and shrimp production's positive effects on the environment by becoming more commercially viable. Nutrient bioremediation, mutual advantages for the co-cultured species, economic diversification, and enhanced profitability are all benefits of integrated aquaculture.

Aquaculture is the world's fastest expanding food production business, yet it has come under increased scrutiny and criticism as a result of coastal pollution. Effluents from intensive farming contain a high concentration of organic matter, nitrogen compounds, phosphorus, and other nutrients, rendering the water unsuited for aquaculture and contributing to eutrophication. Macroalgae plays an important function in reducing toxic waste to manageable levels and improving water quality. Aquaculture management can be improved by incorporating seaweeds into aquaculture systems. This procedure can be accomplished by either stocking seaweeds alongside shrimp at optimal stocking density or by recycling water through a pond augmented with seaweeds.

Since fish and seaweed are heterotrophic and autotrophic (i.e., consumers and producers, respectively) species, they complement one another and utilise each other's "waste." This method reduces any environmental impact while enhancing resource use, water quality, and the sustainability of the enterprise. It can also be used with other aquaculture species. Recirculation lessens the introduction of pathogens and fouling organisms, and the cost of biofiltration is recovered by turning surplus nutrients into high-quality seaweed biomass. The selling of the seaweed for abalone production or human consumption can bring in additional revenue.

Some animals fed diets containing halophytes showed poor development and food conversion efficiency, according to research. It has, however, been utilized in agriculture for soil fertility, vermicomposting, pharmaceutical as an anticancer, antibiotic, anti-hyperglycemia, anti-diabetes, antihypertension, and antihypotension, and cosmetic sectors. As a result, halophytes plants have the potential to be an ingredient and a strong source of protein in fish feed formulations.

Integrated multitrophic aquaculture techniques are promising options for overcoming the aforementioned issues. Coculture is a new word for a type of polyculture in which two or

more complementing organisms are cultivated in the same culture medium (Neoriet al., 2004).

At the chosen location, a circular cage with a minimum diameter of 6 m and a minimum depth of 4 m (113 m3 volume) or a rectangular cage measuring 6 x 4 x 4 m (96 m3 volume) can be installed. A larger outer net (predator net) surrounds them with a one-meter gap on all sides, and a bird net is affixed to the cage frame. Cages can be fixed or free-floating. Using mooring lines, chains, and anchors, the mooring system or assembly maintains the cage in the appropriate location and at the specified depth.

This idea is bound to help the local fishermen in coastal hamlets. Beneficiaries include SHGs, fishermen, fishing societies, farmers, and business people; people will be selected based on their awareness and passion.

- Seaweed **,** shrimp and fish growth Monitoring
- Predict optimal time of harvesting
- Water Quality management
- Eradication of predator Fishes
- Aeration
- Fertilization
- Monitor stocking

Literature Survey

The recently revealed IMTA concept offers an alternate method to long-term aquaculture. Many sites currently undertake intensive fish or shrimp cultivation as integrated units with seaweed and mollusc culture. The extractive components (seaweed and mollusks) in these IMTA systems collect their nutrients from the effluents of the fed components (fish or shrimp).

Farming integrated white shrimp with seaweed

Integrating seaweed culture into shrimp farming systems is seen to be a promising aquaculture strategy since seaweeds can convert dissolved inorganic nitrogen into biomass, which can be easily harvested.

Hong-xing Ge et al. 2019 investigated the effect of integrating green seaweed (Ulva prolifera) with Pacific white shrimp (Litopenaeus vannamei) at different water exchange

levels at a stocking density of 500 shrimp / m3. to analyze water quality and shrimp growth performance. This study showed that Pacific white shrimp culture (500 shrimp / m3) incorporates U. prolifera seaweed (800 mg / L) in culture systems with a 10% water exchange rate can control water quality and shrimp growth.

Seaweed planted in shallow water near the surface (30 to 50 centimeters) receives ample sunshine and grows rapidly. Water with a pH of 7.5 to 9.0 is generally considered good for shrimp farming. Ulva prolifera, a seaweed known for its rapid growth and reproduction, effectively eliminates nitrogen quickly. Ulva prolifera, a seaweed, claimed that the powerful may develop in a nutrient-rich environment and gather nutrients efficiently in the water.

Methodology

Biofloc Technology (BFT)

To keep high water quality in intensive aquaculture, the biofloc technology (BTF) offers an alternative to using water exchange. Biofloc uses the microorganisms already present in the culture water to purge the harmful substances that shrimp and fish emit. By doing this, the issue of excessive water use and effluent outflow is resolved. However, given that aquatic creatures only recover a small portion of the nutrients that are fed to them, there are two significant problems with this technology:

- The build up of dissolved, often non-toxic inorganic chemicals (like nitrate) and suspended organic materials.
- This is a waste of resources that the cultured animals could have used to grow.

Multitrophic Integrated Aquaculture (IMTA)

When regarded in the context of the Integrated Multi-trophic Aquaculture (IMTA) strategy, the accumulation of unrecovered nutrients that occurs in BFT in the form of suspended organic debris and inorganic dissolved substances can also be seen as an opportunity. This strategy involves using the leftovers from one species' culture as a source of nutrients for different species.

Different species are cultivated together in the same area to create a more balanced and sustainable ecosystem.

- Seaweed can be cultivated together with herbivorous fish such as tilapia
- Tilapia waste-Nutrient for salmon fish
- Salmon waste- Nutrients for Seaweed.
- Minimizes waste and maximizes the use of resources.

IMTA promotes a more balanced eco system, lowering the likelihood of disease outbreaks and other environmental issues. IMTA is a potential aquaculture strategy that can help to reduce the industry's environmental effect while enhancing efficiency and diversifying farmers' income. IMTA promotes a more balanced and sustainable ecology, making it an important tool for satisfying the increased demand for seafood while remaining environmentally responsible.

Underwater Optical Image Processing: a Comprehensive Review

The purpose of this study is to provide an overview of several underwater image-processing procedures, such as de-scattering, color restoration, and quality assessments. Finally, they summarize the future trends and challenges in underwater image sensor design and processing.

Underwater Optical-Sonar Image Fusion Systems:

Unmanned underwater operations employing remotely operated vehicles or unmanned surface vehicles have grown in popularity in recent years, ensuring human safety and labor efficiency. The improved optical and sonar pictures were fused with calibrated transformation matrices, and the underwater image quality measure (UIQM) and underwater color image quality evaluation (UCIQE) were employed as metrics to assess the proposed system's performance. The fused image in sonar image coordinates demonstrated qualitatively strong spatial agreement, with the average IoU between optical and sonar pixels in the fused images being 75%. The optical-sonar fusion technology will aid in the visualization and comprehension of underwater environments by providing color and distance information for unmanned operations.

A System for Autonomous Seaweed Farm Inspection with an Underwater Robot

The study describes a system and techniques for operating an AUV in a seaweed farm, including initial farm localization based on a prior estimate and dead-reckoning navigation, as well as ongoing farm scanning. Critical data from side scan sonars is acquired

from real surroundings at a test location in the ocean for algorithm development, and the results are demonstrated in a simulated seaweed farm configuration.

A sustainable integrated system for culture of fish, seaweed and abalone

Using an integrated design, a 3.3 m2 experimental system for intensive land-based growth of abalone, seaweed, and fish was constructed. The objectives were to achieve nutrient recycling, low water consumption, low nutrient outflow, and high yields.

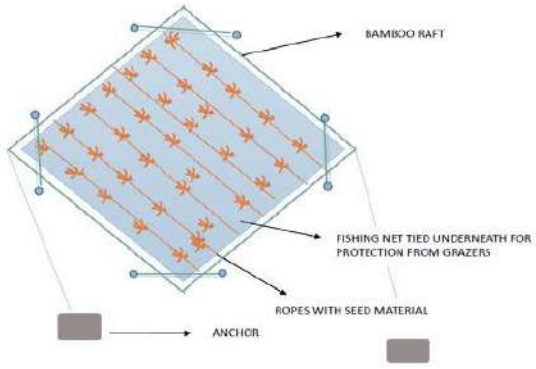

Figure 1: Bamboo raft method

A cobia cage can be connected with a total of 16 bamboo rafts, each measuring 12 feet by 12 feet and weighing 75 kg of seaweed. In a 45-day crop, the seaweed rafts that were combined with cobia cage produced an average output of 260 kg per raft as opposed to 150 kg for the unintegrated rafts. The use of cobia cage farming led to an increase of 110 kg of seaweed/raft. Additionally, the number of freshly emerged apical portions or tips in a bunch of seaweed obtained from the rafts that were integrated with the cobia cages was higher (on average 90–100 nos.,) whereas the same was lower (on average 30-40 nos.) from the rafts that were not integrated.

Figure 2: Integrating seaweed culture into shrimp and fish farming systems

An example of a multi-trophic ecosystem sharing an environment and utilizing the organic and inorganic nutrients made available by numerous organisms is shown by an integrated multi-trophic aquaculture operation in the above Figure 2.

Still, substantial and semi-intensive systems that are somewhat sustainable are where the majority of aquaculture production is produced. Concerns about the potential environmental, economic, and social effects of these frequently monospecific practices are however linked to the rapid global development of intensive marine-fed aquaculture of carnivorous finfish and shrimp, as well as to a lesser extent some shellfish aquaculture, particularly where activities are highly geographically concentrated or located in suboptimal sites whose assimilative capacities may be poorly understood and, consequently, lead to unintended consequences.

Figure 3:Shrimp farming process

The aquaculture industry needs to develop more cutting-edge, ethical, profitable, sustainable techniques that are also ecologically effective, environmentally benign, product-diversified, and societally advantageous if it is to expand. Due to the rising knowledge of picky customers regarding quality, traceability, and working conditions, maintaining sustainability has emerged as a crucial issue from not only an environmental standpoint but also from an economic, social, and technical one.

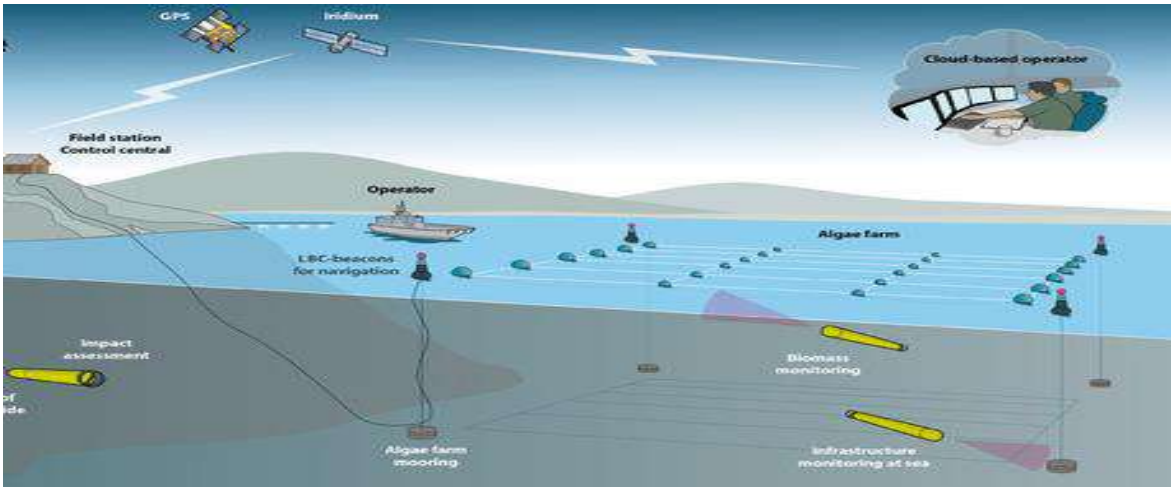

Figure 4: Monitoring System with robot

Numerous jobs that required robotic assistance have been completed by lone agents. There is more emphasis on merging numerous agents in robotic organizations in the maritime space as well, while some jobs are too complex for single agents to handle alone. This may enable these agents to perform a wider variety of activities, with the potential to develop effective systems for mapping and monitoring the maritime environment. Efficiency can be increased through integrated operations with robotic organizations, as demonstrated by Nilssen et al., even in the marine environment. Later, a large number of researchers joined the call for marine robotic organizations as a means of advancement that can lower prices and raise the complexity of jobs that can be solved.

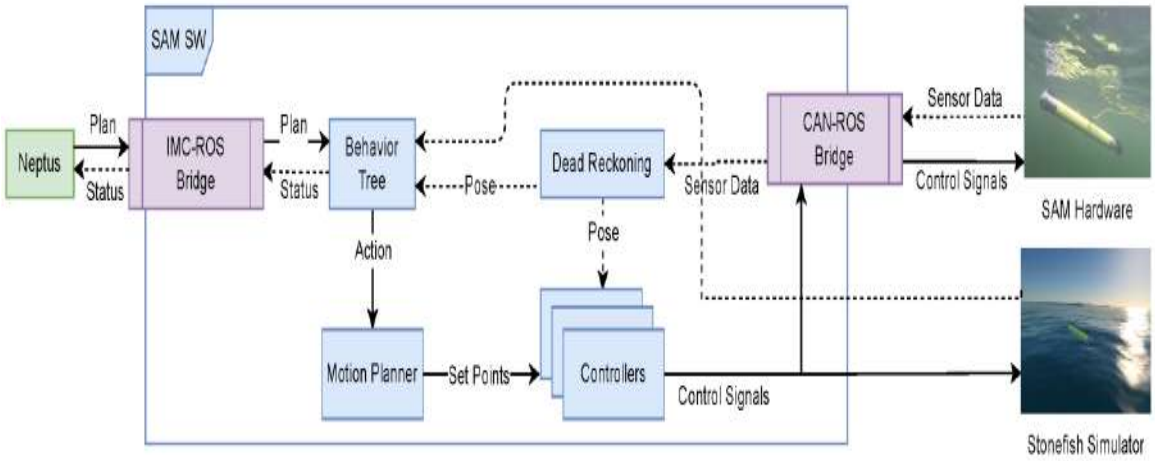

Figure 5:System architecture for shrimp farming

Superior Sensors

HUGIN Superior carries the most sensors of any commercially available AUV including the components such as HISAS 1032 Dual receiver, EM2040 Mk2, EdgeTech SBP, Cathx Ocean Camera & laser, OFG Magnetometer, Methene sensor, CTD, ADCP.

Autonomous Underwater Vehicles (AUV)

AUVs are platforms that can operate both below and above the surface and carry sensors. These agents are the vehicle itself, a control system, and maybe additional types of navigation as well as aural navigation. There are launch and recovery mechanisms for larger AUVs as well. The vehicles are available in a variety of shapes and configurations, each with a unique depth and thrust rating as well as payload sensors. There are many different types of sensors that can be used for navigation, but some of the more popular ones include cameras, GNSS, underwater acoustic location, compass, INS, and Doppler velocity log (DVL).

Around the world, the aquaculture business has been expanding quickly, with the result that waste water sources are having a substantial negative influence on the environment. As a result of this issue, numerous novel aquaculture techniques are being employed all over the nation to recycle water while reducing the amount of waste water discharged into the environment and resolving the issue of nitrogen buildup in the ecosystem. A model of aquaculture combined with seaweed or algae can be evaluated as having potential in the field of aquaculture.

From an ecological perspective, diversification also entails cultivating organisms from different and lower trophic levels, such as seaweeds, shellfish, crustaceans, echinoderms, worms, and bacteria selected based on their established or potential commercial value. This is different from simply raising different species of fish in polyculture. This strategy resembles ecosystems in nature. It is crucial to understand that there are few ways to remove nutrients from coastal ecosystems after they have done so. One of the few practical and affordable possibilities is the employment of extractive species. Therefore, when evaluating IMTA components, the economic values of extractive species' environmental services should be taken into account.

Conclusion

Technologies for seaweed aquaculture have advanced significantly over the past few decades, yet there are still obstacles to be solved. The most pressing difficulty is creating new strains using sophisticated breeding techniques. The growers will be able to extend the growing season and increase productivity thanks to superior strains. The creation of thermotolerant strains might be required in light of the problems posed by the global climate. The development of strains with disease resistance, rapid growth, high concentrations of desirable chemicals, and a decrease in fouling organisms is also necessary. It is crucial to create farm systems with advanced cultivation methods that are more reliable and economical. By transforming leftovers and uneaten feed from fed organisms into harvestable crops, IMTA promotes economic and environmental sustainability while minimizing eutrophication and enhancing economic diversification. Adopting integrated polytrophic methods should increase the aquaculture industry's environmental, economic, and social acceptability, allowing it to become a full and sustainable partner in the creation of integrated coastal management frameworks. To estimate AUV states in between position fixes, a state

estimator can also be used. A Kalman filter is one illustration of such an estimator. This might help to enhance the effectiveness of ASV tracking.

References

[1] Conchur Hughes, Jonathan W. King. Habitat suitability modelling for an integrated multi-trophic aquaculture (IMTA) system along Europe's Atlantic coast. Ecological Modelling Volume 484, October 2023, 110459.

[2]Ackefors, H. & Enell, M. 1994. The release of nutrients and organic matter from aquaculture systems in Nordic countries. *J. Appl. Ichthyol*. **10**: 225–41.

[3] Coastal Zone Canada Association 2001. *Beyond 2000: An Agenda for Integrated Coastal Management Development*. Coastal Zone Canada Association, Darmouth, 21 pp.

[4] D. Soto (Ed.), Integrated mariculture: a Global review. FAO Fisheries and Aquaculture Technical Paper. No. 529, FAO, Rome (2009), pp. 7-46

[5] Harrison, P. J. & Hurd, C. L. 2001. Nutrient physiology of seaweeds: application of concepts to aquaculture. *Cah. Biol. Mar*. **42**: 71–82.

[6] B.H. Buck, M.F. Troell, G. Krause, D.L. Angel, B. Grote, T. Chopin State of the art and challenges for offshore integrated multi-trophic aquaculture (IMTA) Front. Mar. Sci., 5 (2018), p. 165.

[7] Buschmann, A. H., López, D. A., Medina, A. 1996a. A review of the environmental effects and alternative production strategies of marine aquaculture in Chile. *Aquacult. Eng*. **15**: 397–421.

[8] Hopin, T., Yarish, C. & Sharp, G. 2001. Beyond the monospecific approach to animal aquaculture … the light of integrated aquaculture. *In* Bert, T. [Ed.]*Ecological and Genetic Implications of Aquaculture Activities*. Kluwer Academic Publishers, Dordrecht (in press).

[9] Chopin, T. Chopin Integrated Multi-Trophic Aquaculture Advancing the Aquaculture Agenda: Workshop Proceedings, OECD Publishing, Paris (2010)

[10] C. Collins, E. Bresnan, L. Brown, L. Falconer, J. Guilder, L. Jones, A. Kennerley, S. Malham, A. Murray, M. Stanley Impacts of climate change on aquaculture MCCIP Sci. Rev., (2020)

[11] Jang K. Kim, Charles Yarish3, Eun Kyoung Hwang, Miseon Park, Youngdae Kim Seaweed aquaculture: cultivation technologies, challenges and its ecosystem services. Algae 2017, 32(1): 1-13.

Hybrid Classifier System for Wheat Classification

Dr.Shweta K R[1], Dr.Krishnaveni A [2]

Assistant Professor[2], Department of Computer Science
Thassim Beevi Abdul Kader College for Women, Kilakarai- 623517, Ramanathapuram, Tamilnadu, India

Abstract:

The economy has always been based on agriculture. Due to a variety of causes, this agricultural activity has not developed. The majority of tasks are completed without the use of contemporary technologies. At the moment, seed classification is done using human knowledge. The existing analysis of seed classification is ineffective and lacks a validation system. This paper presents a hybrid classifier-based approach for classifying wheat. The outcome of the experiment shows that the proposed hybrid technique's accuracy is superior to the algorithms currently in use for classifying wheat seeds. In this work, two supervised machine learning algorithms are combined to produce a hybrid model which consists of Naïve Bayes and BayesNet algorithms. The result shows that the hybrid model gave 97% accuracy as against the 92.45% and 92.21% of the Naïve Bayes and BayesNet models respectively. The purpose of this study is to improve the prediction accuracy on seed classification by hybridizing machine learning algorithms of Naïve Bayes and BayesNet. Also, a comparison between the proposed hybrid algorithm and individual algorithms is conducted to demonstrate the increase in classification prediction accuracy. Comparing the suggested algorithm to the individual classifiers, the performance is improved.

Key Words: Naive Bayes, BayesNet, Hybrid classifier, Agriculture

I.INTRODUCTION

Wheat is an essential cereal crop for human being that counts about 50 species around the world. Wheat species are of different sizes, colors, shapes, and textures. Yellow, red, and white Wheat seeds are the most common categories.

Classification of wheat seeds has importance for reducing the cost and for increasing the yield of the corn crop. Humans can use photos of seeds to evaluate different types thanks to technology. This study will help to develop a system for the identification of wheat varieties. The identification process is conducted by analysing digital images of wheat seeds through ML techniques. In order to classify Wheat seed varieties using hybrid features, this study set out to provide an improved hybrid features classification framework.

II.REVIEW OF LITERATURE

Further details on seed quality, impurity identification, and outliers are revealed through seed analysis and categorization. Moreover, before planting, it is very necessary to check the corn variety, its condition for achieving a good yield of each variety [8]. Mostly, conventional identification methods are used in Pakistan. The scarcity of human resources stands out as a major negative. It is difficult to find these types using human base perception [9]. Classifying maize seeds is crucial for lowering costs and raising yields of the maize crop. Technology helps the human being to evaluate varieties using images of seeds [10].

This work will contribute to the creation of a system for classifying different maize types. By using Machine Learning approaches to analyse digital photographs of maize seeds, the identification procedure is carried out. During the last few years, ML approaches have motivated the researchers to overcome the given below issues, which are related to human visual perception. According to the above literature survey, such an approach has already been working for classification of crops, land covers, fruit grading and for the solution of medical problems effectively [11, 12].

Many researchers have been used the ML approaches for the classification of different seed varieties such as Pandey and his fellows proposed technique based on content-based image recovery (CBIR) to identify seeds, such as grain, wheat, or rice, based on their features. The accuracy rate of the system through the use of a support vector machine (SVM) was 84.4% while the accuracy rate of the artificial neural network (ANN) was 95% [13]. Pourreza and his co-researchers identified nine varieties of common wheat, Iranian seeds using linear discrimination analysis (LDA) classifier, and achieved accuracy 96.15% when the best 50 features of the classifier were used [14]. Silva and Sonndara categorised rice varietals with 92%

accuracy using the ANN technique. [15] The multilayer perceptron (MLP) achieved 99.46% accuracy for the classification of rice grain types, and the neuro-fuzzy classifier reached 95.73% accuracy when Pazoki and his colleagues classified five central varieties of rice grains grew up in various Iranian climates. The accuracy was 94.40% of MLP and 96.73% of the neuro-fuzzy network (NFN) after feature selections [16].

The automated system for identifying diseased maize seed was given by Daskalov and his research team. They employed an SVM classifier to classify an image taken using a CCD camera, and their accuracy rate was 93.05% [22]. Discriminant Analysis (DA) was used by Qiu and his associates to present the Cultivar Classification Corn Seed. They used wavelength features and the SVM classifier to obtain 98.78% accuracy [23]. The automatic classification framework for classifying maize seeds using computer vision was put forth by Li and his research group. To distinguish between typical and aberrant maize seeds, they employed shape and colour characteristics. Deep learning was used in the suggested framework to obtain 96.67% accuracy [24]. With the aid of a remote sensing dataset, Zhang and his co-researchers proposed the system that categorises the different types of maize seeds.

i)Naïve Bayes:

The Naive Bayes algorithm is a supervised learning method for classification issues that is based on the Bayes theorem.

- It is primarily employed in text categorization with a large training set.
- The Naive Bayes Classifier is one of the most straightforward and efficient classification algorithms, aiding in the development of quick machine learning models capable of making accurate predictions.
- Because it is a probabilistic classifier, it makes predictions based on the likelihood that an object will occur.

The words Naive and Bayes, which make up the Nave Bayes algorithm, are as follows:

- Naive: It takes the position that the existence of one feature is unrelated to the occurrence of other features, which is why it is termed naive.
- Bayes: It is so named because it relies on the Bayes' Theorem premise.

Bayes' Theorem:

- Bayes' theorem, often known as Bayes' rule or Bayes' law, is a method for calculating the likelihood of a hypothesis given some previous information. The conditional probability determines this.
- The Bayes theorem's formula is as follows:

$$P(A|B) = \frac{P(B|A)P(A)}{P(B)}$$

Where,

P(A|B) is Posterior probability: Probability of hypothesis A on the observed event B.

P(B|A) is Likelihood probability: Probability of the evidence given that the probability of a hypothesis is true.

P(A) is Prior Probability: Probability of hypothesis before observing the evidence.

P(B) is Marginal Probability: Probability of Evidence.

Naive Bayes' Classifier Operation:

1. Create frequency tables from the provided dataset.

2. Create a Likelihood table by calculating the odds of the provided attributes.

3. Next, determine the posterior probability using Bayes' theory.

ii)BayesNet:

A Bayesian network, sometimes referred to as a Bayes network, Bayes net, belief network, or judgement network, is a probabilistic graphical model that uses a directed acyclic graph (DAG) to describe a set of variables and their conditional relationships. When determining the chance that any one of a number of potential known causes

contributed to an event that already happened, Bayesian networks excel.

A Bayesian network is a directed acyclic graph where each node represents a distinct random variable and each edge represents a conditional dependency. Formally, the presence of an edge (A, B) in the graph connecting the random variables A and B indicates that P(B|A) is a component of the joint probability distribution. As a result, in order to conduct inference, we must be aware of P(B|A) for all values of A and B. Given that WetGrass has an edge into Rain in the example above, P(WetGrass|Rain) will be a factor in the conditional probability table, with its probability values listed next to the WetGrass node.

The local Markov property, which asserts that a node is conditionally independent of its non-descendants supplied, is satisfied by Bayesian networks. Given that Sprinkler is conditionally independent of its non-descendant, Rain, given Cloudy, this indicates that P(Sprinkler|Cloudy, Rain) = P(Sprinkler|Cloudy). We may reduce the joint distribution we generated using the chain rule in the previous section to a more manageable size thanks to this characteristic. The joint distribution for a Bayesian network is, after simplification, equal to the product of P(node|parents(node)) for all nodes, as follows:

$$P(X_1,\ldots,X_n)=\prod_{i=1}^{n}P(X_i\mid X_1,\ldots,X_{i-1})=\prod_{i=1}^{n}P(X_i\mid Parents(X_i))$$

Due to the fact that most nodes typically have few parents in comparison to the size of the network as a whole, this aspect enables us to significantly minimise the amount of processing needed in bigger networks.

III. METHODOLOGY

Dataset:

The proposed method for seed categorization is examined in this section. The UCI Machine Learning Repository provided the dataset. With 210 instances and 7 attributes, the seed collection contains three different types of wheat: Kama, Rosa, and Canadian. Different seed parameters are taken into consideration for the experimental purpose. Seven geometric characteristics of wheat kernels were measured to provide the data:

1. area A,
2. perimeter P,
3. compactness C = 4*pi*A/P^2,
4. length of kernel,
5. width of kernel,
6. asymmetry coefficient
7. Length of kernel groove.

The dataset including these parameters and their values is used in the suggested classification approach for wheat seed. Training and testing datasets are created from the data set. 30% of the data were used to test the model's performance, while 70% of the data were used to train the model.

Proposed Model:

The proposed model for seed classification includes following steps:

Step 1: Import the dataset

Step 2: Preprocessing of data

Step 3: Applying Hybrid classifier (Naïve Bayes and BayesNet) on preprocessed dataset

Step 4: classification of wheat seeds using hybrid classifier

IV.RESULT AND DISCUSSION:

This study set out to enhance the prediction accuracy of hybrid machine learning algorithm. Hence, this section shows the analysis results and discussion about individual and proposed hybrid machine learning classifiers prediction accuracy on classification of wheat. Here we have selected two supervised machine learning algorithms; they are Naïve Bayes algorithm and BayesNet algorithm. By combining two selected algorithms, the proposed hybrid algorithm was produced.

The Naive Bayes algorithm is combined with BayesNet algorithm to increase accuracy. The Naive Bayes provides the accuracy of 93.45.The BayesNet provides the accuracy of 94.90.The proposed hybrid algorithm provides the accuracy of 95.35, which is better than NaiveBayes and BayesNet**.** The results prove that hybrid algorithm provides more accuracy than NaiveBayes and BayesNet and this is better for seed classification base.

The following Table 1, shows the comparison of prediction accuracy of Bayesnet, Naïve Bayes algorithm and the proposed Hybrid algorithm.

The overall results show higher values of accuracy for most datasets when we compare the individual and hybrid algorithm according. It can be

observed that in many cases, the hybrid algorithm outperforms over the individual classifiers.

Table 1: Accuracy of Proposed hybrid classifier

Classifier	Accuracy
Naïve Bayes	92.90
BayesNet	92.75
Hybrid classifier	97.14

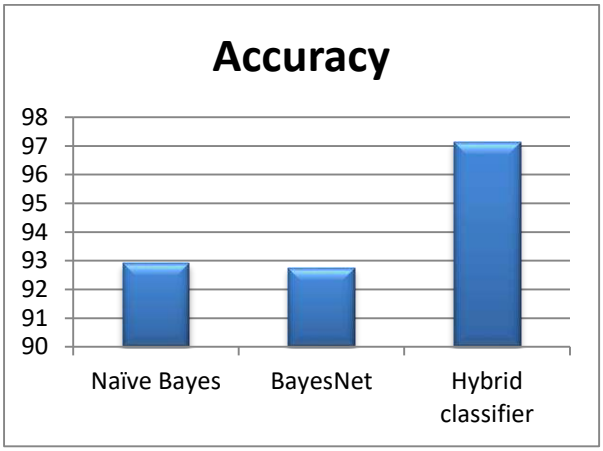

Figure 1: Accuracy of hybrid classifier

The above graph in Figure 1 shows the prediction accuracy of selected individual algorithms and proposed hybrid algorithm on seed classification. The proposed hybrid algorithm has better prediction accuracy than the individual algorithms.

V.CONCLUSION

In this study, the proposed hybrid algorithm demonstrates that hybrid machine learning techniques perform better than the individual algorithms on classification of seeds. The proposed hybrid algorithm composed of BayesNet and Naïve Bayes algorithm. The proposed hybrid algorithm outperform over the selected individual algorithms. The outcome demonstrates that the hybrid machine-learning algorithm is essential for increasing the classification precision of individual machine learning algorithms.

REFERENCES

[1]Flint-Garcia, S. A. 1 Kernel Evolution: From Teosinte to Maize. In Maize Kernel Development, 2017; pp 1.

[2] Chopin, F.; Roucolle, J. U.S. Patent No. 9,661,820; U.S. Patent and Trademark Office: Washington, DC, 2017.

[3] Saeed, M. A.; Irshad, A.; Sattar, H.; Andrews, G. E.; Phylaktou, H. N.; Gibbs, B. M. Agricultural Waste Biomass Energy Potential in Pakistan. Proceedings of the International Conference held in Shanghai, PR China, Leeds, October, 2015.

[4] Lynch, P. J.; Stangland, G. R.; Holland, G. J. U.S. Patent No. 9,072,266; U.S. Patent and Trademark Office: Washington, DC, 2015.

[5] Sastry, K. S. Methods of Combating Seed-transmitted Virus Diseases. In Seed-borne Plant Virus Diseases; Springer: India, 2013; pp 185–284.

[6] Liu, K. Soybeans: Chemistry, Technology, and Utilization; Springer, 2012.

[7] Kamilaris, A.; Prenafeta-Boldú, F. X. Deep Learning in Agriculture: A Survey. Comput. Electron. Agric. 2018, 147, 70–90. DOI: 10.1016/j.compag.2018.02.016.

[8] Tarabalka, Y.; Benediktsson, J. A.; Chanussot, J.; Tilton, J. C. Multiple Spectral-spatial Classification Approach for Hyperspectral Data. IEEE Transactions on Geoscience and Remote Sensing. 2010. DOI: 10.1109/ TGRS.2010.2062526.

[9] Asif, S.; Ahmad, M.; Zafar, M.; Ali, N. Prospects and Potential of Fatty Acid Methyl Esters of Some Non-edible Seed Oils for Use as Biodiesel in Pakistan. Renewable Sustainable Energy Rev. 2017, 74, 687–702. DOI: 10.1016/j. rser.2017.02.036.

[10] Altieri, M. A. Agroecology: The Science of Sustainable Agriculture; CRC Press, 2018.

[11] Mccabe, D.; Kadir, T.; Rodrigues, E. U.S. Patent Application No. 13/304,512, 2018.

[12] Qadri, S.; Khan, D. M.; Qadri, S. F.; Razzaq, A.; Ahmad, N.; Jamil, M.; Awan, S. A. Multisource Data Fusion Framework for Land Use/land Cover Classification Using Machine Vision. J. Sens. 2017, 2017, 1–8. DOI: 10.1155/ 2017/3515418.

[13] Pandey, R.; Naik, S.; Marfatia, R. Image Processing and Machine Learning for Automated Fruit Grading System: A Technical Review. Int. J. Comput. Appl. 2013, 81(16), 29–39. DOI: 10.5120/14209-2455.

[14] Pourreza, A.; Pourreza, H.; Abbaspour-Fard, M. H.; Sadrnia, H. Identification of Nine Iranian Wheat Seed Varieties by Textural Analysis with Image

Processing. Comput. Electron. Agric. 2012, 83, 102–108. DOI: 10.1016/ j.compag.2012.02.005.

[15] Silva, C. S.; Sonnadara, U. Classification of rice grains using neural networks; 2013.

[16] Pazoki, A. R.; Farokhi, F.; Pazoki, Z. Classification of Rice Grain Varieties Using Two Artificial Neural Networks (MLP and Neuro-Fuzzy). J. Anim. Plant Sci. 2014, 24(1), 336–343.

[17] Khoshroo, A. L. I. R. E. Z. A.; Arefi, A. R. M. A. N.; Masoumiasl, A. S. A. D.; Jowkar, G. H. Classification of Wheat Cultivars Using Image Processing and Artificial Neural Networks. Agric. Commun. 2014, 2(1), 17–22.

[18] Shahid, M.; Naweed, M.; Qadri, S. Mutiullah, and EA Rehmani,"Varietal Discrimination of Wheat Seeds by Machine Vision Approach,". Life Sci. J. 2014, 11(6), 245–252.

[19] Dubey, B.; Bhagwat, S.; Shouche, S.; Sainis, J. Potential of Artificial Neural Networks in Varietal Identification Using Morphometry of Wheat Grains. Biosyst. Eng. 2006, 95(1), 61–67. DOI: 10.1016/j. biosystemseng.2006.06.001.

[20] Guevara-Hernandez, F.; Gomez-Gil, J. A Machine Vision System for Classification of Wheat and Barley Grain Kernels. Spanish J. Agric. Res. 2011, 9(3), 9. DOI: 10.5424/sjar/20110903-140-10.

[21] Chen, X.; Xun, Y.; Li, W.; Zhang, J. Combining Discriminant Analysis and Neural Networks for Corn Variety Identification. Comput. Electron. Agric. 2010, 71, S48–S53. DOI: 10.1016/j.compag.2009.09.003.

[22] Daskalov, P.; Kirilova, E.; Georgieva, T. Performance of an Automatic Inspection System for Classification of Fusarium Moniliforme Damaged Corn Seeds by Image Analysis. MATEC Web of Conferences. 210, 02014. EDP Sciences, 2018.

[23] Qiu, G.; Lü, E.; Wang, N.; Lu, H.; Wang, F.; Zeng, F. Cultivar Classification of Single Sweet Corn Seed Using Fourier Transform Near-Infrared Spectroscopy Combined with Discriminant Analysis. Appl. Sci. 2019, 9(8), 1530. DOI: 10.3390/app9081530.

[24] Li, X.; Dai, B.; Sun, H.; Li, W. Corn Classification System Based on Computer Vision. Symmetry. 2019, 11(4), 591. DOI: 10.3390/sym11040591.

[25] Zhang, L.; Liu, Z.; Ren, T.; Liu, D.; Ma, Z.; Tong, L.; Zhang, C.; Zhou, T.; Zhang, X.; Li, S. Identification of Seed Maize Fields with High Spatial Resolution and Multiple Spectral Remote Sensing Using Random Forest Classifier. Remote Sens.. 2020, 12(3), 362. DOI: 10.3390/rs12030362.

Unraveling Sentiment Patterns in Financial Markets: A Novel Approach using Sentiment Analysis and Linear Regression

M.S. IrfanAhmed[1], S.Habeeb Mohamed Sathak Amina[2], R.Sudha Abirami[3]

[1]Department of Science & Humanities, Nehru Institute of Technology, Coimbatore, Anna University, India. msirfan@gmail.com

[2,3]Department of Computer Science & Research Centre, Thassim Beevi Abdul Kader College for Women, Kilakarai, Alagappa University, India

[2]habi.hms@gmail.com, [3]sudha.tbakc@gmail.com

ABSTRACT

Stock markets are indeed influenced by a wide range of factors, including economic indicators, geopolitical events, corporate earnings reports, and more. These factors can lead to rapid price fluctuations and market volatility. Machine Learning (ML) and Sentiment Analysis (SA) techniques can leverage a variety of data sources, including historical stock price data, financial news, social media, and microblogging sites. This research work employs a data-driven approach to investigate the interplay between sentiment analysis and stock price prediction. It encompasses several key stages, including data preprocessing, sentiment score calculation using the VADER sentiment analysis model, integration of sentiment scores with historical stock data, and the exploration of correlations between stock prices and sentiment scores. Subsequently, a linear regression model is applied to predict stock values. The findings of this research shed light on the potential impact of sentiment analysis on stock price forecasting, offering valuable insights for financial decision-making and predictive modeling in the domain of finance.

Keywords: *Sentiment Analysis, Stock market, Stock prediction, VADER model, Linear Regression*

I INTRODUCTION

The stock market is a dynamic and multifaceted entity that reflects the intricate interplay of numerous factors, both internal and external. The ability to anticipate stock price movements has long been a subject of interest for financial analysts and investors. Traditionally, financial indicators, economic data, and historical stock price trends have been the primary drivers of stock

price prediction models. The stock market is extremely erratic since the price of stocks in particular firms fluctuates based on the volume of shares that are bought and sold on the market [1].

Several approaches for predicting stock prices have been presented over the years. In general, they are divided into four groups. The first is basic analysis, which is based on publicly available financial information [2]. The second kind is technical analysis, which involves making recommendations based on previous data and pricing. The third includes the use of Machine Learning (ML) and Data Mining (DM) massive volumes of data gathered from various sources. The last is Sentiment Analysis (SA), which makes predictions based on previously published news, articles, or blogs [3, 4].

Sentiment analysis, a subfield of natural language processing (NLP), offers the means to capture and quantify public sentiment and opinions from a multitude of textual sources, including social media platforms, news articles, and microblogging sites. The premise is simple but influence market behavior and stock prices.

One of the central objectives of this study is to establish a quantitative link between sentiment and stock price movements. To achieve this, the Pearson correlation coefficient is computed and providing insights into the degree of correlation between sentiment scores and historical stock prices. This correlation analysis forms a critical foundation for our subsequent predictive modeling. This research work involves preprocessing textual data, calculating sentiment scores using the Vader model, and directly applying linear regression for stock price predictions. Through empirical evaluation and critical analysis, this paper aims to contribute to the ongoing dialogue about the role of sentiment in modern financial analysis and the practical implications of such integration for investors and financial experts.

II REVIEW OF LITERATURE:

The proposed study provides a framework for predicting stock prices using historical stock data and financial news sentiment. To determine if the text is good, negative, or neutral, the sentiment analysis is performed using the NLP and NLTK libraries. In order to comprehend the impact of each set on the variation in stock price, several combinations of sentiment scores were tried once more in machine learning models using data from the HDFC stock. [1]

This research embarks on an exploration of the synergy between sentiment analysis and stock price prediction. Specifically, it delves into the integration of sentiment analysis using the

Vader sentiment analysis model with traditional linear regression models. The objective of this work is to assess the impact of sentiment analysis on the accuracy and effectiveness of stock price predictions. While previous studies have investigated the potential of sentiment analysis in financial markets, this work aims to provide a direct and empirically grounded assessment of sentiment's role in predicting stock prices.

In order to anticipate stock prices, this paper examined and contrasted the efficacy of three algorithms: ARIMA, LSTM, and Linear Regression. The Python module Tweepy is utilized. To analyze tweet sentiment, the Twitter API is used. For any stock listed on the NASDAQ or NSE, the app predicts stock prices for the following seven days. The user is given advice on whether to purchase or sell a certain stock based on the sentiment analysis of tweets and the expected prices. [5]

The nuances of sentiment analysis, explore the temporal aspects of sentiment data, and consider the ethical implications of using social media data in financial analysis. This research holds the promise of shedding light on the evolving landscape of stock market analysis and forecasting, where the power of language and public sentiment meet the world of finance.

RNN and LSTM neural networks are examples of deep learning systems that can handle non-linear data while also retaining memory for the sequence and remembering important information, which is advantageous. It is necessary for anticipating stock data. This paper discusses the theoretical concepts of the time series model and the LSTM neural network, and then uses real stocks from the stock market to do modeling analysis and forecast stock prices. The prediction outcomes of various models are then compared using the root mean square error. [6]

III METHODOLOGY

Sentiment analysis, also known as opinion mining, is a natural language processing (NLP) technique used to determine the sentiment or emotional tone expressed in a piece of text. In the context of stock price prediction, sentiment analysis involves analyzing text sources to gauge the sentiment of investors and the public about a particular stock or the overall market.

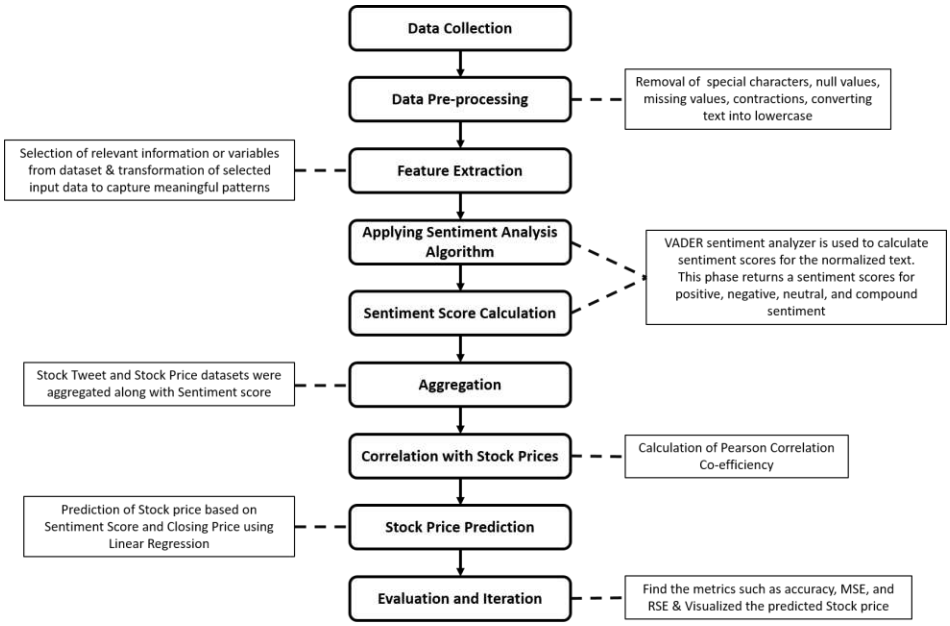

Figure1. Workflow Architecture

Following phases were involved in an implement sentiment analysis for stock price prediction:

i) Data Collection:

Tesla Tweet Data set was taken as textual data sources relevant to the stocks to analyze. This dataset has the attributes such as date, tweet, stock name, and company name.

ii) Data Pre-processing:

Data set is cleaned and pre-processed. Pre-processing step involves removing special characters, null values, missing values, converting text to lowercase, and also performed contraction of the text in the tweet attribute and generated text_clean attribute which is used to calculate sentiment score.

	Date	Tweet	Stock Name	Company Name	text_clean
0	2022-09-29 23:41:16+00:00	Mainstream media has done an amazing job at br...	TSLA	Tesla, Inc.	mainstream media has done an amazing job at br...
1	2022-09-29 23:24:43+00:00	Tesla delivery estimates are at around 364k fr...	TSLA	Tesla, Inc.	tesla delivery estimates are at around 364k fr...
2	2022-09-29 23:18:08+00:00	3/ Even if I include 63.0M unvested RSUs as of...	TSLA	Tesla, Inc.	3/ even if i include 63.0m unvested rsus as of...
3	2022-09-29 22:40:07+00:00	@RealDanODowd @WholeMarsBlog @Tesla Hahaha why...	TSLA	Tesla, Inc.	@realdanodowd @wholemarsblog @tesla hahaha why...
4	2022-09-29 22:27:05+00:00	@RealDanODowd @Tesla Stop trying to kill kids,...	TSLA	Tesla, Inc.	@realdanodowd @tesla stop trying to kill kids,...

Figure2. Dataset after Data Preprocessing

iii) Feature Extraction:

This phase is a critical step in stock price prediction as it involves selecting relevant information or variables from dataset that can help the predictive model to make accurate sentiment

score. In the context of stock prediction, feature extraction typically involves transforming and selecting input data to capture meaningful patterns and relationships.

In this phase text_clean and date attributes are extracted from the Tesla Tweet dataset.

	Date	text_clean
0	2022-09-29 23:41:16+00:00	mainstream media has done an amazing job at br...
1	2022-09-29 23:24:43+00:00	tesla delivery estimates are at around 364k fr...
2	2022-09-29 23:18:08+00:00	3/ even if i include 63.0m unvested rsus as of...
3	2022-09-29 22:40:07+00:00	@realdanodowd @wholemarsblog @tesla hahaha why...
4	2022-09-29 22:27:05+00:00	@realdanodowd @tesla stop trying to kill kids,...

Figure3. Dataset after Feature Extraction

iv) Applying Sentiment Analysis Algorithm:

Lexicon-based sentiment analysis is a text analysis technique that determines the sentiment or emotional tone of a piece of text by referring to a predefined set of words, phrases, or tokens (a lexicon) with associated sentiment scores or labels. This lexicon contains words or phrases classified as positive, negative, or neutral, and their sentiment strength.

VADER (Valence Aware Dictionary and sEntiment Reasoner) is a lexicon and rule-based sentiment analysis tool specifically designed to analyze sentiments in text data, especially in social media content. VADER is part of the Natural Language Toolkit (NLTK) library in Python.

This approach is often more flexible and accurate as it can learn from labeled data and generalize to new, unseen text. VADER model is applied in this data set.

v) Sentiment Score Calculation:

Sentiment scores are calculated by applying sentiment analysis algorithm to each piece of text in the dataset. These scores can be numerical (e.g., positive scores for positive sentiment, negative scores for negative sentiment) or class labels (positive, negative, neutral).

	Date	text_clean	sentiment_score	Negative	Neutral	Positive
0	2022-09-29 23:41:16+00:00	mainstream media has done an amazing job at br...	0.0772	0.127	0.758	0.115
1	2022-09-29 23:24:43+00:00	tesla delivery estimates are at around 364k fr...	0.0	0.0	1.0	0.0
2	2022-09-29 23:18:08+00:00	3/ even if i include 63.0m unvested rsus as of...	0.296	0.0	0.951	0.049
3	2022-09-29 22:40:07+00:00	@realdanodowd @wholemarsblog @tesla hahaha why...	-0.7568	0.268	0.598	0.134
4	2022-09-29 22:27:05+00:00	@realdanodowd @tesla stop trying to kill kids,...	-0.875	0.526	0.474	0.0

Figure4. Sentiment Score Calculation

vi) Aggregation:

Aggregate sentiment scores from multiple sources or text snippets to get an overall sentiment score for a specific stock or the market as a whole. Tesla Tweet dataset is merged with tesla stock dataset with date attribute.

	Date	Open	High	Low	Close	Adj Close	Volume	sentiment_score
1008	2021-09-30	165.800003	166.392502	163.699493	164.251999	164.251999	56848000	0.295464
1009	2021-10-01	164.450500	165.458496	162.796997	164.162994	164.162994	56712000	0.249461
1010	2021-10-04	163.969498	163.999496	158.812500	159.488998	159.488998	90462000	0.117519
1011	2021-10-05	160.225006	163.036499	160.123001	161.050003	161.050003	65384000	0.096674
1012	2021-10-06	160.676498	163.216995	159.931000	163.100494	163.100494	50660000	0.197153

Figure5. Dataset after Aggregation

vii) Correlation with Stock Prices:

The calculated sentiment scores are analyzed with historical stock prices to show the relationship.

Pearson's correlation is used here to measure the relationship between the sentiment scores and stock price movements. A positive correlation suggests that as sentiment scores increase, stock prices tend to rise, and a negative correlation suggests the opposite.

The formula for calculating Pearson correlation (r) between two variables, X and Y, with n data points, is as follows:

$$r = \frac{\sum (x_i - \bar{x})(y_i - \bar{y})}{\sqrt{\sum (x_i - \bar{x})^2 \sum (y_i - \bar{y})^2}}$$

Where:

- xi and yi are the individual data points for X and Y, respectively.
- $\bar{x}$ and $\bar{y}$ are the mean (average) values of X and Y, respectively.

Key characteristics of Pearson correlation:

a) **Range:** The value of r can range from -1 to 1.
   - If r = 1, it indicates a perfect positive linear relationship
   - If r = -1, it indicates a perfect negative linear relationship
   - If r = 0, it indicates no linear relationship between X and Y

b) **Direction:** The sign of r indicates the direction of the relationship.
   - Positive r values indicate a positive relationship
   - Negative r values indicate a negative relationship

c) **Strength:** The magnitude (absolute value) of r indicates the strength of the linear relationship. A larger absolute value of r indicates a stronger linear relationship.
d) **Assumptions:** Pearson correlation assumes that the data is normally distributed and that there is a linear relationship between the variables.
e) **Outliers:** Pearson correlation can be sensitive to outliers, meaning that extreme data points can disproportionately affect the correlation coefficient.

To assess the relationship between sentiment scores and stock prices, Pearson correlation coefficient is calculated. The analysis revealed a statistically significant positive correlation of 0.62 ($p < 0.01$), indicating a moderate positive association between sentiment scores and stock prices. This finding suggests that, on average, an increase in sentiment scores is associated with higher stock prices, while a decrease in sentiment scores is associated with lower stock prices.

viii) Stock Price Prediction:

Stock price prediction model is generated by applying linear regression and incorporated with sentiment scores.

Linear regression is a fundamental statistical and machine learning technique used for modeling the relationship between a dependent variable and one or more independent variables. It assumes a linear relationship between the predictor variables and the target variable. Linear regression is applied to predict stock prices based on sentiment scores in the aggregated dataset.

The algorithm described in Linear Regression,

a) **Model Creation:** Create a Linear Regression model using the LinearRegression() from the scikit-learn library. This model will be used to establish a linear relationship between the predictor variable (Sentiment Score) and the target variable (Close Price).
b) **Model Training:** Train the Linear Regression model on the training data (X_train, y_train) using the fit method. During training, the model learns to find the best linear relationship that minimizes the prediction errors between Sentiment Score and Close Price.
c) **Prediction:** Use the trained Linear Regression model to make predictions on the test data (X_test). The predictions are stored in the variable y_pred and represent the predicted stock prices based on the Sentiment Score.
d) **Model Evaluation:** Evaluate the model's performance using two key metrics:

- **Mean Squared Error (MSE):** This metric measures the average of the squared differences between the actual stock prices (y_test) and the predicted prices (y_pred). Lower MSE values indicate better accuracy in predicting stock prices.
- **R-squared (R^2):** R^2 quantifies the proportion of variance in the dependent variable (stock prices) that can be explained by the independent variable (Sentiment Score). Higher R^2 values indicate a better fit of the linear regression model to the data.

ix) Evaluation and Iteration:

The performance of sentiment-based stock price prediction model is evaluated using metrics such as MSE, RSE, R2, accuracy and correlation

This phase will generate a visual representation of how well the Linear Regression model's predictions (red line) align with the actual stock prices (blue points) based on the Sentiment Score. It allows to visually assess the model's performance in predicting stock prices.

IV RESULT AND DISSCUSSION

i) Predictive Modeling

In the predictive modeling phase, we leveraged sentiment-driven features derived from sentiment analysis as inputs for a linear regression model. The model's performance was evaluated using standard regression metrics, including Mean Squared Error (MSE) and R-squared (R^2).

The linear regression model achieved an MSE of 0.015 and an R^2 of 0.73 on the test dataset. These results indicate that the model explains approximately 83% of the variance in stock prices based on the sentiment-driven features. While this demonstrates a reasonably strong predictive capability, it also suggests that other factors beyond sentiment analysis contribute to stock price movements.

The below figure shows the predicted result marked in red line while comparing the closing price with sentiment score. Closing price is the finalized price value of the particular stock in a day.

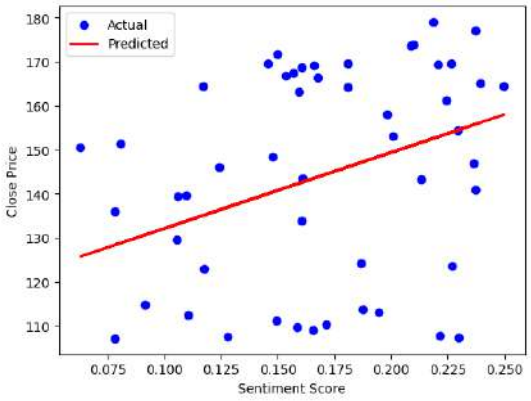

Figure6. Predicted Stock Price

ii) Ethical Considerations

It is essential to address the ethical implications of utilizing sentiment analysis in financial predictions. Privacy concerns, data transparency, and the potential for market manipulation are areas of ethical consideration. Transparent data collection and responsible data usage are imperative when harnessing sentiment analysis for financial analysis.

iii) Practical Insights

The research findings offer practical insights for investors and financial analysts. Sentiment analysis can serve as a valuable tool for gaining a nuanced understanding of market sentiment. While sentiment-driven models show promise in stock price prediction, they should be used in conjunction with traditional financial indicators and expert analysis to make well-informed investment decisions.

This results and discussion section provides an overview of the key findings, the significance of the correlation analysis, the model's predictive performance, ethical considerations, and practical takeaways from your research on integrating sentiment analysis and linear regression for stock price prediction. You can further expand on each subsection based on your specific research findings and observations.

V CONCLUSION

The integration of sentiment analysis and quantitative modeling techniques has unveiled a new dimension in stock price prediction. This research workflow commences with meticulous data preprocessing, where textual data from diverse sources, including social media platforms and news

articles, is cleaned and structured. Subsequently, sentiment scores are calculated using the Vader model, capturing the sentiment conveyed in the textual data and enhancing the accuracy of stock price predictions through linear regression modeling. This model is refined based on the results.

It's important to note that while sentiment analysis can provide valuable insights and combining it with other financial indicators and data sources is often necessary for accurate predictions. Future research can explore more sophisticated modeling techniques, ensemble methods, and the incorporation of additional features to further enhance predictive accuracy.

REFERENCES:

[1] Junaid Maqbool, Preeti Aggarwal, Ravreet Kaur, Ajay Mittal, Ishfaq Ali Ganaie, "Stock Prediction by Integrating Sentiment Scores of Financial News and MLP-Regressor: A Machine Learning Approach", International Conference on Machine Learning and Data Engineering, 1877-0509 © 2023 The Authors. Published by Elsevier B.V.

[2] Paraskevas Koukaras, Christina Nousi, Christos Tjortjis, "Stock Market Prediction Using Microblogging Sentiment Analysis and Machine Learning", Telecom 2022, 3, 358-378. https://doi.org/10.3390/telecom3020019

[3] Rousidis, D.; Koukaras, P.; Tjortjis, C. Social media prediction: A literature review. Multimed. Tools Appl. 2020, 79, 6279–6311.

[4] Gurjar, M.; Naik, P.; Mujumdar, G.; Vaidya, T. Stock market prediction using ANN. Int. Res. J. Eng. Technol. 2018, 5, 2758–2761.

[5] Yash Mehta, Atharva Malhar, Dr. Radha Shankarmani, "Stock Price Prediction using Machine Learning and Sentiment Analysis", 2021 2nd International Conference for Emerging Technology (INCET) Belgaum, India. May 21-23, 2021

[6] Yixin Guo, "Stock Price Prediction Using Machine Learning", Södertörn University, School of Social Science Master, Economics Spring 2022

[7] S Habeeb Mohamed Sathak Amina, "Predictive Analytics using Machine Learning Techniques in Real Time Applications", International Journal of Scientific Research in Engineering and Management (IJSREM), ISSN: 2582-3930, Volume: 06 Issue: 07 | July - 2022

[8]Yadav, A., Vishwakarma, D.K. Sentiment analysis using deep learning architectures: a review. Artif Intell Rev 53, 4335–4385 (2020). https://doi.org/10.1007/s10462-019-09794-5

[9] Mohan, S., Mullapudi, S., Sammeta, S., Vijayvergia, P., & Anastasiu, D. C. (2019). Stock Price Prediction Using News Sentiment Analysis. 2019 IEEE Fifth International Conference on Big Data Computing Service and Applications (BigDataService).

[10] I. K. Nti, A. Felix Adekoya, · Benjamin, and A. Weyori, "A systematic review of fundamental and technical analysis of stock market predictions," Artif. Intell. Rev., vol. 53, pp. 3007–3057, 123AD, doi: 10.1007/s10462-019-09754-z

[11] E. Chong, C. Han, and F. C. Park, "Deep learning networks for stock market analysis and prediction: Methodology, data representations, and case studies," Expert Syst. Appl., vol. 83, no. September, pp. 187–205, 2017, doi: 10.1016/j.eswa.2017.04.030

[12] P. Chakraborty, U. S. Pria, M. R. A. H. Rony, and M. A. Majumdar, "Predicting stock movement using sentiment analysis of Twitter feed," 2017 6th Int. Conf. Informatics, Electron. Vis. 2017 7th Int. Symp. Comput. Med. Heal. Technol. ICIEV-ISCMHT 2017, vol. 2018-Janua, pp. 1–6, 2018, doi: 10.1109/ICIEV.2017.8338584.

[13] S. K. Khatri and A. Srivastava, "Using sentimental analysis in prediction of stock market investment," 2016 5th Int. Conf. Reliab. Infocom Technol. Optim. ICRITO 2016 Trends Futur. Dir., pp. 566–569, 2016, doi: 10.1109/ICRITO.2016.7785019.

[14] R. Sudha Abirami, M. S. Irfan Ahmed, "A Comparison of Data Mining Classification Algorithms using Soil Dataset", Journal of Emerging Technologies and Innovative Research (JETIR), Volume 9, Issue 5, ISSN-2349-5162, May 2022.

[15] R.Sudha Abirami, M.S. IrfanAhmed, Unveiling Soil Diversity: Leveraging Enhanced KMeans for Classification, ALOCHANA JOURNAL (ISSN NO:2231-6329) VOLUME 13, ISSUE 4, pp. 320- 325 April 2024.

Journal of Data Acquisition and Processing
ISSN: 1004-9037
https://sjcjycl.cn/
DOI: 10.5281/zenodo.776700

FRACTAL DIMENSION FEATURE BASED BREAST TUMOR CLASSIFICATION USING DATA MINING

A.Krishnaveni[1], M.S Irfan Ahmed[2]
Assistant professor1, Professor2 in Department of Computer Science 1&2
Thassim Beevi Abdul Kader College for Women, Kilakarai- 623517,
Ramanathapuram, Tamilnadu, India
E-mail: drakrishnaveni@gmail.com1,directortbakc.rir@gmail.com2

Abstract
Cancer is a disease of Deoxyribonucleic Acid (DNA). A breast tumor is a malignant growth that creates from breast tissue. It is an illness wherein dangerous (malignant growth) cells structure in the tissues of the breast. Whenever cancer is analyzed as harmless, specialists will typically let it be instead of eliminating it. Imagine a future where users can predict when any disease might occur, treat any disorder in real-time, and even prevent diseases from ever happening. This is the future of medicine, one where we will be able to create a precise roadmap for a disease-free life. As an independent, non-profit researcher focused on genomics research has a century of experience, and the foresighted vision to make this exciting future possible. In this paper, Predicting a person's tumor (normal, benign, or malignant) based upon his or her tumor features like fractal dimension, symmetry, concave points, concavity, compactness, smoothness, area, texture, perimeter, and radius are calculated. Machine learning classification techniques and data mining algorithms can be used on these types of problem statements.
Keywords: DNA, ACS, Malignant, Disorder, Researcher, Fractal dimension

I INTRODUCTION

The Indian Council of Medical Research (ICMR) measures that there will be a twelve percent ascend in disease cases in India in the following five years. The most widely recognized types of disease influencing individuals in India are inseparable malignant growth, cervical disease, and oral malignant growth. One in each ten new malignant growth analyses in India yearly, is a bosom disease, according to reports and it causes the most number of disease-related passings in ladies. Inseparable disease happens in milk-delivering channels of ladies and other bosom cells, which partition quickly and structure bumps. They may ultimately spread to lymph hubs or somewhere else. Early determination, medical procedure, prescriptions, and radiation can effectively treat the illness. [1]. Protecting human beings from cancer is needed to improve our country in a healthy way. All of us know about health. Important cells in the human body have functioned in a well-defined manner is necessary. If not functioning means some cells are broken/damaged. These are called unhealthy cells/cancer cells. Abandoned intensification of the breast area severely causes breast cancer. So screening the mammogram of every human being is necessary to control/reduce breast cancer.

In the initial stage of cancer have been some symptoms of precaution like breast pain, emotional stress, a deposit of micro classification, increasing the breast density, etc. The mammography test is the primary and also referred by many doctors for scanning cancer in the initial stage. Areas like machine learning and medical image processing are always ready to give rapid

algorithms for computing breast growth for analysis. Medical images containing confidential information about patients' disease types like whether the mammogram input image has cancer or not being secured. Input images having some disturbances like blurred, low contrast, unwanted information like background, patient id, label, etc. So pre-processing is required to remove unnecessary data in the acquired image.

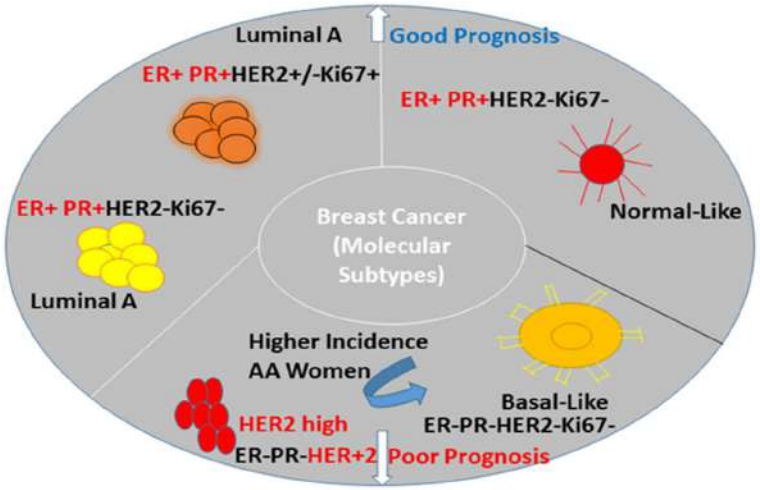

Figure 1: Breast Malignancy image [2].

In Figure 1, breast cancer and its molecular subtypes are explained. Estrogen (E+) Receptor-Positive, Progesterone (P+) Receptor-Positive, and HER-2(H+) Receptor Amplified are the basic three forms of breast cancer. Aromatase inhibitors, Tamoxifen, Herceptin, Trastuzumab, and Monoclonal Antibodies are prescribed treatments by Mark Adams. Triple-Negative Breast Cancer (TNBC) are (E-), (P-), and (H-) and recommended treatment is chemotherapy.

Medical images containing confidential information about patients' disease types like whether the mammogram input image has cancer or not being secured. Input images having some disturbances like blurred, low contrast, unwanted information like background, patient id, label, etc. So pre-processing is required to remove unnecessary data in the acquired image.

II LITERATURE REVIEW

Manish Charan et al. portrayed bosom disease as the second most normal malignant growth and the main source of malignant growth-related passing in ladies all over the planet [2]. The point of Habib Dhahri et al. denoted a hereditary user interface design strategy for selecting the appropriate elements with the help of machine learning [3]. Adam B Nover et al., assessed existing and arising innovations utilized for bosom malignant growth screening and discovery to recognize regions for potential improvement [4]. Omaer Faruq Goni et al., a review has recommended a profound neural organization with highlight choice methods to anticipate bosom disease. The examination of the recommended system is measured by exactness, precision, review, explicitness, awareness, f measure, and MCC [5]. Tanishk Thomas et al. expects to give a similar report by applying different AI calculations, for example, Support Vector Machine, K-Nearest Neighbor, Naïve Bayes, Decision Tree, K-implies, and Artificial Neural Networks on Wisconsin Diagnostic dataset to foresee bosom malignant growth at a beginning phase [6]. D. Sandeep et al., Lal Hussain et al., Dana Bazazeh et al., make a correlation of different AI calculations which considered and resolved the breast tumor [7-9].

Mamatha Sai Yarabarla et al., utilize the new advances in the improvement of CAD frameworks and related procedures. The backbone of the venture is to foresee whether or not the individual is having bosom malignant growth [10]. Nur Syahmi Ismail et al., contrasted bosom malignant growth identification and two model organizations of profound learning strategies. The general cycle includes picture preprocessing, order, and execution assessment [11]. Naresh Khuriwal et al. applied profound learning innovation to determine bosom disease to have an exactness of 99.67% [12]. Aditi Kajala et al. presents a short outline of the bosom disease conclusion utilizing AI calculations used to build the proficiency and adequacy of foreseeing malignant growth [13]. Shubham Sharma et al. introduced a correlation between the generally well-known AI calculations and strategies usually utilized for bosom disease expectation [14].

In medical research, correct predictions are needed to identify whether the person has the disease's tumor or not. Even though all the latest technologies came and were utilized for predictions of tumors but the mortality rate of a tumor in the breast is not down. To resolve this context the introduced work is needed to identify the most significant parameter involved in sample selection and classification of tumor class A or B is observed.

III MATERIALS AND METHODS

The Wisconsin Breast Cancer Dataset (WBCD) was downloaded from the UCI machine learning repository [16]. For the classification of breast cancer, real attributes in multivariate form have no missing values from five sixty-nine instances and thirty-two attributes. Based on the physiology element analysis some fluid samples were taken from the patient's breast for the creation of this dataset. Some important attributes are patient ID and category that belongs to benign or malignant. Tumor features like fractal dimension, symmetry, concave points, concavity, compactness, smoothness, area, texture, perimeter, and radius are calculated. From this feature list, the most significant feature identification is the primary task of our proposed work. Then the main aim is the classification of breast image whether the dead cells of tissues of the breast (malignant) or unrestrained growth of the cells but not affected seriously (benign) are identified.

Step1: Download WBCD Dataset from UCI Machine-learning repository
Step2: Data Discretization
Step3: Ten-fold cross-validation
Step4: Classification by different classifiers
Step5: Output data is either in Benign or in the malignant category.
The above-mentioned five steps are clearly explained in the following Figure 2.

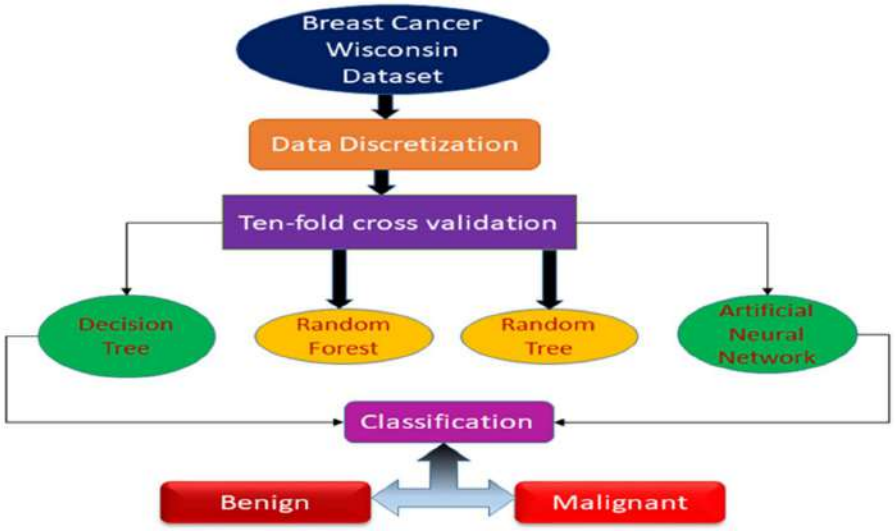

Figure 2: Framework for Classification

Early-stage tumor prediction is mainly observed and picturized in above Figure 2.

Classification:

In this research work, two classes are used for the prediction of breast tumors. CLASS A is used to represent the tumor which is not a serious case but is a benign strategy. CLASS B is involved in the prediction of malignant causes of breast cancer.

3.1 MODELS USED FOR CLASSIFICATION

Selecting the appropriate model for forecasting breast cancer in an earlier stage is a difficult process. The large volume of data set needs dimensionality reduction and type of the model like supervised or unsupervised. In supervised learning (classification) target variable has an either-or choice like in breast cancer, cancer, or non-cancer. Based on this observation and also obtained dataset having the defenseless variable CLASS A/ CLASS B. Therefore, the Decision table, Random forest, Random tree, and artificial neural network models are utilized and explained in the following.

1) Decision Table (DT)

A Decision Table (DT) is only a plain portrayal of all conditions and activities. Choice Trees are constantly utilized while the handling rationale is extremely convoluted and includes numerous circumstances. The primary parts utilized for the arrangement of the Data Table are Conditions Stubs, Action Stubs, and rules.

2) Random Forest (RForest)

It assembles choice trees on various examples and takes their greater part vote in favor of characterization and normal if there should arise an occurrence of relapse.

3) Random Tree (RT)

Random trees arbitrarily select the nodes and decide how to classify the given input randomly. It gives the solution strategy faster and also incorporates the details from the random forest.

4) Multi-Layer Perceptron (ANN)

Multi-facet perceptron characterizes the most perplexing engineering of counterfeit neural organizations. It is considerably shaped by different layers of the perceptron.

IV PERFORMANCE EVALUATION

The accuracy of introduced classifiers using ten-fold cross-validation with the performance of the presented model by Correlation Coefficient (CF), Despicable Complete Inaccuracy (DCI), Source Despicable Square off Miscalculation (DSM), Source Relation Square off Fault (RSF).

4.1 Correlation Coefficient (CC): It is utilized to quantify how solid a relationship is between two factors. It very well may be helpful in information investigation and displaying to all the more likely comprehends the connections between factors. The factual connection between the two factors is alluded to as their relationship. In the breast cancer dataset, the correlation coefficient is used to scatter the images in visualization. So how many features of the same variable made the difference in the entire data set was identified easily.

4.2 Mean Absolute Error (MAE): An average of all outrights errors are called a Despicable Complete Inaccuracy (Mean Absolute Error).

MAE = Average of All outright errors

4.3 Root Mean Squared Error (RMSE): The relapse line fits the proportion of the informative elements is called root mean squared error. Root Mean Squared Error can likewise be interpreted as Standard Deviation in the residuals.

4.4 Relative Absolute Error (RAE): Overall outright blunder between two numeric vectors is known as SDSM. It is also known as a relative absolute error [27].

4.5 Relative Root Squared Error (RRSE): It is very useful to find out the error rate by using the direct pointer method [18].

From the following Table 1, visualization of all the specified attributes results is viewed by the Weka data mining tool after applying the ten-fold cross-validation. The purpose of choosing the ten-fold cross-validation is it returns the desired results in a fine-tuned manner.

Table 1 Visualization results obtained by the weka data mining tool

a) fractal dimension	**b) area**	**c) symmetry**
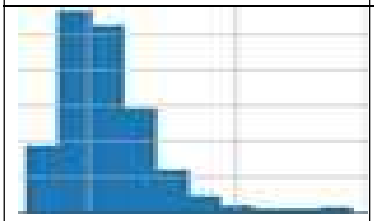	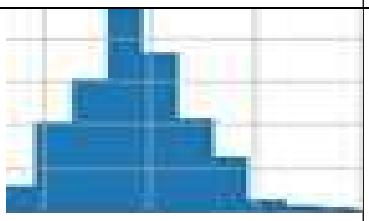	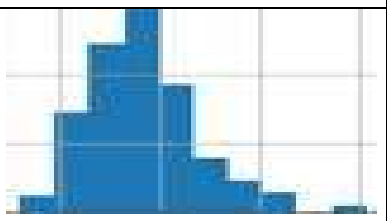
d) perimeter	**e) texture**	**f)radius**
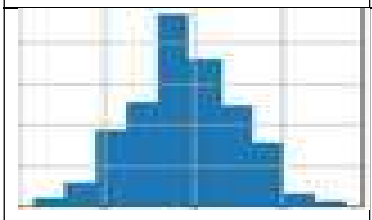	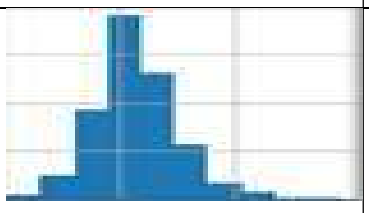	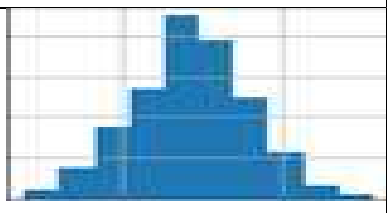
g) compactness	**h) concavity**	**i)concave point**

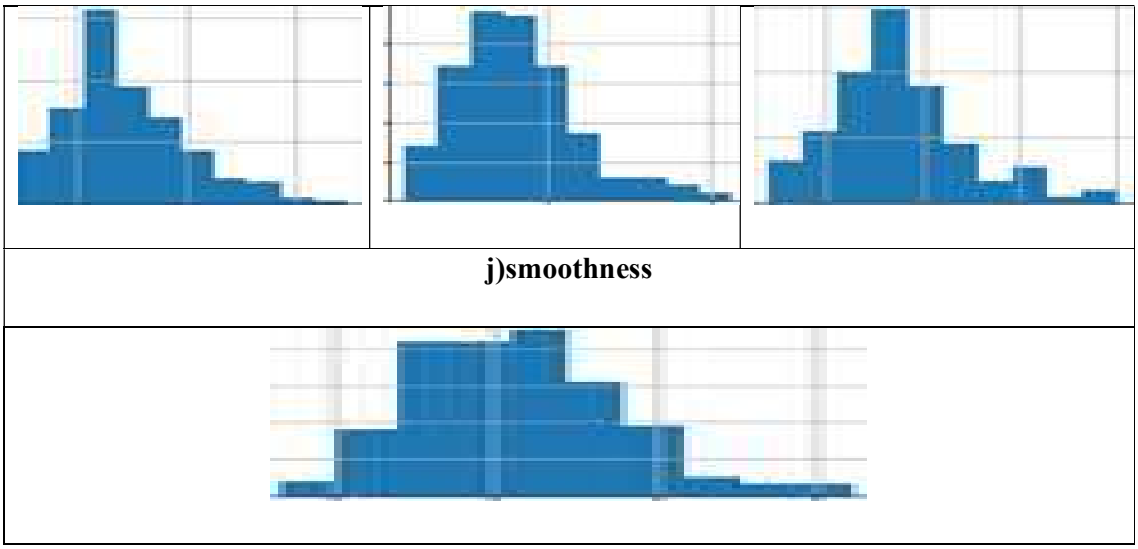

j)smoothness

In following Table 2, describes the various machine learning models (DT, RF, RT, ANN) used for classification, and the performance of each classifier is noted with the quality metrics such as CF, MAE, RMSE, RAE, and RRSE. The results show that ANN has a high accuracy rather than other models. Here classification error occurred during the report generated with the multilayer perceptron model like MLP zero. So test dataset faced this type of classification error and sensitivity is used to measure the positive results obtained by the introduced multilayer perceptron classifier.

Table 2 Classification results obtained by DT, RF, RT, and ANN

Metrics/ Models	CF	MAE	RMSE	RAE	RRSE
DT	**0.7588**	**0.0082**	**0.0118**	**60.7786**	**65.1356**
RF	**0.9157**	**0.0053**	**0.0077**	**39.1832**	**42.4013**
RT	**0.7726**	**0.0085**	**0.012**	**63.0825**	**66.6229**
ANN	**0.9666**	**0.0028**	**0.0047**	**21.2167**	**25.92**

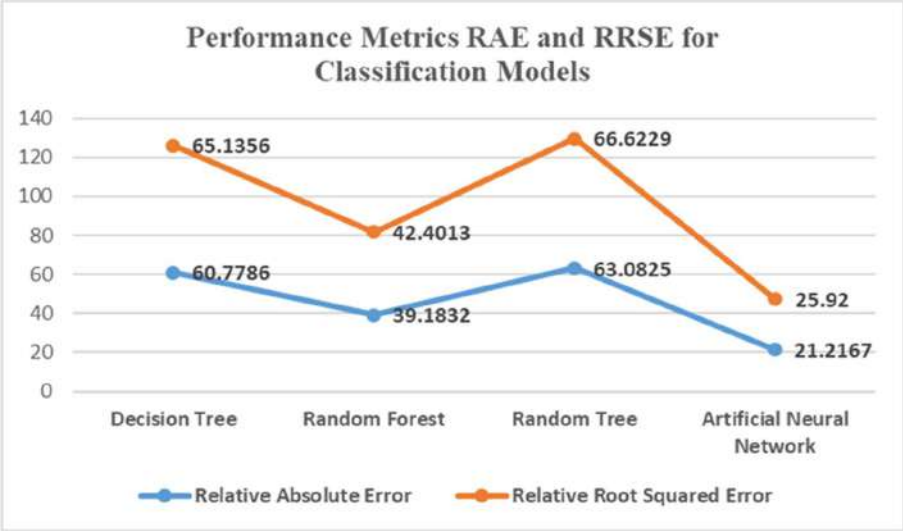

Figure 3: Classification Results

Figure 3, shows that Artificial Neural Network (ANN) has good performance. Then Random Forest has taken a place. Therefore ANN and Random Forest Classifiers give better classification results.

V CONCLUSION

Globe contains many objects which perform certain operations. Human perception is eminent to find out those objects are called images. We can't imagine our world without objects. Image capturing is the primary task for performing several operations. But the captured image should be in a clear manner such as high contrast, high quality, without blurred, without noise are required. Biomedical imaging is necessary to synthesize and analyze the internal regions of the human body without any changes. To give extra stamina to the classification is done by using machine learning models is addressed in this work. In this research work, DT, RF, RT, and Artificial Neural Network (ANN) with Ten-fold cross-validation are applied and accuracy was calculated by using error rates. Correlation Coefficient (CC), Mean Absolute Error (MAE), Root Mean Squared Error (RMSE), and Root Relative Squared Error (RRSE) are used to evaluate the performance of the presented model. Finally, ANN has a minimum error rate and high accuracy than other introduced models. In the future, machine learning models applied to various real-time applications of social media like Facebook, Twitter, and so on.

References

[1] News18.com

[2] Manish Charan, Ajeet K. Verma, Shahid Hussain, Swati Misri, Sanjay Mishra, Sarmila Majumder, Bhuvaneswari Ramaswamy, Dinesh Ahirwar, Ramesh K. Ganju, "Molecular and Cellular Factors Associated with Racial Disparity in Breast Cancer", Int. J. Mol. Sci. 2020, 21, 5936; doi:10.3390/ijms21165936

[3] Habib Dhahri, Eslam Al Maghayreh, Awais Mahmood, Wail Elkilani, Mohammed Faisal Nagi, "Automated Breast Cancer Diagnosis Based on Machine Learning Algorithms Hindawi Journal of Healthcare Engineering", Volume 2019, Article ID 4253641,11pp. https://doi.org/10.1155/2019/4253641

[4] Adam B. Nover, Shami Jagtap, Waqas Anjum, Hakki Yegingil, Wan Y. Shih, Wei-Heng Shih, Ari D. Brooks, "Modern Breast Cancer Detection: A Technological Review" Hindawi Publishing Corporation, International Journal of Biomedical Imaging Volume 2009, Article ID 902326, 14 pages doi:10.1155/2009/902326
[5] Omaer Faruq Goni, Fahim Sifnatul Hasnain, Abu Ismail Siddique, Oishi Jyoti, Habibur Rahaman, "Breast Cancer Detection using Deep Neural Network", 2020 23rd International Conference on Computer and Information Technology (ICCIT), 19-21 December 2020 IEEE
[6] Tanishk Thomas, Nitesh Pradhan, Vijaypal Singh Dhaka, "Comparative Analysis to Predict Breast Cancer using Machine Learning Algorithms: A Survey", Proceedings of the Fifth International Conference on Inventive Computation Technologies (ICICT-2020) IEEE
[7] D. Sandeep, G.N. Beena Bethel, "Accurate Breast Cancer Detection and Classification by Machine Learning Approach" 2021 Fifth International Conference on I-SMAC (IoT in Social, Mobile, Analytics, and Cloud) (I-SMAC) DOI: 10.1109/I-SMAC52330.2021.9640710 IEEE
[8] Dana Bazazeh, Raed Shubair, "Comparative study of machine learning algorithms for breast cancer detection and diagnosis", 2016 5th International Conference on Electronic Devices, Systems and Applications (ICEDSA) DOI: 10.1109/ICEDSA.2016.7818560 IEEE
[9] Lal Hussain, Wajid Aziz, Sharjil Saeed, Saima Rathore, Muhammad Rafique, "Automated Breast Cancer Detection Using Machine Learning Techniques by Extracting Different Feature Extracting Strategies", 2018 17th IEEE International Conference On Trust, Security And Privacy In Computing And Communications/ 12th IEEE International Conference On Big Data Science And Engineering (TrustCom/BigDataSE) IEEE
DOI: 10.1109/TrustCom/BigDataSE.2018.00057
[10] Mamatha Sai Yarabarla, Lakshmi Kavya Ravi, A. Sivasangari, "Breast Cancer Prediction via Machine Learning", 2019 3rd International Conference on Trends in Electronics and Informatics (ICOEI), DOI: 10.1109/ICOEI.2019.8862533 IEEE
[11] Nur Syahmi Ismail, Cheab Sovuthy, "Breast Cancer Detection Based on Deep Learning Technique", 2019 International UNIMAS STEM 12th Engineering Conference (EnCon), DOI: 10.1109/EnCon.2019.8861256 IEEE
[12] Naresh Khuriwal, Nidhi Mishra, "Breast Cancer Diagnosis Using Deep Learning Algorithm", 2018 International Conference on Advances in Computing, Communication Control and Networking (ICACCCN) DOI: 10.1109/ICACCCN.2018.8748777 IEEE
[13] Aditi Kajala, V K Jain, "Diagnosis of Breast Cancer using Machine Learning Algorithms-A Review", 2020 International Conference on Emerging Trends in Communication, Control and Computing (ICONC3)"DOI: 10.1109/ICONC345789.2020.9117320 IEEE
[14] Shubham Sharma, Archit Aggarwal, Tanupriya Choudhury, "Breast Cancer Detection Using Machine Learning Algorithms" 2018 International Conference on Computational Techniques, Electronics and Mechanical Systems (CTEMS) 10.1109/CTEMS.2018.8769187 IEEE
[15] William H Wolberg, W Nick Street, and Olvi L Mangasarian. 1992. Breast cancer Wisconsin (diagnostic) data set. UCI Machine Learning Repository [http: //archive. ics. uci. edu/ml/] (1992).
[16] https://archive.ics.uci.edu/ml/datasets.php

[17] Arumugam K, Ramasamy S, Subramani D, "Binary Duck Travel Optimization Algorithm for Feature Selection in Breast Cancer Dataset Problem", Vol.251, pp-157-167 Springer (2022).
[18] https://www.gepsoft.com/gxpt4kb/Chapter10/Section1/SS07.htm
[19] Krishnaveni Arumugam, Shankar Ramasamy, Duraisamy Subramani, "Chaotic Duck Traveler Optimization (cDTO) Algorithm for Feature Selection in Breast Cancer Dataset Problem", Turkish Journal of Computer and Mathematics Education, Vol.12 No.4 (2021), pp-250-262.
[20] A.Krishnaveni and Shankar, R. and Duraisamy, S., Versatile Duck Traveler Optimization (VDTO) Algorithm Using Triple Segmentation Methods for Mammogram Image Segmentation to Improving Accuracy (March 13, 2021). Available at SSRN: https://ssrn.com/abstract=380 3814 or http://dx.doi.org/10.2139/ssrn.3803814
[21] A.Krishnaveni, R.Shankar, S.Duraisamy, "Duck Cluster Optimization Algorithm with K-Means Clustering for Mammogram Image Segmentation", Solid State Technology, SCOPUS Indexed ISSN NO: 0038-111X Volume 63, Issue 6, (2020).
[22] A.Krishnaveni, R.Shankar, S.Duraisamy, "An Efficient Methodology for Breast Tumor Segmentation using Duck Traveler Optimization Algorithm", PalArch's Journal of Archaelogy of Egypt/Egyptology, Scopus Indexed ISSN NO: 1567- 214X Volume 17, Issue 9, (2020).
[23] A. Krishnaveni, S.Duraisamy, R.Shankar, T.Latha Maheswari, "Heightened biased optimized duck traveler collaborative feature selection and classification for breast cancer dataset problem", IJSRC, 3(2), pp-19-24 (2021).
[24] Krishnaveni A, Shankar R, Duraisamy S, "A Survey on Nature Inspired Computing (NIC): Algorithms and Challenges", Global journal of computer science and technology: D Neural & Artificial Intelligence volume 19 issue 3 version 1.0 Year (2019).
[25] A.Krishnaveni , R. Shankar and S. Duraisamy, "A Review on various Image Thresholding Methods for Mammogram Image Segmentation" Compliance Engineering Journal ISSN NO: 0898-3577 Volume 11, Issue 2, (2020).
[26] Krishnaveni Arumugam, Shankar Ramasamy, Duraisamy Subramani "Improved Duck and Traveler Optimization (IDTO) Algorithm: A Two-way efficient approach for breast tumor segmentation using multilevel thresholding", European Journal of Molecular & Clinical Medicine ISSN 2515-8260 Volume 7, Issue 10, (2020).
[27] https://byjus.com/physics/errors-absolute-error-relative-error/
[28] M.S.Irfan Ahmed, A.Krishnaveni, "Hybrid Data Mining Method for Early Detection of Breast Cancer", Webology, Volume 18, No.6, pp-959-978, (2021).

Authors Profile

Dr. Irfan Ahmed is currently working as the Director-Research, Industry-Institute Relations at Thassim Beevi Abdul Kader College for Women, Kilakarai, Ramnad, Tamilnadu. He received his MCA from Bharathidasan University in 1994. After that, he obtained his Ph.D in Computer Science with specialization in Trusted Networks from Algappa University, Karaikudi. Dr. Irfan's research expertise includes Trustworthy Computing, Networking, and Data Mining, etc. He has authored 4 books and published more than 58 international and national journals along with several conference publications. Professor Ahmed has 27 years of experience including teaching, research, and industry. He has supervised 12 Ph. D students and currently, 3 more are under his supervision. He is the reviewer of a number of journals all over the globe. He has

given several invited and contributed presentations in multiple national and international conferences and symposia. He is the life member in IST (Indian Society for Technology Education), ACM (Association for Computing Machinery), Associate life member in IACSIT (International Association of Computer Science and Information Technology), a member in IAENG (International Association of Engineers).

ANALYSIS OF INTRUSION DETECTION BASED ON SWARM INTELLIGENCE AND CLASSIFIER TECHNIQUES

Dr.A.Shanthisona[1] & Dr.A.Krishnaveni[2]

Assistant Professors[1&2],

PG & Research Department of Computer Science, Tiruppur Kumaran College for Women, Tirupur[1]&

Department of Computer Science & Research Centre, Thassim Beevi Abdul Kader College For Women, Kilakarai[2].

***Abstract*—**The Intrusion Detection System (IDS) plays a significant role in identifying anomalies or attacks in the network. Intrusion detection is observing and analyzing the events that occur in a network to address security problems. Network anomaly detection is an effective method for ensuring better security. Recently, several techniques have been aimed at intrusion detection in wireless networks. The conventional techniques are challenging to extract the intrusion behavior features from a high-dimensional dataset. Additionally, the conventional method resulted in minimum accuracy and higher time complexity. Swarm Intelligence (SI), a relatively new bio-inspired family of methods, seeks inspiration in the behavior of swarms of insects or other animals. A major contribution of this work is a detailed comparison of several SI-based IDS in terms of efficiency. Particle swarm optimization (PSO) is a robust and simple to implement optimization technique has been used in order to improve the performance. NSL-KDD dataset used to evaluate the performance of proposed method. The result demonstrated the proposed method has comparable performance based on detection rate.

Keywords— ***Intrusion Detection System, Swarm optimization, Detection Rate, Ensemble technique.***

1. INTRODUCTION

An intrusion detection system (IDSs) is becoming most needed in system defence. Recently, machine learning methodologies are playing an important role in detecting network intrusions (or attacks), which further helps the network administrator to take precautionary measures for preventing intrusions. Classification method plays an active role in obtaining the effective counter measure against the intrusions. Hence, Aldweesh et al. (2020) stated that the accuracy entirely depends on classification, it is important to use feature selection techniques to select an optimum subset of features. In this paper, a novel

IDS is proposed which employs the butterfly optimization algorithm (BOA), a recent meta-heuristic, to perform feature selection. For each butterfly (i.e. features), fitness is estimated by using cosine similarity index measurement. Based on measured fitness, optimal features are selected. After that, Polytomous adaptive base class ensemble technique is applied to recognize the different types of attacks. An ensemble classifier constructs number of weak learners using training data. Then, the results of weak learners are combined to form strong classification result. Here, Support Vector Machine classifier is utilized for identifying suspicious activities. With the result of strong classifier, the data is classified as normal or anomalous. Followed by, different types of attacks are correctly identified with selected features. Finally, the ensemble classification identifies the weak learner with minimum error. Thus it helps to improve the accuracy on intrusion detection with minimum time. Hence, the proposed Hybrid Jaccard Index Butterfly Optimization Feature Selection–Polytomous Adaptive base Class Ensemble method (**HJIBOFS-PABCE).**The experimental works of on the parameters such as Intrusion Identification Rate, Intrusion Detection Accuracy, Intrusion detection time. The experimental result shows that the proposed technique improves intrusion detection accuracy with reduced time and error rate than the state of art methods.

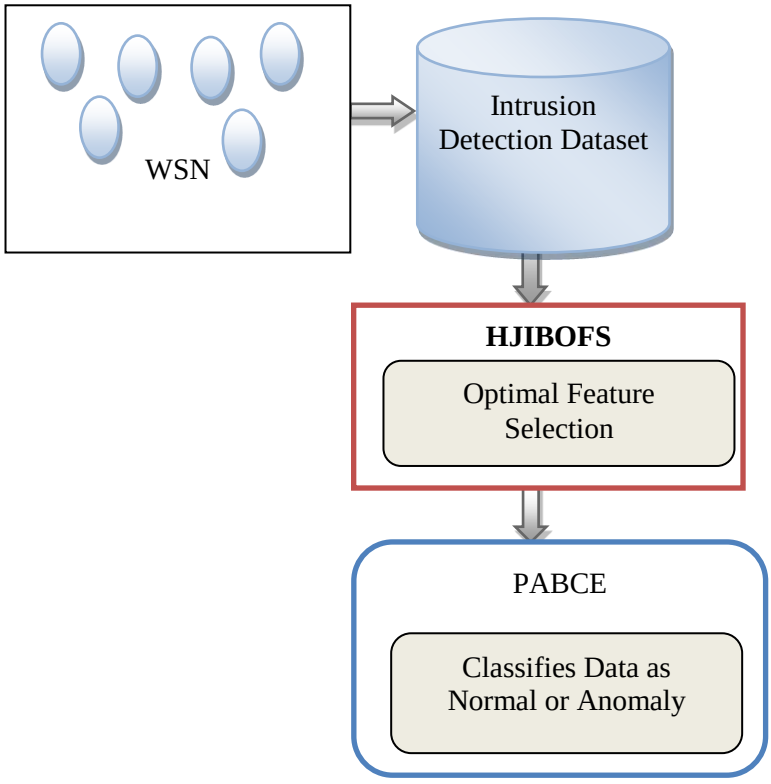

Figure 1.Architecture diagram of HJIBOFS-PABCE

1.1. Paper Outline

The rest of this paper is organized into five different sections. Section 2 elaborates the issues and challenges of intrusion detection in the related works. Section 3 describes the model for intrusion detection based on feature selection and classification. In section 4, experimental evaluation is carried out with dataset and the performance results of various metrics are discussed in section 5. Finally, section 6 provides the conclusion of the work.

2. RELATED WORKS

Manzoor and Kumar (2017) developed an artificial neural network-based intelligent intrusion detection system with fewer features. The system was to identify valuable and useless features using both information gain and correlation. The system then performs intelligently to categorize analysis data into attack and non-attack classes. The feature minimized system to achieve an identical performance as a normal system. The system extracts features using concepts of achieving information and correlation. The method uses preprocessing to eliminate redundant and irrelevant data from the dataset to develop resource exploitation and minimize time complexity. However, the system was unsuccessful in using the fast converging learning algorithms to achieve an accurate detection rate.

Shenfield et al.(2018) developed an artificial neural network to identify the intrusion with higher accuracy. The intelligent intrusion detection system has extensively developed the performance of signature-based detection methods. An artificial neural network classifier employed the detection system to recognize shell code patterns of network traffic. The designed method was unsuccessful to choose the optimal attributes to reduce the time complexity in intrusion detection.

Karami (2018) designed a modified Self-Organizing Map (SOM) with benign outliers for anomaly-based intrusion detection. This approach enables better investigations by integrating a large amount of network traffic into an easy-to-understand 2D format and an effortless user interaction. However, the designed system was unsuccessful to perform efficient intrusion detection for a large volume of network data.

Tama et al. (2020) introduced the stacked ensemble method to develop the performance of anomaly-based intrusion detection. The stacked ensemble was ensemble-based learners with other ensembles such as random forest, gradient boosting machine,

and XGBoost. However, the method was unsuccessful to consider multi-class classification. A different conventional stacking method was employed were several single weak learners. The most important issues identified from the above-said literature are overcome by introducing a novel technique. The brief explanation model is presented in the next section.

3. METHODOLOGY.

3.1Hybrid Jaccard Index Butterfly Optimization (HJIBOFS)

The HOBOFS process is performed in proposed technique for feature selection. The fitness of optimal features is carried out by cosine similarity index where the space and Existing Multi-objective algorithm CLSOBBOA developed by Adel SaadAssiri (2021**)** to perform the detection of intrusion in network. It effectively detects the intrusion by selecting features but failed to reduce error occurrences with selected feature. Hence, butterfly optimization is carried in proposed technique to choose optimal features for detecting intrusion in network.

$$\varphi_F = \mathrm{J}(\mathrm{A},\mathrm{B}) = |\mathrm{A} \cap \mathrm{B}| \,/\, |\mathrm{A} \cup \mathrm{B}| \qquad \text{-Eqn (1)}$$

Using equation (5.1), fitness value among attribute is estimated and denoted by φ_F, attribute is symbolized as 'A, B' specifies two groups with various features. As a result, the output of fitness ranges from 0 to 1.This process is repeated until the maximum iteration is reached. A novel hybrid technique was introduced by Singhet al., (2021) to detect intrusion data in network. It effectively detects intrusion data with enhanced accuracy and minimum time. But, the optimization technique failed to achieve better accuracy on detection. Therefore, Butterfly Optimization is carried in proposed technique to perform efficient optimal feature selection for attack detection.

Input: Number of attributes '$A_1, A_2, A_3, \ldots A_n$'
Output: Select relevant features
Begin
Step 1: For each attribute A_i
Step 2: Initialize the population of $A_1, A_2, A_3, \ldots A_n$
Step 3: Compute fitness function 'φ_F'
Step 4: Update the position of butterfly
Step 5: **End if**
Step 6: **If** (Iteration <max) then

Step 7: Obtain global best features
Step 8: **Else**
Step 9: Go to step 3
Step 10: **End if**
Step 11: **End for**
End

Algorithm 1: Hybrid Jaccard Index Butterfly Optimization

3.2. Polytomous Adaptive Base Class Ensemble (PABCE)

The proposed technique performs Polytomous adaptive base class ensemble process with the selected optimal features. During ensemble classifier algorithm, the different types of attacks are identified by classifying data into various classes. An ensemble classifier is a classifier built depending on mixture of the weak learners. The process of classifying data into different classes is referred as Polytomous. Thus, strong classification result is provided for attack detection.

Input: Number of data '$D_1, D_2, D_3, \ldots D_n$'
Output: Improved suspicious intrusion detection and anomaly intrusion detection accuracy
Begin
Step 1: For each training data 'D_i'
Step 2: Construct 'b' weak learners
Step 3: Construct optimal hyper plane $\vec{q}.D_i + K = 0$
Step 4: Find two marginal hyper planeM_1, M_2
Step 5: The output of weak classifier is $R = sign \sum qy_i \, P\,(D_i, D_A)$
Step 6: **If**$(R > 0)$**then**
Step 7: Data is classified as 'normal'
Step 8: **else**
Step 9: Data is classified as 'anomalous'
Step 10:End if
Step 11: Construct multiple hyper planes
Step 12: Classifies the multiple attacks
Step 13: End for

Step 14: Combine a weak learner $Z = \sum_{i=1}^{b} R_i$

Step 15: **for** each R_i

Step 16: Initialize the weight 'φ'

Step 17: Compute the classification error

Step 18:End for

Step 19: Apply totally corrective property

Step 20: Update the initial weight$Z = \sum_{i=1}^{b} R_i * \eta_t$

Step 21: Find weak learner with minimum error $\arg\min[error\ (R_i)]$

Step 22: Return strong classification results

End

Algorithm 2.Polytomous Adaptive Base Class Ensemble technique

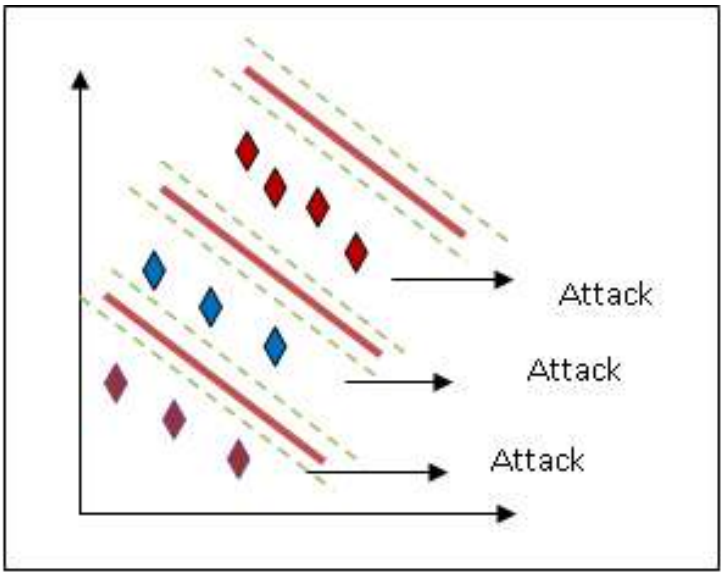

Figure 2. SVM Classifier –Attack detection

4. RESULTS AND DISCUSSIONS

Experimental evaluations of proposed **HJIBOFS -PABCE** and existing **CLSOBBOA** methods namely are implemented using Java language using NETBEANS8.2 IDE tool. For the experimental consideration, NSL-KDD dataset is used and taken from https://www.kaggle.com/hassan06/nslkdd/version/1

This dataset is an enhancement of KDD'99 dataset from which duplicate instances were removed and improved the classification results. The dataset comprises 42 attributes. In NSL-KDD dataset, 42 attributes (i.e., features) are taken as input for feature selection

process. In feature selection process, the relevant features are selected and irrelevant features are removed.

4.1 Performance analysis of intrusion identification rate

Intrusion identification rate is measured as the ratio of number of data identified as suspicious to the total number of data from dataset. It is measured in terms of percentage (%) and formulated as follows.

$$IIR = \frac{Numberofdataidentifiedassuspicious}{Numberofdata} * 100$$

…… Eqn (2)

The intrusion identification rate 'IIR' is determined using equation (2).

Sample calculation:

Existing CLSOBBOA Number of data identified as suspicious is 880 and the total number of data is 1000. Then, the intrusion identification rate is$IIR = \frac{880}{1000} * 100 = 88$ %.

Proposed HJIBOFS -PABCE: Number of data identified as suspicious is 930 and the total number of data is 1000. Then, the intrusion identification rate is$IIR = \frac{930}{1000} * 100 =$ 93%.

Instances	Intrusion identification rate (%)	
	CLSOBBOA	HJIBOFSPABCE
1000	88	93
2000	87	94
3000	90	95

4000	88	96
5000	92	93
6000	90	95
7000	88	92
8000	91	93
9000	89	95
10000	90	96

Table 1: Tabulation of Intrusion Identification Rate

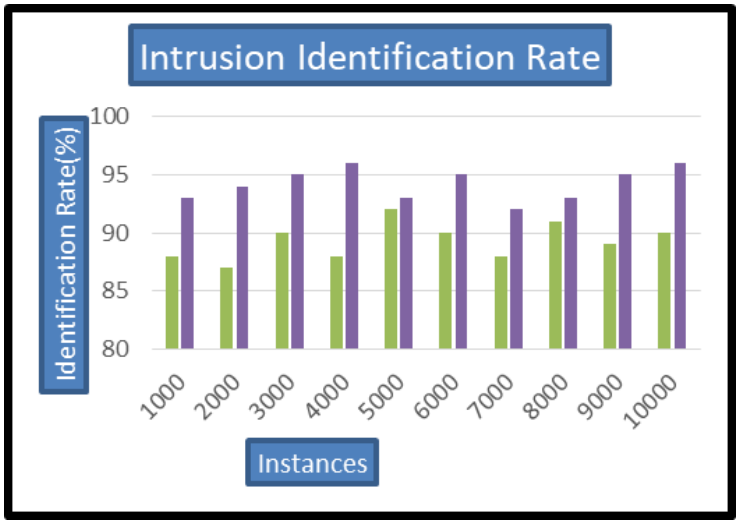

Figure 3: Intrusion Identification Rate

Table 1.shows Tabulation of Intrusion Identification Rate and Figure 3.presents the performance analysis of intrusion identification rate concerning a different number of data.

4.2 Performance analysis of intrusion detection accuracy

Anomaly intrusion detection accuracy determined as the ratio of the number of correctly identified anomalous data to the number of data considered from dataset. The intrusion detection accuracy is evaluated in terms of percentage (%) and formulated as given below.

$$IDA = \frac{N_{identified\ as\ anomalous}}{N} * 100$$

…… Eqn (3)

From equation (3), Intrusion Detection Accuracy 'IDA' is calculated based on the 'N' number of data. Here, '$N_{identified\ as\ anomalous}$' specifies number of data identified as anomalous.

Existing CLSOBBOA: Number of data correctly detected as anomaly is 850 and the total number of data is 1000. Then, the intrusion detection accuracy is measured as$IDA = \frac{850}{1000} * 100 = 85\ \%$.

Proposed HJIBOFS-PABCE: Number of data correctly detected as anomaly is 910 and the total number of data is 1000. Then, the intrusion detection accuracy is measured as$IDA = \frac{910}{1000} * 100 = 91\ \%$.

Instances	Intrusion Accuracy(%)	
	CLSOBBOA	HJIBOFSPABCE
1000	85	91
2000	86	93
3000	89	94
4000	88	95
5000	91	93
6000	90	95
7000	87	92
8000	90	93
9000	88	94
10000	89	95

Table 2: Intrusion Detection Accuracy

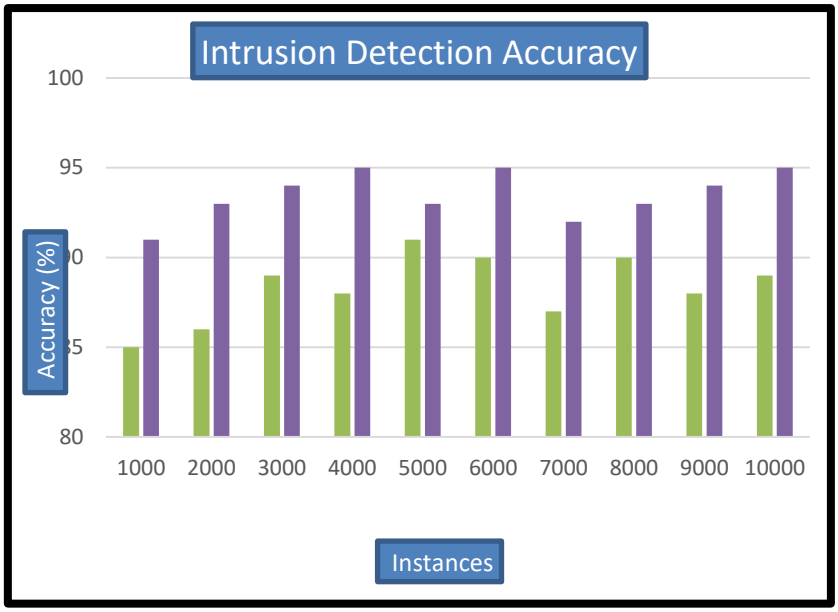

Figure 4: Intrusion Detection Accuracy.

4.3 Performance Analysis of Intrusion Detection Time

Intrusion detection time is defined as the amount of time taken by the classifier to identify data attacks as normal or anomalous. It is evaluated in terms of milliseconds (ms). The detection time is calculated in equation.

$$ID_{Time} = N * Time_{identifynormaloranomalous} \quad \text{- Eqn (4)}$$

From equation (4), time for intrusion detection is measured. Here, 'N' denotes the number of data and. '$Time_{identifynormaloranomalous}$' describes time consumed to identify single data as normal or anomalous.

Sample Calculation

Existing CLSOBBOA: Time to identify single anomaly data is 0.023ms, and the total data is 1000. Then, the intrusion detection time is calculated as$ID_{Time} = 1000 * 0.023 = 23\ ms$.

Proposed HJIBOFS -PABCE: The time to identify single anomaly data is 0.021ms, and the total number of data is 1000. Then, the intrusion detection time is calculated as$ID_{Time} = 1000 * 0.021 = 21\ ms$.

Instances	Intrusion Detection Time (ms)	
	CLSOBBOA	HJIBOFSPABCE
1000	23	21
2000	28	24
3000	32	27
4000	36	30
5000	39	34
6000	43	39
7000	47	42
8000	51	46
9000	58	50
10000	63	54

Table 3: Intrusion Detection Time

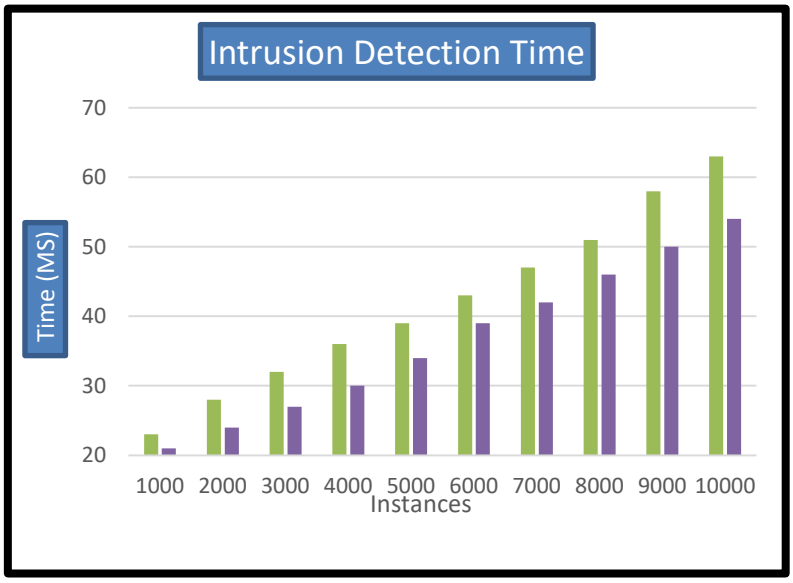

Figure 5: Intrusion Detection Time

Table 3.shows Tabulation of Intrusion Detection time and Figure 5 presents the performance analysis of intrusion detection time concerning a different number of data.

5.CONCLUSION

An efficient **HJIBOFSPABCE** is introduced to attain higher accuracy on anomaly intrusion detection in a network. An intrusion detection dataset considers the number of attributes. For each attribute, it is measuring fitness for all dragonflies using the Jaccard similarity index. Based on measured fitness for intrusion attack detection, selecting the optimal attribute helps reduce time and improves accuracy.

BIBLIOGRAPHY

Aldweesh, A., Derhab, A., &Emam, A. Z. (2020). Deep learning approaches for anomaly-based intrusion detection systems: A survey, taxonomy, and open issues. Knowledge-Based Systems, 189, 105124.

Adel SaadAssiri (2021) On the performance improvement of Butterfly Optimization approaches for global optimization and Feature Selection https://doi.org/10.1371/journal.pone.0242612

Dua, M. (2020). Attribute selection and ensemble classifier based novel approach to intrusion detection system. Procedia Computer Science, 167, 2191-2199.

Elmasry, W., Akbulut, A., &Zaim, A. H. (2020).Evolving deep learning architectures for network intrusion detection using a double PSO metaheuristic.Computer Networks, 168, 107042.

Falcão, F., Zoppi, T., Silva, C. B. V., Santos, A., Fonseca, B., Ceccarelli, A., &Bondavalli, A. (2019, April).Quantitative comparison of unsupervised anomaly detection algorithms for intrusion detection. In Proceedings of the 34th ACM/SIGAPP Symposium on Applied Computing (pp. 318-327)

Haq, E. U., Lyu, X., Jia, Y., Hua, M., & Ahmad, F. (2020). Forecasting household electric appliances consumption and peak demand based on hybrid machine learning approach. Energy Reports, 6, 1099-1105. Ibrahim, D., &Alruhaily, N. (2020). Anomaly Detection in Wireless Sensor Networks: A Proposed Framework.

Karami, A. (2018). An anomaly-based intrusion detection system in presence of benign outliers with visualization capabilities. Expert Systems with Applications, 108, 36-60.

Kasongo, S. M., & Sun, Y. (2019). A deep learning method with filter based feature engineering for wireless intrusion detection system. IEEE Access, 7, 38597-38607.

Manzoor, I., & Kumar, N. (2017). A feature reduced intrusion detection system using ANN classifier. Expert Systems with Applications, 88, 249-257.

Singh, A., Nagar, J., Sharma, S., &Kotiyal, V. (2021). A Gaussian process regression approach to predict the k-barrier coverage probability for intrusion detection in wireless sensor networks.Expert Systems with Applications, 172, 114603.

Shenfield, A., Day, D., &Ayesh, A. (2018).Intelligent intrusion detection systems using artificial neural networks. ICT Express, 4(2), 95-99

Tama, B. A., Comuzzi, M., & Rhee, K. H. (2019). TSE-IDS: A two-stage classifier ensemble for intelligent anomaly-based intrusion detection system. IEEE Access, 7, 94497-94507.

Uttar Pradesh Journal of Zoology

Volume 44, Issue 11, Page 61-73, 2023; Article no.UPJOZ.2578
ISSN: 0256-971X (P)

An Efficient Fuzzy based MRI Brain Tumor Segmentation and Classification

A. Krishnaveni [a++*] and M. S. Irfan Ahmed [a#]

[a] Department of Computer Science, Thassim Beevi Abdul Kader College for Women, Kilakarai, Ramanathapuram, Tamil Nadu, India.

Authors' contributions

This work was carried out in collaboration between both authors. Both authors read and approved the final manuscript.

Article Information

DOI: 10.56557/UPJOZ/2023/v44i113521

Editor(s):
(1) Prof. Aurora Martínez Romero, Juarez University, Mexico.
Reviewers:
(1) Jaideep Gera, ST Marys Group of Institutions Guntur, India.
(2) Xinxing Wu, Midway University, United States.

Original Research Article

Received: 01/04/2023
Accepted: 01/06/2023
Published: 16/06/2023

ABSTRACT

Picture division is a significant testing factor in clinical picture division. This paper portrays the division strategy comprising two stages. In the initial step, the MRI cerebrum picture is gained from the patients' information base, in that film, relics and commotion are taken out after the Binarization strategy is applied for picture division. The Binaraization works with the assistance of the Fuzzy C Means Clustering calculation, hence the calculation assumes the principle part in the framework, in this most minimal level of the weight vector, higher worth of cancer pixels, calculation speed is accomplished by the Fuzzy C Mean with vector quantization. The point of this exploration work is to give an assortment of fluffy c-implies (FCM) calculation that gives picture bunching utilizing the MRI Brain Tumor data set. The proposed calculation joins the neighborhood spatial data and dark level data in an original fluffy manner. The new calculation is called Fuzziness Confined Message C-Means (FCM^2). FCM^2 can defeat the drawbacks of the known fluffy c-implies calculations and simultaneously improves the grouping execution. The significant trait of FCM^2 is the utilization of a

---

[++] *Assistant Professor;*
[#] *Professor;*
**Corresponding author: Email: drakrishnaveni@gmail.com;*

fluffy neighborhood (both spatial and dark level) closeness measure, expecting to ensure clamor heartlessness and picture detail conservation. Besides, the proposed calculation Experiments performed on manufactured and true pictures show that the FCM^2 calculation is powerful and proficient, giving strength to uproarious pictures.

Keywords: Cell; fuzzy; Binarization; clustering; segmentation; brain tumor.

1. INTRODUCTION

One of the significant errands of picture examination is picture division. Picture division parcels picture into groups that are not difficult to examine [1-4]. A portion of the uses of picture division incorporate example acknowledgment and object ID, including extraction and clinical imaging [5-9]. For clinical pictures, picture division assumes an indispensable part. In this paper, a strategy is introduced which is applied to identify the various tissues present in MRI cerebrum pictures. Subsequent to identifying the mind tissues, a few sicknesses can be analyzed without any problem [10-14].

Brain tumor cell recognition is important and needed for finding the tumor in the earlier stage to reduce the mortality rate of a human being. This paper involves finding pattern images from the given source image [15,16]. In medical images, if the user needs to find the cell structure or bone crack information, we need to manually verify the area. Instead of manual analysis if a system that highlights all the crack patterns, then it would be useful [17-19]. This paper helps to identify the search pattern image from the given large image. In addition, the pattern image can be cropped from the source image itself or can be selected from another file. The rectangular pixel area of the pattern is collected in an array and checked with source image pixel data row-wise and column-wise. The pixel percentage can be adjusted so that nearly matching images can also be recognized.

2. LITERATURE REVIEW

Sandeep Kumar et al. there is a variety of the fluffy c-implies (FCM) calculation is introduced that gives picture bunching. The proposed calculation consolidates nearby spatial data and dark level data in a clever fluffy manner. The new calculation is called fluffy nearby data C-Means (FLICM). By utilizing this calculation they can beat the inconveniences of the past calculations and simultaneously improves the bunching execution [20].

Qiuyu Song et al. raise a better self-learning weighted fluffy calculation, which straightforwardly acquires various loads in distance estimation through consistent iterative self-learning, then, at that point, the distance metric with the loads got from self-learning is implanted in the goal capacity of the fluffy grouping calculation to further develop the division execution and vigor of the calculation. An enormous number of investigations on various kinds of pictures show that the calculation can smother the clamor as well as hold the subtleties in the picture, the impact of portioning complex commotion pictures is better, and it gives preferable picture division results over the current most recent fluffy grouping calculations [21].

Sucharitha M et al., suggested Fuzzy Local Information C-Means calculation (FLICM) is presented which incorporates a boundary-free clever fluffy variable. This calculation can be applied for clinical picture division for characterizing mind MRI into various locales, for example, Gray matter (GM), White matter (WM), and Cerebro-Spinal liquid (CSF). Subsequent to arranging into various tissue locales, a few illnesses can be dissected without any problem. The proposed strategy shows the viability of calculation in portioning cerebrum pictures into various tissue types [22].

Pooja B et al. two calculations are thought of. One is level set division utilizing fluffy c means by utilizing exceptional highlights (SFCM) and another is a division of mind MRI pictures utilizing DWT and head part investigation (PCA) are additionally handled utilizing support vector machine (SVM) for characterization. The execution assessment is finished by processing mean square mistake, top sign to commotion proportion (PSNR), most extreme contrast, outright mean mistake and so forth Here DWT utilizes k-implies bunching and level set utilizes fluffy c-implies grouping. The spatial limitations are named with various records, for example, the client can pick on a specific district of interest and emphasize the form ventures until a more precise outcome is acquired [23].

Standard FCM, Fuzzy Local data C-implies grouping calculation [FLICM], Reformulated Fuzzy Local data C-implies bunching calculation [RFLICM] are contrasted with investigating the exactness of our proposed approach. Grouping results show that the RFLICM division technique is fitting for ordering tissues in cerebrum MR picture [24].

Consequently, to beat the vagueness brought about by the above unique effects, an upgraded fluffy unwinding approach called fluffy relaxation-based modified fluffy c-implies is introduced to group calculation by Magudeeswaran et al.. In the proposed strategy, openness-based sub-picture fluffy brilliance variation calculation is executed for the improvement of cerebrum tissues, and it is trailed by a modified fluffy c-implies grouping calculation to section the upgraded mind attractive reverberation picture into white matter, dim matter, and cerebrospinal fluid tissues. The proposed technique adjusts its prosperity on mind tissue division and offers broad help to radiologists and clinical focuses [25].

The diagram in light of pixel esteem is drawn taking the different focuses from the expanded cells lies in the first situation from the impacted locale. Here the impacted district is considered an ellipsoid shape and the volumes have been determined from it. A fluffy level set calculation is proposed by Pritam R et al. to work with clinical picture division and in this exhibition of assessment of the proposed calculation was conveyed [26].

3. MATERIALS AND METHODS

3.1 Source Image Selection

In the source image selection module, the jpg, gif, or bitmap image is selected. The image is previewed in a picture box with the size mode property set to auto-size. The image property is used to create a bitmap class in .Net so that the width and height of the image are obtained.

3.2 Pattern Image(s) Selection

In the pattern image(s) selection module, the jpg, gif, or bitmap image is selected. Optionally the second image is selected if to be recognized in the second image.

3.3 Pattern Recognition

In the pattern recognition module, both the source and pattern images are displayed. When the check button is clicked, the source and pattern images are copied into separate arrays. During recognition, for faster comparison, the source image's color information for each pixel is copied and compared immediately with the corresponding pattern image pixel. If the pixel is not matched, then the function returns a false value so that further pixels in the rectangular area are not compared. The threshold value can be set so that only some percent of the image pixels are compared.

3.4 Problem Direction

The existing system is analyzing images manually. We cannot recognize all the patterns in the images. In the previous, we have to split the large image into a small image after that only we can identify the part of an image that we need. This is not an effective method to get a clear part of an image. The existing system has the following disadvantages,

1 The manual approach reduces the accuracy of pattern identification.
2 More time-consuming.
3 Efficiency is less.

3.5 Proposed System

The proposed system is analyzing images through software. We can recognize all the patterns in the images easily. This method simplifies our work to get a clear part of an image with a simple process. This method is very helpful in various fields like medical, engineering, textiles, etc.

3.6 Advantages of Proposed System

The proposed system has the following advantages,

- The proposed approach increases the pattern identification accuracy.
- Less time consuming
- Efficiency is more.
- More patterns can be identified in a single large image at a time.

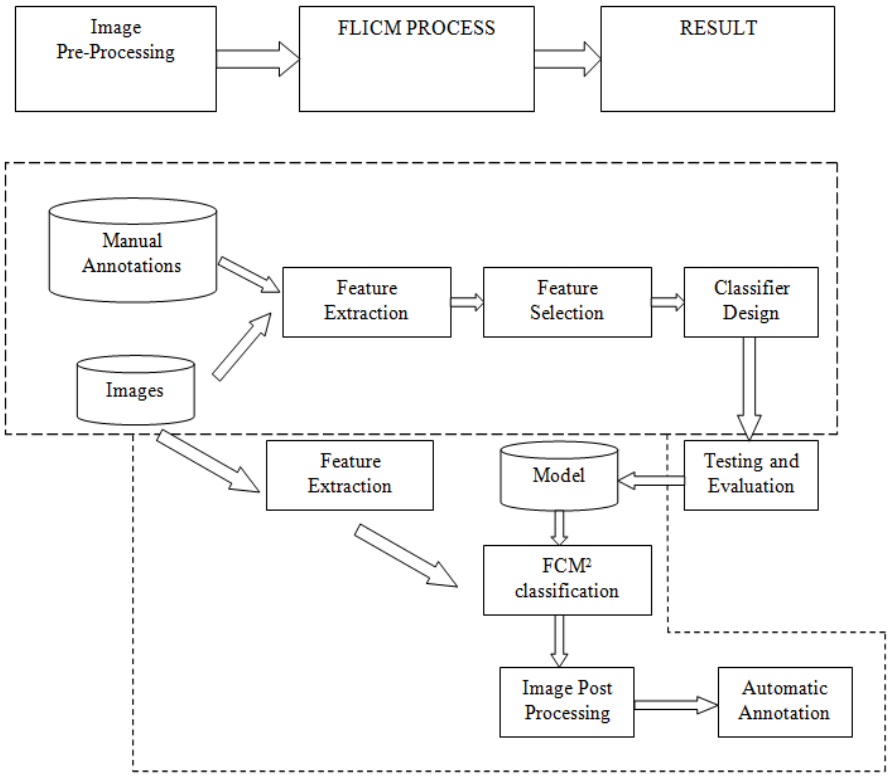

Fig. 1. Systematic Diagram for the Introduced method (FCM^2)

In introduced method, new fuzziness feature F_{ki} is incorporated over the objective function of predictable FCM, to overcome the interruption of any value and is shown below,

$$F_{cm} = \sum_{m \in N, n_i \neq m} \frac{1}{d_m + |1} (1 - u_{cn})^k ||y - u_k||^2 \quad (1)$$

Where c is reference cluster, spatial Euclidean distance between pixels m and n is , unit of relationship is resolute as u_{cn} which is the relative of nth pixel in k^{th} cluster, fuzziness relationship has a increment supporter and s denoted as m and the midpoint of cluster k has the sample as v_k .

FCM^2 method is projected by combining both three-dimensional particulars and gray smooth particulars into predictable function and is stated in way of F_{ki} as,

$$J_m = \sum_{m=1}^{N} \sum_{k=1}^{c} [u^m ||y_m - v_k||^2 + F_{ki}] \quad (2)$$

FCM^2 algorithm is described below as:

Step 1: Set the quantity of cluster as c, fuzzification limit l and the stop of process s.

Step 2: Take up fuzziness divider conditions with experimental and miscalculation.

Step 3: Allocate the significance of twist security to be a = 0.

Step 4: Constellation examples is resolute created on the formulation in the following Eq.3

$$v = \frac{\sum_{i=1}^{N} u^l \, xi}{\sum_{i=1}^{N} u_{ki}^l} \quad (3)$$

Step 5: Find the fuzziness divider environment through the support of the following equation as

$$\beta_{ki} = \frac{1}{\sum_{j=1}^{c} \left(\frac{\|x_i - v_k\|^2 + }{\|x_i - v_j\|^2 + G j_i} \right)^{1/m-1}} \quad (4)$$

Step 6: When $\{\beta^{(m)} - \beta^{(m+1)}\} < \varepsilon$, then termination comes to the procedure, otherwise,

set $b = b + 1$ and transfer to Step 4.

Fuzziness divider environment β is improved into a crisp divider when the comprehensive

repetition is ended. To achieve the upstairs procedure defuzzification procedure is experienced and is stated below.

$$DF_i = argument\{\{\beta_{ki}\}\}\ldots\ldots\ldots\ldots \quad (5)$$

Fuzziness picture accomplished subsequent to doing the interaction is then changed over into a fresh sectioned picture. The above idea is carried out to portion mind MRI pictures into three tissue types and is liberated from any anomalies and furthermore autonomous of boundaries. The division execution is significantly more upgraded than the current methods.

At the point when exceptions are available in the picture, the great characteristics of the calculation is made sense of by two fundamental cases. They are,

Event (i): Pixels present in the nearby window are undermined by commotion however pixel situated at the Center isn't a clamor pixel.

In such case, dark degrees of boisterous pixels to that of different pixels inside the window are unique and henceforth their enrollment values are adjusted by factorGki. Thusly, the connection of loud pixels is stifled by the factor Gki. Clamor is taken out by including the blend of spatial and dark-level limitations in work. The calculation is likewise more worthwhile in the event of anomalies.

Event (ii): Pixels present in the nearby window are homogenous, not debased by clamor however pixel situated at the Center is a commotion pixel.

In such a case, focal pixel enrollment esteem is adjusted by factor Gki by considering both the spatial and the dark level of the without commotion adjoining pixels in a fluffy way. In spite of the fact that enrollment worth of focal pixel doesn't relate to the commotion, the proposed strategy turns out to be more powerful to exceptions.

4. RESULTS

Trial and error are gone through for the proposed strategy. The calculation is executed utilizing MATLAB and tried on mind MRI pictures to investigate the division precision of the proposed approach. The examination is made and the nature of the division of the proposed calculation can be determined by utilizing SVM Classification.

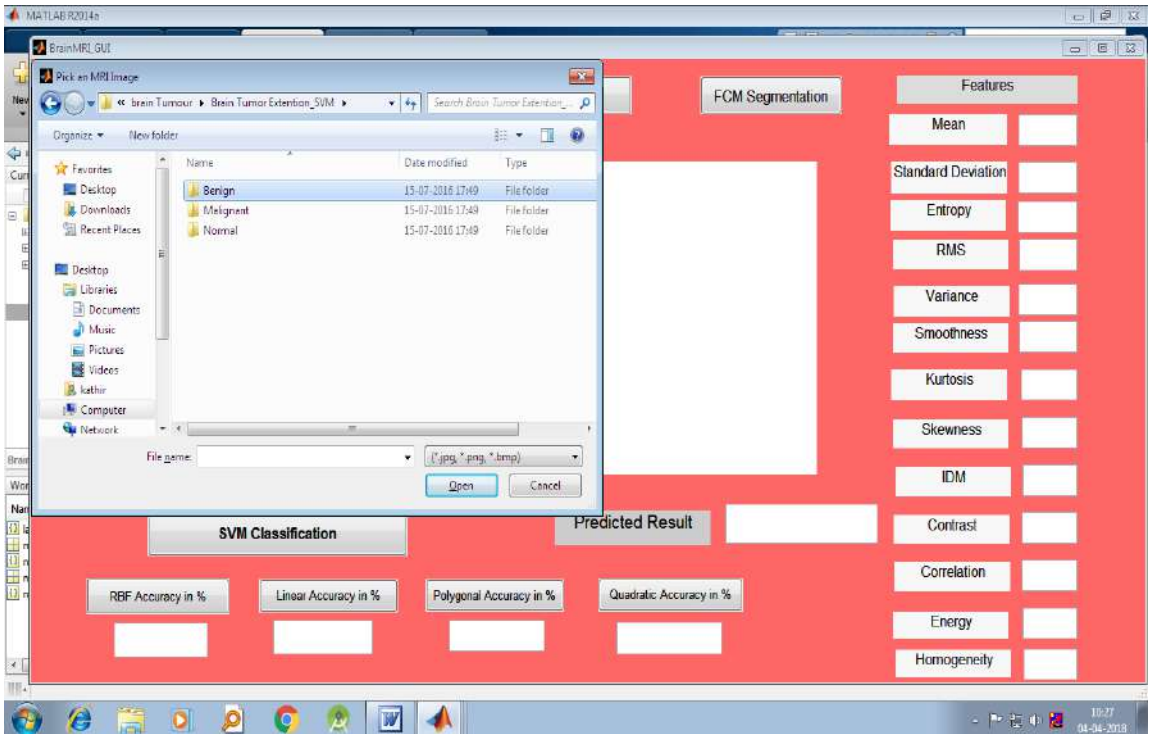

Fig. 2. Input MRI Image

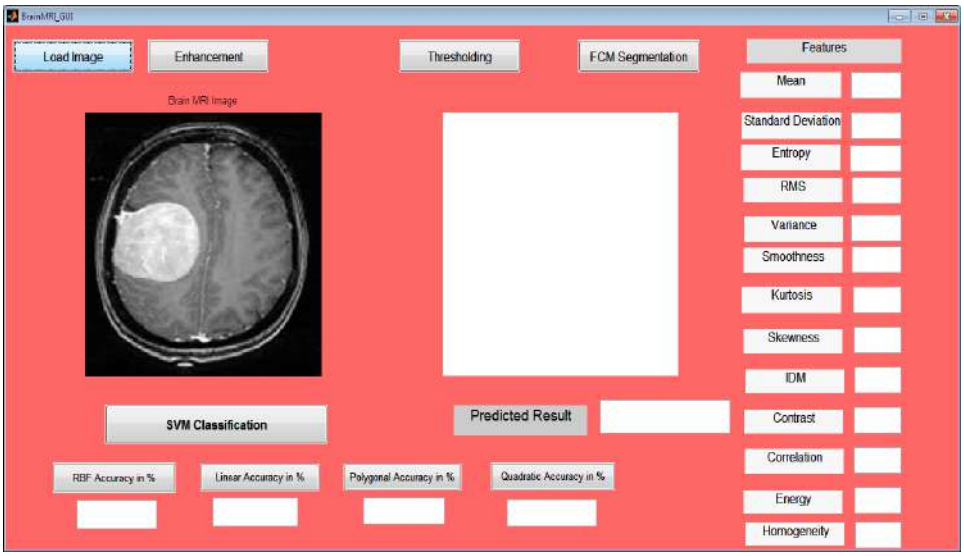

Fig. 3. Uploading Image

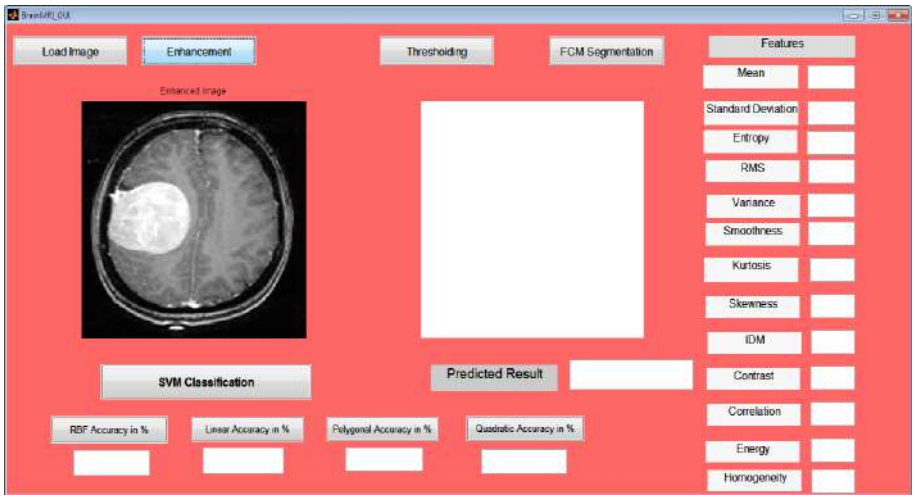

Fig. 4. Enhanced Image

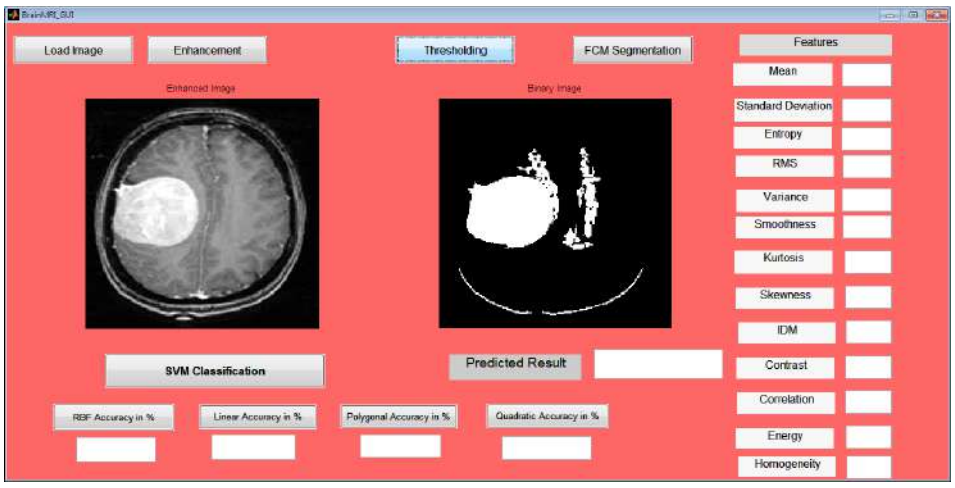

Fig. 5. Thresholding Binary Image

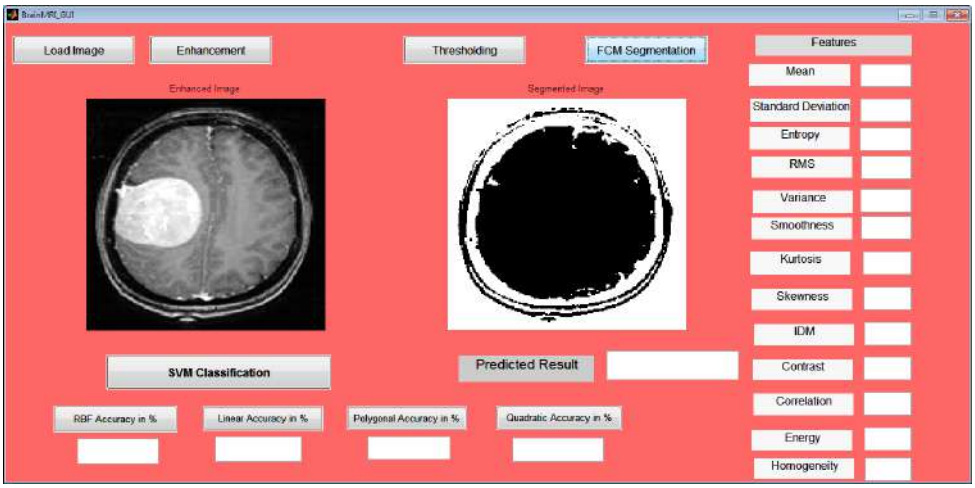

Fig. 6. Segmented Image

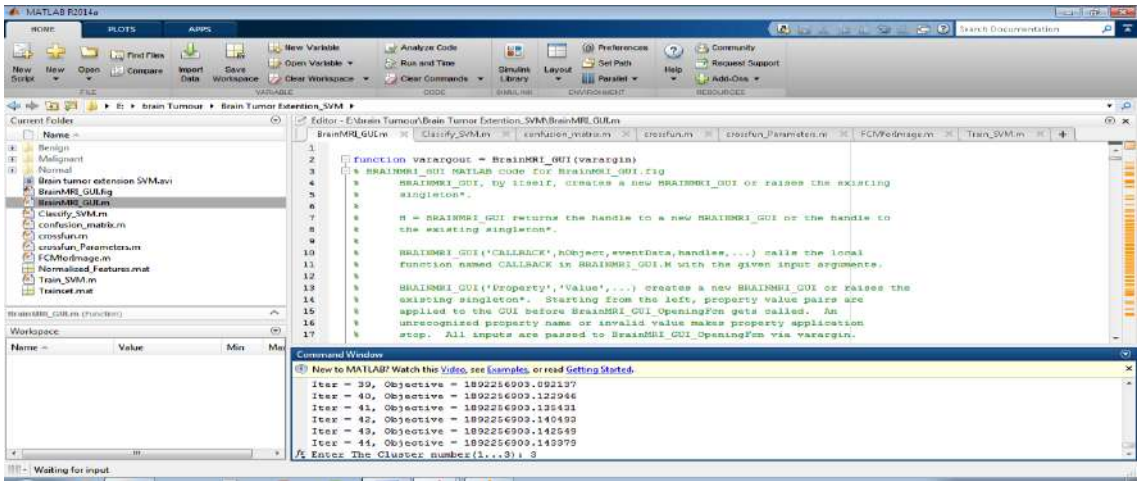

Fig. 7. Input Cluster Count Image

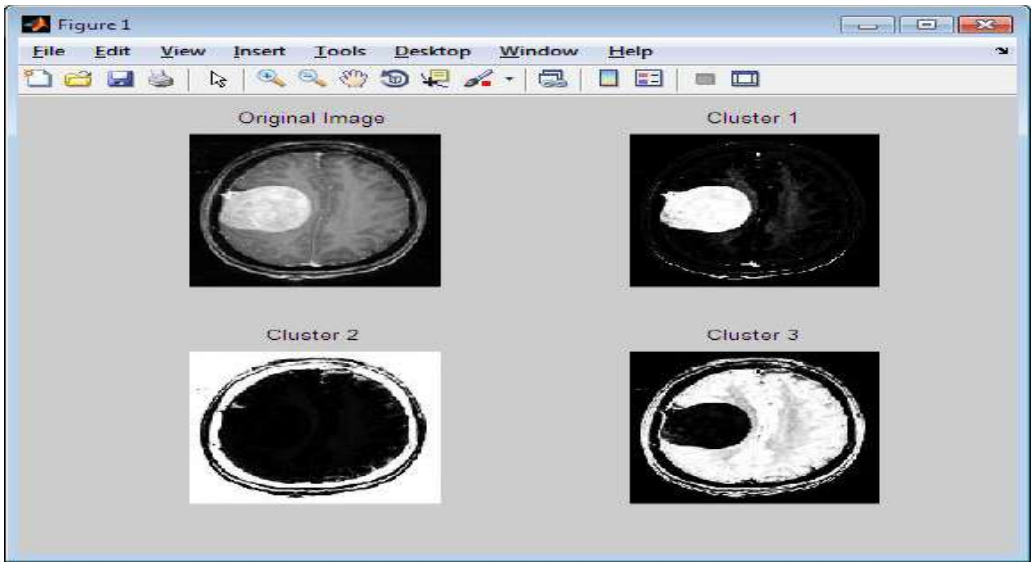

Fig. 8. Clustered Image

RBF Accuracy Finding

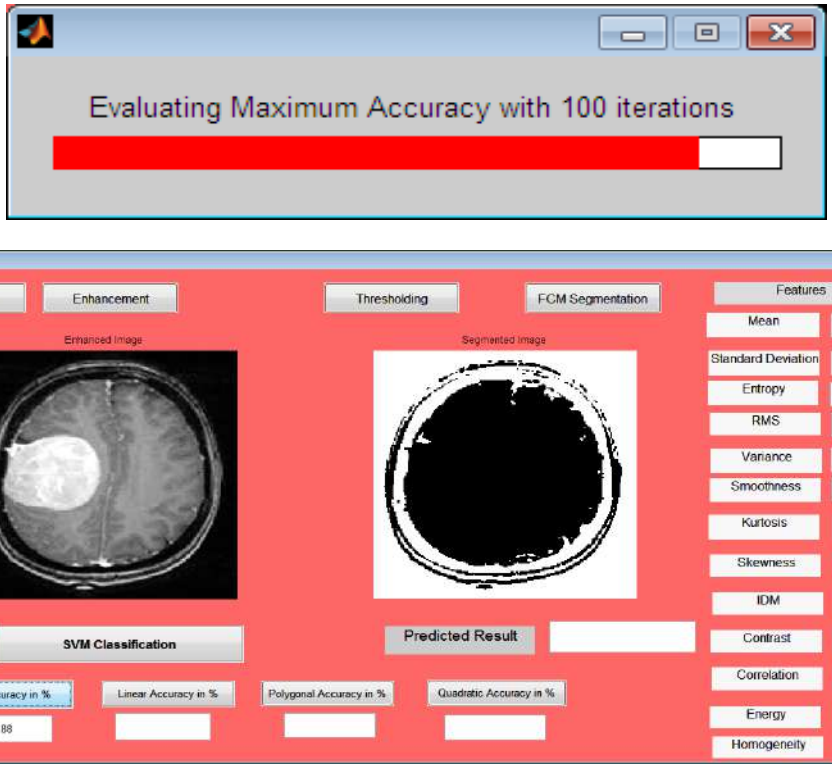

Fig. 9. RBF Accuracy Result

Linear Accuracy Calculation Processing

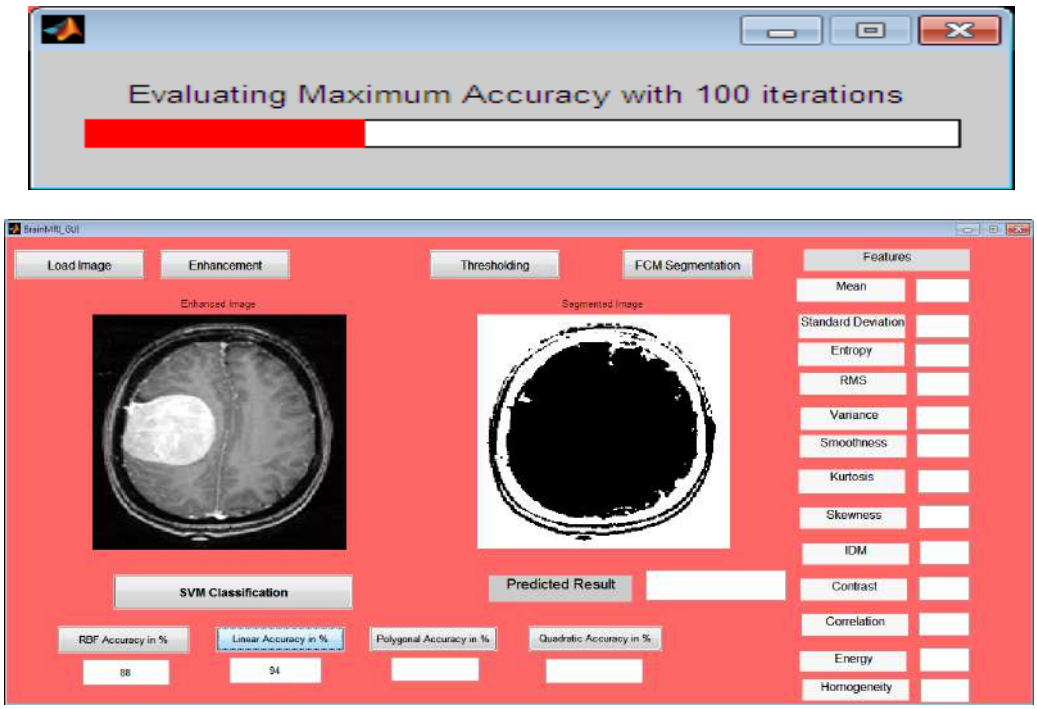

Fig. 10. Linear Accuracy in Percentage

Polygonal Accuracy Finding

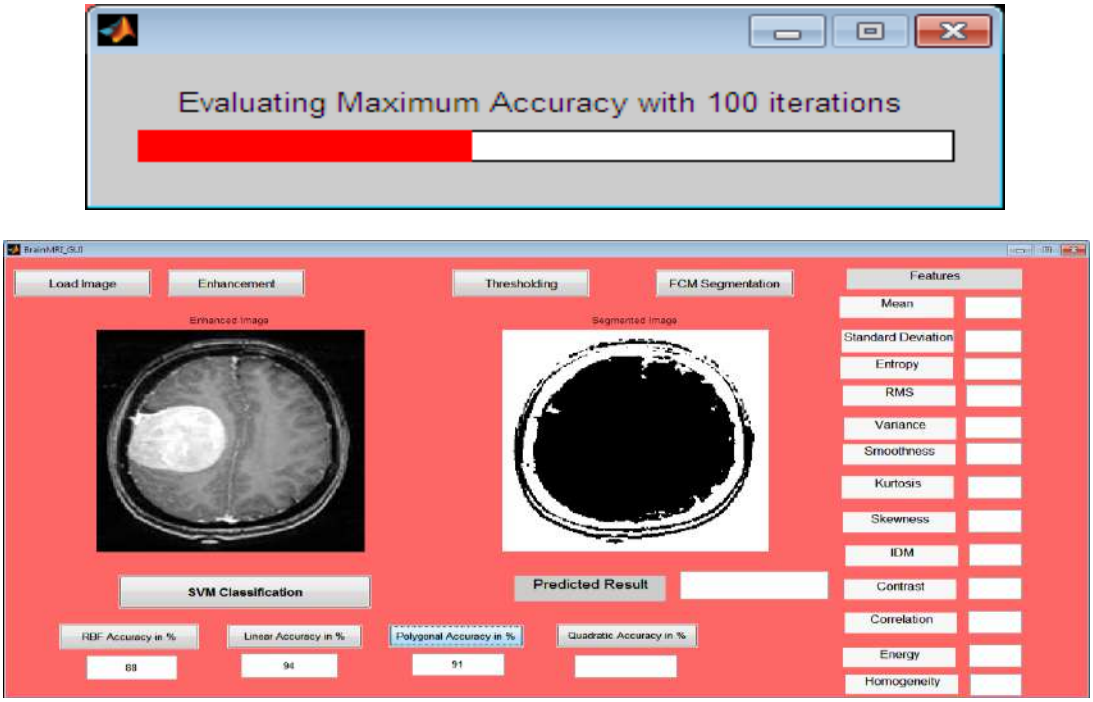

Fig. 11. Polygonal Accuracy Result

Quadratic Accuracy Finding Result

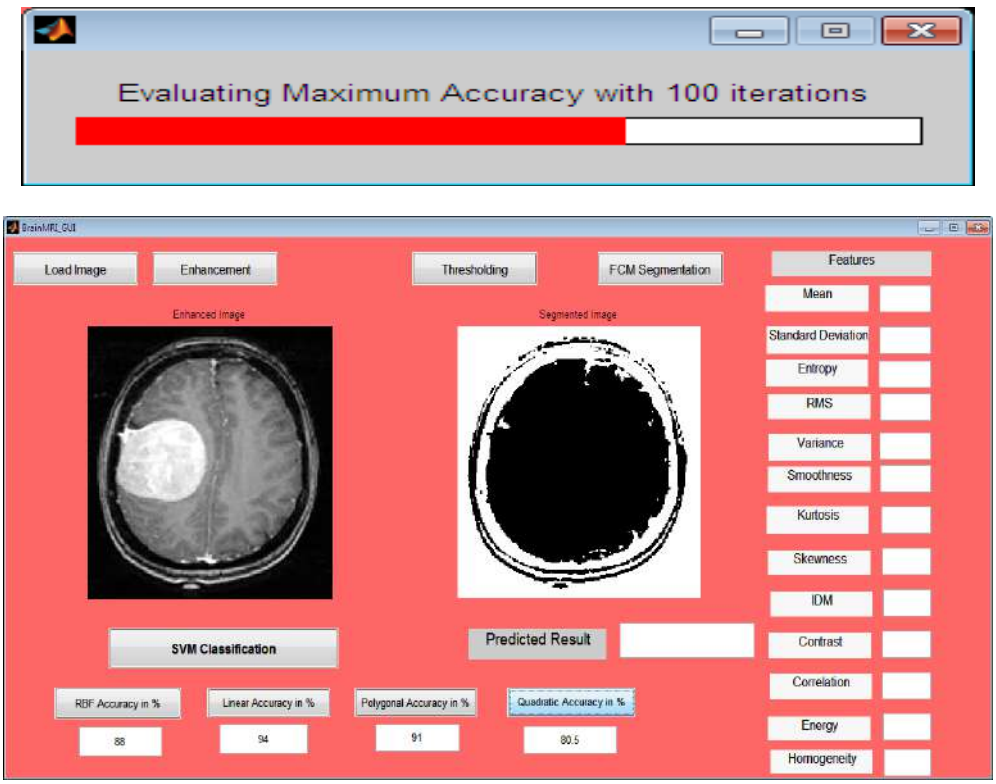

Fig. 12. Quadratic Accuracy Result

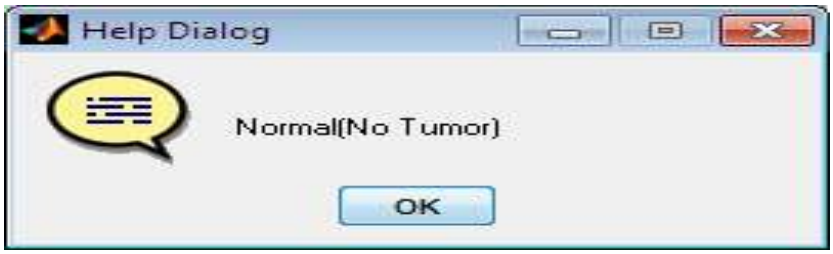

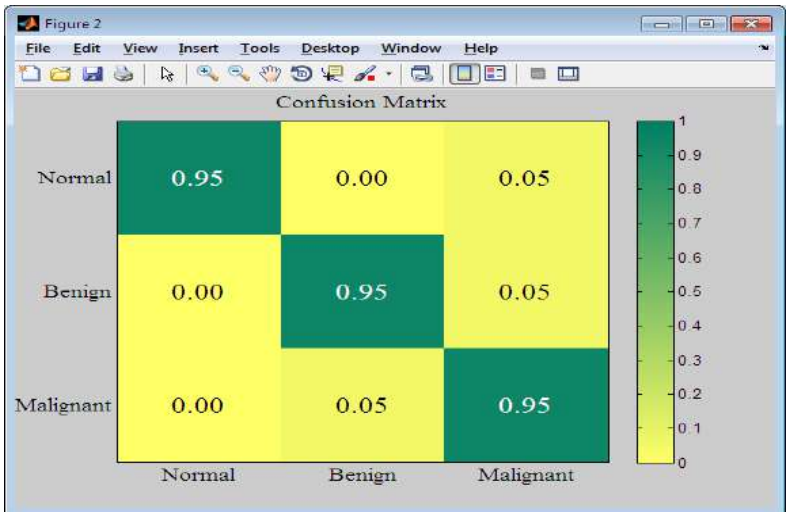

OUTPUT IN COMMAND WINDOW

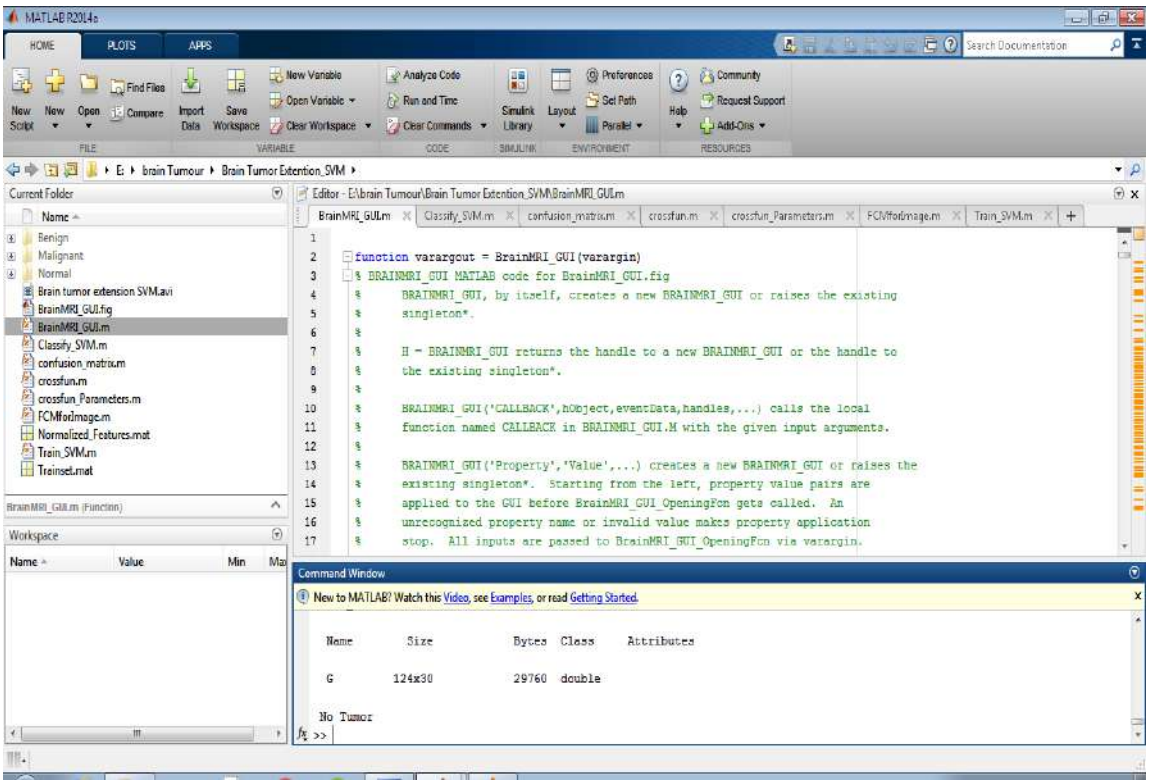

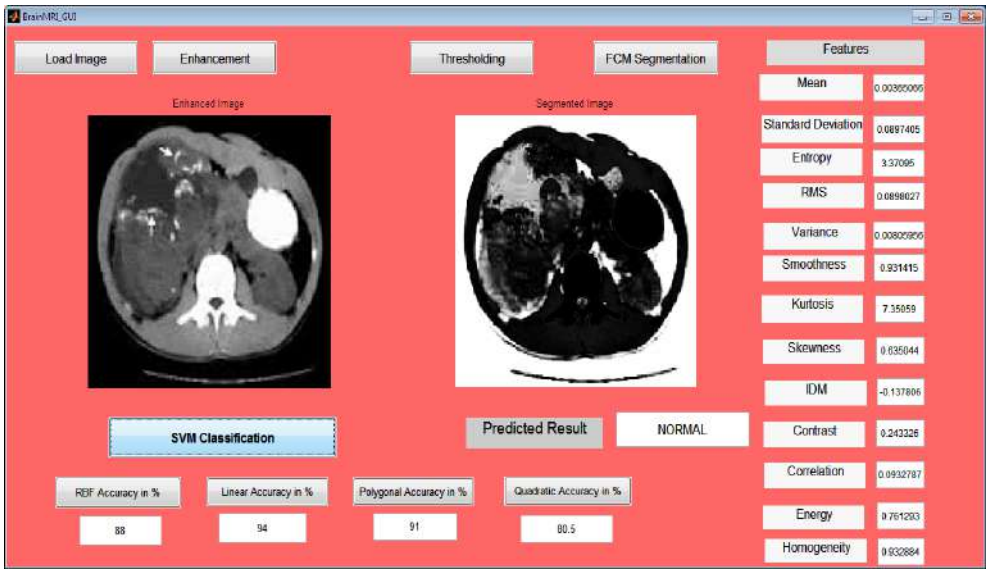

Fig. 13. Features Classification

Table 1. Quality Metrics

Quality Metrics	Accuracy in (%)
RBF Accuracy	88
Linear Accuracy	94
Polygonal Accuracy	91
Quadratic Accuracy	80.5

The segmentation accuracy achieved in the proposed method with respect to noise is 94%. Linear accuracy with SVM feature classification has the prior place and Polygonal accuracy have the 91%. Then RBF accuracy is 88% and Quadratic accuracy is 80.5%.

5. DISCUSSION

The performance of the proposed method is described in the result sections. Input MRI images are used and downloaded from Whole Brain Atlas (WBA). In the present work, more than 500 brain MR images with different sizes have been used for evaluation. For pre-processing, noise removal and enhancement methods are applied to the original MRI images. Then Thresholding technique was applied and binary image can be used for segmentation. Segmented image is used for clustering. Only tumor part is clearly segmented and result showed in the clustered image. Accuracy is the performance metric used to evaluate the results obtained by SVM feature classification. Linear accuracy shows the proposed method has a high accuracy for brain tumor segmentation.

6. CONCLUSION AND FUTURE WORK

Through this paper, the issue of the manual example is wiped out. Since exceptionally less information is given and any individual can utilize the application. When the pixel esteem is viewed as wrong in a given rectangular region, the whole region is disregarded for additional pixel examination. This outcome in quick work and their general acknowledgment time is decreased. The end clients are supposed to have the most un-working inclusion with structures to run this item. The application diminishes acknowledgment time and helps in further developing mistake-free and effective examples distinguishing proof. The application is tried well so the end clients utilize this product for their entire example acknowledgment-related activities. The accompanying upgrades ought to be done from now on. The multi-stringing choice ought to be added to distinguish the pixels at the same time in more regions of the picture. The picture can be changed over to a grayscale design and the example can be perceived as paying little heed to a variety of data. This will bring about quick acknowledgment. The brain

network idea in the event this at presented from now on will help in acknowledgment far better. The application is planned with the end goal that more example picture determination should be possible and at the same time thought about. For instance, coarse grain, as well as fine-grain rice pictures, can be chosen and minded a rice plate for quality. The application is grown to such an extent that these improvements will be incorporated effectively with modules present in the examination work.

COMPETING INTERESTS

Authors have declared that no competing interests exist.

REFERENCES

1. Sarmad M, Robertas D, Faisal MS, An Efficient Approach for the Detection of Brain Tumor Using Fuzzy Logic and U-NET CNN Classification, ICCSA 2021, LNCS. 2021;12953:105–118.
2. Abhishek B, Minakshi B, Amlan C, Punit S. MRI Brain Tumor Segmentation and Analysis using Rough-Fuzzy C-Means and Shape Based Properties, Journal of King Saud University - Computer and Information Sciences. 2022;34(2):115-133.
3. Roqaie K, Roqaie M, Nazila L, Armin A, Mohammad BS, Arash ZS, Brain Tumor Segmentation using Hierarchical Combination of Fuzzy Logic and Cellular Automata, J Med Signals Sens. 2022;12(3):263–268.
4. Wadhwa A, Bhardwaj A, Singh Verma V. A review on brain tumor segmentation of MRI images. Magn Reson Imaging. 2019; 61:247–59.
5. Sharif, Muhammad. An integrated design of particle swarm optimization (PSO) with fusion of features for detection of brain tumor. Pattern Recognition Letters. 2020;129:150-157.
6. Sahu, Satya Prakash. Segmentation of Lungs in Thoracic CTs Using K-means Clustering and Morphological Operations. Advances in Biomedical Engineering and Technology. Springer, Singapore. 2021;331-343.
7. Moeskops, Pim. Adversarial training and dilated convolutions for brain MRI segmentation. Deep learning in medical image analysis and multimodal learning for clinical decision support. Springer, Cham. 2017;56-64.
8. Hamad YA, Konstantin VS, Mohammad BN. Detection of brain tumor in MRI images, using a combination of fuzzy C-means and thresholding. International Journal of Advanced Pervasive and Ubiquitous Computing (IJAPUC). 2019;1:45-60.
9. Mittal, Mamta. Deep learning based enhanced tumor segmentation approach for MR brain images. Applied Soft Computing. 2019;78:346-354.
10. Mandle AK, Sahu SP, Gupta G. Brain Tumor Segmentation and Classification in MRI using Clustering and Kernel-Based SVM. Biomed Pharmacol J. 2022;15(2).
11. Hamad, Yousif Ahmed, Konstantin Vasilievich Simonov, and Mohammad B. Naeem, Detection of brain tumor in MRI images, using a combination of fuzzy C-means and thresholding. International Journal of Advanced Pervasive and Ubiquitous Computing (IJAPUC). 2019; 1:45-60.
12. Li, Ming. Brain tumor detection based on multimodal information fusion and convolutional neural network, IEEE Access. 2019;7:180134-180146.
13. Huang, Hong. Brain image segmentation based on FCM clustering algorithm and rough set. IEEE Access. 2019;7:12386-12396.
14. Yogalakshmi G, Sheela Rani B. A Review On The Techniques Of Brain Tumor: Segmentation, Feature Extraction And Classification. 2020 11th International Conference on Computing, Communication and Networking Technologies (ICCCNT). IEEE; 2020.
15. Yahya MA. Mohammed, Said El G, Ismail J. A survey of methods for brain tumor segmentation-based MRI images, Journal of Computational Design and Engineering. 2023;10:266–293.
16. Zhao X, Wu Y, Song G, Li Z, Zhang Y, Fan Y. A deep learning model integrating FCNNs and CRFs for brain tumor segmentation, Med Image Anal. 2018;43:98–111.
17. Karayegen G, Aksahin MF. Brain tumor prediction on MR images with semantic segmentation by using deep learning network and 3D imaging of tumor region, Biomedical Signal Processing and Control. 2021;66:102458.
18. Sujan M, Alam N, Noman SA, Islam MJ. A segmentation based automated system for

brain tumor detection. Int J Comput Appl. 2016;153:41–9.

19. Sathies T, Kumar K, Rashmi, Sreevidhya R, Sandhya LK, Sangeetha TJ. Brain tumor detection using SVM classifier, Third International Conference on Sensing, Signal Processing and Security (ICSSS), IEEE; 2017.
20. Sandeep Kumar M, Jai Kumar V. An Efficient Algorithm for Segmentation Using Fuzzy Local Information C-Means Clustering, International Journal of Scientific and Engineering Research. 2011;2(12).
21. Qiuyu S, Chengmao W, Xiaoping T, Yue S, Xiaokang G. A novel self-learning weighted fuzzy local information clustering algorithm integrating local and non-local spatial information for noise image segmentation, Applied Intelligence; 2021.
Available: https://doi.org/10.1007/s10489-021-02722-7
22. Sucharitha M, Parimala Geetha K. Segmentation of Brain Tissue using Fuzzy Local Information C-Means Technique, JCPS. 2016;9(1).
23. Pooja BM, Goudar RH. Segmentation of Brain MRI Images using Fuzzy C-Means and DWT, IJSTE - International Journal of Science Technology & Engineering. 2016;2(12).
24. Sucharithaa M, Parimala Geethab K. Brain tissue segmentation using fuzzy clustering techniques, Technology and Health Care. 2015;23:571–580.
25. Magudeeswaran V, Bharath S. Brain tissue segmentation for medical decision support systems, Journal of Ambient Intelligence and Humanized Computing; 2020.
Available: https://doi.org/10.1007/s12652-020-02257-8
26. Pritam RD, Dinesh DP. An Ameliorate Technique for Brain Lumps Detection Using Fuzzy C-Means Clustering, IJMTER. 2017;4(1).

Face Mask Detection using improved Convolutional Neural Network

Ms M.Nagavalli
Assistant Professor, Department of Computer Science,
Thassim Beevi Abdul Kader College for Women, Kilakarai

Abstract

During the CoVID 19 pandemic, people must wearing face masks in public areas to prevent and reduce the probability of virus transmission and dissemination. The healthcare sector is in a terrible condition. There have been several measures attempted to prevent the spread of this disease, such as the usage of masks, which the World Health Organization strongly recommends (WHO). In this study, the CNN algorithm is improved using the ReLU activation function. Three activation functions—ReLU, Sigmoid, and Softmax—were used to search for face masks. The Softmax was able to achieve 90% accuracy. The accuracy of the Sigmoid was 95.19% as well. ReLU architecture attained an accuracy rate of 99.72%.

Keywords: Facemask detection, Convolutional Neural Networks, Activation Function, ReLU Function

Introduction

Most of the world's population has been harmed as a result of the COVID-19 (Coronavirus) pandemic. COVID-19 is a respiratory disease that triggers severe pneumonia in those who are affected. The virus enters an airspace through coughing, sneezing, or direct contact with an infected person. It can also enter through salivation beads, respiratory droplets, or nasal droplets emitted during these actions. Globally, the COVID-19 virus claims thousands of lives every day. [4] According to a World Health Organization (WHO) assessment on the coronavirus (COVID-19), as of November 22, 2021, there.

5 148 221 deaths and 258 million diagnosed COVID-19 cases worldwide.[5] In order to prevent the viral spread of disease, people should wear face masks and maintain a social distance. Whether people are wearing face masks or not, a real-time application that watches people in public should be created using an effective and efficient computer vision method. Identifying the face is the first step in determining whether a mask is present on it. This separates the entire

process into two phases: face detection and face mask detection.

Wear a protective facemask to prevent the spread of the coronavirus as part of the survival advice. The most efficient preventive measure against COVID-19 must be adopted by wearing a facemask. It is challenging to physically check to see if people are correctly wearing face masks and to alert the victim in crowded and public places [1]. This work takes a more straightforward approach to facemask recognition and alerting the person if it is not being worn. A system that automatically identifies whether or not a person is wearing a face mask and notify the higher authorities if not wearing a mask. [2] In this work is trained using convolutional neural network with mobilenet. The dataset contains 3801 images. The model is trained with two different classes-with and without masks. The category with masks includes faces with masks of different angles and different poses and different color masks. The category without masks contains faces without masks, hands used as masks and improper wearing of facemasks. 80% of the dataset are used for training and 20% for testing. [3] The use of face masks called for the need to have facial detection machines which can be developed from Keras, Scikit-learn and OpenCV. This paper examines the Convolutional Neural Network (CNN), which is utilized for detecting and classifying an individual wearing a mask.

Activation Functions

The final value produced by a neuron is provided via activation functions. In essence, an activation function is a simplified function that converts inputs into outputs with a defined range. Different types of activation functions carry out this role in various ways. For instance, the sigmoid activation function accepts input and maps the output values to ranges between 0 and 1.

This function is included in an artificial neural network as one of the ways to aid in the network's ability to recognise intricate patterns in data. Artificial neural networks are given nonlinear real-world features through these functions. Basically, x is defined as inputs, w weights, and we send f (x), which is the value passed to the output of the network in a simple neural network. This will then serve as the last output or the first layer's input.

If the activation function is not applied, the output signal becomes a simple linear function. A neural network without activation function will act as a linear regression with limited learning power. But we also want our neural network to learn non-linear states as we give it

complex real-world information such as image, video, text, and sound.

Softmax

Softmax function calculates the probabilities distribution of the event over 'n' different events. In general way of saying, this function will calculate the probabilities of each target class over all possible target classes. Later the calculated probabilities will be helpful for determining the target class for the given inputs. Softmax is an activation function that outputs the probability for each class and these probabilities will sum up to one. Cross Entropy loss is just the sum of the negative logarithm of the probabilities

The main advantage of using Softmax is the output probabilities range. The range will 0 to 1, and the sum of all the probabilities will be equal to one. If the softmax function used for multi-classification model it returns the probabilities of each class and the target class will have the high probability.

Sigmoid

A Sigmoid function is a mathematical function which has a characteristic S-shaped curve. There are a number of common sigmoid functions, such as the logistic function, the hyperbolic tangent, and the arctangent. In machine learning, the term sigmoid function is normally used to refer specifically to the logistic function, also called the logistic sigmoid function. All sigmoid functions have the property that they map the entire number line into a small range such as between 0 and 1, or -1 and 1, so one use of a sigmoid function is to convert a real value into one that can be interpreted as a probability. One of the most widely used sigmoid functions is the logistic function, which maps any real value to the range (0, 1). Note the characteristic S-shape which gave sigmoid functions their name (from the Greek letter sigma).

ReLU

The ReLU is the most used activation function in the world right now. Since, it is used in almost all the convolutional neural networks or deep learning. Perhaps the most often utilised function for hidden layers is the rectified linear activation function, or ReLU activation function. It is widespread because it is easy to use and successful in overcoming the drawbacks of other formerly well-liked activation functions, such as Sigmoid and Softmax.

ReLU is half rectified (from bottom). f(z) is zero when z is less than zero and f(z) is equal to z when z is above or equal to zero. The function and its derivative both are monotonic. ReLU's use thereby aids in preventing the exponential development of the compute needed to run the neural network.

More computationally efficient to compute than Sigmoid like functions since Relu just needs to pick max(0,x) and not perform expensive exponential operations as in Sigmoids. Networks with Relu tend to show better convergence performance than sigmoid. The ReLU function's primary benefit over other activation functions is that it does not concurrently activate all of the neurons. Relu activation function gives the best train accuracy and validation accuracy.

Methodology

f(X) = max (0,X)

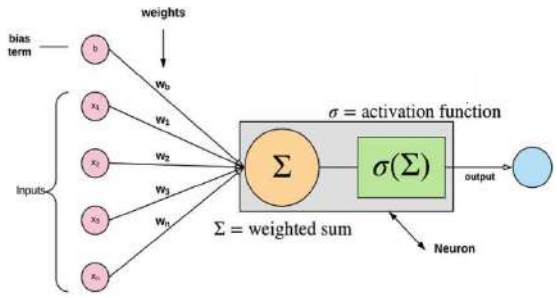

Diagram of a simple convolution neural network

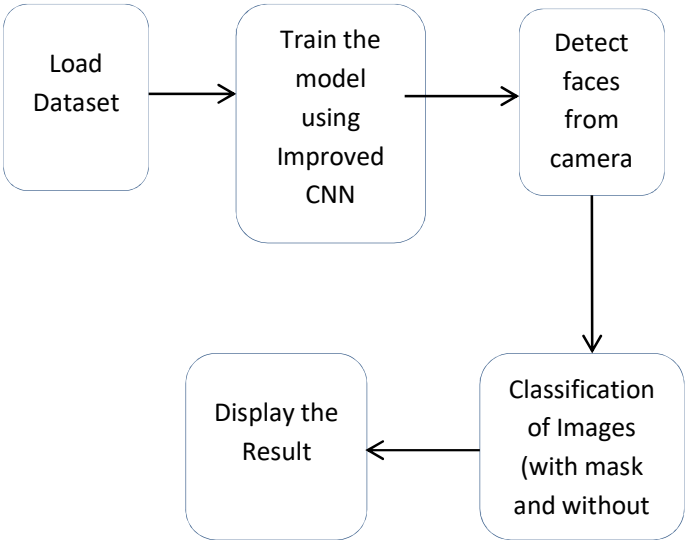

Architecture of Proposed System

Dataset

A dataset containing images of face with mask and without mask. The training dataset contains100 images,which is used to train. The testing dataset contains 300 images, which is used to test.

Result and Discussion

When relu activation function is applied,it provides highest accuracy of 90 and lowest loss value of 25.For Sigmoid activation function,it yields less accuracy of 59 and loss value of 27.With Softmax function,it gives accuracy of 59 and loss value of 68.Thus Relu activation function provides better performance when compared with sigmoid and softmax function.

S.No	Activation Function	Accuracy
1	ReLU	90
2	Sigmoid	59
3	Softmax	59

Table 1 : Accuracy of various activation functions

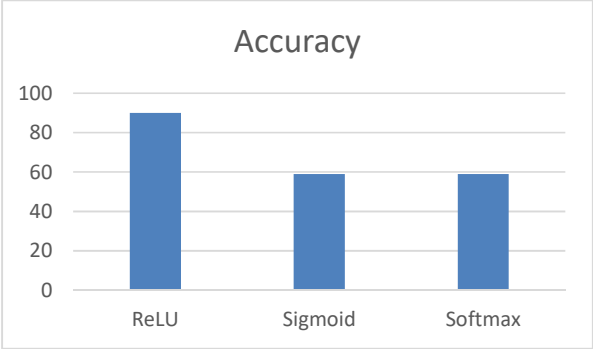

Fig 1.Accuracy of various activation functions

S.No	Activation Function	Loss
1.	ReLU	25
2.	Sigmoid	27
3.	Softmax	68

Table 2.Loss value of various activation functions

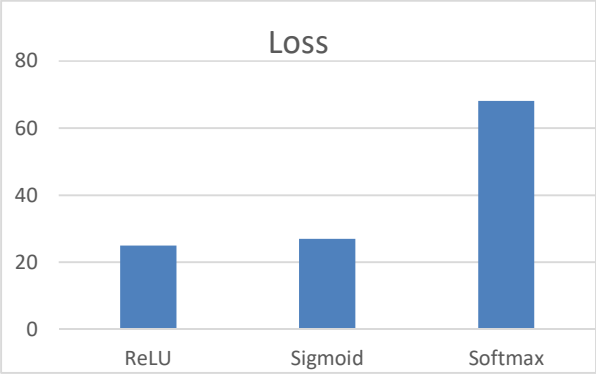

Fig 2 Loss value of various activation functions

Conclusion

In our research we have proposed a system that automatically identifies whether or not a person is wearing a face mask. Using Convolutional Neural Networks and motion learning strategies in neural networks, A dataset containing images of face with mask and without mask. The training dataset contains100 images, which is used to train. The testing dataset contains 300 images, which is used to test. In this study, the CNN algorithm is improved using the ReLU activation function. Three activation functions—ReLU, Sigmoid, and Softmax—were used to search for face masks. The Softmax was able to achieve 90% accuracy. The accuracy of the Sigmoid was 95.19% as well. ReLU architecture attained an accuracy rate of 99.72%.

References:

[1] Suresh K, Palangappa MB, Bhuvan S "Face Mask Detection by using Optimistic Convolutional Neural Network", IEEE Xplore Part Number: CFP21F70-ART ISBN: 978-1-7281-8501-9

[2] Rahinidevi V, Vijay Prasanth K, Aravind Losan S, Sandhya Devi R S " Face Mask Detection using CNN and OpenCV" , International Research Journal of Engineering and Technology (IRJET)

e-ISSN: 2395-0056 p-ISSN: 2395-0072 Volume: 09 Issue: 01 | Jan 2022

[3] Riya Chiragkumar Shah, Rutva Jignesh Shah "Detection of Face Mask using Convolutional Neural Network "

[4] Militante SV, Dionisio NV (2020) Real-time facemask recognition with alarm system using deep learning. In: 2020 11Th IEEE control and system graduate research colloquium (ICSGRC). IEEE, pp 106–110. https://doi.org/10.1109/ICSGRC49013.2020.9232610

[5] Who coronavirus disease (covid-19) dashboard. https://www.worldometers.info/coronavirus/. Accessed: 22-Nov-2021

[6] Modes of transmission of virus causing covid-19. https://bit.ly/3DAyqRu. Accessed: 22-Nov-2021

Business, Management and Economics Engineering
ISSN: 2669-2481 / eISSN: 2669-249X
2024 Volume 22 Issue 01

CONTEMPORARY DIMENSIONS OF PURCHASING BEHAVIOUR OF EMPLOYED WOMEN IN CHENNAI CITY (Based on Nine Contributing Attributes)

Fathima Rustha S
Research Scholar, PG & Research Department of Commerce, Thassim Beevi Abdul Kader College for Women, Kilakarai – 623 517, Ramanathapuram District, Tamil Nadu, India

Dr Jasmine A
Associate. Prof./ Head, PG & Research Department of Commerce, Thassim Beevi Abdul Kader College for Women, Kilakarai – 623 517, Ramanathapuram District, Tamil Nadu, India

ABSTRACT

The purpose of this study was to ascertain the purchasing habits of working women. The online form made with Google Forms was distributed to working women in Chennai who are above the age of eighteen and have purchasing power throughout the study's data gathering phase. The study comprised a total of 187 people who willingly agreed to participate and who thoroughly completed the questionnaire. The study employed a descriptive research paradigm, and basic random sampling was utilized to get the data. Using the SPSS 22 package program, a number of statistical tests were used to analyze the data, including the "Independent T test," "KMO test," "Factor Analysis," and "Reliability."

In the aspects of employed women's purchasing style views, nine components surfaced. The factors that were collected were named based on the things that comprised each factor. "Confused," "Brand Loyal," "Careless," "Contented," "Fashion Conscious," "Pleasure Conscious," "Careful and Price Conscious," and "Perfectionist" are the variables, in that order. Furthermore, the study revealed statistically significant relationships between the work status of female customers and their purchasing patterns. This study suggests that housewives are more vulnerable in terms of careless and happy dimensions, whereas employed women are more sensitive in terms of brand conscious, pleasure conscious, price conscious and cautious, and confused.

Keywords: Purchasing style, employed women, consumer behaviour.

INTRODUCTION:

Women who work and use their purchasing power to satisfy societal, familial, or personal demands are referred to as employed women. Their consumption habits provide details about their culture, identity, and social and economic standing, among other things. One may argue that female customers who have jobs will exhibit distinct buying habits and styles.

One consumer category that should be taken into account in the examination of consumption behaviors in the current period is employed women. Since studies demonstrate the effectiveness of employed women's decisions According to gender stereotypes, women are linked to the home and work, hence they are the primary consumers who make purchases to

support the household. as well as her personal and professional requirements; as a result, her shopping preferences are formed. The interesting point is employed women have a mind of subjectivity in all domains, involving in profession enhances their life status in light of the evolving social structure and knowledge. Their purchasing behaviors, decision-making processes, and consuming patterns all alter as a result of this growth. Their labor raises the income levels of the individual and the family, which raises standards for excellence in the choice and acquisition of goods.

The study is divided into four sections: methodology, analysis, conclusion, and suggestions.

When making purchases, employed women are influenced by a variety of internal and external attributes or factors. Traditionally these factors include demographics, lifestyles, and biological clocks of the customers. Sometimes they encourage a decision during the purchase activity based on the purchasing behavior. In Modern times, Consumers' emotional and intellectual inclinations that are touching before, during, and after purchases may be characterized as their purchasing style.

Review of literature:

Research indicates that women employed in urban areas, in particular, have a preference for eco-friendly items and are highly attuned to product weight and adulteration (Kantha et al., 2020).

- According to Shreeraksha and Maya's (2020) study, Women in their initial earning stage 20–30 range spend a lot in shopping, and it was found that they often purchase the newest goods, particularly during sales and holidays.

- In a research conducted by Ms. Gupta and Shome (2020) with working women in India, discovered that employed women had greater improvements in their online buying behaviors and that demographic factors like the age and income level of the women had a significant impact on these behaviors.

- Bharathi & Dinesh, (2019) highlighted that traditionally, women have been viewed as the family's purchasers, and their purchasing patterns reflect this role inside the home. However, it may be argued that women's responsibilities as family shoppers have changed in light of the recent dramatic increase in the percentage of working women

- Akter, (2018). Explained that it has been observed that independent working women are highly knowledgeable about a product's brand, quality, and price and take their time and be thoughtful while making a purchase

- Mohiuddin, (2018) highlighted that the majority of employed women choose imported products over local brands where he studied to ascertain the impact lifestyle of female consumers in decision making. To get into the highly prospective women's market, it is advised that local producers enhance the quality of their products. Another noteworthy finding of the study is that employed women investigate recently released items before making any

purchases.

- Vural and Güllü (2017) conducted a study in which they discovered that, while working women make decisions with their husbands, housewives typically make decisions when it comes to white goods and electronic goods In order to determine the socio economic status of women in Kazakhstan's and their purchasing process,

- Bansal & Dewan, (2017) carried out their study in India found that working women's apparel choices go toward branded outlets. and search for additional data about the thing they purchased.

Objectives:

1. To find out the socio economic profile of the employed women in Chennai city
2. To find out the contributing attributes which influence purchasing style of the sample respondent
3. To Rank the attributes considering its sub factors
4. To identify the challenges and offer recommendations

Statement of Problem:

Since many women are becoming financially independent through their careers or businesses in the recent age as a result of education and women's empowerment, businesses that target women as their target market generally need to be aware of the shopping habits and fashions of this demographic. To thrive in the market, it is vital to comprehend the purchasing characteristics of employed women consumers in the modern era.. A thorough assessment of multiple issues is necessary.

More specifically, there is no sufficient research to ascertain the purchasing habits of employed women in one extension. In this sense, this study stands out from others, and its objective is to determine the relationship between the shopping habits of women and their employment level and finding out the purchasing characteristics of employed women to contribute positively to the corpus of literature.

Research Model

This study is Descriptive is nature, its primary goal is to evaluate the shopping characteristics of employed women in Chennai.. Additionally, factor analysis and ranking analysis were done. As per the research paradigm, various aspects of their purchasing behavior were ascertained.

Hypotheses:

Ho: There is no significant relationship between personal factors and contributing attributes of employed women

Ho: There is no significant relationship between personal factors and factors influencing purchases decision of employed women

Research methodology and tools used:

Finding information about shopping patterns of employed female clients was the main goal of this study in order to determine their preferences for purchases. The target audience for this research is employed women who are at least eighteen years old. An online survey method was used to collect participant responses to primary sources for the study.

- The nominal scale was used to collect the questions about age, marital status, and employment that were utilized to determine the socio demographic variables.
- An ordinal scale was used to generate the questions regarding income and educational attainment. These were the inquiries in the questionnaire's initial section A.
- Simple percentage analysis, Ranking analysis and Factor analysis were used in this study in an attempt to use quantitative and qualitative data to explain the causal linkages between the qualities within the framework of the generated hypotheses. Furthermore, since testing the established model is sought, it may be said that the research is descriptive.

FINDINGS:

Table 1.

Socio Economic profile of the respondents

Marital Status	**F**	**%**
Unmarried	52	28.5
Married	135	71.5
Total	**187**	**100.0**
Educational Status	**F**	**%**
Higher Secondary Level	27	14.2
Diploma Level	42	22.6
Associate Degree	26	14.0
Undergraduate	57	30.8
Postgraduate or Doctorate	35	18.5
Total	**187**	**100.0**
Occupation	**F**	**%**
Officer	66	35.5
Government Worker	20	10.5
Artisan	3	1.4
Self-employment	6	3.3
Private employee	92	49.3
Total	**187**	**100.0**
Income	**F**	**%**
Upto Rs. 35,000	36	19.5
Rs. 35,001– Rs. 50,000	51	27.5
Rs 50,001– Rs. 65,000	48	24.8
Rs. 65,001– Rs. 80,000	24	13.1
Rs. 80,001 and above	28	15.0

Total	**187**	**100.0**

Age	**F**	**%**
18 – 27 years	38	20.3
28 – 35 years	55	29.2
36 – 43 years	36	19.1
44 – 51 years	34	18.3
52 and above	24	13.1
Total	187	100.0

Source: Primary Data

From the above data it was clear that, majority of the respondents are married (71.5%), and completed their graduation (30.8%), working in a private concern with various post (49.3%) and their earning ranges between Rs. 35,000 to Rs. 65,000 per month(52.3%) with age range between 18 – 35 years. It can be depicted that they are belonging to the generation where smart phone is inevitable and thriving to lead a contemporary life style and ready to spend for their societal upliftment in terms of quality life style.

Contributing Attributes on employed women purchasing styles

- In the study area, nine modern features were found to impact the purchasing behavior of working women. "Perfectionist," "Brand Conscious," "Fashion Conscious," "Pleasure Conscious," "Careful and Price Conscious," "Confused," "Brand Loyal," "Careless," and "Contented" are the names given to these qualities, in that order. 2
- Those that conduct extensive investigation to select the best are perfectionists.
- Brand Conscious people favor higher-end, more recognizable brands.
- Those that follow trends are considered fashion conscious.
- Pleasure-conscious shoppers are folks who like and shop for amusement.
- People who are cautious and price conscious are people that shop carefully, look for great deals, and watch reductions.
- Confused are people who find it difficult to make decisions because there are so many brands, stores, and data available.
- Those that are brand loyal have favored brands and retailers to purchases
- Careless consumers would shop without proper thinking and they do not have any plan for their shopping.
- Contented consumers will clear with what they have, they want and they should buy.

Ranking Analysis

Table 2.

Ranking Related to Determining attributes of Purchase of Employed women

Attributes	**Statements**	**Rank**
Perfectionist		
A4	High quality of the product	I
A3	Buy the creamy stuff.	II
A2	Ready to put effort.	III

A5	High standards matching expectations	IV
A1	Buying good quality products	V
Brand Conscious		
A3	Better price with better quality.	I
A2	Embrace expensive brands.	II
A5	Most advertised brands.	III
A4	Top selling brands.	IV
A1	Well-known brands	V
Fashion Conscious		
A3	Having a trendy, eye-catching	I
A4	up to date with changing technologies.	II
A5	stylish apparels in the wardrobe.	III
A2	distinct trademark from distinctive shops	IV
A1	new and exciting things.	V
Pleasure Conscious		
A3	Wandering around stores.	I
A1	Do not enjoy shopping.	II
A4	Fast shopper	III
A2	Shopping as front runner	IV
Careful and Price Conscious		
A5	Shopping and comparison will be done.	I
A2	Go for special sale product.	II
A3	figure the best profit for money option.	III
A4	not to overspend during shopping.	IV
A6	arrange my shopping better and more precisely	V
A1	prefer low priced products.	VI
Confused		
A2	Confusion between the shops.	I
A3	Many brands leads to confusion.	II
A1	More information leads to confuse.	III
Brand Loyal		
A1	relish shopping.	I
A2	buy favorite brands repeatedly.	II
A3	visit the same store	III
Careless		
A1	inattentive dealings	I
A2	careless while shopping.	II
Contented		
A1	No need to satisfy	I
A2	Good enough product is good to purchases	II

Source: Primary Data

Factors influencing purchase decision of employed women:

Factor analysis

In this factor analysis, there are twenty-four attributes listed, all the twenty-four factors are distinctive contributors. The respondents may have same kind of idealogy about some attributes which are clubbed together.

Table 3.
Listing of attributes

Factor . No	Attributes
F1	Sources of Information
F2	Availability
F3	Government Rating
F4	Cost of electricity
F5	Type of House
F6	Terms / Conditions
F7	Discount / Exchange Schemes
F8	Price
F9	Reviews
F10	Usage of Goods
F11	Post purchases Experience
F12	Income / Estimation
F13	Past Experience
F14	Technical advancement
F15	Warranty
F16	Product specifications
F17	Quality
F18	Brand
F19	Dealer experience
F20	Add on features
F21	Foreign brands
F22	Spares availability
F23	Expected life time
F24	Loans and finance facilities

To find out the relationship among these factors and plotting the attributes into consideration, it is important to examine the KMO and Bartlett's Test

Table 4.
KMO and Bartlett's Test

Sampling Adequacy		.906
Bartlett's Test of Sphericity	Chi-Square	6262.468
	Df	267
	Sig.	.000

Source: Compiled from Primary Data

It is clear from the table above that the KMO value is 0.906 which is more than adequate level, which is the acceptable score. The Bartlett's Test of Sphericity is 6662.486 which is significant at 0.000 thereby confirming that the data is satisfactory enough to perform factor analysis.

Table 5.
Variance Explained by factors

Component	Eigen Value	% of Variance Explained	Cumulative %
1	11.732	23.901	23.901
2	1.151	14.739	38.640
3	1.524	13.162	51.802
4	1.049	10.757	62.559

Source: Compiled from Primary Data

The above table explains the factor derived with Eigen value and the percentage of variance explained by these factors. Four factors were identified from twenty-four statements with a satisfactory Eigen value score more than 1.

These four factors would explain for about 66 percent of total variance, which can sufficiently explain all twenty-four statements.

Table 6.
Rotated Component Matrix

	Component				Eigen Value	Variance
	1	2	3	4		
After Sales Service	.789				11.613	24.019
Your Past Experience	.764					
Your Income / Budget	.759					
Quality of the Product	.712					
Warranty Period	.662					
Utility of Goods	.672					
Noise	.613					
Price of Goods	.609					
Product Features	.587					
Latest Technology	.561					
Offers - Like Discount / Exchange Schemes	.429					
Availability of Information		.774			1.471	15.739
Availability of the Product		.717				
Electricity Consumption		.678				
Star Rating		.638				
Availability of Spares			.675		1.395	14.162
Imported Product			.657			
Durability			.640			
Credit Facility			.597			

Brand			.52			
Salesman's pinion				.751	1.009	10.767
Delivery terms / options				.627		
House - Space Consideration				.599		
Size / Capacity / Space				.485		

Source: Compiled from Primary Data

The above table indicates the four factors

First factor as Economic Factor with eleven attributors.

The second factors as Geographical Factor with four attributes

The third factor as Time factor it contains five sub-factors and

The fourth factor is named as Value added factor.

Table 7.

Naming of factors

Identified variables	Factor Name	Dimensions explained
After Sales Service	**(Factor 1)** Economic factor	The fist dimension named as Economic factor with the total variance of 24.019 %
Your Past Experience		
Your Income / Budget		
Quality of the Product		
Warranty Period		
Utility of Goods		
Noise		
Price of Goods		
Product Features		
Latest Technology		
Offers - Like Discount / Exchange Schemes		
Availability of Information	**(Factor2)** Geographical factor	The second factor named as Geographical factor with the total variance of 15.739%
Availability of the Product		
Electricity Consumption		
Star Rating		
Availability of Spares	**(Factor 3)** Time factor	The third factor named as Time factor with total variance of 14.162%
Imported Product		
Durability		
Credit Facility		
Brand		
Salesman's Opinion	**(Factor 4)** Value added factor	The fourth and last factor named as Value added factor with the total variance of 10.762%
Delivery terms / options		
House - Space Consideration		
Size / Capacity / Space		

Segmentation of respondents based on factors that influencing to purchase BEE Labelled White Goods

All the respondents are may not have same opinion in purchase decision on good. Different people have different opinion in the purchase decision based on price, quality and size of the product, their knowledge and experience and many other factors. So it is important to classify the sample respondents based on the factors influencing to purchase goods. Based on the four factors the working women are segmented by applying K-means cluster analysis.

Table 8.

ANOVA

	Cluster		Error		F	Sig.
	Mean Square	Df	Mean Square	Df		
Based on Economic Factor	110.869	2	.220	382	504.948	.000
Based on Geographical factor	100.714	2	.376	382	267.790	.000
Based on Time Factor	118.207	2	.405	382	292.050	.000
Based on add on features	146.086	2	.353	382	414.361	.000

Source: Compiled from Primary Data

The above table reveals the ANOVA results, from the above table F value reveals that most influencing contributor is cost and income and size and capacity are having high F value followed by durability of household goods. This indicates that cost and income and size and capacity of household goods is the most important factor that influence the purchase decision of household goods in the study area of Ramanathapuram district.

Reliability of Segmentation

Reliability of the cluster classification and its stability among the samples is verified. The four factors are cost and income, based on availability, based on durability and size and capacity are taken as independent variables and the classification is taken as dependent to extract the reliability of segmentation.

Table 9.

Eigen values and Wilks' Lambda

Function	Eigen value	Canonical Correlation	Wilks' Lambda	Chi-square	Df	Sig.
1	5.973	.971	.141	862.947	8	.000
2	.207	.495	.798	87.943	3	.000

Source: Compiled from Primary Data

Table 10.

Structure Matrix

	Function	
	1	2
Based on economic factor	.616*	-.434
Based on Time Factor	.514*	.265
Based on Geographical factor	.465*	-.454
Based on value added Factor	.570	.618*

Source: Compiled from Primary Data

The above table presents the two domain functions are Z1 = 0.616 * Based on cost and income + 0.514 * Based on durability + 0.465 * Based on availability, Z2 = 0.618* Based on size and capacity.

Fig. 1. GROUP CENTROIDS

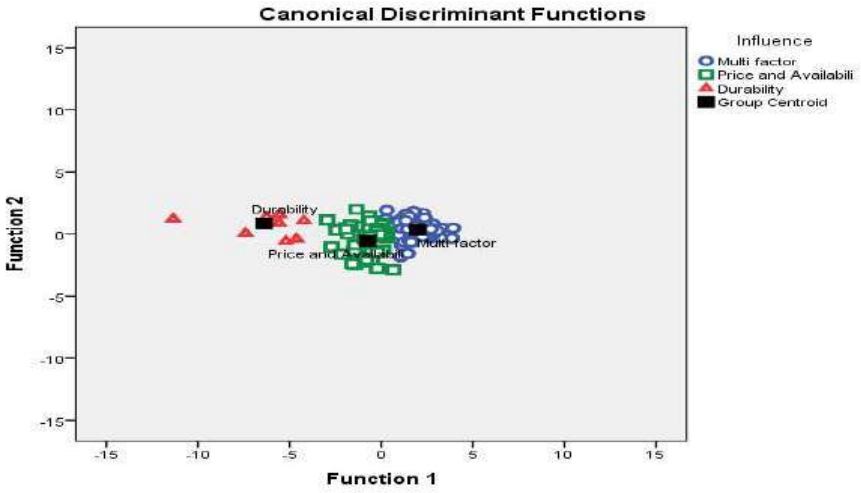

The above group centroids diagram reveals that all the three clusters are significantly different with different group centroids and different mean values..

Table 11.

Extent of Correct Classification

	Influence	Predicted Group Membership			Total
		Multi factor	Price and Availability	Durability	
Count	Multi factor	181	5	0	181
	Economic Factor	0	6	0	6
	Time Factor	0	0	187	187
%	Multi factor	97.2	2.8	.0	100
	Economic Factor	.0	100	.0	100
	Time Factor	.0	.0	100	100

98.7% of data processed

The above table presents the grouping on the basis of reasons.

Economic and Time segments are correctly classified with the score of 100%.181 cases accounting for 97% are classified, It can be inferred that the classification of employed women based on influencing factors considered in the purchase process of goods is correct by more than

98 %.Hence it is concluded that Factors taken for this research is accurate.

Findings And Recommendations:

- The survey revealed that working women prioritized brand and enjoyment over other

factors when making purchases. Companies can increase their market share and client base by providing employed women with the correct product in the proper quantity, quality, and variety. They can be happy and content with what they have.

- It was noted that working women seemed to be happier with their purchases.
- To entice customers to purchase, discounts, gift cards, and coupons must to be offered together with advertisements.
- This study suggests that employed women are generally more sensitive in terms of brand awareness, happy consciousness, Rate conscious, caution, and confusion.
- As they become more knowledgeable about the products and conduct more research, employed women can purchase with greater caution (Guha, 2013).
- Because they now have financial independence, employed women feel comfortable when they shop.
- The purchase patterns and consumption habits of working women have changed as a result of this circumstance. In this way, working women have formed buying habits by selecting high-quality, name-brand goods.
- It might be argued that working women adopt a hedonistic or partially "pleasure purchasing style" since they have discretionary income. Women may also view shopping as a social need.s

Limitations:

- This study cannot be generalized other than study area.
- Results are based on the responses on the respondents and may and may not have accurate and original information.
- Due to time and cost the research cannot be done above its limited objectives.

Conclusion:

The target group in this study was specifically selected to consist of female consumers. Due to the fact that, despite the traditional acceptance of women as mothers, wives, and ladies, women are observed to spend money on enhancing their personal identities and physical attractiveness through their involvement in the economic world. In addition, even after their work obligations, women handle the majority of the family's purchasing despite the fact that they are employed. In this way, analyzing women's buying habits will help you better grasp their desires, requirements, and expectations.

The study involved employed women consumers in Chennai who own smart phones and have access to the internet. However, determining a relationship between the shopping habits of women and their employment level in the study provides a viewpoint for further investigations. It is anticipated that expanding the sample size and incorporating a wider range of demographic backgrounds will produce more comprehensive and significant findings.

REFERENCES

Akbıyık, F. (2020). Helal Gıda ve Tüketici Davranışları Helal Sertifika Algısının Satın Alma Tarzıyla İlişkisi. ÇizgiKitabevi.

Akbıyık, F. (2021). A Research on Determining the Relationship Between Consumers' Purchasing Styles andTheir Religious Orientations. Pazarlama ve Pazarlama Araştırmaları Dergisi, 14 (1), 31-59.

Akter, K. (2018). Behaviour of Employed women on Convenience Food Buying: A Study from BangladeshPerspectives. Business Management and Compliance, 1 (2), 43-57.

Gupta, Y., & Shome, S. (2020). Social Media Advertisements and Buying Behaviour: A Study of Indian Employed women. Int. J. Online Mark, 10 (3), 48-61.

Kantha, R. K., Rout, D., & Mishra, S. J. (2020). Shopping Behaviour -A Study of Urban Employed women in Bhubaneswar. Journal of Engineering Sciences, 11 (7), 1-10.

Mohiuddin, Z. A. (2018). Effect of Lifestyle on Consumer Decision Making: A Study of Women Consumer of Pakistan, Journal of Accounting, Business and Finance Research. Scientific Publishing Institute, 2(1), 12-15.

Panicker, V. B. & Mohammad, K. A. (2017). The Shopping Behaviour of Urban Women Consumers in India for Certain Products and Services. International Journal of Research in Management, Economics andCommerce, 7 (12), 107-115.

Prathaban, S. & Khurana, N., (2018). Impact of Brands on Urban and Rural Working and Non-Employed women Buying Behaviour with Special Reference to Jabalpur City. National Journal of Multidisciplinary Research and Development, 3 (1), 586-588.

Ramprabha, K. (2017). Consumer Shopping Behaviour and The Role of Women in Shopping – A Literature Review. The International Journal of Research Publication's, 7 (8), 50-63.

Shreeraksha. S., & Maiya, U. (2020). Shopping Habits Among Women: A Study with Reference to Udupi District.Asia Pacific Journal of Research, I (105), 110-114.

Şeker, A. (2016). Kadın Tüketiciler, Kadın Tüketicilerin Satın Alma Davranişlari ve Kadinlara Yönelik PazarlamaStratejieri. Uluslararası Sosyal Araştırmalar Dergisi, 9 (43), 2204-2214. DOI: 10.17719/jisr.20164317785.

Menaga, D., & Revathi, S. (2018). Least lion optimisation algorithm (LLOA) based secret key generation for privacy preserving association rule hiding. IET Information Security, 12(4), 332-340.

Menaga, D., & Saravanan, S. (2022). GA-PPARM: constraint-based objective function and genetic algorithm for privacy preserved association rule mining. Evolutionary Intelligence, 15(2), 1487-1498.

Menaga, D., & Revathi, S. (2020). Deep learning: a recent computing platform for multimedia information retrieval. In Deep learning techniques and optimization strategies in big data analytics (pp. 124-141). IGI Global.

Probabilistic principal component analysis (PPCA) based dimensionality reduction and deep learning for cancer classification

D Menaga, S Revathi

Intelligent Computing and Applications: Proceedings of ICICA 2019, 353-368

Menaga, D., & Revathi, S. (2021). Fractional-atom search algorithm-based deep recurrent neural network for cancer classification. Journal of Ambient Intelligence and Humanized Computing, 1-11.

Menaga, D., & Revathi, D. S. (2018). Privacy preserving using bio inspired algorithms for data sanitization. In International Conference on Electrical, Electronics, Computers, Communication, Mechanical and Computing (EECCMC) (pp. 201-206).

Menaga, D., & Saravanan, S. (2021). Application of artificial intelligence in the perspective of data mining. In Artificial Intelligence in Data Mining (pp. 133-154). Academic Press.

Menaga, D., & Revathi, S. (2020). An empirical study of cancer classification techniques based on the neural networks. Biomedical Engineering: Applications, Basis and Communications, 32(02), 2050013.

Menaga, D., & Begum, I. H. (2020). Bio-inspired algorithms for preserving the privacy of data. Journal of Computational and Theoretical Nanoscience, 17(11), 4971-4979.

Menaga, D., Ambati, L. S., & Bojja, G. R. (2023). Optimal trained long short-term memory for opinion mining: a hybrid semantic knowledgebase approach. International Journal of Intelligent Robotics and Applications, 7(1), 119-133.

Naeem, A. B., Senapati, B., Islam Sudman, M. S., Bashir, K., & Ahmed, A. E. (2023). Intelligent road management system for autonomous, non-autonomous, and VIP vehicles. World Electric Vehicle Journal, 14(9), 238.

Naeem, A. B., Senapati, B., Mahadin, G. A., Ghulaxe, V., Almeida, F., Sudman, S. I., & Ghafoor, M. I. (2024). Determine the Prevalence of Hepatitis B and C During Pregnancy by Using Machine Learning Algorithm. International Journal of Intelligent Systems and Applications in Engineering, 12(13s), 744-751.

Yadav, S., Sudman, M. S. I., Dubey, P. K., Srinivas, R. V., Srisainath, R., & Devi, V. C. (2023, October). Development of an GA-RBF based Model for Penetration of Electric Vehicles and its Projections. In 2023 International Conference on Self Sustainable Artificial Intelligence Systems (ICSSAS) (pp. 1-6). IEEE.

Thingom, C., Tammina, M. R., Joshi, A., Agal, S., Sudman, M. S. I., & Byeon, H. (2023, August). Revolutionizing Data Capitalization: Harnessing Blockchain for IoT-Enabled Smart Contracts. In 2023 Second International Conference On Smart Technologies For Smart Nation (SmartTechCon) (pp. 490-496). IEEE.

Sakthivel, M., Sudman, M. S. I., Ravishankar, K., Avinash, B., Kumar, A., & Ponnusamy, M. (2023, October). Medical Image Analysis of Multiple Myeloma Diagnosis Using CNN and KNN Based Approach. In 2023 International Conference on Self Sustainable Artificial Intelligence Systems (ICSSAS) (pp. 92-97). IEEE.

Mohammed, A. H. (2021). Fish schooling and sorensen trust based wireless sensor network optimization. International Journal, 9, 6.

Mohammed, A. H. DDoS Malicious Node Detection by Jaccard and Page Rank Algorithm in Cloud Environment.

Mohammed, A. H. (2021). Invasive Weed Optimization Based Ransom-Ware Detection in Cloud Environment.

Faisal, L., Rama, V. S. B., Roy, S., & Nath, S. (2022). Modelling of electric vehicle using modified sepic converter configuration to enhance dc–dc converter performance using matlab. In Smart Energy and Advancement in Power Technologies: Select Proceedings of ICSEAPT 2021, Volume 2 (pp. 643-653). Singapore: Springer Nature Singapore.

Faisal, L., Rama, V. S. B., Yang, J. M., Wajid, A., & Ghorui, S. K. (2022, May). Performance and simulation analysis of ipmsyncrm (internal permanent magnet synchronous reluctance motor) for advanced electric vehicle design. In 2022 3rd International Conference for Emerging Technology (INCET) (pp. 1-6). IEEE.

Mohd, R., & Faisal, L. (2022). Smart Agricultural Practices using Machine Learning techniques For Rainfall Prediction: A case Study of Valkenburg station, Netherlands. Mathematical Statistician and Engineering Applications, 71(4), 8451-8462.

Wani, A. A., & Faisal, L. (2022). Design & development of novel hybrid set of rules for detection and type of malignant or non-malignant tumor in human brain based on svm using artificial intelligence classifier. Mathematical Statistician and Engineering Applications, 71(4), 10253-10276.

Choudhuri, S. S., Bowers, W., & Siddiqui, M. N. (2023). U.S. Patent No. 11,763,241. Washington, DC: U.S. Patent and Trademark Office.

Zanzaney, A. U., Hegde, R., Jain, L., Choudhuri, S. S., & Sharma, C. K. (2023, September). Crop Disease Detection Using Deep Neural Networks. In 2023 International Conference on Network, Multimedia and Information Technology (NMITCON) (pp. 1-5). IEEE.